



University of Bradford eThesis

This thesis is hosted in [Bradford Scholars](#) – The University of Bradford Open Access repository. Visit the repository for full metadata or to contact the repository team



© University of Bradford. This work is licenced for reuse under a [Creative Commons Licence](#).

**EFFECTS OF GRAPHENE OXIDE *IN VITRO* ON DNA
DAMAGE IN HUMAN WHOLE BLOOD AND
PERIPHERAL BLOOD LYMPHOCYTES
FROM HEALTHY INDIVIDUALS
AND PULMONARY DISEASE PATIENTS:
ASTHMA, COPD, AND LUNG CANCER**

E. E. AMADI

Ph.D

UNIVERSITY OF BRADFORD

2019

**EFFECTS OF GRAPHENE OXIDE *IN VITRO* ON DNA DAMAGE IN HUMAN
WHOLE BLOOD AND PERIPHERAL BLOOD LYMPHOCYTES FROM
HEALTHY INDIVIDUALS AND PULMONARY DISEASE PATIENTS:
ASTHMA, COPD, AND LUNG CANCER**

Emmanuel Eni Amadi

B.Pharm, University of Nigeria Nsukka (Nigeria)

MSc, Analytical & Pharmaceutical Sciences, Loughborough University (UK)

PG. Diploma in Pharmacy, University of Brighton (UK)

Executive MBA, Lancaster University Management School (UK)

Submitted for the degree of

Doctor of Philosophy

Faculty of Life Sciences

University of Bradford

2019

Abstract

Name: Emmanuel Eni Amadi

Title: Effects of Graphene Oxide *in vitro* on DNA Damage in Human Whole Blood and Peripheral Blood Lymphocytes from Healthy individuals and Pulmonary Disease Patients: Asthma, COPD, and Lung Cancer.

Keywords: Graphene Oxide, human whole blood, peripheral blood lymphocytes, asthma, COPD, lung cancer, Comet assay, Micronucleus assay, Western Blot, RT-qPCR.

For the past few decades, the popularity of graphene oxide (GO) nanomaterials (NMs) has increased exceedingly due to their biomedical applications in drug delivery of anti-cancer drugs. Their unique physicochemical properties such as high surface area and good surface chemistry with unbound surface functional groups (e.g. hydroxyl - OH, carboxyl /ketone C=O, epoxy/alkoxy C-O, aromatic group C=C, etc) which enable covalent bonding with organic molecules (e.g. RNA, DNA) make GO NMs as excellent candidates in drug delivery nanocarriers. Despite the overwhelming biomedical applications, there are concerns about their genotoxicity on human DNA. Published genotoxicity studies on GO NMs were performed using non-commercial GO with 2-3 layers of GO sheets, synthesized in various laboratories with the potential for inter-laboratory variabilities. However, what has not been studied before is the effects of the commercial GO (15-20 sheets; 4-10% edge-oxidized; 1 mg/mL) *in vitro* on DNA damage in human whole blood and peripheral blood lymphocytes (PBL) from real-life patients diagnosed with chronic pulmonary diseases [asthma, chronic obstructive pulmonary disease (COPD), and lung cancer], and genotoxic endpoints compared with those from

healthy control individuals to determine whether there are any differences in GO sensitivity. Thus, in the present study, we had characterized GO NMs using Zetasizer Nano for Dynamic Light Scattering (DLS) and zeta potential (ZP) in the aqueous solution, and electron microscopy using the Scanning Electron Microscope (SEM) and Transmission Electron Microscope (TEM) in the dry state, respectively. Cytotoxicity studies were conducted on human PBL from healthy individuals and patients (asthma, COPD, and lung cancer) using the Methylthiazolyldiphenyl-tetrazolium bromide (MTT) and Neutral Red Uptake (NRU) assays, respectively. The genotoxicity (DNA damage) and cytogenetic effects (chromosome aberration parameters) induced by GO NMs on human whole blood from healthy individuals and patients were studied using the Alkaline Comet Assay and Cytokinesis-blocked Micronucleus (CBMN) assay, respectively. Our results showed concentration-dependent increases in cytotoxicity, genotoxicity, and chromosome aberrations, with blood samples from COPD and lung cancer patients being more sensitive to DNA damage insults compared with asthma patients and healthy control individuals. Furthermore, the relative gene and protein expressions of TP53, CDKN1A/p21, and BCL-2 relative to GAPDH on human PBL were studied using the Reverse Transcription Quantitative Polymerase Chain Reaction (RT-qPCR) and Western Blot techniques, respectively. Our results have shown altered gene and protein expression levels. Specifically, GO-induced cytotoxicity, genotoxicity, and micronuclei aberrations were associated with TP53 upregulation - a biomarker of DNA damage - in both patients and healthy individuals. These effects show that GO NMs have promising roles in drug delivery applications when formulated to deliver drug payload to COPD and cancer cells. However, the fact that

cytotoxicity, genotoxicity, chromosome instability, and gene/protein expressions - biomarkers of cancer risk - were observed in healthy individuals are of concern to public health, especially in occupational exposures at micro levels at the workplace.

Acknowledgement

I am grateful to my PhD Principal Supervisor, Professor Diana Anderson, The Established Chair of Biomedical Sciences, Faculty of Life Sciences, University of Bradford for her support throughout my PhD studies. Her ability to guide and accommodate me, starting from 2015 when I was interviewed at her office till my graduation in 2019, despite my weaknesses have been deeply appreciated. Secondly, I am grateful to Dr Mojgan Najafzadeh, my Associate Supervisor and a Research Fellow in Medical Research/Lecturer at University of Bradford. She was instrumental in the arrangement of all blood samples from patients used in this study. I also wish to acknowledge Dr Adi Baumgartner, a Senior Lecturer in Biomedical Sciences, School of Health Sciences, York St. John University. Dr Adi was my first PhD supervisor (2006-2017) before taking up his current post at York St. John University in 2017.

To my beloved wife, Mrs Ewa Amadi, and our two sons: **Michael Chidozie Amadi** and **Anthony Chibuike Amadi** - for their unalloyed love throughout these difficult years. May the soul of my dear, late mother, Late Mrs Lucy Ugo Amadi, who passed on to eternal glory on 12th March 2018 R.I.P. with the Lord. To my eldest brother, Sir Charles Ifeanyi Amadi (KSJI), you have played key roles of a father to me since I was a child. May God bless you.

Finally, I wish to acknowledge the Trustees of The Leverhulme Trade Charities Trust, London for the PhD Bursary award without which it would have been difficult to continue with my PhD studies. I pray God to bless me so I can be a blessing to others (Acts 20: 35).

Table of Contents

Abstract	i
Acknowledgement	iv
Table of Contents.....	v
List of Figures	xv
List of tables.....	xviii
Abbreviations	xxiii
Chapter 1: General Introduction	1
1.0 Introduction	2
1.1 Nanoparticles and Nanomaterials	4
1.2 Nanotechnology	5
1.3 Graphene Oxide Nanomaterials.....	6
1.4 Applications of Graphene Oxide in Biomedical Sciences.....	8
1.4.1 Drug delivery.....	9
1.4.2 Gene therapy	11
1.4.3 Tissue engineering.....	11
1.5 Pathogenesis of nanoparticles-induced pulmonary diseases.....	12
1.5.1 Nanoparticle deposition and clearance in human lungs.....	13
1.5.2 Inflammation of the lungs.....	14
1.5.3 Oxidative Stress and Reactive Oxygen Species	15
1.5.4 Genotoxicity of Nanomaterials	16
1.6 Diseases of the Pulmonary System	17
1.6.1 Asthma.....	18
1.6.2 Chronic Obstructive Pulmonary Disease	19
1.6.3 Lung Cancer	20
1.7 Methods used for assessment of Genotoxicity (DNA Damage), chromosome instability, and gene and protein expressions in human whole blood and peripheral blood lymphocytes.....	21
1.7.1 Genotoxicity assay	21
1.7.1.1 Comet assay.....	21
1.7.2 Cytogenetic assay.....	23
1.7.2.1 Cytokinesis Blocked Micronucleus (CBMN) Assay.....	23

1.7.3 Gene Expression assay (RT-qPCR)	24
1.7.4 Western Blot	25
1.8 Aim and Objectives of the Project	25
1.8.1 Aim.....	25
1.8.2 Objectives	27
Chapter 2: Materials and Methods.....	29
2.0 Materials and Methods.....	30
2.1 Materials	30
2.1.1 Chemicals	30
2.1.2 Equipment.....	32
2.2 Methods	34
2.2.1 Ethical Approval.....	34
2.2.2 Recruitment of volunteers	34
2.2.3 Collection of Blood Samples	36
2.2.4 Isolation of Peripheral Human Lymphocytes (PBL).....	37
2.2.5 Cell Counting with Haemocytometer.....	38
2.2.6 Determination of lymphocyte concentration	38
2.2.7 Cell viability test with Trypan Blue Exclusion assay	39
2.2.8 Particle Characterization of Graphene Oxide Nanomaterials.....	40
2.2.8.1 Materials	40
2.2.8.1.1 Preparation of GO dilution in aqueous suspension	41
2.2.8.1.2 Dynamic Light scattering	41
2.2.8.1.3 Zeta Potential	42
2.2.8.1.4 Scanning Electron Microscope.....	42
2.2.8.1.5 Transmission Electron Microscope.....	43
2.2.9 <i>In Vitro</i> Cytotoxicity Assays.....	44
2.2.9.1 MTT Cell Proliferation /Cell survival Assay	44
2.2.9.1.1 Materials.....	45
2.2.9.1.1.1 Demographic Data of blood donors used in the MTT and NRU assays	45
2.2.9.1.2 Methods	46
2.2.9.1.2.1 Preparation of Reagents.....	46
2.2.9.1.2.2 Treatment of Lymphocytes with GO NMs.....	46

2.2.9.1.2.3 Treatment of lymphocytes with MTT dye solution	47
2.2.9.1.2.4 Spectrophotometric Analysis (Absorbance).....	48
2.2.9.1.2.5 Data Analysis	48
2.2.9.1.2.5.1 Calculation of Percentage (%) Cell survival in the MTT Assay	48
2.2.9.1.2.5.2 Statistical Analysis	49
2.2.9.2 Neutral Red Uptake (NRU) Assay	49
2.2.9.2.1 Materials.....	50
2.2.9.2.1.1 Demographic Data of blood donors used in the NRU Assay	50
2.2.9.2.2 Methods	50
2.2.9.2.2.1 Treatment of Lymphocytes with GO	50
2.2.9.2.2.2 Treatment of Lymphocytes with Neutral Red Solution.....	51
2.2.9.2.2.3 Spectrophotometric Analysis (Absorbance).....	51
2.2.9.2.2.4 Data Analysis	52
2.2.9.2.2.4.1 Calculation of % Cell survival in the NRU Assay	52
2.2.9.2.2.4.2 Statistical Analysis	52
2.2.10 Genotoxicity Assay	53
2.2.10.1 Alkaline Comet Assay.....	53
2.2.10.1.1 Materials.....	54
2.2.10.1.1.1 Demographic Data of blood donors.....	54
2.2.10.1.2 Methods.....	58
2.2.10.1.2.1 Treatment of human Whole Blood with Chemical Agents	58
2.2.10.1.2.2 Cell Lysis	59
2.2.10.1.2.3 DNA Unwinding and Alkaline Electrophoresis	60
2.2.10.1.2.4 Neutralisation	61
2.2.10.1.2.5 DNA Staining with Ethidium Bromide	61
2.2.10.1.2.6 DNA Damage Scoring	62
2.2.10.1.2.7 Statistical Analysis.....	62
2.2.11 Cytogenetic Assay	63
2.2.11.1 Cytokinesis-Blocked Micronucleus (CBMN) Assay.....	63
2.2.11.1.1 Materials.....	63
2.2.11.1.1.1 Demographic Data of participants in CBMN Assay	63
2.2.11.1.2 Methods.....	64

2.2.11.1.2.1 Preparation of Basic Culture Medium	64
2.2.11.1.2.2 Blood Cell Culture: Day 1; Time point: 0 h.....	64
2.2.11.1.2.3 Chemical Treatment with GO: Day 2; Time point: 24 h	65
2.2.11.1.2.4 Treatment with Cyto-B: Cytokinesis Block: Day 3; Time point: 44 h.....	65
2.2.11.1.2.5 Cell Harvesting and Preparation: Day 4; Time point: 72 h	66
2.2.11.1.2.6 Treatment with Cold KCl (Hypotonic Shock)	66
2.2.11.1.2.7 Cell Fixation.....	67
2.2.11.1.2.7.1 Fixation with Formaldehyde	67
2.2.11.1.2.7.2 Fixation without Formaldehyde	67
2.2.11.1.2.8 Slide Preparation: Day 5.....	67
2.2.11.1.2.9 Giemsa Staining: Day 6.....	68
2.2.11.1.2.10 Slide Mounting: Day 7	69
2.2.11.1.2.11 Micronuclei (MNI) Scoring: From Day 8 onwards	69
2.2.11.1.2.12 Data Analysis	70
2.2.11.1.2.12.1 Calculation of Nuclear Division Index.....	70
2.2.11.1.2.12.2 Statistical Analysis.....	70
2.2.12 Gene Expression Assay using Reverse Transcription Quantitative Polymerase Chain Reaction (RT-qPCR).....	71
2.2.12.1 Materials.....	71
2.2.12.1.1 Demographic Data of participants in RT-qPCR.....	71
2.2.12.2 Molecular Biology Methods for RT-qPCR.....	72
2.2.12.2.1 Extraction of Total RNA from human lymphocytes.....	72
2.2.12.2.1.1 First Column Wash.....	73
2.2.12.2.1.2 Second Column Wash.....	73
2.2.12.2.1.3 Third Column Wash.....	73
2.2.12.2.1.4 Optional Spin (to dry the column)	73
2.2.12.2.1.5 Elution of Pure RNA	74
2.2.12.2.2 Quantification of RNA concentrations and purity	74
2.2.12.2.3 Primer Design.....	75
2.2.12.2.4 Reverse Transcription	76
2.2.12.2.4.1 Priming with RNA or Oligo (dT) ₁₅ Primers	76
2.2.12.2.4.2 Preparation of Reverse Transcription Mixture	77

2.2.12.2.4.3 Synthesis of Complementary DNA (cDNA)	78
2.2.12.2.5 Quantitative Polymerase Chain Reaction (qPCR)	79
2.2.12.2.6 Gene Expression Data Analysis	81
2.2.12.2.6.1 Calculation of Relative Gene Expression or Fold-Change using the Double-Delta ($2^{-\Delta\Delta Cq}$) (Livak) Method	83
2.2.12.2.6.2 Calculation of Average Cq values from triplicate results ..	83
2.2.12.2.6.3 Normalization (ΔCq) of GOI relative to reference gene ...	83
2.2.12.2.6.4 Normalisation ($\Delta\Delta Cq$) of treated samples (ΔCq) relative to untreated samples (ΔCq).....	84
2.2.12.2.6.5 Calculation of Fold-differences ($2^{-\Delta\Delta Cq}$).....	84
2.2.12.2.6.6 Statistical Analysis.....	85
2.2.13 Protein Expression using Western Blot (WB) Method.....	85
2.2.13.1 Materials.....	85
2.2.13.1.1 Demographic Data of participants used in WB analysis	85
2.2.13.2 Molecular Biology Methods in WB	85
2.2.13.2.1 Protein Extraction	86
2.2.13.2.2 Determination of Protein Concentrations.....	87
2.2.13.2.3 Preparation of Sodium Dodecyl Sulfate-Polyacrylamide Gel Electrophoresis (SDS-PAGE)	88
2.2.13.2.3.1 Preparation of 12.5% Resolving Gels.....	88
2.2.13.2.3.2 Preparation of 6% Stacking Gels.....	90
2.2.13.2.4 Loading Proteins and SDS-PAGE Electrophoresis	90
2.2.13.2.5 Protein transfer to PVDF membrane	91
2.2.13.2.6 Blocking of unbound Proteins.....	92
2.2.13.2.7 Incubation with Primary Antibodies	92
2.2.13.2.8 Incubation with Secondary Antibody	92
2.2.13.2.9 Detection of proteins with Chemiluminescent Substrate	93
Chapter 3: Particle Characterization	94
3.0 Characterization of GO nanomaterials.....	95
3.1 Introduction	95
3.2 Materials	95
3.3 Methods	95
3.4 Results	95

3.4.1 Agglomeration state / particle size distribution and Zeta Potential (Surface charge) analyses	95
3.4.2 SEM and TEM Analyses	99
3.5 Discussion.....	106
Chapter 4: Cytotoxicity Assays	110
1.0 Cytotoxicity of GO NMs in human lymphocytes from healthy individuals and patients (asthma, COPD, and lung cancer).....	111
4.1 Introduction	111
4.1.1 Hypothesis: GO may be cytotoxic to human lymphocytes	111
4.1.2 Materials and Methods.....	112
4.2 Results	112
4.2.1 Cytotoxicity of GO NMs in human lymphocytes in the MTT and NRU assays	112
4.2.2 Confounding Factors.....	119
4.3 Discussion.....	119
Chapter 5: Genotoxicity Assay	124
5.0 Genotoxicity (DNA Damage) Effects of GO in vitro in human whole blood from healthy individuals and patients (asthma, COPD, and lung cancer)	125
5.1 Introduction	125
5.1.1 Hypothesis: GO may be genotoxic in human whole blood.....	125
5.2 Materials and Methods.....	126
5.3 Results	126
5.3.1 H ₂ O ₂ Concentration-dependent DNA Damage in Healthy individuals ..	126
5.3.2 GO-induced DNA damage on human whole blood from Healthy Individuals and patients (asthma, COPD, and lung cancer).....	129
5.3.3 Confounding Factors.....	133
5.4 Discussion.....	134
Chapter 6: Cytogenetic Assay	137
6.0 Analysis of the Effects of GO on genetic instability endpoints (Chromosome aberration and Micronuclei (MNi)) in healthy individuals and patients (asthma, COPD, and lung cancer) in the Cytokinesis-Blocked Micronucleus (CBMN) Assay	138

6.1 Introduction	138
6.1.1 Hypothesis: GO may cause mutagenesis in human whole blood	139
6.2 Materials and Methods.....	142
6.3 Results.....	142
6.3.1 Analysis of Genetic Instability Endpoints (Mononucleated cells (MonoNC), Binucleated cells (BiNC), Multinucleated cells (MultiNC), Micronuclei (MNi), Nucleoplasmic bridges (NPBs), and Nuclear Buds (NBUDs)) induced after treatment with GO in healthy individuals and patients (asthma, COPD, and lung cancer) in the CBMN Assay.....	142
6.4 Confounding Factors.....	157
6.5 Discussion.....	157
Chapter 7: Gene Expression Analysis	164
7.0 Effects of GO NMs on the Relative Gene Expression of Cell-Cycle signalling genes (TP53, CDKN1A, and BCL-2) in Human Lymphocytes from healthy individuals and patients (asthma, COPD, and lung cancer) using RT-qPCR Method.....	165
7.1 Introduction	165
7.1.1 Hypothesis: GO may affect gene expression of cell-cycle signalling genes involved in the cascade of DNA damage.....	166
7.2 Materials and Methods.....	166
7.3 Results.....	167
7.3.1 Effects of GO NMs on the Relative Gene Expression of cell-cycle signalling genes (TP53, CDKN1A, BCL-2) relative to GAPDH in Human Lymphocytes from healthy individuals and patients (asthma, COPD, and lung cancer) using the RT-qPCR Method	167
7.3.2 Confounding Factors.....	174
7.4 Discussion.....	174
Chapter 8: Protein Expression Analysis.....	178
8.0 Analysis of the Effects of GO on Protein Expression of Cell-Cycle signalling proteins (p53, p21, BCL-2) relative to GAPDH in Human Lymphocytes from healthy individuals and patients (asthma, COPD, and lung cancer) using Western Blot Method.....	179

8.1 Introduction	179
8.1.1 Hypothesis: GO may affect protein expression in the cell-cycle signalling pathways (p53, p21, and BCL-2 relative to GAPDH) involved in the cascade of DNA Damage.....	180
8.2 Materials and Methods.....	180
8.3 Results.....	180
8.3.1 Effects of GO on Protein Expression on the Cell-Cycle signalling proteins (p53, p21, BCL-2) in Human Lymphocytes from healthy individuals and patients (asthma, COPD, and lung cancer) using WB Method	180
8.3.2 Confounding Factors.....	183
8.4 Discussion.....	183
Chapter 9: General Discussion.....	185
9.0 General Discussion.....	186
9.1 Discussion on GO particle characterization (Chapter 3)	188
9.2 Discussion on the cytotoxicity of GO NMs in human lymphocytes from healthy individuals and patients (asthma, COPD, and lung cancer) using MTT and NRU assays (Chapter 4).....	190
9.3 Discussion on the genotoxicity (DNA damage) of GO NMs in human whole blood from patients and patients (asthma, COPD, and lung cancer) using the Alkaline Comet Assay (Chapter 5)	192
9.4 Discussion on the cytogenetic (mutagenesis) effects of GO on human whole blood from patients and patients (asthma, COPD, and lung cancer) using CBMN Assay (Chapter 6)	194
9.5 Discussion on the Effects of GO on Gene and Protein Expression of p53/TP53, CDKN1A/p21, and BCL-2 on human lymphocytes from healthy individuals and patients (asthma, COPD, and lung cancer) using the RT-qPCR Method (Chapter 7).....	197
9.6 Conclusion	201
9.7 Future work	206
References.....	207
References.....	208
Appendix	227

Appendix 1: Consent Forms.....	228
Appendix 2: Abstracts & Oral Presentations attended	235
Appendix 2.1: NANO Boston Conference under the “Emerging Researcher Forum;” Crown Plaza, Boston-Newton, Boston, MA, USA, 22-24 April 2019	235
Appendix 2.2: Postgraduate Research Symposium, Faculty of Life Sciences, University of Bradford; Mon. 4 th June 2018; Abstract Book, p6.	238
Appendix 2.3: Postgraduate Research Symposium, Faculty of Life Sciences, University of Bradford; Abstract & Oral Presentation: Wed. 7 th June 2017; Abstract Book, pp10-11.....	240
Appendix 3: Poster Presentation: Life Sciences Research and Development Open Day, Tuesday 5 th June 2018; Faculty of Life Sciences, University of Bradford, UK.	243
Appendix 4: Raw Date for Neutral Red Uptake Assay	244
Appendix 5: Raw Date for MTT Assay	247
Appendix 6: Reagents for Comet assay.....	249
Appendix 7: Raw data of DNA damage in the Comet assay.....	251
Appendix 7.1: H ₂ O ₂ -concentration dependent DNA damage in healthy individuals (n=5).....	251
Appendix 7.2: Effects of GO and 100 µM H ₂ O ₂ on human DNA in vitro on human whole blood from Healthy individuals and patients (asthma, COPD, and lung Cancer) in the Comet assay.	252
Appendix 8: Reagents used in the CBMN Assay	253
Appendix 9: Summary of Chemical Treatments, volumes, and treatment sequences in the CBMN assay	253
Appendix 10: Chemicals and mixtures used in RNA Isolation	255
Appendix 11: Western Blot materials	256
Appendix 12: Amplification curves obtained during qPCR data analysis	263
Appendix 12.1: Amplification curves for Healthy Individuals	263
Appendix 12.2: Amplification curves for asthma Patients	264
Appendix 12.3: Amplification curves for COPD patients	265
Appendix 12.4: Amplification curves for lung cancer patients	266
Appendix 13: RT-qPCR RAW DATA.....	267
Appendix 13.1 RT-qPCR raw data for Healthy	267

Appendix 13.2 RT-qPCR raw data for asthma patients	268
Appendix 13.3 RT-qPCR raw data for COPD Patients	269
Appendix 13.4 RT-qPCR raw data for lung cancer patients.....	270
Appendix 14: Graphene Oxide Safety Data Sheet.....	271
Appendix 15: E-mail Correspondences with Sigma-Aldrich	277

List of Figures

Figure 1.1: Cisplatin-DNA cross-linking adducts: (A) 1,2-intrastrand cross-link, (B) Interstrand cross-links, (C) Mono-functional adduct, and (D) protein-DNA cross-link. The main site of attack of Cisplatin to DNA is on the N7 of Guanine (Fahmy 2014)	3
Figure 1.2: Structure of Graphene Oxide	7
Figure 1.3: Synthetic routes of Graphene Oxide and reduced Graphene Oxide, using graphite as a starting material (Sur 2012).....	8
Figure 1.4: Schematic diagram showing different biomedical applications of Graphene and GO, including gene and drug delivery, tissue engineering, etc (Dasari Shareena et al. 2018).	9
Figure 1.5: A schematic drawing showing the synthesis of GO, a model structural change (GON-PEG), Dox loading /cross-linking, and reduction-triggered release of the CPMAA cross-linked nano GO polyethylene glycol barriers.	10
Figure 1.6: Relationship between asthma and COPD.....	20
Figure 2.1: Schematic illustration of Isolation of lymphocytes from human whole blood using density-gradient Lymphoprep™ (Bharadwaj et al. 2012)	37
Figure 2.2: Illustrative photos of the Zetasizer Nano ZS-90 during sample loading (Malvern Panalytical Ltd 2018)	41
Figure 2.3: A Zetasizer cell photograph taken during zeta potential analysis with the aid of a Samsung Galaxy S9+ Mobile Phone with 12 MP camera . The photo shows the internal sections of the cell – the electrodes and a capillary.....	42
Figure 2.4: Photographic images of the particle preparation on the left and the interior of the SEM during SEM analysis	43
Figure 2.5: Conversion of soluble, yellow tetrazolium MTT dye (A) (Grant 2014) to insoluble, purple Formazan crystals (B) by reductase enzymes inside the mitochondria of living cells (Shinryuu 2010).	45
Figure 2.6: Representative image of a 96-well plate during NRU assay	51

Figure 2.7: Photographs taken during the Comet assay:	60
Figure 2.8: A schematic representation of duplicate slides with markings (x) indicating where 2 x 20 μ L of cell suspensions were added.....	68
Figure 2.9: BioDrop™ Touch Duo Spectrophotometer (BioDrop Ltd 2012)	74
Figure 2.10: Primer design websites: (a) KiCqStart™ (Sigma-Aldrich), and (b) Ensemble website.	75
Figure 2.11: Representative example of an amplification plot of 5 samples (1,2,3 and 4). As the cDNA is amplified in the samples, their fluorescence increased.....	82
Figure 2.12: Calibration curve obtained using the Bradford assay at 595 nm. .	87
Figure 2.13: Photographic images taken during Western Blot analysis	89
Figure 3.1: Measurement of particle size-distribution (hydrodynamic diameter) by DLS (size vs. intensity) using Zetasizer Nano ZS-90, Model ZEN3600 (Malvern Instruments Ltd, UK). Average particle size of GO (15-20 sheets), Z-Average (d.nm): A = 806.1 nm, PDI = 0.768; B = 779.1 nm, PDI = 0.899; and C = 693.8 nm, PDI = 0.929. Abbreviations: Z-Average = average size; d.nm = diameter; and PDI = polydispersity index	97
Figure 3.2: Measurement of the Zeta Potential (surface charge) using Zetasizer Nano ZS-90, Model ZEN3600 (Malvern Instruments Ltd, UK). Zeta Potential: (A) = - 21.7 mV; (B) = - 26. 1 mV; and (C) = structure of GO with terminal groups: epoxy /alkoxy (C-O), carboxyl (C=O), aromatic (C=C), etc (Song et al. 2014; PubChem 2018).....	98
Figure 3.3: 20K SEM micrographs of GO aggregates: (A) in 10 μ g/mL; and (B) 20 μ g/mL in in aqueous solution.....	101
Figure 3.4: 20K SEM micrographs of GO: (A) 50 μ g/mL suspension in RPMI, and (B) in 100 μ g/mL suspension in RPM.....	102
Figure 3.5: TEM micrographs of GO at 50 x magnification: (A) 10 μ g/mL; (B) 20 μ g/mL; (C) 50 μ g/mL, and (D) 100 μ g/mL	103
Figure 3.6: TEM micrographs of GO aggregates: (A) x 1K magnification (50 μ g/mL) and (B) 10K magnification (20 μ g/mL)	104

Figure 3.7: TEM micrograph of GO aggregates: (A) x 1K magnification (50 µg/mL) and (B) 2.5K magnification (100 µg/mL)	105
Figure 4.1: Cytotoxicity of Graphene Oxide (15-20 sheets) in peripheral human lymphocytes after 24 h exposure to different concentrations of GO (10, 20, 50 and 100 µg/mL). The mitochondrial activities were assessed with NRU and MTT assays.....	118
Figure 5.1: H ₂ O ₂ concentration-dependent DNA damage in human whole blood from healthy individuals after exposure to four different concentrations of H ₂ O ₂ (10, 30, 60, and 100 µM) compared with untreated whole blood as the negative control (NC).	128
Figure 5.2: GO-induced DNA damage in human whole blood from healthy individuals and patients (Olive tail moment).....	131
Figure 5.3: GO-induced DNA damage in human whole blood from healthy individuals and patients (% tail DNA).	132
Figure 5.4: Representative Comet images formed after migration of broken DNA	133
Figure 6.1: Schematic illustration of cell cycle. It comprises two major components: (1) The Interphase (G ₀ , G ₁ , S & G ₂), and (2) the Mitotic phase (mitosis & cytokinesis) (Lumen Learning 2017; CNX 2019).	140
Figure 6.2: Photographs of genetic instability parameters obtained during Micronucleus assay scoring.	156
Figure 6.3: Photographs of genetic instability parameters obtained during Micronucleus assay scoring.	156
Figure 8.1: Effects of GO (50, 100, 150, and 200 µg/mL) on the induction of p53, BCL-2, and p21 proteins relative to GAPDH human lymphocytes from healthy individuals. The protein bands were differentially induced.....	182

List of tables

Table 2-1: Chemicals, manufacturers, and CAS number/Catalogue number...	30
Table 2-2: Equipment and other materials	32
Table 2-3: Characteristics of GO NMs.....	40
Table 2-4: Demographic data of patients and healthy individuals used in the MTT and NRU Assay.	45
Table 2-5: Chemical Treatment table	47
Table 2-6: Components of In Vitro Toxicology Neutral Red based assay kit	50
Table 2-7: Demographic data of patients and healthy individuals used in the Comet and CBMN assays.	54
Table 2-8: Preparation of Bulk Basic Culture medium from a bottle of 500 mL RPMI 1640-with Glutamax-1.	64
Table 2-9: Demographic data of patients and healthy individuals used in RT- qPCR and Western Blotting methods (n=3)	71
Table 2-10: Detailed information of the Human Primers used in RT-qPCR, including their sequences (5'-3'), length, conc. (nmol), volume of nuclease free water (μ L) added to reconstitute each primer to 100 μ M and their annealing temperatures	76
Table 2-11: Mixture No. 1: Priming with RNA or Oligo (dT)15 Primer	77
Table 2-12: Mixture No. 2: Components of Reverse Transcription mixture	78
Table 2-13: Cycling Conditions for the Synthesis of cDNA.....	79
Table 2-14: qPCR Reaction Mixture (20 μ L) and a photo of a 96-Well plate....	80
Table 2-15: qPCR Thermal Cycling Conditions	81
Table 2-16: Reagents for the preparation of Resolving and Stacking Gels	88
Table 3-1: Characterization of GO showing agglomeration states (Z-Average): hydrodynamic diameter (nm), Polydispersity Index and surface charge (Zeta Potential) in aqueous solution assessed using DLS. Particle size range = 693.8 to 806.1 nm; and Zeta Potential = - 21.7 to - 26.1 mV.	96

Table 3-2: Particle distance of GO (10, 20, 50, and 100 µg/mL) measured with SEM and TEM. The average distance was between 360 and 450 nm. ...	100
Table 3-3: Mean distance of 2-3 layers of GO synthesized in-house by other researchers and size distance measured with dynamic force microscope (DFM) (Song et al. 2014).....	100
Table -4-1: NRU Assay measurements of the % cell survival rates and % cell reduction of metabolic activities of human lymphocytes from healthy individuals and patients (asthma, COPD and lung cancer) after treatment with different concentrations of GO (10, 20, 50, and 100 µg/mL) in 3 independent experiments (n = 3). The NC, untreated lymphocytes have 100% metabolic activity.....	116
Table 4-2: MTT Assay measurements of the % Cell survival rates and % cell reduction of metabolic activities of human lymphocytes from healthy individuals and patients (asthma, COPD and lung cancer) after treatment with different concentrations of GO (10, 20, 50, and 100 µg/mL) in 3 independent experiments (n = 3). The NC, untreated lymphocytes have 100% metabolic activity.....	117
Table 6-1: Mean values of various genetic instability parameters in human whole blood after treatment with different concentrations of GO (0, 10, 20, 50 and 100 µg/mL) and 0.4 µM MMC in Healthy Individuals in the CBMN Assay. DNA damage events were scored specifically in once divided binucleated cells. Statistical analyses were performed using GraphPad Prism, version 8.1.2 (332) with built-in One-Way ANOVA and Dunnett's multiple comparisons tests to compare cytogenetic parameters in treated samples relative to the negative control (NC). Statistical significance was rated at p < 0.05; where * = p<0.05 and ns = not significant; 5 x independent experiments (n = 5).	152
Table 6-2: Mean values of various genetic instability parameters in human whole blood after treatment with different concentrations of GO (0, 10, 20, 50 and 100 µg/mL) and 0.4 µM MMC in asthma patients in the CBMN Assay. DNA damage events were scored specifically in once divided binucleated cells. Statistical analyses were performed using GraphPad	

Prism, version 8.1.2 (332) with built-in One-Way ANOVA and Dunnett's multiple comparisons tests to compare cytogenetic parameters in treated samples relative to the negative control (NC). Statistical significance was rated at $p < 0.05$; where * = $p < 0.05$ and ns = not significant; 5 x independent experiments (n = 5). 153

Table 6-3: Mean values of various genetic instability parameters in human whole blood after treatment with different concentrations of GO (0, 10, 20, 50 and 100 $\mu\text{g/mL}$) and 0.4 μM MMC in COPD patients in the CBMN Assay. DNA damage events were scored specifically in once divided binucleated cells. Statistical analyses were performed using GraphPad Prism, version 8.1.2 (332) with built-in One-Way ANOVA and Dunnett's multiple comparisons tests to compare cytogenetic parameters in treated samples relative to the negative control (NC). Statistical significance was rated at $p < 0.05$; where * = $p < 0.05$ and ns = not significant; 5 x independent experiments (n = 5). 154

Table 6-4: Mean values of various genetic instability parameters in human whole blood after treatment with different concentrations of GO (0, 10, 20, 50 and 100 $\mu\text{g/mL}$) and 0.4 μM MMC in lung cancer patients in the CBMN Assay. DNA damage events were scored specifically in once divided binucleated cells. Statistical analyses were performed using GraphPad Prism, version 8.1.2 (332) with built-in One-Way ANOVA and Dunnett's multiple comparisons tests to compare cytogenetic parameters in treated samples relative to the negative control (NC). Statistical significance was rated at $p < 0.05$; where * = $p < 0.05$ and ns = not significant; 5 x independent experiments (n = 5). 155

Table 7-1: Relative Gene Expression of cell-cycle signalling genes (TP53, CDKN1A, and BCL2) normalized with reference gene (GAPDH) in human lymphocytes from healthy individuals after 24 h treatment with different concentrations of GO (150 and 200 $\mu\text{g/mL}$) in RT-qPCR. Relative gene expression was expressed as fold-change/fold difference of treated samples relative to untreated samples using the double delta method ($2^{-\Delta\Delta\text{Cq}}$). Statistical analyses were performed using GraphPad Prism, version

8.1.2 (332) with built-in One-Way ANOVA and Dunnett's multiple comparisons tests to compare expressed genes of interest in treated samples relative to the untreated. Statistical significance was rated at $p < 0.05$; where * = $p < 0.05$ and ns = not significant.); three independent experiments (n=3) were performed in triplicate. 170

Table 7-2: Relative Gene Expression of cell-cycle signalling genes (TP53, CDKN1A, and BCL2) normalized with reference gene (GAPDH) in human lymphocytes from asthma patients after 24 h treatment with different concentrations of GO (150 and 200 $\mu\text{g/mL}$) in RT-qPCR. Relative gene expression was expressed as fold-change/fold difference of treated samples relative to untreated samples using the double delta method ($2^{-\Delta\Delta Cq}$). Statistical analyses were performed using GraphPad Prism, version 8.1.2 (332) with built-in One-Way ANOVA and Dunnett's multiple comparisons tests to compare expressed genes of interest in treated samples relative to the untreated. Statistical significance was rated at $p < 0.05$; where * = $p < 0.05$ and ns = not significant.); three independent experiments (n=3) were performed in triplicate. 171

Table 7-3: Relative Gene Expression of cell-cycle signalling genes (TP53, CDKN1A, and BCL2) normalized with reference gene (GAPDH) in human lymphocytes from COPD patients after 24 h treatment with different concentrations of GO (150 and 200 $\mu\text{g/mL}$) in RT-qPCR. Relative gene expression was expressed as fold-change/fold difference of treated samples relative to untreated samples using the double delta method ($2^{-\Delta\Delta Cq}$). Statistical analyses were performed using GraphPad Prism, version 8.1.2 (332) with built-in One-Way ANOVA and Dunnett's multiple comparisons tests to compare expressed genes of interest in treated samples relative to the untreated. Statistical significance was rated at $p < 0.05$; where * = $p < 0.05$ and ns = not significant.); three independent experiments (n=3) were performed in triplicate. 172

Table 7-4: Relative Gene Expression of cell-cycle signalling genes (TP53, CDKN1A, and BCL2) normalized with reference gene (GAPDH) in human lymphocytes from lung cancer patients after 24 h treatment with different concentrations of GO (150 and 200 $\mu\text{g/mL}$) in RT-qPCR. Relative gene

expression was expressed as fold-change/fold difference of treated samples relative to untreated samples using the double delta method ($2^{-\Delta\Delta Cq}$). Statistical analyses were performed using GraphPad Prism, version 8.1.2 (332) with built-in One-Way ANOVA and Dunnett's multiple comparisons tests to compare expressed genes of interest in treated samples relative to the untreated. Statistical significance was rated at $p < 0.05$; where * = $p < 0.05$ and ns = not significant.); three independent experiments (n=3) were performed in triplicate. 173

Abbreviations

ACOS: Asthma-COPD overlap syndrome

ALS: Alkaline labile sites

ANOVA: Analysis of variance

APS: Ammonium persulfate

ATP: Adenosine triphosphate

BAL: Brocho-alveolar lavage

BiNC: Binucleated cells

BMP: Bone morphogenetic protein

BRI: Bradford Royal Infirmary

BSA: Bovine Serum Albumin

CAS: Chemical Abstracts Service

CBMN: Cytokinesis-blocked Micronucleus assay

CDKN1A: Cyclin-dependent kinase inhibitor

cDNA: Complementary DNA

COPD: Chronic obstructive pulmonary disease

CPI: Consumer Products Inventory

CPMAA: Cysteine polymethacrylic acid

Cq: Quantitative cycle

Cyto-B: Cytochalasin-B

Dex: Dexamethasone

DFM: Dynamic force microscope

DLS: Dynamic Light Scattering

DMSO: Dimethyl sulfoxide

DNA: Deoxyribonucleic acid

DFW: DNase Free Water

dNTP: Deoxyribonucleotide triphosphate

DOX: Doxorubicin

D/RFW: DNase/ RNase Free water

DSB: Double-strand breaks

ECL: Enhanced chemiluminescence

EDTA: Ethylenediaminetetraacetic acid

ENMs: Engineered nanomaterials

ENPs: Engineered nanoparticles

EtBr: Ethidium bromide

FBS: Fetal Bovine Serum

GAPDH: Glyceraldehyde 3-phosphate dehydrogenase

GO: Graphene Oxide

GOFNMs: Graphene oxide family nanomaterials

GOI: Gene of interest

G-phase: Growth phase

GSH: Glutathione

HRP: Horseradish peroxidase enzyme

IARC: International Agency for Research on Cancer

ISO: International Organization for Standardization

IRAS: Integrated Research Application System

i.v.: Intravenous

kDa: Kilodalton

kV: Kilovolt

LABA: Long-acting beta-2 agonists

LH: Lithium Heparin

LMP: Low Melting Point

mA: Milliamp

MAPK: Mitogen-activated protein kinase

MN: Micronucleus

MNi: Micronuclei

MMC: Mitomycin-C

Mono NC: Mononucleated cells

M-phase: Mitotic phase

mRNA: Micro RNA

mV: Millivolts

MTT: Methylthiazolyldiphenyl-tetrazolium bromide

MultiNC: Multinucleated cells

MWCNTs: Multi-walled carbon nanotubes

NBUDs: Nuclear buds

NC: Negative control

NCBI: National Centre for Biotechnology Information

NDI: Nuclear division index

NFDM: Non-fat dry milk

NFW: Nuclease Free Water

NGS: Nano-graphene sheets

NHS: National Health Service

NMP: Normal melting point

NMs: Nanomaterials

NP: Nonyl phenoxy polyethoxylethanol

NPBs: Nucleoplasmic bridges

NPs: Nanoparticles

NRU: Neutral Red Uptake

OTM: Olive tail moment

PAGE: Polyacrylamide Gel Electrophoresis

PBL: Peripheral blood lymphocytes

PBS: Phosphate buffered saline

PC: Positive Control

PCR: Polymerase Chain reaction

PDI: Polydispersity Index

PEG: Polyethylene Glycol

PEI: Polyethyleneimine

PEI-GO: Polyethyleneimine Graphene Oxide

PEN: Project on Emerging Nanotechnologies

Pen-Strep: Penicillin-Streptomycin

PHA: Phytohaemagglutinin

PMAA: Polymethacrylic acid

PVDF: Polyvinylidene difluoride

REC: Research Ethics Committee

rGO: Reduced GO

RIPA: Radioimmunoprecipitation assay

RNA: Ribonucleic acid

RFW: RNase Free Water

ROS: Reactive oxygen species

RPMI: Roswell Park Memorial Institute

RT: Room temperature

RT-qPCR: Reverse Transcription quantitative polymerase chain reaction

SABA: Short-acting beta-2 agonists

SCA: Structural Chromosome aberrations

SCGE: Single-cell gel electrophoresis

SDS: Sodium dodecyl sulphate

SEM: Scanning Electron Microscope

S.E.M: Standard Error of the Mean

SP: Substance P

S-phase: Synthesis phase

SSB: Single-strand breaks (SSB)

TBST: Tris-buffered saline-Tween 20

TEM: Transmission Electron Microscope

TEMED: Tetramethylethylenediamine

TfR: Transferrin receptors

Ti: Titanium

Ti-GO: Titanium-Graphene oxide

UPR: Unfolded protein responses

WB: Western Blot

WHO: World Health Organization

ZP: Zeta potential

2-D: 2-dimensional

3-D: 3-dimensional

5FU: 5-Fluorouracil

Chapter 1: General Introduction

1.0 Introduction

Presently, chronic pulmonary diseases such as lung cancer, asthma, and chronic obstructive pulmonary diseases (COPD) are amongst the deadly diseases and global health issues. For cancer, the treatment type is dependent on its location, the size, extent of metastasis, and the general wellbeing of the patient. The most common treatment options for stage 3 lung cancer are a combination of surgery, chemotherapy, high dose of radiotherapy, and gene therapy (Cancer Research UK 2017; American Cancer Society 2018; Dana-Farber Cancer Institute 2018). Among all four options, chemotherapy is the most common treatment and has been used for different kinds of cancers. However, chemotherapy has its own limitations, including drug resistance, low therapeutic efficiency, low cellular uptake efficiency, and side effects (Fisher et al. 2012; MacMillan Cancer Support 2012). Among chemotherapy drugs, 5-Fluorouracil (also known as **5FU**) and **cisplatin** family drugs are the most commonly used anti-cancer agents (Cancer Research UK 2016). Although, 5FU is among the oldest anti-cancer agents, it is still very useful in the treatment of solid tumours (e.g. breast cancer, colon, head, and neck cancers, etc). It belongs to the pyrimidine family of anti-metabolites. They resemble small molecules in the body and therefore, inhibit the activities of cancer cells by interfering with their metabolic activities. To achieve the required therapeutic level with 5FU, high doses of 400-600 mg/m² are administered per week using a small pump which the patient carries around for many days (Kamm et al. 2003). A number of side effects have been reported (He et al. 2003). On the other hand, Cisplatin, a well-known anticancer agent, is used for the treatment of various types of cancers including lung cancer, head and neck, testicular cancers, etc (Dasari and Bernard Tchounwou 2014; MacMillan Cancer Support

2018). Ototoxicity and nephrotoxicity are common side effects. Similarly, to achieve the required therapeutic level in the blood, high doses of cisplatin (50-100 mg/m² IV) are required (Medscape 2019).

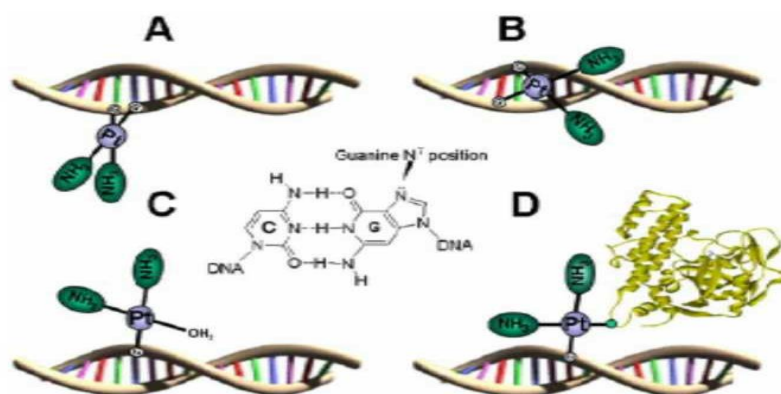


Figure 1.1: Cisplatin-DNA cross-linking adducts: (A) 1,2-intrastrand cross-link, (B) Interstrand cross-links, (C) Mono-functional adduct, and (D) protein-DNA cross-link. The main site of attack of Cisplatin to DNA is on the N7 of Guanine (Fahmy 2014)

As shown in **Figure 1.1**, Cisplatin functions by cross-linking with the purine base of the DNA of cancer cells leading to DNA damage, especially DNA double strand breaks (DSB), disturbance of the DNA repair system and ultimately causing apoptosis (programmed cells deaths) in cancer cells (Dasari and Bernard Tchounwou 2014). It also inflicts injury to healthy, normal somatic cells and induce germ cell loss in *in vitro* cell experiments (Netdoctor 2012; Smart et al. 2018). Globally, research is ongoing to finding alternative treatments and drug delivery carriers to deliver anti-cancer drugs directly to tumour cells with minimal damage to healthy cells, hence the emergence of GO NMs. Following the discovery of Graphene, GO and other graphene oxide family nanomaterials (GOFNMs) have emerged into the world of nanotechnology. The emergence has

redefined and transformed scientists' perception of nanomaterials due to their unique properties relevant to biomedical applications. Currently, the paradigm of GO FNMs applications has shifted dramatically from the field of engineering (such as Graphene semi-conductor chips, GO conductive film/ electrodes; solar energy, Graphene Computer Memory, etc) (ACS Material 2019), to the field of biomedical sciences such as tissue engineering, imaging techniques, photodynamic therapies, drug delivery of anti-cancer drugs (e.g. GO-Dox) , and in gene therapy (Zhou and Liang 2014). Nanomaterials could be structurally modified with various chemical components of interest, allowing conjugation with ligands, genes or drugs to specifically target certain parts of the body such as tumour sites, with less damage to healthy tissues or organs (Handy and Shaw 2007).

1.1 Nanoparticles and Nanomaterials

According to the World Health Organization (WHO), **nanoparticles** (NPs) are particles of any material with **at least one** dimension < 100 nm in the nano-sized form either in the length, width/diameter, or thickness (WHO 2017). The International Organization for Standardization (ISO) defines **nanomaterials** (NMs) as any material (i.e. nanostructured material – either internal or surface structure) or object (i.e. nano-object) which has either **one, two or three** external dimensions in the nanoscale (1 nm = 10^{-9} m) (Hatto 2011). Thus, engineered nanomaterials (ENMs) possess extremely high surface area-to-volume ratio and have been structurally and commercially produced on a large scale to exhibit specific properties. NPs have size range of 1-100 nm in every dimension. However, at the industrial level, NMs are any material having particle size up to 1,000 nm in at least one dimension (Jeevanandam et al. 2018). Although they

are > 100 nm in size, GO with thickness up to 1,000 nm is regarded as a nanomaterial since it exhibits the same unique properties similar to NPs (Omlor et al. 2015).

1.2 Nanotechnology

Nanotechnology is the engineering process of the manufacture and subsequent applications of NMs at the nanoscale. Structural manipulation of NPs enables surface modification and attachment of different functional groups (e.g. OH⁻, antibodies, etc), thereby opening the way for a wide range of applications in biomedicine and biotechnology (Mody et al. 2010). In the last few decades, nanotechnology had advanced leading to the production of various kinds of novel applications in many industries. In recent years, applied nanotechnology market has grown at the rate of 12.1%, and it is estimated to reach \$196.02 billion (US Dollar) by the year 2020 (Radiant Insights 2014).

In 2004, two US companies - the Project on Emerging Nanotechnologies (PEN) and the Woodrow Wilson International Centre for Scholars – collaborated and produced a Nanotechnology Inventory, initially in a PDF format, now called the Nanotechnology Consumer Products Inventory (CPI) (The Project on Emerging Nanotechnologies 2019). The aim was to have on record, the number and details of nanoparticle-based products that were evolving, and which had made it to the commercial market. Since then, a high record number of nanomaterial-based products recorded had increased from 54 products in 2005 to 1,814 by the end of March 2015 (Vance et al. 2015). If the trend continues in

this way, it was estimated that by 2020, the number of nanomaterial-based products could reach 3,400 (The Project on Emerging Nanotechnologies 2019).

As new applications of nanotechnology are emerging and industries continuously seeking more avenues to produce more variants, engineered nanoparticles (ENPs) could also become emerging pollutants and a threat to human life (Lei et al. 2015). Nanomaterials acquire unique properties due to their altered physicochemical properties such as their small particle size and large surface area to volume ratio (Osman et al. 2010). Bulky materials possess constant physicochemical properties regardless of their dimensions. However, as their bulk sizes decrease to the nanoscale level, they exhibit diverse and unique properties. Previous studies have shown that the same unique properties of NPs could ironically be responsible for their toxicity potential (Tang et al. 2015). Their extremely small particle size and high surface reactivity have led to increased concerns on their safety in humans as in both acute and long-term exposures might lead to inflammation of the respiratory lungs, oxidative stress, genotoxicity, and pulmonary diseases (Lu et al. 2014).

1.3 Graphene Oxide Nanomaterials

GO NMs are carbonaceous single-layer sheet of graphite oxide (See **Figure 1.2**). We have chosen these NMs because of their unique physical and chemical properties such as high surface area -to-volume ratio; 2-dimensional (2-D) surface planar; surface chemistry: 4-10% edge-oxidization; and heavily unbound, surface functional groups such as hydroxy - OH, carboxyl /ketone C=O,

epoxy/alkoxy C-O, and aromatic C=C groups (Wang et al. 2011b; Mohamadi and Hamidi 2017). Their unique surface chemistry enables covalent bonding with biocompatible polymers such as Chitosan, Polyethylene Glycol (PEG) (Wu et al. 2015), and organic molecules (e.g. proteins, RNA, DNA, and drugs) making GO excellent nanocarriers in drug delivery (Rebuttini et al. 2015). It is their biomedical applications which made GO more popular than other nanomaterials. Chemically, GO is made up of carbon, oxygen, and hydrogen, with a chemical formula and structure shown in **Figure 1.2** below.

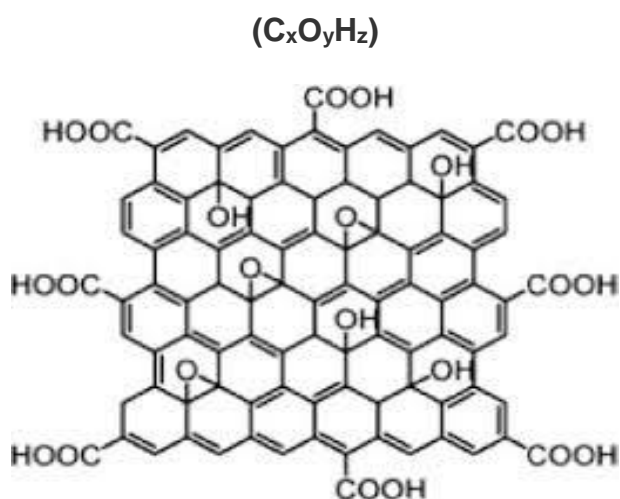


Figure 1.2: Structure of Graphene Oxide

Because of this composition, GO can easily be chemically reduced by removing oxygen and hydroxyl (OH) components to form a thin film derivative known as reduced GO (rGO). Unlike GO with good dispersibility and stability in aqueous solution, rGO with fewer OH intercalation (see **Figure 1.3, page 8**) is less soluble, less stable, and has low electrical conductivity compared to ordinary GO (Konios et al. 2014; Zhou and Liang 2014). In addition to the above qualities, GO and rGO are the only forms of graphene family NMs that could be produced commercially on a large scale (Sur 2012).

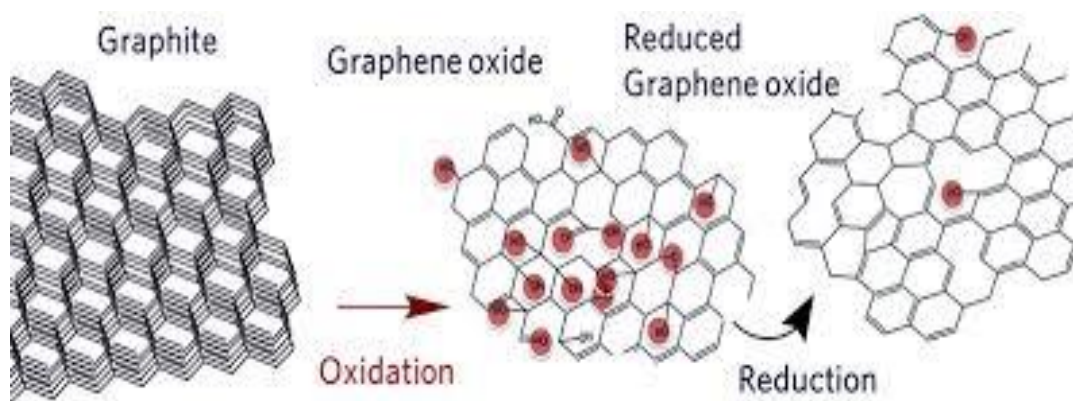


Figure 1.3: Synthetic routes of Graphene Oxide and reduced Graphene Oxide, using graphite as a starting material (Sur 2012).

One of the striking features of GO, as shown in **Figure 1.3**, is the insertion of molecules of water (H, O, and OH) into the atomic structure during the oxidation process, thereby causing an increase in interplanar spacing and disruption of sp² binding network (Zhu et al. 2010; De La Fuente 2013). However, despite the good surface chemistry, GO NMs cannot be used independently on their own as nanocarriers due to their tendency to agglomerate in physiological solutions (Tang et al. 2017). To reduce this limitation, surfactants, polymers, and proteins are being incorporated as dispersants in drug delivery formulations (Ma et al. 2017). However, these dispersants do not prevent severe side effects associated with anti-cancer drugs, such as DOX (Zhang et al. 2017).

1.4 Applications of Graphene Oxide in Biomedical Sciences

GO NMs have several applications in nanomedicine including drug delivery, gene therapy, tissue engineering, nanomedical devices, etc (see **Figure 1.4**).

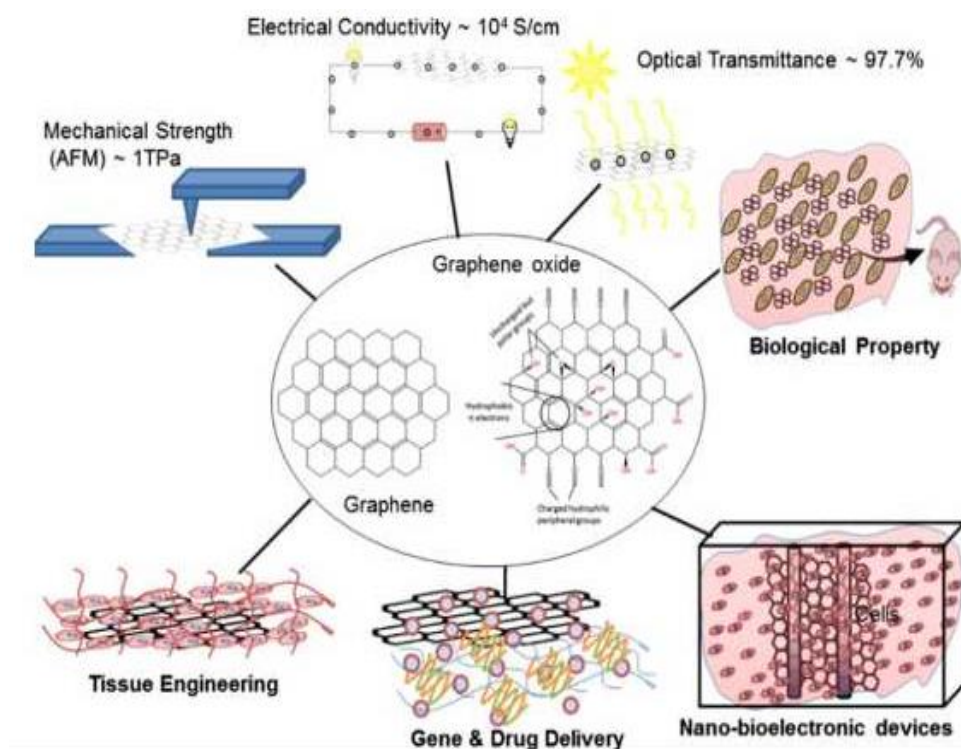


Figure 1.4: Schematic diagram showing different biomedical applications of Graphene and GO, including gene and drug delivery, tissue engineering, etc (Dasari Shareena et al. 2018).

1.4.1 Drug delivery

The popularity of GO NMs has increased significantly due to their application as a drug delivery platform for the treatment of several chronic diseases. The properties which make GO unique compared to other nanomaterials are the surface chemistry, two-dimensional planar structure, and high surface area of 2,600 m²/g (Liu et al. 2013a; Wu et al. 2015). They have also been used to deliver different therapeutic agents including proteins, small drug molecules, antibodies, and DNA (Parveen et al. 2012). The large specific surface area of a single layer of nano-graphene sheets (NGS) (See **Figure 1.5**) allows significant number of drugs to be loaded into its structure (Sun et al. 2008). Research using xenograft

tumour mouse models show that NGS have a high uptake into tumour cells (Yang et al. 2010).

A number of factors have been identified to influence the effectiveness of GO-based drug delivery systems, including the structural design, drug loading capacity, biocompatibility in blood, and the efficiency of drug release at the right tumour site (Wang et al. 2011a; Liu et al. 2013a). To improve the specificity of nanocarriers, the surface is conjugated with ligands such as transferrin receptors (TfR) (Daniels et al. 2006); folic acid (Nasongkla et al. 2004); and polyclonal antibodies specific to certain tumour cells (Dinauer et al. 2005).

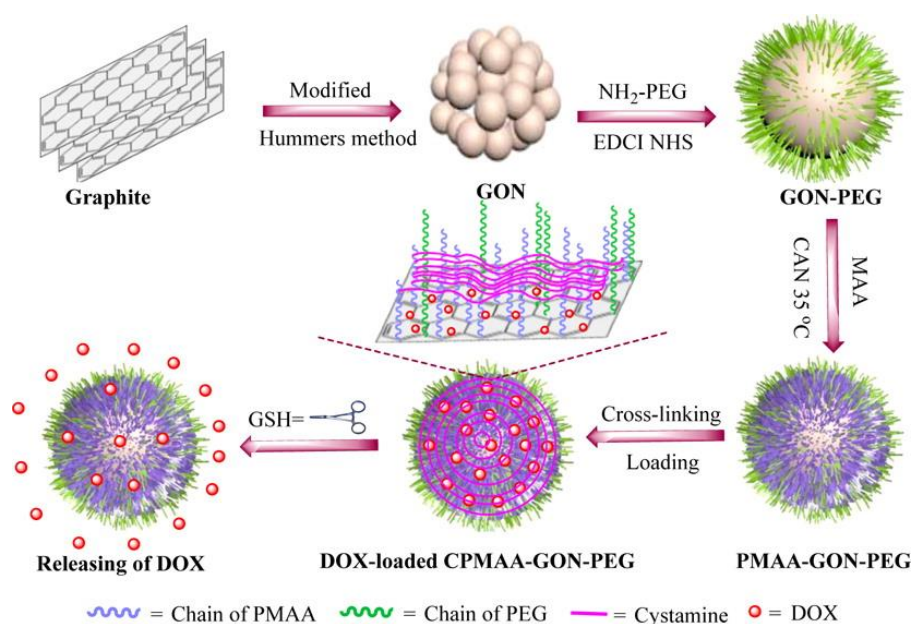


Figure 1.5: A schematic drawing showing the synthesis of GO, a model structural change (GON-PEG), Dox loading /cross-linking, and reduction-triggered release of the CPMAA cross-linked nano GO polyethylene glycol barriers.

Abbreviations: GON = GO nanoparticles; PEG = polyethylene glycol; GSH = glutathione; DOX = doxorubicin; CPMAA = cysteine polymethacrylic acid; PMAA = polymethacrylic acid (Zhao et al. 2015).

Functionalisation of GO with PEG (PEG-GO) also known as PEGylation increases the solubility of insoluble drugs and oily aromatic compounds in the serum and aqueous solutions (Liu et al. 2008; Yang et al. 2010).

1.4.2 Gene therapy

Gene therapy is an innovative and hopeful method for the treatment of various genetic diseases such as cystic fibrosis, cancer, etc (Yang et al. 2007; Ziello et al. 2010; Williams 2014). It involves the use of both viral vectors (e.g. adenoviruses, retroviruses, etc) and non-viral vectors (e.g. liposomes) to accurately deliver the genes of interest to the target sites from where they are taken up by endocytosis and then released (Foldvari et al. 2016). To achieve success in gene therapy formulation, the gene vector must protect the DNA from nuclease enzyme damage and enable efficient cellular uptake of the DNA, and increase gene transfection efficiency (Naldini et al. 1996; Li et al. 2017). Gene vector efficiency and safety are some of the problems facing the gene therapy industry (Mintzer and Simanek 2009). Previous studies showed that GO grafted with polyethyleneimine (PEI) using electrostatic interactions resulted in significant reduction in cytotoxicity and increased transfection efficiency of plasmid DNA compared to unbound polymer, making PEI-GO a good conjugate in gene delivery (Chen et al. 2011; Feng et al. 2011).

1.4.3 Tissue engineering

GO is widely applied in tissue engineering for the delivery of specific proteins, such as substance P (SP) factors which are responsible for the induction of stem-cell factor in the bone marrow, bone morphogenetic proteins (BMP) -2 and -7,

and growth factors for bone healing and regeneration (Rameshwar and Gascon 1995; Bishop and Einhorn 2007; Gautschi et al. 2007). BMP-2 and -7 have been approved for clinical application in open fractures of long bones, spinal fusion, etc (Haubruck et al. 2016). Administration of high dose of BMP-2 results in severe side effects such as inflammation and unrestrained bone development. However, a study by La et al. (La et al. 2014) showed that when the surface of Titanium (Ti) implant was coated with GO, and the resulting Titanium-Graphene Oxide (Ti-GO) implant filled with various BMPs and SPs, the results showed the highest bone formation evidenced by the highest level of alkaline phosphatase activity in bone-forming cells compared with implants without GO (La et al. 2014). Alkaline phosphatase activity, a biomarker of bone formation, is vital for bone mineralization (Dimai et al. 1998).

1.5 Pathogenesis of nanoparticles-induced pulmonary diseases

The pulmonary system is the primary route through which nanomaterials enter the body, making the lungs the most target risk area of nanomaterial exposure and accumulation. After inhalation in the aerosol form, these tiny, ultrafine particles (1-100 nm) migrate from the trachea into the bronchi, and then easily deposited on the alveoli. Due to their small particulate sizes, they permeate the alveoli tissues and eventually cross the alveoli-blood barrier. From there, they can pass into our blood system and finally end up being deposited in our tissues and organs (e.g. liver, spleen, etc). Since some NPs have half-lives ($t_{1/2}$) of approximately 700 days in human lungs, they could pose occupational health risk to factory workers in nanotechnology manufacturing sectors (Bahadar et al. 2016). It has been reported that long-term exposure to NPs could be linked to

serious damage to human lungs, and may interact with macromolecules such as DNA leading to a host of pulmonary diseases such as pulmonary fibrosis, lung cancer, etc (Rim et al. 2013). Researchers have found that NPs < 10 nm have aerodynamic sizes and behave like gas (Sanchez et al. 2012), and thus when inhaled they can diffuse in and out of the alveoli with ease or be deposited on the lungs and alter the lung's normal physiological functions (Bahadar et al. 2016). Despite the high-profile commercial interests garnered by GO NMs, few studies were reported on their genotoxicity on human DNA, but none was reported on their toxicity on blood samples and BPL from patients with chronic pulmonary diseases.

1.5.1 Nanoparticle deposition and clearance in human lungs

Inhaled NPs can induce acute or chronic lung injury which may ultimately lead to some form of lung diseases such as asthma, COPD, emphysema, and even lung cancer. The extent of NPs-induced lung damage is dependent on the NPs achieving a critical lung burden (Lu et al. 2014). The lung burden is controlled by the rate determining steps of particle-deposition versus particle clearance, provided the solid NPs do not obstruct NPs clearance mechanisms. The bioavailability and genotoxicity of nanoscale ultrafine particulate matters are dependent not only on their chemical properties (e.g. chemical composition), but mainly also on their physical properties such as size, shape, crystallinity, and surface reactivity. Depending on their size, they can migrate into the alveoli (Li and Chen 2011), and then cross over through the thin alveolar-blood barrier into the blood circulation, and into the regional lymph nodes (Oberdörster et al. 1994; Sager et al. 2008). There is a body of evidence that showed that when NPs reach

the alveoli, the lung reacts to clear the NPs through macrophage phagocytosis (Lu et al. 2014). Carbonaceous NMs such as multiwalled carbon nanotubes (MWCNTs) have physical resemblances with asbestos fibres (Sanchez et al. 2009). Long-term exposure to asbestos fibres, usually over many years, has been reported to cause asbestosis. Asbestosis is a chronic inflammation and scarring of the lungs characterised by cough, shortness of breath, wheezing, and dyspnoea. Complications may include granulomas, lung cancer, mesothelioma, pulmonary heart disease, etc like those observed in animals and humans exposed to asbestos (Lu et al. 2014). Since MWCNTs are members of GOFNMs with similar chemical structural relationships, the carcinogenic potentials of asbestos-exposure and the toxicity of GONMs are an area of research interest. Studies showed that the lower the concentration of inhaled NPs on the lungs, the lower the alveolar clearance rate, and vice-versa: the more the concentration of NPs on the lungs, the more the alveolar clearance rates, and the potential for increased retention half-life (Sanchez et al. 2009).

1.5.2 Inflammation of the lungs

Inhaled NPs are foreign bodies which trigger pro-inflammation cytokines leading to acute or chronic inflammatory responses (Ge et al. 2011; Kim et al. 2012b). Studies by MacNee (2005) showed that tests with bronchial biopsies as well as induced sputum had confirmed the presence of lung inflammation in people who smoked cigarettes compared to non-smokers (MacNee 2005; Tudor and Petrache 2012). Abnormal responses to inhaled NPs outside the normal protective inflammatory responses are characteristic features of COPD (Vijayan 2013). The presence of inflammatory cells in the lungs of mice has also been

investigated. In a study by Lu et al. (2014), six mice were administered with 50 µg of aqueous solution of GO straight into the lungs for 24 h. Thereafter, they observed the formation of hyaline membrane and severe acute lung inflammation on the alveolar exudates. Further observation after a 21-day exposure, showed lung inflammation, protein leaking into the alveolar space, broncho-alveolar lavage (BAL) fluid, and increased level of pro-inflammatory cytokines in the BAL (Lu et al. 2014). There is also a close association between inflammatory response and oxidative stress through pro-inflammatory gene transcription (Li et al. 2013a). It has been shown that NPs induce the pro-inflammatory pathway - the mitogen-activated protein (MAP) kinases – responsible for oxidative stress (Lu et al. 2014).

1.5.3 Oxidative Stress and Reactive Oxygen Species

Adenosine triphosphate (ATP) is produced in the mitochondria (the Powerhouse of the cells) and produces energy through a series of coupled proton-electron transfer processes where molecular oxygen is reduced to water (H₂O) (Lodish et al. 2000). During this process, some of the oxygen is not reduced completely, leading to the formation of highly reactive free radicals called reactive oxygen species (ROS) such as peroxides, superoxide anion radicals, hydroxyl radicals (OH[•]), singlet oxygen and other oxygen-containing radicals. Therefore, ROS are the by-products or derivatives of cellular oxidative metabolism, the majority of which take place inside in the mitochondria (Li et al. 2013c).

Our lungs are constantly generating ROS during normal respiratory activities such as gaseous exchange in a Redox-reaction process. Nanomaterials such as GO with abundant source of oxygen radicals [O[•]], could induce pulmonary

disease through induction of ROS in the mitochondrial (Fu et al. 2014). Excessive production of ROS has been inherently associated with many cancers (Ježek et al. 2018). Oxidative stress occurs in a number of ways: (1) when there is an imbalance between the amount of ROS generated and the amount removed during normal physiological activities; that is when the body is unable to remove excess ROS; (2) when the body is unable to repair any damage caused by the presence of ROS generated either directly inside the cell or within cellular vicinity, or indirectly by affecting mitochondrial respiration, and (3) depletion of anti-oxidant species within the cell (Xia et al. 2008; Lu et al. 2014). The extent of damage caused by oxidative stress and ROS over a long period of time could be among the leading causes of life-threatening conditions such as Alzheimer's, Parkinson's disease, diabetes, etc (Fu et al. 2014).

1.5.4 Genotoxicity of Nanomaterials

Nanomaterials could damage the integrity of the genome, either directly (primary DNA damage mechanism) or indirectly (secondary DNA damage mechanism). Primary DNA damage occurs when nanomaterials bind directly to the DNA and damage the superficial network and integrity of the DNA. On the other hand, indirect DNA damage occurs when nanomaterials bind to the cell component of cell division apparatus, causing oxidative/cellular stress which give rise to free radicals (ROS) and destroy the centromeres or the spindle of the microtubule.

When GO is administered intratracheally, it interacts with the cell membrane and is subsequently transferred into the cytoplasm and the nucleus through endocytosis (Liu et al. 2016). Long-term exposure to the lungs exposes the DNA

to a constant cycle of damage-and-repair mechanisms. It is the irreparable, permanent damage that progressively leads to mutagenesis (Liu et al. 2013c).

1.6 Diseases of the Pulmonary System

Asthma, COPD and lung cancer are among the most frequently diagnosed respiratory diseases in the UK (Denholm et al. 2017). Statistics from the British Lung Foundation show that in 2012, approximately, 12.7 million people in the UK had a history of asthma, COPD or another form of long-term respiratory health disease (British Lung Foundation 2017). Figures obtained from the General Practice (GP) records across the country also suggested that over 8 million people were diagnosed with asthma, 1.2 million with COPD and 86,000 people with lung cancer (British Lung Foundation 2017). In terms of death ratio of the same year (by cause, all ages (> 28 days)), records showed that 1,246 people died of asthma, 29,776 died of COPD and a record number of 35,419 died of lung cancer (British Lung Foundation 2017). The above statistics showed that lung cancer was the highest cause of death (6.2 %) followed by COPD (5.3%).

The incidence of cancer presents a huge challenge to the individual patient in a number of ways such as psychological impacts, personality traits, social behaviours, disease coping styles, distress and depressive signs (Anderson et al. 2014; Shimizu et al. 2015), but also comes with enormous economic burden to the society. According to reports published by the Health Economics Research Centre, University of Oxford, lung cancer costs the UK National Health Service (NHS) over \$2.4 billion per year compared with other forms of cancer, including

bowel cancer (£1.6bn), breast cancer (£1.5bn), and prostate cancer (£0.8bn). Early diagnosis and treatment can potentially prolong death and simultaneously reduces the costs associated with lung cancer (Anderson et al. 2014).

1.6.1 Asthma

Allergic asthma is a chronic inflammatory disease of the airway linked with hyper-responsiveness and ultra-structural changes of the respiratory tract leading to airway remodelling (Bousquet et al. 2007). Some patients with asthma have a history of rhinitis and dyspnoea on exertion. Damage to the lungs is not completely reversed by existing therapeutic methods such as inhaled steroid preventers. Inhaled corticosteroids are the main treatment of choice to control asthma, their pharmacological impacts on the lungs are relatively longer, usually given twice each day (Lu et al. 2014). Also, their use is limited due to their systemic side effects such as suppression of adrenocorticoids, Cushing's syndrome / hypercortisolism e.g. fat deposition on the face leading to round face, high blood pressure, thinning of the skin, reddish-purple stretch marks, libido), myasthenia gravis (muscle weakness), and osteoporosis (bone weakness) (Dahl 2006; Lefebvre et al. 2015). Despite the several treatment options available such as short-acting Beta-2 agonists (SABA), e.g. salbutamol (Ventolin® Evohaler), long-acting Beta-2 Agonists (LABA), and the standardised international guidelines for managing asthma, yet a huge number of patients suffering from asthma have poor control of the disease. There is an urgent need to find a better treatment option for asthma; researchers are looking elsewhere to find an alternative, or a novel therapy that could tackle asthma once and for all, especially

for those suffering from severe asthma attacks. This is where nanoparticles could play a role.

In 2013, a study by Kenyon, et al. demonstrated that nanoparticles could become the future alternative to current treatment options. Using asthmatic mice, dexamethasone (Dex), a steroid drug, was encapsulated with self-assembling nanoparticles forming Dex-NPs complex. This complex was systemically administered directly targeting the lungs, which to a greater extent resulted in a drastic decrease in allergic inflammatory conditions and hypersensitivity compared to the same dose of Dex administered alone (Kenyon et al. 2013). However, this has not been tested in humans, and as such, more caution is required as the genotoxicity of the Dex-NPs complex has not been assessed.

1.6.2 Chronic Obstructive Pulmonary Disease

Chronic obstructive pulmonary disease (COPD) is a medical condition of the pulmonary system characterised by inflammatory conditions of the airways leading to constriction of the airway muscles and damages to the air sacs in the lungs. It is caused by a multi-dimensional factor. Injury to the lungs could lead to a number of diseases, but involves a number of stages such as the **initiation stage** – during exposure to genotoxic agents such as cigarette smoke, air pollutants, infectious agents, and nanoparticles, **progression stage** and finally, **the consolidation stage** (Tuder and Petrache 2012).

Although some COPD symptoms such as wheezing (especially when breathing out), shortness of breath, coughing, and chest tightness can overlap with those

of asthma symptoms, leading to asthma-COPD overlap syndrome (ACOS) (see **Figure 1.6**), there are many distinguishing differences between the two (Global Initiative For Asthma 2014).

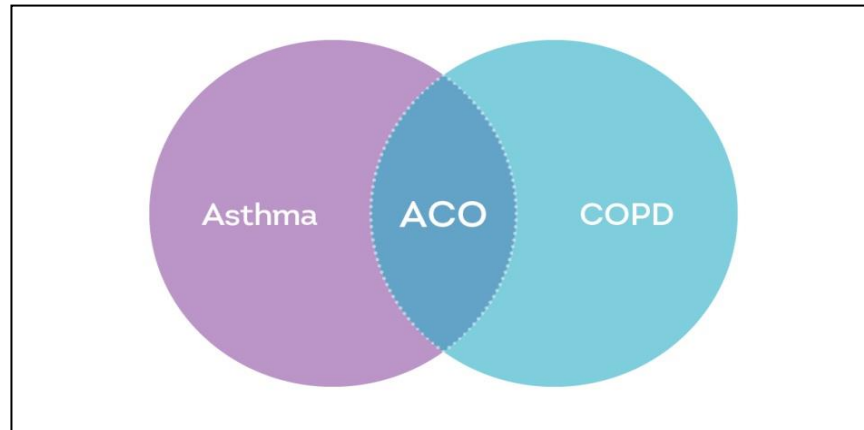


Figure 1.6: Relationship between asthma and COPD.

The intersection – the asthma-COPD Overlap Syndrome (ACOS) - sometimes makes it difficult for doctors to work out which medications to prescribe for patients suffering from either of the two diseases (Asthma UK 2016).

In COPD, there is more mucus or phlegm production than normal, and tends to occur at the age of ≥ 40 years old with persistent symptoms (Asthma UK 2016). Cigarette smoking is the major cause of COPD. However, it can also be caused by long-term exposure to environmental or workplace toxic particles (including nanoparticles), air pollution, dust, fumes, or gases. Some people who do not smoke can also suffer from COPD due to poorly controlled long-term asthma.

1.6.3 Lung Cancer

Lung cancer is the 3rd most common cancer in the UK, with over 46,388 new cases diagnosed in 2015 and 35,620 deaths in 2016 (Cancer Research UK 2015). Cigarette smoking is the major single cause of lung cancer in the UK,

accounting to 72%, while 79% of all lung cancer incidences are preventable. The most common method of treatment is chemotherapy and it is usually commenced after the visible cancer had been surgically removed, but severe side effects limit its usage. However, to overcome the side effects associated with chemotherapy, GO NMs are being proposed as drug delivery carrier-conjugates to efficiently target and deliver anti-cancer drugs to tumour cells with little damage to healthy tissues (Vinardell and Mitjans 2015).

Previous studies have established a close relationship between lung cancer, COPD, and asthma (Denholm et al. 2017). Inhaled NPs have been shown to be effective *in vivo* in the treatment of mouse-induced lung cancer. In this study, mice-induced lung cancer were treated with inhalable NPs powder in the solid state incorporated with 30 µg of Dox; one treated through the nasal route and the other with intravenous (i.v.) administration. The results demonstrated a higher recovery rate in the nasal route compared to the i.v. route (Roa et al. 2011; Lu et al. 2014; Muralidharan et al. 2015).

1.7 Methods used for assessment of Genotoxicity (DNA Damage), chromosome instability, and gene and protein expressions in human whole blood and peripheral blood lymphocytes

1.7.1 Genotoxicity assay

1.7.1.1 Comet assay

The Comet assay, also known as the single-cell gel electrophoresis (SCGE), is a valuable assay routinely used to detect and quantify DNA damage and repair of

individual eukaryotic cells (Andem et al. 2013). The Comet assay has gained tremendous popularity in biomedical sciences because it is a simple, rapid, and sensitive tool capable of assessing DNA damage in normal cells in the absence of cytotoxicity and also in necrotic and apoptotic cells (Gunasekarana et al. 2015). Because of its versatility, it has been widely modified and optimised for DNA damage assessment across various models such as cell cultures, bacteria, yeast cells, sperm, human whole blood, solid tumours reduced to single cells, etc (Nandhakumar et al. 2011). Single-cell (Comet) assay has been widely applied in medicine in the field of genotoxicity experiments – for determination of DNA damage; human biomonitoring – to assess the route of entry into our body and their negative impact / susceptibility in our system; in drug discovery – for the selection of cancer therapeutics; and occupational exposure to genotoxic chemicals (AMS Biotechnology 2016).

Historically, the Comet assay technique was developed by Swedish scientists, Ostling & Johanson (1984) to assess the effects of gamma-irradiation on mammalian DNA under a neutral pH condition (Andem et al. 2013). Over the next 4 years, Singh et al. (1988) discovered that the neutral pH condition limited the use of the assay to assess different types of DNA damage and mainly detected DNA double-strand breaks (DSB) (Collins 2004). However, the above claim was criticised and disputed by Andem et al. (2013) because their own research showed that both DSB and single-stranded breaks (SSB) were detectable at the neutral pH condition (Andem et al. 2013). In 1990, the Alkaline Comet assay version was further modified and optimised by introducing electrophoresis under alkaline pH condition (pH >13) (Olive et al. 1990; Tice et al. 2000).

1.7.2 Cytogenetic assay

1.7.2.1 Cytokinesis Blocked Micronucleus (CBMN) Assay

The Cytokinesis-Blocked Micronucleus (CBMN) also known as the Micronucleus (MN) Assay is the most comprehensive technique to detect and quantify DNA injury, cytotoxicity, and cytostatic events in cells (Fenech and Michael 2007).

DNA damage or injury is scored specifically at the binucleated (BN) stage of cell division and comprises three components: Micronuclei (MNI) – biomarkers of chromosomal breakage and/or the loss of an entire chromosome; Nucleoplasmic bridges (NPBs) - biomarkers of DNA disrepair/telomere end-fusions; and Nuclear buds (NBUDs) – biomarkers of amplified DNA exclusion and/or DNA repair complexes. **Cytotoxicity** is measured through necrotic and/or apoptotic cell ratios while **cytostatic events** (inhibition of cell growth) are measured according to the proportions of mono-, bi- and multinucleated cells.

The CBMN assay can detect and measure changes in both the structure and the number of chromosomes of dividing cells. In cells undergoing cell division, cells that contain DSB divide to form two daughter cells. Some of the whole chromosomes or chromosome fragments lag at the anaphase stage or are simply unable to migrate effectively to the spindle throughout cellular mitosis and subsequently wrapped together, leading to the formation of MNI.

Scoring of MNI is carried out especially in cells which have completed nuclear division. Blockage of cytokinesis with Cytochalasin-B (Cyto-B) results in the accumulation of MonoNC, BiNC, MultiNC. Cyto-B is an alkaloid and a well-known mycotoxin. It binds strongly/irreversibly to the actin – the rigid, skeletal framework

of the cell - and restricts microfilament ring formation which holds two daughter nuclei together during cytokinesis (the separation of materials among daughter cells). These nuclear materials are then specifically scored per 1,000 cells (i.e. 500 cells per slide per concentration) using an optical microscope. **The Nuclear division index (NDI)** – an indicator of cytostatic events and a biomarker of cell proliferation and mitogenic response - is then calculated using the values of the MonoNC, BiNC, and MultiNC. Studies elsewhere show that the NDI could be used as a biomarker in the screening of colorectal cancer patients for adenomas and carcinomas (Ionescu et al. 2011).

1.7.3 Gene Expression assay (RT-qPCR)

Reverse-transcription quantitative polymerase chain reaction (RT-qPCR) is a molecular biology technique to quantify copies of micro RNA (mRNA) (Chovancova et al. 2017). It is a popular method for gene expression analysis and has been used in clinical laboratories for disease diagnosis (e.g. prognosis of leukaemia), tissue-response profiling, and cancer phenotyping (Bernard and Wittwer 2002; Bustin and Mueller 2005). There are two types of RT-qPCR: One-step RT-qPCR and two-step RT-qPCR (Wacker and Godard 2005). Both methods follow the same method of reverse transcription of RNA into a complementary DNA (cDNA), followed by using the cDNA template for subsequent qPCR amplification. However, the main difference between the two methods is on how they were prepared. In the one-step RT-qPCR method, reverse transcription and PCR reactions take place inside the same tube, whereas in the two-Step RT-qPCR method, the two reaction steps are conducted separately: first, the synthesis of cDNA in one tube, and thereafter transferred

into the PCR reaction tube. The two-step method was the method of choice used in this PhD study because it permits all messages in the mRNA of the sample in each tube to be fully transcribed into a cDNA, and allows the user to store the samples for future use (Wacker and Godard 2005). However, both methods are time-consuming, especially during total RNA isolation procedures where it takes an average of 30 to 60 min to complete a single isolation.

1.7.4 Western Blot

Western Blot (WB) is a one of the most commonly used techniques for the detection of proteins (Mahmood and Yang 2012; ThermoFisher-Scientific 2015). It is based on the method which includes separation of proteins through gel electrophoresis according to their molecular size (kDa); protein transfer or blotting from gel to a suitable membrane (e.g. PVDF); probing with primary antibodies and detected with secondary antibodies conjugated with Horseradish Peroxidase (HRP); followed by visualisation with chemiluminescent substrates using an appropriate software, and bands quantified using the relevant software (e.g. ImageJ). Historically, WB was initially described in 1979 by H. Towbin and his colleagues as an **electrophoretic transfer of proteins** from polyacrylamide gels to nitrocellulose sheets (Towbin et al. 1979). However, two years later in 1981, the name Western Blot was coined by W. Neal Burnette (Burnette 1981).

1.8 Aim and Objectives of the Project

1.8.1 Aim

The aim of this PhD study was to evaluate *in vitro* the cytotoxicity, genotoxicity (DNA Damage), chromosome instability, and gene/ protein expressions of cell-

cycle signally genes (TP53, CDKN1A/p21, and BCL-2) on human whole blood and peripheral blood lymphocytes (PBL) from healthy individuals and patients with chronic pulmonary diseases: asthma, COPD, and lung cancer after treatment with different concentrations of commercially available, multi-walled GO NMs [GO, 15-20 sheets, 4-10% edge-oxidized; Concentration: 1 mg/mL; Dispersion in H₂O; Sigma-Aldrich, USA] to determine whether there are any differences in GO sensitivity in patients compared to healthy control individuals.

Previous studies on GO NMs were conducted mostly with 2-3 layers of GO synthesized locally in various laboratories with the potential of interlaboratory variabilities. While some of the studies demonstrated that GO induced cytotoxicity and mutagenicity on mice (Liu et al. 2013b), others reported that GO NMs were haemocompatible with serum albumin and human lymphocytes (Wang et al. 2011a; Ding et al. 2014; Kiew et al. 2016) and no obvious cytotoxicity in murine lung epithelial cells (Bengtson et al. 2016). However, none of the studies were performed with the commercial GO used in this study, and no previous studies were conducted on human whole blood and PBL from patients with chronic pulmonary diseases (asthma, COPD, and lung cancer) and results compared with healthy control individuals to determine whether there are any differences in sensitivity to the GO NMs.

In this study, five hypotheses were proposed:

1. Hypothesis 1: GO may be cytotoxic to human lymphocytes.
2. Hypothesis 2: GO may induce DNA damage in human whole blood.

3. Hypothesis 3: GO may cause cytogenetic effects and alter chromosome stability parameters.
4. Hypothesis 4: GO may affect gene expression of cell-cycle signalling genes TP53, Cyclin Dependent Kinase Inhibitor 1A (CDKN1A), and BCL-2) involved in the cascade of DNA damage.
5. Hypothesis 5: GO may affect protein expression of cell-cycle signalling proteins p53, p21, and BCL-2 in human lymphocytes.

1.8.2 Objectives

To achieve the aim, our objectives were:

First, to characterize GO NMs to understand their physicochemical properties, such as the mean hydrodynamic diameter/ particle size; shape, agglomeration state; and surface charge in aqueous dispersion and in the dry state. We would achieve this objective using the Zetasizer Nano Instrument for Dynamic Light scattering (DLS) and Zeta Potential (ZP), followed by electron microscope using the Scanning Electron Microscope (SEM) and Transmission Electron Microscope (TEM), respectively.

Secondly, to assess the cytotoxicity of GO NMs on human lymphocytes from patients (asthma, COPD, and lung cancer) and results compared with those from healthy individuals using the MTT and Neutral Red Uptake Assay (NRU) assays.

Thirdly, to establish the hydrogen peroxide (H₂O₂) concentration with the highest genotoxic insult (DNA damage), but at a non-cytotoxic concentration on human whole blood from health individuals to be used as the positive control (PC) in the Alkaline Comet assay. Thereafter, to determine the genotoxicity of different

concentrations of GO NMs (10, 20, 50, and 100 µg/mL) vis-à-vis the PC on human whole blood from patients (asthma, COPD, and lung cancer) and the results compared with those from healthy control individuals. The cytogenetic studies (chromosomal abnormalities) were conducted using the Cytokinesis-blocked Micronucleus (CBMN) assay; and

Finally, to evaluate the effects of GO NMS on the gene expression of mRNA tumour suppressor genes: TP53, CDKN1A, and apoptotic/anti-apoptotic BCL-2 relative to GAPDH reference oligonucleotides; and protein expression of p53, p21, and BCL-2 to GAPDH from patients (asthma, COPD, and lung cancer) and the results compared with those from healthy control individuals using the RT-qPCR and Western Blot techniques, respectively.

The next chapter (Chapter 2) will describe the materials and methods used to accomplish each of the above objectives.

Chapter 2: Materials and Methods

2.0 Materials and Methods

2.1 Materials

2.1.1 Chemicals

The table below contains an alphabetical list of all the chemicals and reagents used in the study, including their manufacturers and the CAS/ Catalogue number.

Table 2-1: Chemicals, manufacturers, and CAS number/Catalogue number

Chemicals, Reagents or Media	Manufacturers	CAS / Cat. Number
Acrylamide/ Bis-Acrylamide (30%)	Sigma-Aldrich, UK	1610158
Ammonium persulfate (APS)	Sigma-Aldrich, UK	7727-54-0; A3678
Anti-BCL-2 antibody	Abcam, UK	ab196495
Anti-GAPDH anti-body	Abcam	ab181602
Anti-p21 antibody (EPR362) – Rabbit monoclonal to p21	Abcam, UK	ab109520
Anti-p53 antibody	Abcam, UK	ab131442
Anti-Rabbit IgGVHH Single Domain Antibody (HRP) monoclonal	Abcam, UK	ab191866
Bromophenol Blue	Sigma-Aldrich, UK	115-39-9
Bovine Serum Albumin (BSA)	Sigma-Aldrich, UK	9048-46-8; A2153
Clarity™ Western ECL Substrate	Bio-Rad, UK	1705061
Cytochalasin B (Cyto-B), from <i>Drechslera dematioidea</i>	Sigma-Aldrich, UK	14930-96-2
Dimethyl sulfoxide (DMSO)	Sigma-Aldrich, UK	67-68-5
DPX Mountant for histology	Sigma-Aldrich, UK	06522
Ethidium bromide	Sigma-Aldrich, UK	1239-45-8
Ethylenediaminetetraacetic acid (Na ₂ EDTA)	Sigma-Aldrich, UK	10378-23-1
Fetal Bovine Serum (FBS)	Thermo Fisher Scientific™, USA	26140087
Formaldehyde solution (37%)	Sigma-Aldrich, UK	50-00-0
GenElute™ Mammalian Total RNA Miniprep Kit	Sigma-Aldrich, UK	RTN70
Giemsa's stain improved R66 solution Gurr® for microscopy	VWR, UK	350864X
Glacial Acetic acid	Sigma-Aldrich, UK	64-19-7
Glycine	Sigma-Aldrich, UK	56-40-6
Glycerol	Sigma-Aldrich, UK	56-81-5

Goat Anti-Rabbit IgG H&L (HRP)	Abcam, UK	ab205718
Graphene Oxide 15-20 sheets, 4-10% edge-oxidized, 1 mg/mL, dispersion in H ₂ O.	Sigma-Aldrich, USA	794341; PubChem Substance ID: 329768441
Halt™ Protease and Phosphatase Inhibitor Cocktail, EDTA-Free (100X)	Thermo Fisher Scientific™, UK	78441; TF267772
Hydrogen peroxide (30%w/w)	Sigma-Aldrich, UK	7722-84-1
ImProm-II™ Reverse Transcription System	Promega, USA	A3800
In vitro Toxicology Assay Kit Neutral Red Based	Sigma-Aldrich, USA	Tox-4
iQ™ SYBR® Green Supermix	Bio-Rad, UK	170-8885
Lymphoprep™	Stemcell Technologies, Canada	07851
Low Melting Point (LMP) Agarose (UltraPure™)	Invitrogen/ Thermo Fisher Scientific™, UK	16520-050
2-mercaptoethanol (B-mercaptoethanol)	Bio-Rad, UK	1610710
Methanol	Sigma-Aldrich, UK	67-56-1
Mitomycin C	Sigma-Aldrich, UK	50-07-7
MTT molecular probes (Methylthiazolyldiphenyl-tetrazolium bromide) (MW=414), 1g	Invitrogen (by Thermo Fisher Scientific™), UK	M6494; 199029
Normal melting point (NMP) agarose	Thermo Scientific™, UK	17850
Marvel Original Dry Skimmed Milk (Non-Fat Dry milk)	Premier Foods Group, UK	7888067
Oligonucleotide FH1_TP53	Sigma-Aldrich, UK	8812338657-10/0
Oligonucleotide RH1_TP53	Sigma-Aldrich, UK	8812338657-10/1
Oligonucleotide FH1_BCL2	Sigma-Aldrich, UK	8812338657-20/0
Oligonucleotide RH1_BCL2	Sigma-Aldrich, UK	8812338657-20/1
Oligonucleotide FH1_CDKN1A	Sigma-Aldrich, UK	8812338657-30/0
Oligonucleotide RH1_CDKN1A	Sigma-Aldrich, UK	8812338657-30/1
Oligonucleotide FH1_GAPDH	Sigma-Aldrich, UK	8812338657-40/0
Oligonucleotide RH1_GAPDH	Sigma-Aldrich, UK	8812338657-40/1
Penicillin-Streptomycin (Pen. Strep)	Sigma-Aldrich, UK	P4333
Phosphate buffered saline (PBS)	Sigma-Aldrich, UK	P3813

Phytohaemagglutinin (PHA), M-form	Gibco™ /Thermo Fisher Scientific, UK	10576015
Potassium chloride (KCl)	VWR, UK	7447-40-7
Precision Plus Protein™ Dual Colour Standards	Bio-Rad, UK	161-374S
Quick Start™ Bradford Protein Assay Kit 2	Bio-Rad, UK	5000202
RIPA Lysis & Extraction Buffer	Thermo Fisher Scientific™, UK	89900
RPMI Medium-1640 (x1) + GlutaMAX™	Thermo Fisher Scientific™, UK	61870-010
RPMI-1640 Medium	Sigma-Aldrich, UK	R8758
Sodium Chloride (NaCl)	Sigma-Aldrich, UK	7647-14-5
Sodium hydroxide (NaOH)	Sigma-Aldrich, UK	S5881
Sodium dodecyl sulphate (SDS)	Sigma-Aldrich, UK	151-21-3
Sodium Phosphate dibasic	VWR, UK	7558-79-4
Sodium Phosphate monobasic	VWR, UK	7558-80-7
TEMED (Tetramethylethylenediamine)	Thermo Fisher Scientific™, UK	17919
Triton X-100	Sigma-Aldrich, UK	9002-93-1
Trizma base	Sigma-Aldrich, UK	77-86-1
Tween®-20	Sigma-Aldrich, UK	9005-64-5

2.1.2 Equipment

The table below show an alphabetical list of the equipment and materials used and their manufacturers/distributors.

Table 2-2: Equipment and other materials

Equipment and other materials	Manufacturers/ distributors
Amersham™ Hybond™ Polyvinylidene difluoride (PVDF) Blotting Membrane (0.45 µM x 150 mm)	GE Healthcare Life Sciences, Germany
BioDrop™ Touch Duo Spectrophotometer	BioDrop Ltd, Cambridge, UK
BRAND® Filter Flask with lateral socket / Vacuum glass bottle	Sigma-Aldrich, UK
BRAND® Staining Trough / incubation box with tray	Sigma-Aldrich, UK
Corning® 15 mL centrifuge Tubes	Sigma-Aldrich, UK
Corning® cell culture flasks (25 cm ²)	Sigma-Aldrich, UK
Cover Glass (24 x 50 mm);	VWR, UK
Duran™ Staining Jar, Coplin Type Brand	Fisher Scientific, UK
Electrophoresis tank (H30)	Scie-Plas, UK

Eppendorf® Tubes (1mL)	Sigma-Aldrich, UK
Electrophoresis Power supply	Consort (E861), Belgium
Falcon tubes (15 mL)	BD, Swindon, UK
Fluorescent Microscope	Leica, Wetzlar, Germany
Freezer - 20°C	Sanyo, Ultra Low, Japan
Freezer - 80°C	Sanyo, Ultra Low, Japan
G:Box i Chemi XR Software	GENESys, UK
Hera Cell culture incubator (37°C and 5% CO ₂)	Leec Ltd, UK
Insulin syringe (Gauge 28 ½)	MediSupplies, UK
Ice Maker	Scotsman, UK
Kinetic Imaging CCD Camera	Andor® Technologies, UK
Kinetic Imaging Statistic Software	Andor Bioimaging (formerly Kinetic Imaging), UK
Komet® 6 Software	Andor® Technologies, UK
Magnetic stirrer	Stuart Scientific, Essex, UK
Micropipettes (Pipetman®) 10-100 µL + 200-1,000 µL	Gilson, UK
Micropipette tips (2-200µL) + 200 to 1,000 µL)	Sigma-Aldrich, UK
Microscope slides (76 x 26 mm) Superfrost	Thermo Scientific, UK
Microwave oven	Sanyo, Bucks, UK
MSE Micro Centaur Centrifuge	MSE (UK) Ltd, London
Multiscan™ FC Microplate Reader (version 1.00.79)	Thermo Fisher Scientific, UK
Neubauer haemocytometer	VWR Scientifics, West Chester, UK
Optical reaction plates (MicroAmp™ Optical Adhesive Film Kit, 96-well)	Applied Biosystems Thermo Scientific, UK
PCR Sprint Thermal Cycler	Thermo Electron Corporation, USA
pH Meter	Dunmow, UK
qPCR CT000 Touch™ Thermal Cycler (CFX96™ Real-Time System)	Bio-Rad, UK
Scanning Electron Microscope (SEM) (FEI Quanta 400)	Cambridge, UK
Stuart™ Orbital Shaker	Thermo Fisher Scientific™, UK
Transmission Electron Microscope (TEM), JEM-2100	JEOL Ltd., Tokyo, Japan
Vibra-Cell™ Ultrasonic Liquid Processors	Sonics & Materials Inc, Newtown, USA
Vacurette® (LH Lithium Heparin, 9 mL) tubes	Greiner Bio-One (Austria)
Vortex mixer (LSE)	Fisher Scientific
Water bath	Grant Instruments, Cambridge, UK
Whatman® quantitative Filter paper, Ashless, Grade 41, circles, diam. 125mm pack of 100	Sigma-Aldrich, UK
Zetasizer Nano ZS-90, Model ZEN3600	Malvern Instruments Ltd, UK

2.2 Methods

2.2.1 Ethical Approval

This research was approved by the University of Bradford Research Ethics Committee for human individuals (Ref. No: 0405/8); the Integrated Research Application System (IRAS) approval was obtained by the University of Bradford, Faculty of Life Sciences as reviewed by Leeds East Research Ethics Committee (REC), (REC reference Number: 12/YH/0464), and by the Research Support and Governance Office of the Bradford Teaching Hospitals NHS Foundation (Ref: RE DA:1202), Bradford, West Yorkshire, UK.

2.2.2 Recruitment of volunteers

Before completing the consent forms, each participant was given a Participant Information Sheet consisting of two parts (see **Appendix 1**):

Part 1: Tells the participant the purpose of the study, the reason they had been invited followed with emphasis on voluntary participation; and

Part 2: Provides more detailed information about what would happen to participants if they took part in the study; study tests being non-predictive for individual participants; people who cannot take part in the study; and people to contact for queries.

Healthy volunteers (males and females, aged between 18 and 70 years) from mixed ethnicities were recruited from staff and students at the University of Bradford and some residents in Blackley, North Manchester, UK after giving informed consent. They were recruited between August 2016 and January 2019.

For healthy normal volunteers, the inclusion criteria were:

- Willingness to complete the informed consent form;
- Agreeing to have blood samples taken or stored at the University of Bradford;
- Data collected might be examined at by individuals from the NHS Trust and the University of Bradford Sub-Committee for human individuals;
- Do not have pulmonary diseases such as asthma, COPD, inflammatory lung diseases, pre-cancerous states or a family history of lung cancer and;
- Are not receiving medications for pulmonary diseases.

Patients with chronic pulmonary diseases (asthma, COPD, and lung cancer) were recruited from the hospital wards, and the Ambulatory / Respiratory clinic of Professor Badie Jacob at Bradford Royal Infirmary (BRI) and Dr Abid Aziz a Respiratory Consultant at St Luke's Hospital, Bradford, West Yorkshire, UK.

Inclusion criteria were:

- Willingness to complete the informed consent form;
- Agreeing to have blood samples taken or stored at the University of Bradford;
- That data collected might be examined at by individuals from the NHS Trust or researchers at the University of Bradford,
- Have been clinically diagnosed to have any of the pulmonary diseases: asthma, emphysema / pleural disease, COPD, or lung cancer.

Confounding factors such as age, gender, ethnicity, and cigarette smoking habits were taking into consideration.

2.2.3 Collection of Blood Samples

Human whole blood samples were collected in 9 mL heparinised tubes (Vacurette[®], LH Lithium Heparin) from patients and healthy individuals, aged: 24-77). Patients with chronic diseases – asthma, COPD, and lung cancer – were diagnosed at the Outpatient department of the Respiratory/Oncology unit, Bradford Royal Infirmary (BRI), Bradford, West Yorkshire, UK. Healthy individuals were recruited from the University of Bradford staff and student Community and volunteers from Blackley area of North Manchester, UK.

Blood samples used in this project were used immediately or on the same day of collection. For general knowledge, although blood samples in Lithium Heparin Tubes (with anti-coagulant) could be stored for up to 72 h (3 days), it is advisable to use them as soon as possible or within 48 hours as they might become unstable with longer storage. Blood samples (human liquid **biopsies**) were chosen for this PhD study instead of surgical biopsies because it is faster to detect traces of COPD and cancer's DNA in the blood or biomarkers of DNA damage due to genotoxic agents early in blood samples from patients undergoing treatment or from healthy individuals who visit their GP surgeries for routine checks. Early detection of traces of DNA damage in blood samples could potentially increase people's chances of living longer with a better quality of life, than late detection when diseases such as COPD and lung cancer could have spread into advanced stages or in healthy individuals at the risk of developing chronic pulmonary diseases (Pantel 2016).

2.2.4 Isolation of Peripheral Human Lymphocytes (PBL)

Human PBL from healthy individuals and patients (asthma, COPD, and lung cancer) were isolated from whole blood using the Lymphoprep™ density gradient centrifugation method with slight modification (Böyum 1968; STEMCELL Technologies 2017). Described briefly, human whole blood was diluted 1:1 in NaCl (0.9%) and gently mixed (See **Figure 2.1**). Three mL (3 mL) of Lymphoprep™ was added into a 15 mL Falcon tube, and 6 mL of the diluted blood sample (Blood-NaCl mixture) carefully layered on top of the Lymphoprep™ without disturbing the mixture. The Falcon tubes were centrifuged at 1,900 rpm (800 x g) for 20 min at room temperature (RT) forming four different layers of blood components: red blood cells (erythrocytes and granulocytes) on the bottom; Lymphoprep™ layer; a layer of white blood cells (lymphocytes and monocytes) and platelets; and a layer of plasma on the top.

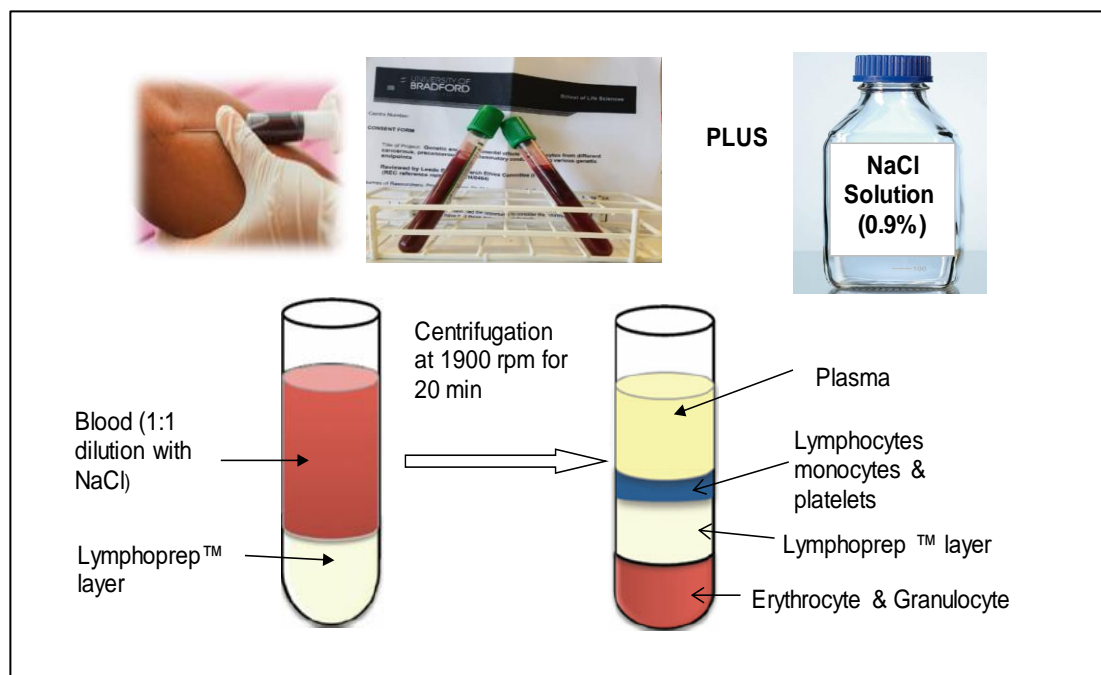


Figure 2.1: Schematic illustration of Isolation of lymphocytes from human whole blood using density-gradient Lymphoprep™ (Bharadwaj et al. 2012)

The cloudy, buffy coat layer containing white blood cells (lymphocytes and monocytes) and platelets (immediately above the Lymphoprep™ layer) was then carefully collected from the interface using Pasteur pipette. The lymphocyte-containing layer was transferred into a 50 mL Universal tube prefilled with 10 mL of 0.9% NaCl. The Universal tube containing the Lymphocyte-NaCl mixture was then centrifuged at 1,500 rpm (630 x g) for 15 min at RT to concentrate the cells. The supernatant was discarded leaving the pellets on the base of the tube undisturbed.

2.2.5 Cell Counting with Haemocytometer

The lymphocytes were suspended in 700 µL of RPMI-1640 medium and mixed with the aid of a micropipette. Cell counts were performed to determine cell concentration, which also helps to calculate the volume of lymphocyte suspension to be used in cell culture and treatment. Briefly, 10 µL of lymphocyte suspension was pipetted and transferred into a Neubauer Haemocytometer, followed by adding a drop of water to each corner of the Haemocytometer and then covered with a glass cover slip. Cells were observed under the Inverted Microscope at x10 Eyepiece lenses and x100 magnification (objective lenses) and cells counted on 4 squares from each of the 4 corners [1 square = 1 mm; = 16-smaller squares of 0.05 mm (= $2.5 \times 10^{-3} \text{ mm}^2$)].

2.2.6 Determination of lymphocyte concentration

An average of the four readings was taken and the result (**a**) multiplied by 10^4 cells/µL to give us the concentration of lymphocytes in the lymphocyte-RPMI mixture. That is, $C_1 = \mathbf{a} \times 10^4 \text{ cells}/\mu\text{L}$; where **a** = average cell counts, and 10^4

cells = the standard number of cells in a 1-square volume of the haemocytometer.

Overall, the following equation was used:

$$C_1V_1 = C_2V_2 \text{ or } V_1 = \frac{C_2V_2}{C_1}$$

Where:

V₁ = unknown volume of the lymphocyte-RPMI-1640 mixture we require for incubation and treatment with chemical.

C₂ = 20×10^4 cells/ μ L (a standard cell concentration).

V₂ = 1 mL (1,000 μ L) (a standard final volume).

C₁ = known concentration (**a**) of lymphocytes we had earlier counted.

2.2.7 Cell viability test with Trypan Blue Exclusion assay

Prior to treatment of human whole blood and lymphocytes with chemical agents, cell viability was performed using the Trypan Blue Exclusion assay to determine the cell membrane integrity or cell viability (Avelar-Freitas et al. 2014). Briefly, 10 μ L of blood + RPMI mixture or lymphocyte + RPMI mixture was mixed 1:1 with 10 μ L of Trypan blue dye (0.4% w/v), making a final volume of 20 μ L. Thereafter, 10 μ L of this mixture was pipetted into a Neubauer Haemocytometer and incubated for 10 mins. When the integrity of the cell membrane has been compromised, non-viable dead cells absorb the Trypan blue dye and appear blue in colour while viable, unstained cells would not take up the blue colour and appear white in colour. In this present study, the cells were normally between 90 and 95% viable (Thermo Fisher Scientific 2018).

2.2.8 Particle Characterization of Graphene Oxide Nanomaterials

2.2.8.1 Materials

Table 2-3: Characteristics of GO NMs

Product Name	Graphene Oxide 15-20 sheets, 4-10% edge-oxidized; 1 mg/mL; dispersion in H ₂ O (PCode: 794341, Sigma-Aldrich, USA)
TESTS	Specifications provided by the manufacturer (Sigma-Aldrich, USA) at the National Centre for Biotechnology Information (NCBI), PubChem Substance (PubChem 2018)
Preparation Method	Modified Hummer's method (Chemical Exfoliation of graphite) (Hummers and Offeman 1958)
Appearance (Colour)	Very dark brown to black
Appearance (Form)	Suspension
Molecular weight	4,239.48 g/mol (Sigma-Aldrich) and 2,043.856 g/mol (PubChem 2018)
Molecular Formula	C ₁₄₀ H ₄₂ O ₂₀ (NCBI)
Bulk density	~1.8 g/cm ³
Carbon (Dry Basis)	> 50 %
Oxygen (Dry Basis)	< 11 %
Residue on Evaporation	0.9- 1.4 mg/mL
Sulphur Content	N/A
Oxidization level	≥ 95% (AC Materials: High Surface Area of Graphene Oxide)

Commercial GO from Sigma-Aldrich was prepared by the chemical exfoliation method / oxidation of graphite with two strong oxidizing agents - MnO₄ (permanganate) and NaNO₃ in H₂SO₄/ H₃PO₄ (Hummers and Offeman 1958; Song et al. 2014). Large flakes of GO NMs similar to the one used in this study, could have been prepared using a precursor such as poly-dispersed hyper-branched polyphenylene to yield large flakes of NMs (Zhi and Müllen 2008). All other chemicals were of analytical grade and were listed in Section 2.1.1. Several techniques were used to characterise GO NMs in order to understand their physicochemical behaviour in the aqueous dispersion medium. To study these

characteristics, the following methods were used: DLS, ZP, SEM, and TEM, respectively.

2.2.8.1.1 Preparation of GO dilution in aqueous suspension

For nanoparticle characterisation, different concentrations of the working of GO (10, 20, 50, and 100 µg/mL) in a final volume of 1,000 µL of aqueous solution were prepared from the stock dispersion of GO (1mg/mL) using the equation,

$V_1 = \frac{C_2V_2}{C_1}$, and the final concentrations sonicated for 5 min at 30 W (Ultrasonics).

2.2.8.1.2 Dynamic Light scattering

The particle size distribution of GO in dH₂O was determined using DLS technique with the aid of a Zetasizer Nano ZS-90 (Model ZEN 3600) (See **Figure 2.2**). A small volume of the working stock prepared in section 2.2.8.1.1 was transferred into disposable cuvettes and measurements performed in triplicate at RT (25°C).



Figure 2.2: Illustrative photos of the Zetasizer Nano ZS-90 during sample loading (Malvern Panalytical Ltd 2018)

2.2.8.1.3 Zeta Potential

Zeta potential (ZP) was performed using the Zetasizer Nano ZS-90 (Model ZEN 3600) to determine the surface charge of GO NMS in aqueous dispersion.

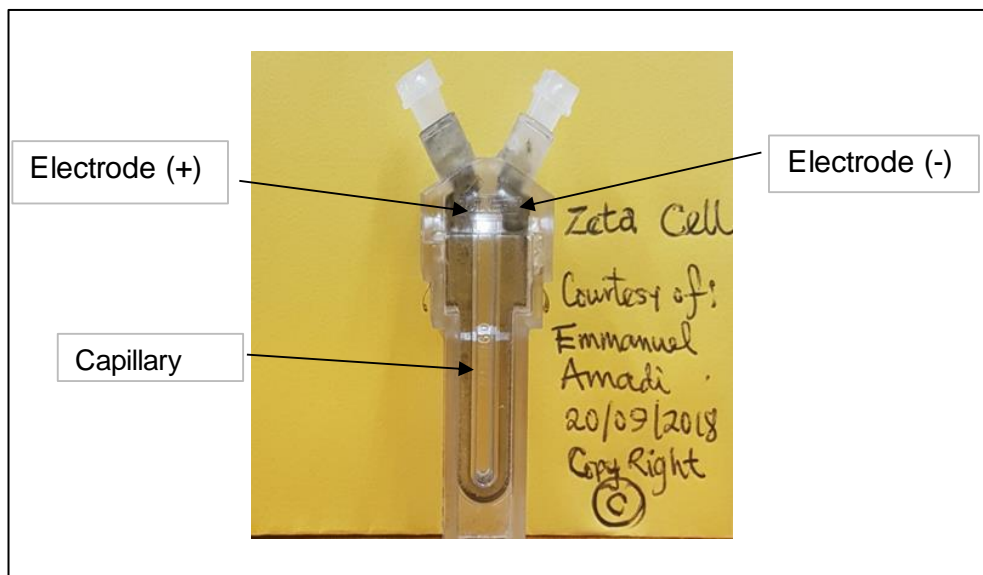


Figure 2.3: A Zetasizer cell photograph taken during zeta potential analysis with the aid of a Samsung Galaxy S9+ Mobile Phone with 12 MP camera . The photo shows the internal sections of the cell – the electrodes and a capillary.

The different concentrations of the working stock (10, 20, 50, and 100 $\mu\text{g/mL}$) in 1000 μL were transferred to a clean Zetasizer cell as shown in Figure 2.3above, and then measured in triplicate at RT (25°C) with 16 runs each.

2.2.8.1.4 Scanning Electron Microscope

The beam of electrons from the SEM were scanned on the surface of the dried GO samples to determine their surface morphology, physicochemical aggregation, and particle size. Briefly, four different concentrations of GO working stock (10, 20, 50 and 100 $\mu\text{g/mL}$) in aqueous suspension were pipetted to special adhesives (specimen substrates/mount in black colour as shown in **Figure 2.4**) and allowed to sediment and filter.



Figure 2.4: Photographic images of the particle preparation on the left and the interior of the SEM during SEM analysis

They were gently allowed to dry with the aid of a hair drier at a 1-metre distance to avoid blowing off the particles. Samples were loaded in the sample stub/holder and then transferred to the sample stage. The sample stub was then tightened with a screw/tape and positioned in place to obtain better image. The sample stage was then placed inside the sample chamber and the compartment closed. The pumps were turned on to allow the system to reach vacuum. The SEM software was opened, and the operating voltage was set at 20.0 kV, and two-dimensional (2-D) SEM images analysed with 20K magnification (FEI Quanta 400, Cambridge, UK).

2.2.8.1.5 Transmission Electron Microscope

TEM was applied to the dried GO samples to measure their size, and aggregation characteristics. Different concentrations of GO (10, 20, 50 and 100 $\mu\text{g}/\text{mL}$) were prepared by first filtering them through carbon-coated copper TEM grids (300 mesh), followed by washing off excess particles from the grids by dipping them 50 x in dH_2O (i.e. 50 dips consisting of 20 dips in dH_2O , followed by 2 x 15 dips).

Finally, the solvent was allowed to dry, and the TEM grid fixed on the TEM sample holder and the particles scanned using TEM (JEM-2100, JEOL Ltd., Tokyo, Japan) at 20.0kV at various magnifications (50x; 1,000x; and 2,500x) and three-dimensional (3-D) TEM micrographs obtained.

2.2.9 *In Vitro* Cytotoxicity Assays

In Vitro Cytotoxicity assays (Roggen 2011) - MTT and NRU assays - were performed using isolated lymphocytes to assess cell survival rates / metabolic profiles after treatment with different concentrations of GO NMs. Treating healthy living cells with cytotoxic chemicals may lead to inhibition of cell growth (cytostasis), necrosis (accidental cell death) or apoptosis (programmed cell death) (Çelik 2018).

2.2.9.1 MTT Cell Proliferation /Cell survival Assay

The MTT assay, developed by Tim Mossman, is a colorimetric assay which measures the metabolic activities of living cells inside the mitochondrial (the Powerhouse of the cells) (Mossman 1983). We had chosen the MTT assay because it is a robust and sensitive test used in drug screening due to its ability to give linearity of results over a wide range of cell densities and cytotoxicity risks (Niles et al. 2009). As the cells undergo metabolic redox-reaction in order to deal with so many particles around them, the mitochondria reductase enzymes convert the soluble tetrazolium MTT dye from yellow colour to insoluble, purple formazan crystals (Liu et al. 1997) in the mitochondria of living cells as presented in Figure 2.5.

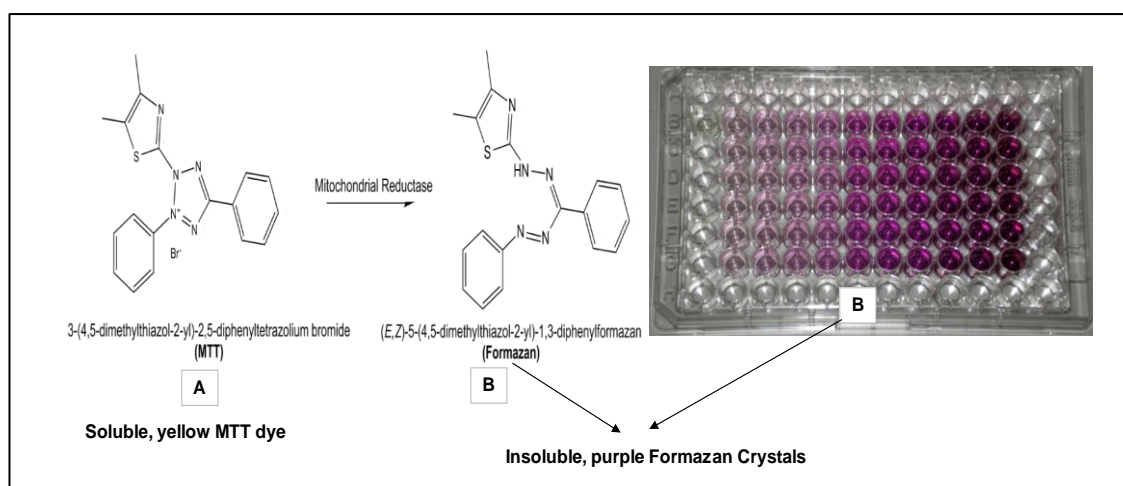


Figure 2.5: Conversion of soluble, yellow tetrazolium MTT dye (A) (Grant 2014) to insoluble, purple Formazan crystals (B) by reductase enzymes inside the mitochondria of living cells (Shinyuu 2010).

2.2.9.1.1 Materials

The materials used in the MTT Cell Proliferation assay were listed in section 2.1.1.

2.2.9.1.1.1 Demographic Data of blood donors used in the MTT and NRU assays

Table 2-4: Demographic data of patients and healthy individuals used in the MTT and NRU Assay.

No	Code/ Hospital Number	Age	Gender	Ethnicity	Smoking history
Healthy Individuals					
1	AM	45	F	Caucasian	Non-Smoker
2	WJ	47	M	Caucasian	Non-Smoker
3	AN	43	M	Caucasian	Non-Smoker
Asthma patients					
4	0809845	26	F	Caucasian	Non-Smoker
5	N/A	64	F	Asian	Non-Smoker

6	N/A	46	F	Asian	Non-Smoker
COPD patients					
7	N/A	58	M	Caucasian	Past Smoker
8	N/A	54	F	Caucasian	Past Smoker/ tobacco
9	0290072	57	M	Caucasian	Smoker; 30/day; alcohol
Lung Cancer patients					
10	N/A	55	F	Asian	Past Smoker
11	4360497856	57	M	Caucasian	Smoker; 30/day
12	0795624	65	M	Caucasian	30 pack/ year

2.2.9.1.2 Methods

The MTT assay was performed to measure the cell proliferation rate in the mitochondria of living cells using the MTT dye according to the original method discussed elsewhere (Mossman 1983).

2.2.9.1.2.1 Preparation of Reagents

12 mM MTT stock solution was prepared by adding 5 mg of MTT dye to 1 mL of PBS. The solution was mixed thoroughly using a vortex mixer to increase solubility of the dye. Excess MTT solution was stored at 4°C for future use.

2.2.9.1.2.2 Treatment of Lymphocytes with GO NMs

Specified volumes of lymphocyte mixtures (V_1) from healthy individuals, asthma, COPD, and lung cancer patients previously calculated in Section 2.2.6 were added to 5 wells of a 6-Well Plate.

Table 2-5: Chemical Treatment table

Wells	GO Final Conc.	Volume of GO stock required (μL)	V_1 = vol. of Lymphocyte+ RPMI mixture calculated (μL)	Vol. of fresh RPMI 1640 (1X)	Final volume (μL)
1	NC	0	V_1	$1,000 - V_1$	1,000
2	10 $\mu\text{g}/\text{mL}$	10	V_1	$1,000 - (10 \mu\text{L} + V_1)$	1,000
3	20 $\mu\text{g}/\text{mL}$	20	V_1	$1,000 - (20 \mu\text{L} + V_1)$	1,000
4	50 $\mu\text{g}/\text{mL}$	50	V_1	$1,000 - (50 \mu\text{L} + V_1)$	1,000
5	100 $\mu\text{g}/\text{mL}$	100	V_1	$1,000 - (100 \mu\text{L} + V_1)$	1,000

Using the chemical treatment Table above, human lymphocyte-RPMI mixtures in four wells (2, 3, 4, and 5) were treated with 4 different concentrations of GO (10, 20, 50, and 100 μL) while the 5th well, the NC, was treated with fresh RPMI-1640 (1X) medium, supplemented with glutamine (GlutaMax™) 15% heat inactivated FBS, 100 U/mL penicillin and 100 $\mu\text{g}/\text{mL}$ streptomycin were added to the wells. Thereafter, they were incubated overnight for 24 h in an incubator (37°C, 5% CO₂) and the cells allowed to adhere to the base of the plate.

2.2.9.1.2.3 Treatment of lymphocytes with MTT dye solution

After incubation, the cells were transferred into Eppendorf® Tubes and centrifuged at 1,000 rpm ($\approx 418 \times g$) for 5 min to concentrate the cells, and the medium discarded. The pellets were resuspended in 100 μL of fresh RPMI-1640 medium and then transferred in triplicate into a 96-Well plate to commence treatment with MTT dye. The first wells of the 96-well plate were loaded with 100

μ L of RPMI-1640 medium to serve as the NC/ blank (with no cells), while the rest of the wells contain 100 μ L of cells in triplicate. Ten microlitres (10 μ L) of 12 mM MTT stock solution was added into each well to discriminate between genotoxicity and cytotoxicity in the pathogenesis of DNA DSB. Thereafter, they were incubated at 37°C for 4 h, followed by removal of all medium, but 25 μ L of medium left with cells per well. Thereafter, the MTT dye absorbed by the cells in each well was solubilized by adding 50 μ L of DMSO and thoroughly mixed by gentle pipetting up and down or using vortex mixer. They were incubated at 37°C for 15 min and absorbance readings taken immediately.

2.2.9.1.2.4 Spectrophotometric Analysis (Absorbance)

The amounts of MTT dye absorbed by cells are directly proportional to the proliferative activities of the cells. They were quantified by measuring the absorbance readings at 540 nm using the Multiscan™ FC Microplate reader.

2.2.9.1.2.5 Data Analysis

2.2.9.1.2.5.1 Calculation of Percentage (%) Cell survival in the MTT Assay

First, the corrected absorbance readings were obtained by subtracting all the background readings (Absorbance of empty wells) from each of the absorbance readings from treated cells (NC, 10, 20, 50 and 100 μ g/mL), followed by taking the average of the triplicate readings (n=3). The control readings were obtained from the absorbance readings of the first wells containing only the RPMI medium (with no cells) and MTT stock solution. The amount of the corrected absorbance values is proportional to the number of proliferating cells. The % Cell Survival

rates, which measures metabolic activities and cytotoxicity, was calculated using the following equation:

$$\% \text{ Cell survival} = \frac{\text{Absorbance (Treated Cells)}}{\text{Absorbance of Control (Medium only)}} \times 100.$$

2.2.9.1.2.5.2 Statistical Analysis

The graph of % cell survival rates in the MTT Assay of treated lymphocytes (healthy, asthma, COPD, and lung cancer) was plotted against different concentrations of GO (10, 20, 50 and 100 µg/mL) while the untreated lymphocytes (NC = 0 µg/ml) had 100% absorbance. Graphs were plotted using GraphPad Prism® software, version 7.04 (Fay Avenue, La Jolla, CA, USA), and statistical analysis performed using the same software with built-in One-Way ANOVA and Dunnett's post-hoc multiple comparison test to determine differences in cytotoxicity of treated lymphocytes relative to the untreated, NC samples. Statistical significance was accepted at $p < 0.05$, where * = $p < 0.05$; ** = $p < 0.01$; *** = $p < 0.001$; and ns = not statistically significant.

2.2.9.2 Neutral Red Uptake (NRU) Assay

The NRU assay measures the metabolic activity of lysosomes of living cells in the presence of chemicals agent (Sigma-Aldrich USA 2018). The lysosomes are located inside the cytoplasm and serve as the digestives system of the cells. They contain hydrolytic enzymes that liquify nutrients by breaking down individual proteins or whole microorganism. The Neutral Red is a eurhodin dye which is taken up by active transport into the cell lysosomes, and is subsequently stained red, whereas non-viable, dead cells cannot take up this dye. The amount of dye

absorbed, which is proportional to the amount of active living cells, is then quantified using a spectrophotometer (Multiscan™ FC Microplate reader).

2.2.9.2.1 Materials

The Neutral Red Assay kit (Sigma-Aldrich, USA) is listed in section 2.1.1: Chemicals, and contains three ready-to-use components (Table 2-6).

Table 2-6: Components of In Vitro Toxicology Neutral Red based assay kit

Product No.	Item	Quantity
N 2889	Neutral Red Solution 0.33% in Dulbecco's phosphate-buffered saline (PBS) buffer	20 mL
N 4270	Neutral Red Assay Fixative, 0.1% Calcium Chloride (CaCl ₂) in 0.5% Formaldehyde	125 mL
N 4395	Neutral Red Assay Solubilization Solution (1% Acetic Acid in 50% Ethanol)	125 mL

2.2.9.2.1.1 Demographic Data of blood donors used in the NRU Assay

The demographic data, containing Age, Gender, Ethnicity and Smoking history of blood donors used in the NRU assay are listed Section 2.2.9.1.1.1

2.2.9.2.2 Methods

2.2.9.2.2.1 Treatment of Lymphocytes with GO

Lymphocytes from patients (asthma, COPD, and lung cancer) and healthy individuals were treated with GO as previously described (Section 2.2.9.1.2.2). After 24 h of treatment, the culture medium was discarded and replaced with 100 µL fresh RPMI-medium. The cells were transferred in triplicate into a 96-Well

plate, while the negative control/blank wells (with no cells) on the first lane were loaded with only 100 μ L of RPMI-1640 medium.

2.2.9.2.2.2 Treatment of Lymphocytes with Neutral Red Solution

10 μ L of Neutral Red Solution, equivalent to 10% of the culture medium, was added into each well and incubated for 3 h at 37°C and 5% CO₂. Thereafter, the cells were fixed with 100 μ L Neutral Red Assay Fixative (0.5% Formalin; and 1% CaCl₂) and subsequently transferred to Eppendorf® tubes. They were centrifuged at 1,000 rpm (\approx 418 x g) for 7 min and thereafter the Fixative was carefully removed without disrupting the cells. The cells were solubilised with equal volume (100 μ L) of Neutral Red Solubilisation Solution (1% acetic acid; and 50% ethanol), mixed thoroughly and transferred back into the 96-Well plate. They were incubated for 10 min at RT before absorbance readings were taken.

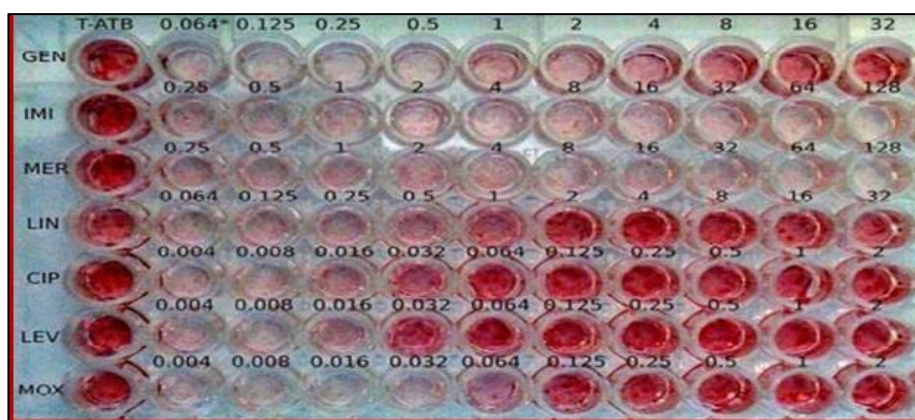


Figure 2.6: Representative image of a 96-well plate during NRU assay

2.2.9.2.2.3 Spectrophotometric Analysis (Absorbance)

The amount of Neutral Red dye absorbed into the lysosomes of the cells is directly proportional to the proliferative activities of the cells, vis-à-vis cytotoxicity

of the agent and the absorbance read at 540 nm using the Multiscan™ FC Microplate reader (version 1.00.79; Thermo Fisher Scientific, UK). A second absorbance was read at 595 nm, which is the background absorbance of the multiwell plate.

2.2.9.2.2.4 Data Analysis

2.2.9.2.2.4.1 Calculation of % Cell survival in the NRU Assay

First, we obtained the corrected absorbance readings by subtracting all the background readings (Absorbance of empty wells) at 595 nm from absorbance at 540 nm for each of the treated cells (NC, 10, 20, 50 and 100 µg/mL). The control readings were obtained from the absorbance readings of the first wells containing only the RPMI medium (with no cells) and Neutral Red dye solution. The final, corrected absorbance values are proportional to the number of proliferating cells. The average of the triplicate readings (n=3) were taken. The % Cell Survival rates in the NRU assay, which measures metabolic activities and drug cytotoxicity, was calculated using the following equation:

$$\% \text{ Cell survival} = \frac{\text{Absorbance of cells treated with GO (540-595nm)}}{\text{Absorbance of Control (540-595 nm)}} \times 100.$$

2.2.9.2.2.4.2 Statistical Analysis

The graph of % cell survival rates in the NRU Assay of treated lymphocytes (healthy, asthma, COPD, and lung cancer) was plotted against different concentrations of GO (10, 20, 50 and 100 µg/mL) while the untreated lymphocytes (NC = 0 µg/ml) had 100% absorbance. Graphs were plotted using GraphPad Prism® software, version 7.04 (Fay Avenue, La Jolla, CA, USA), and

statistical analysis performed using the same software with built-in One-Way ANOVA and Dunnett's post-hoc multiple comparison test to determine differences in cytotoxicity of treated lymphocytes relative to the untreated, NC samples. Statistical significance was accepted at $p < 0.05$, where * = $p < 0.05$; ** = $p < 0.01$; *** = $p < 0.001$; and ns = not statistically significant.

2.2.10 Genotoxicity Assay

The Genotoxicity (DNA damage) assay is aimed at determining the level of DNA damage in human whole blood after exposure to GO NMs. DNA damage can occur either directly by damaging the genetic materials within the DNA molecules or indirectly through the activation of surface receptors which trigger ROS, and the ROS subsequently triggers oxidative stress which then activates the cell-cycle signalling pathways. Both effects could induce mutations which could be transferred from generation to generation. Short-term DNA damage by genotoxic agents could lead to DNA damage recovery and repair, while in extreme cases, long-term DNA damage may lead to non-recovery and be irreparable. It is the irreparable damaged DNA that subsequently leads to either programmed cell death (apoptosis), necrosis (accidental cell death), or frequent mutations (mutagenesis) and finally cancer (Liu et al. 2013b).

2.2.10.1 Alkaline Comet Assay

Hydrogen peroxide (H_2O_2) concentration with the highest non-toxic DNA damage was used as the positive control (PC) in this study as the standard reference chemical in the Comet assay. H_2O_2 is naturally produced in the body during normal metabolic process.

2.2.10.1.1 Materials

The amounts of buffers/Reagents used in the Comet assay were prepared from the chemicals /Reagents listed in **Section 2.1.1** and **Appendix 6**.

2.2.10.1.1.1 Demographic Data of blood donors

The demographic data of patients and healthy individuals are listed in Table 2-7, comprising age, gender, ethnicity, smoking history, and past medical history.

Table 2-7: Demographic data of patients and healthy individuals used in the Comet and CBMN assays.

	Sample Number	Age	Gender	Ethnicity	Smoking history	Past Medical History
Healthy Individuals						
1	10335	39	M	Caucasian	Non - Smoker	N/A
2	10329	39	F	“”	“”	“”
3	10331	69	M	“”	“”	“”
4	JW 27-8-15 (Box 91)	40	M	“”	“”	“”
5	23-24 (Box 84)	44	F	“”	“”	“”
6	No-35-36	56	F	“”	“”	“”
7	17-06-15 MA	47	M	“”	“”	“”
8	MS 23-06-15	39	M	“”	“”	“”
9	10588	32	F	Asian	“”	“”
10	10-12-18	47	M	Caucasian	“”	“”
11	AM	45	F	Caucasian	Non-Smoker	“”
12	WJ	47	M	Caucasian	“”	“”
13	AN	43	M	Caucasian	“”	“”
14	HC	56	M	“”	“”	“”
15	JH	24	M	“”	“”	“”

16	TA	42	F	“”	“”	“”
17	PN	39	F	“”	“”	“”
18	AH	48	M	“”	“”	“”
19	NA	50	M	“”	“”	“”
20	EW	46	F	“”	“”	“”
ASTHMA PATIENTS						
21	27-10-15 R	45	M	Caucasian	Smoker, 3-5/day	N/A
22	21-10-15 R	32	F	Caucasian	Non-smoker	“”
23	13-3-17 R4 0339423	31	F	Asian	“”	“”
24	13-3-17 R2 0505001	61	M	Caucasian	Smoker; 40/day; 30/year	Asthma & COPD
25	13-3-17 R3 0538130	54	F	Caucasian	Smoker; 15-20/ day	Asthma & COPD
26	R 21-10-15	32	F	Caucasian	Non - Smoker	NA
27	RAE 0144596	47	F	Caucasian	Not recorded	“”
28	9/3/17 R2 RAE 1317552	54	F	Caucasian	Past Smoker	“”
29	R4 13-3-17	64	M	Caucasian	Non - Smoker	“”
30	24/2/17 RAE 0797968	38	F	Caucasian	Not recorded	“”
31	9-3-17	49	M	Caucasian	Smoker; 3/day	“”
32	03-12-18	64	F	Asian	Non - Smoker	“”
33	6-12-18	46	F	Asian	Non - Smoker	“”
34	1182462; 4500698388	61	M	Caucasian	Non - Smoker	“”
35	N/A	65	M	“”	Non- Smoker	N/A
36	N/A	58	F	“”	Non- Smoker	“”
37	N/A	60	M	“”	Non- Smoker	“”

38	0809845	26	F	Caucasian	Non-Smoker	“”
39	N/A	64	F	Asian	Non-Smoker	“”
40	N/A	46	F	Asian	Non-Smoker	“”
COPD PATIENTS						
41	5-8-15 R2	52	M	Caucasian	Smoker; 20/ day	“”
42	09-06-15 R	65	F	Caucasian	Smoker; 5- 10/day	“”
43	13-3-17 R2 0505001	61	M	Caucasian	Smoker; 40/day; 30/year	Asthma & COPD
44	13-3-17 R3 0538130	54	F	Caucasian	Smoker; 15-20/ day	Asthma & COPD
45	13-3-17 R1 1308631	56	F	Caucasian	Past Smoker	N/A
46	R 09-06-15	55	M	Caucasian	Smoker; 20-80/day	“”
47	R2 05-08-15	64	M	Caucasian	Smoker	“”
48	R1 27-2-17; RAE 0255865	64	M	Caucasian	Smoker; 20/day	“”
49	R3 27-2-17 DJ1	54	F	Caucasian	Smoker; 6- 8/day	“”
50	R3 28-2-17	69	M	Caucasian	Smoker	“”
51	R1 2-3-17 RAE 1165577	64	M	Caucasian	Smoker; 20/day	“”
52	R2 2-3-17 RAE 0716425	70	F	Caucasian	Smoker; 15-20/day for 20 years	Severe COPD/ recurrent chest infection
53	9/3/17 R1 RAE 0292614	49	M	Asian	Smoker; 20/day; Cannabis; pop usually	COPD; Schizophren ia
54	6-12-18	54	F	Caucasian	Past Smoker; Tobacco	“”

55	3340032	57	M	Caucasian	Smoker	“”
56	367885	59	M	Caucasian	Smoker; 30/day	“”
57	4360497856	57	M	Caucasian	Smoker	“”
58	N/A	58	M	Caucasian	Past Smoker	“”
59	N/A	54	F	Caucasian	Past Smoker/ tobacco	“”
60	0290072	57	M	Caucasian	Smoker; 30/day; alcohol	“”
LUNG CANCER PATIENTS						
61	5-8-15 R3	64	M	Caucasian	Smoker; 8/ day	N/A
62	29-7-15 R	62	M	Caucasian	Smoker; 10-15/day	“”
63	05-08-15 R	62	F	Asian	Non - Smoker	“”
64	06-08-15 R2	74	M	Caucasian	10-15/day	“”
65	05-08-15 R1	60	F	Asian	Non - Smoker	“”
66	R1 7-12- 2016	64	M	Caucasian	Smoker	“”
67	R2 7-12- 2016	77	F	Caucasian	Smoker	“
68	12-1-17	64	M	Caucasian	Smoker	Lung nodule
69	13-12-18	55	F	Asian	Past Smoker	N/A
70	0795624	65	M	Caucasian	Smoker; 30 pack/ year	“”
71	0564145	72	F	Caucasian	Smoker	
72	0290072	57	M	Caucasian	Smoker; 30/day	Pulmonary fibrosis; COPD
73	N/A	60	F	Caucasian	Past Smoker	N/A”
74	N/A	50	M	Caucasian	Past Smoker	“”
75	N/A	65	M	Asian	Past Smoker	“”

76	N/A	61	F	Caucasian	Past Smoker	“”
77	N/A	68	M	Caucasian	Past Smoker	N/A
78	N/A	55	F	Asian	Past Smoker	“”
79	4360497856	57	M	Caucasian	Smoker; 30/day	“”
80	0795624	65	M	Caucasian	30 pack/ year	“”

2.2.10.1.2 Methods

2.2.10.1.2.1 Treatment of human Whole Blood with Chemical Agents

The aims of the Comet assay were twofold, namely:

1. To determine the concentration of H₂O₂ (10, 30, 60, and 100 µM) with the highest DNA damage to be used as a non-toxic reference standard; and
2. To evaluate the DNA damage caused by GO (10, 20, 50, and 100 µg/mL) and H₂O₂ (PC) on human whole blood relative to untreated samples.

The Comet assay experiments from each of the treatment groups - healthy and patients (asthma, COPD, and lung cancer) - were performed independently as previously described elsewhere (Karbashi and Cooke 2014). Briefly, 890 µL of RPMI medium was pipetted into each of empty Eppendorf® tubes. For H₂O₂-concentration dependent DNA damage, they were treated with 10 µL of the aforementioned H₂O₂ concentrations. For the assessments of GO-induced DNA damage, 10 µL of different GO concentrations and the PC (H₂O₂) were added into their respective tubes while the NC received RPMI medium. 100 µL of human whole blood then added to each tube, making a total final volume of 1,000 µL. They were immediately incubated for 30 min in the cell culture incubator (37°C,

5% CO₂). During the incubation period, super frosted microscope slides pre-coated with 1 % NMP agarose were prepared in duplicate per treatment concentration. After cell incubation, the cells were immediately centrifuged at 3,000 rpm (300 x g) for 3 min to concentrate the cells, and 900 µL of the supernatant removed, leaving a small volume of ~ 100 µL with the cell pellets on the base of the tube. The cell pellets were re-suspended (1:1 ratio) with equal volume (100 µL) of 0.5% LMP agarose making a final volume of 200 µL agarose-cell suspension. They were gently mixed thoroughly with pipette tips to avoid destruction of the cells or gently mixed with a vortex mixer, and 100 µL of the agarose-cell suspension was carefully layered onto each of the 2 duplicate slides. The slides were immediately covered with glass coverslips (24 x 50 mm) to flatten the cell suspension, and then transferred to an ice tray or kept inside the refrigerator (4°C) for 5 min (to allow the agarose-cell suspension to polymerise and gel, thereby reducing further DNA damage). Thereafter, the coverslips were carefully removed and discarded without disrupting the agarose-layer.

2.2.10.1.2.2 Cell Lysis

The slides were carefully arranged horizontally in a slide tray, and then immersed in the black incubation box (See **Fig. 2.7B**) (BRAND® Staining Trough, Sigma-Aldrich) containing 200 mL of freshly prepared, ice-cold hypertonic lysis buffer (2.5 M NaCl, NaOH, 100 mM Na₂EDTA, 10 mM Trizma base, 10% DMSO, 1% Triton X-100) (See **Appendix 6**).

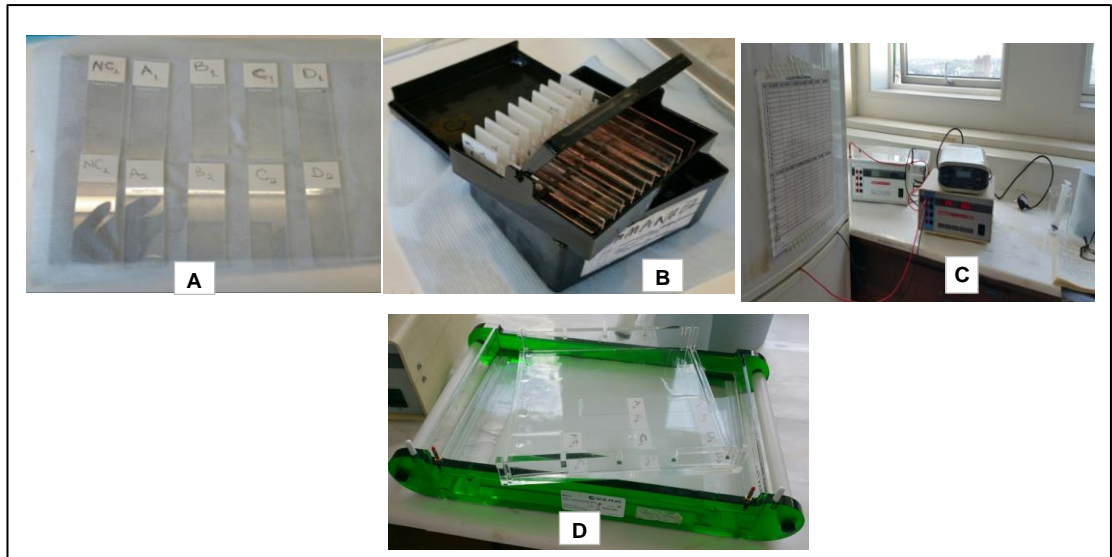


Figure 2.7: Photographs taken during the Comet assay: **(A)** duplicate slides; **(B)** slides arranged in the slide tray with black box, ready for incubation and cell lysis overnight; **(C)** DNA unwinding and electrophoresis inside the refrigerator (4°C); and **(D)** slides on the electrophoresis tank during neutralization.

This was covered securely with a black cover and stored in the dark inside the refrigerator at 4°C for at least 1 hour, or preferably left overnight according to the protocol. However, in this project, the cells were incubated overnight (24 h) to ensure maximum contact with the lysis solution as would be in normal human exposure conditions. Prior to this stage, the lysis solution was prepared fresh on the day of the experiment and stored in the refrigerator (4°C) for at least, 30 to 60 min to cool down before use.

2.2.10.1.2.3 DNA Unwinding and Alkaline Electrophoresis

After cell lysis, the slide-containing cells were removed from the lysis solution and placed horizontally, side by side to each other in the electrophoresis tank containing 2,000 mL of freshly prepared cold alkaline electrophoresis buffer (10 M NaCl, 200 mM Na₂EDTA, pH > 13.5, 4°C). The tank was then transferred into

the refrigerator (4°C) and incubated for 30 min for DNA unwinding to take place. The previously relaxed/super-coiled DNA unwinds in the presence of the alkaline electrophoresis medium. Double-strand DNA would break up into two components: single-strand breaks (SSB) and alkaline labile sites (ALS). Thereafter, electrophoresis was performed for further 30 min at a Voltage of 25V and 300 mA current (I). During electrophoresis, small particles of fragmented DNA would migrate faster from the negative cathode (-) towards the positive anode under an electric current, while larger particles of DNA fragments migrate slowly and are separated at a shorter distance.

2.2.10.1.2.4 Neutralisation

After electrophoresis, the power supply was turned off and the tank removed from the refrigerator. The slides were carefully removed from the electrophoresis tank and the buffer discarded. The slides were placed horizontally on a rectangular plastic with a flat surface, making sure the slides were not on top of each other. Using a plastic Pasteur[®] pipette, the slides were then neutralised three times with a neutralising buffer (400 mM Trizma base, pH 7.5) for 5 min each, by washing the slides drop by drop with the neutralisation buffer. This process could take up to 15 min to complete.

2.2.10.1.2.5 DNA Staining with Ethidium Bromide

After neutralisation, the slides were transferred into the dark room (with a dim light) and stained with filtered Ethidium bromide (EtBr) (20 µg/mL). Briefly, a volume of 60 µL of EtBr was pipetted on top of each slide, and then covered with

cover slips (24 mm x 50 mm). Excess EtBr was wiped off with clean tissue, and then covered appropriately to protect the slides from dehydration during scoring.

2.2.10.1.2.6 DNA Damage Scoring

The slides were viewed under the fluorescent microscope (Leica, Wetzlar, Germany) coupled to a Comet[®] 6 analysis software (Andor[®] Technology Ltd, Belfast UK). Particles of migrated damaged DNA appear as Comets and are manually scored. DNA damage was scored as the Olive tail moment (OTM) (tail intensity x DNA migration distance) and percentage of the DNA in the tail (% Tail DNA). A total of 100 cells (i.e. 50 cells from each of the 2 duplicate slides) were scored at random per treatment concentration. Comet images were captured with the aid of a CCD Camera (Kinetic Imaging K2) coupled to the top of the microscope and linked to the Komet[®] 6 image analysis software. Five independent Comet assays for H₂O₂ concentration-dependent DNA damage were performed using 5 blood samples from healthy individuals. Thereafter, further 80 independent Comet assay experiments were conducted on GO-induced DNA damage comprising 20 blood samples from healthy individuals, 20 from asthma patients, 20 from COPD patients, and 20 from lung cancer patients. Data obtained from the Komet[®] 6 Image analysis Software were analysed with Kinetic Imaging Data Analysis Macro software (Andor[®] Bio-Imaging Division) with built-in powerful Microsoft Excel.

2.2.10.1.2.7 Statistical Analysis

The data were expressed as the Mean \pm SEM (Standard Error of the Mean). Bar Charts (for H₂O₂-concentration dependent DNA damage) and Histograms (for

GO-induced DNA damage, PC, and NC) were plotted using GraphPad Prism® software, version 7.04 (Fay Avenue, La Jolla, CA, USA), and statistical analysis performed using the same software with built-in One-Way ANOVA and Dunnett's post-hoc multiple comparison test to determine differences in DNA damage (OTM and % Tail DNA) of treated blood samples relative to the untreated, NC samples. Statistical significance was accepted at $p < 0.05$, where * = $p < 0.05$; ** = $p < 0.01$; *** = $p < 0.001$; and ns = not statistically significant. Bars indicate standard errors.

2.2.11 Cytogenetic Assay

2.2.11.1 Cytokinesis-Blocked Micronucleus (CBMN) Assay

The CBMN assay experiments were performed using the protocol described by (Fenech 2007). A total of 20 different experiments were performed using twenty (20) different freshly collected blood samples, comprising 5 from healthy individuals; 5 from asthma patients; 5 from COPD patients; and 5 from lung cancer patients.

2.2.11.1.1 Materials

The chemicals and equipment used in the CBMN Assay are listed in Sections 2.1.1 and 2.1.2.

2.2.11.1.1.1 Demographic Data of participants in CBMN Assay

The demographic data, containing Age, Gender, Ethnicity, Smoking history, and past medical history of blood donors used in the CBMN Assay are listed in Section 2.2.10.1.1.1.

2.2.11.1.2 Methods

2.2.11.1.2.1 Preparation of Basic Culture Medium

The bulk basic culture media were prepared under strict sterile condition inside the sterile fume hood (Table 2-8).

Table 2-8: Preparation of Bulk Basic Culture medium from a bottle of 500 mL RPMI 1640-with Glutamax-1.

Chemicals	Basic cell culture	Final conc.
RPMI-1640 medium with Glutamax-I	84 mL	84%
FBS	15 mL	15%
Pen-Strep	1 mL	1%
Total Volume	100 mL	
Divided into aliquots of 4.5 mL x 22 and stored frozen (-20°C) till when required		
Prior to use defrost and add 130 µL PHA		
1 x aliquot	4.5 mL	
PHA	130 µL	

Basic culture medium was divided into 4.5 mL aliquots and stored in the freezer (-20°C) for future use.

2.2.11.1.2.2 Blood Cell Culture: Day 1; Time point: 0 h

Prior to blood cell culturing, five (5) frozen aliquots of the basic cell culture medium (4.5 mL) representing the NC, 10, 20, 50, and 100 µg/mL were transferred from the freezer (-20°C) into the Cell culture incubator (37°C, 5% CO₂) and allowed to equilibrate for at least 30 min. Thereafter, they were transferred

into the sterile fume hood. A volume of 130 μL of PHA was added into each of the culture flasks and gently mixed by briefly shaking them after each addition. At time 0-h, Day No. 1, a volume 400 μL of fresh human whole blood samples were carefully added into each of the flasks and mixed gently. They were transferred into the incubator (37°C, 5% CO_2) for 24 h.

2.2.11.1.2.3 Chemical Treatment with GO: Day 2; Time point: 24 h

At 24 h incubation, the blood cell cultures were treated with 50 μL of GO (10, 20, 50, and 100 $\mu\text{g}/\text{mL}$) while the NC flask received no chemical treatment. The PC control flask was treated with 50 μL of 0.4 μM Mitomycin-C (MMC) to inhibit DNA synthesis. According to the company's safety data sheets, MMC reacts covalently with DNA, *in vivo* and *in vitro*, to form cross-links between the DNA complementary strands and inhibit DNA replication (Sigma-Aldrich 2017). Finally, the flasks were then transferred back to the cell culture incubator (37°C, 5% CO_2) for further 20 h of chemical treatment or till 44-h of cell incubation.

2.2.11.1.2.4 Treatment with Cyto-B: Cytokinesis Block: Day 3; Time point: 44 h

After 44 h of blood cell culturing or 20 h of treatment with GO NMs, 30 μL of Cyto-B were added into each of the flasks. The Cyto-B impairs cytokinesis at the M-phase of cell division (i.e. the physical division of the cytoplasm of cells forming two daughter cells). Cytokinesis occurs simultaneously with nuclear divisions (mitosis and meiosis). By blocking cytokinesis, Cyto-B inhibits actin filaments formation, leading to the formation of BiNC, MNi, and other cytogenetic damage

parameters. The cells were incubated in the cell culture incubator (37°C, 5% CO₂.) for further 28 h or 72 h of cell culture.

2.2.11.1.2.5 Cell Harvesting and Preparation: Day 4; Time point: 72 h

On the 4th day, after 72 h of blood culturing, sterile conditions were no longer required, and the cells were harvested on the workbench. This is because after blocking cytokinesis with Cyto-B, the cells were no longer actively dividing. Cell cultures in Corning® Culture Flasks (25 cm²) were transferred to 15 mL Falcon® tubes and centrifuged at 800 rpm ($\approx 333 \times g$) for 8 min to concentrate the cells. The supernatants were removed using a vacuum pump, containing 300 mL of virkon (2%), until 500 μ L of the cells were left, and thereafter re-suspended by patting the tubes.

2.2.11.1.2.6 Treatment with Cold KCl (Hypotonic Shock)

The cells were gently treated with 5 mL of freshly prepared cold KCl (110 mM, 4°C) and then mixed thoroughly using a vortex mixer. Thereafter, they were transferred to the refrigerator (4°C) for 15 min to allow the cells to swell and the chromosomes to spread and avoid overlapping of the micronucleus boundary with the nuclear boundary (Fenech et al. 2003b). The cells were centrifuged at 800 rpm ($\approx 333 \times g$) for 8 min and supernatants removed using the vacuum pump, leaving a volume of 500 μ L.

2.2.11.1.2.7 Cell Fixation

Cell fixation involves the addition of Carnoy's solution (1 part of glacial acetic acid and 3 parts of methanol (1:3 ratio) into the cells to induce necrosis (accidental cell death). The cells were fixed in two stages, namely:

2.2.11.1.2.7.1 Fixation with Formaldehyde

The cells were resuspended using the vortex mixer. A volume of 5 mL of freshly prepared Carnoy's solution was gently added to the cell cultures, followed by 3 drops of 37% Formaldehyde using a plastic Pasteur pipette. Formaldehyde is a fixative which dehydrates cells/ tissues, causing proteins to denature and precipitate. The tubes were then centrifuged at 800 rpm ($\approx 333 \times g$) for 8 min and supernatants removed using a vacuum pump, leaving a small volume of 500 μL .

2.2.11.1.2.7.2 Fixation without Formaldehyde

The cell pellets were re-suspended on a vortex mixer, and 5 mL of Carnoy's solution added with no formaldehyde. They were centrifuged at 800 rpm ($\approx 333 \times g$) for 8 min and supernatants removed using the vacuum pump, leaving a small volume of 500 μL . This process was repeated twice without addition of formaldehyde. On the last step, the supernatant was not removed, and the cells were stored with the Carnoy's solution in the refrigerator (4°C) overnight.

2.2.11.1.2.8 Slide Preparation: Day 5

On the 5th day, the tubes were removed from the refrigerator (4°C) and the cells centrifuged at 800 rpm ($\approx 333 \times g$) for 8 min to concentrate the cells. The

supernatants were removed with the vacuum pump, leaving ~ 100 μ L. Depending on the size of the pellets left in the tube, cells were re-suspended with 200-300 μ L of freshly prepared Carnoy's solution and mixed thoroughly with a vortex mixer.

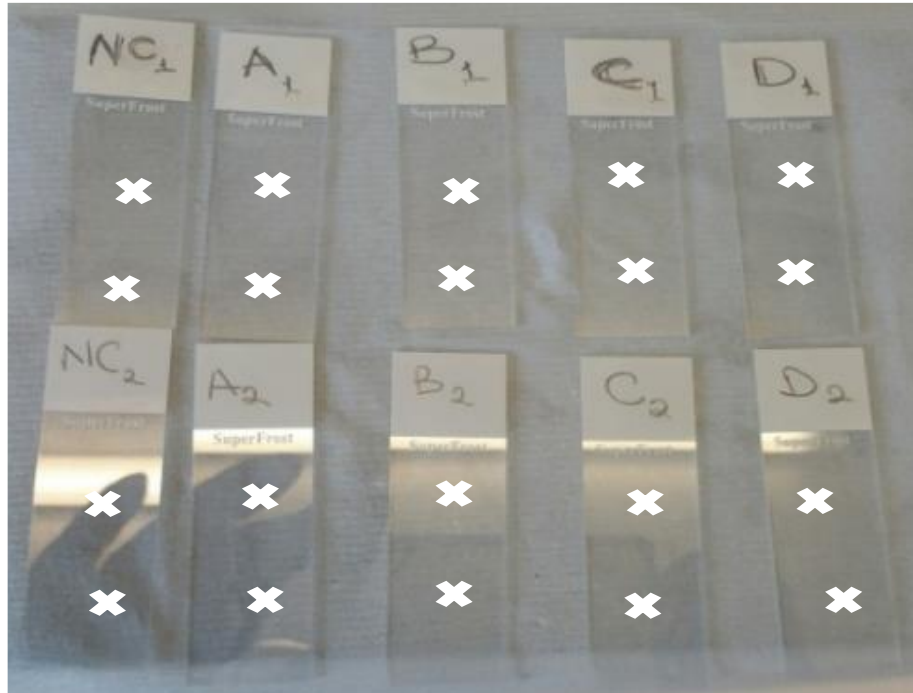


Figure 2.8: A schematic representation of duplicate slides with markings (x) indicating where 2 x 20 μ L of cell suspensions were added.

Thereafter, 2 x 20 μ L of the cell suspension were dropped onto pre-marked duplicate slides (**Fig. 2.8**) previously marked (x) 13 mm from the edges and 13 mm from the frosted end of the slide as shown above. The slides were left overnight to dry at RT before staining from the 6th day.

2.2.11.1.2.9 Giemsa Staining: Day 6

A volume of 200 mL of 5% Giemsa in Sorenson buffer was prepared fresh and filtered twice using Whatman[®] Filter papers (41, Ashless, Circles, 125 mm,

Whatman® Schleicher & Schuell). The slides were stained for 20 min in a Glass Coplin Staining Jar. Thereafter, the slides were rinsed with dH₂O for 2 min and allowed to air-dry overnight at RT before mounting glass coverslip on the 7th Day.

2.2.11.1.2.10 Slide Mounting: Day 7

After air-drying overnight, the slides were placed on a heat block (40°C), and 3 drops of DPX Mountant applied unto the slides using a plastic Pasteur pipette. The slides were covered with cover slips (24 x 50 mm²) and allowed to air-dry overnight at RT before being scored under the microscope from day 8.

2.2.11.1.2.11 Micronuclei (MNi) Scoring: From Day 8 onwards

On the 8th day, the slides were visualised under a digital microscope (AmScope; 40X-2500X; LED Digital Binocular Compound microscope) coupled with a camera (3D Stage + 3MP USB Camera, USA). For high powered magnification, a drop of immersion oil (339200-0010, Reactifs RAL, France) was dropped on the slides and viewed using the immersion Objective lens (x 100) and Eyepiece (x 10), (total magnification = 1,000). The frequencies of cytogenetic (chromosome aberration) parameters such as MNi, MonoNC, BiNC, MultiNC, NPBs and NBUDs were scored using hand-held tally counters. A minimum of 1,000 cells per treatment concentration (i.e. 500 cells per duplicate slide) were scored according to the criteria as described by Fenech (2007). Each experiment was repeated 5 times, comprising 5 experiments with 5 healthy blood samples; 5 experiments with 5 blood samples from asthma patients; 5 experiments with 5 blood samples from COPD patients; and 5 experiments with 5 blood samples from lung cancer patients.

2.2.11.1.2.12 Data Analysis

2.2.11.1.2.12.1 Calculation of Nuclear Division Index

The nuclear division index (NDI) – an indicator of cytostatic effect of GO - was calculated using the formula:

$$\mathbf{NDI} = \frac{M_1 + 2M_2 + 3M_3}{N}$$

Where M_1 = MonoNC; M_2 = BiNC; M_3 = MultiNC; and N = total number of viable cells scored (1,000) per concentration.

Other parameters scored were Mono with MNi, BiNC with MNi, BiNC with Buds, and BiNC with NPBs and values calculated as a percentage of the total number of cells scored (1,000).

2.2.11.1.2.12.2 Statistical Analysis

The data were expressed as the Mean \pm SEM, and statistical analysis performed using the GraphPad Prism[®] software, version 7.04 (Fay Avenue, La Jolla, CA, USA) with built-in One-Way ANOVA and Dunnett's post-hoc multiple comparison test to determine differences in the frequencies of cytogenetic parameters (MNi, MonoNC, BiNC, MultiNC, NPBs and NBUDs) in treated blood samples (healthy individuals and patients: asthma, COPD, and lung cancer) relative to the untreated, NC samples. Statistical significance was accepted at $p < 0.05$, where * = $p < 0.05$; ** = $p < 0.01$; *** = $p < 0.001$; and ns = not significant.

2.2.12 Gene Expression Assay using Reverse Transcription Quantitative Polymerase Chain Reaction (RT-qPCR)

2.2.12.1 Materials

Materials and equipment used in RT-qPCR are list in Sections 2.1.1 and 2.1.2 respectively.

2.2.12.1.1 Demographic Data of participants in RT-qPCR

Table 2-9: Demographic data of patients and healthy individuals used in RT-qPCR and Western Blotting methods (n=3)

No	Code/ Hospital Number	Age	Gender	Ethnicity	Smoking history
Healthy Individuals					
1	AM	45	F	Caucasian	Non-Smoker
2	WJ	47	M	Caucasian	Non-Smoker
3	AN	43	M	Caucasian	Non-Smoker
Asthma patients					
4	0809845	26	F	Caucasian	Non-Smoker
5	N/A	64	F	Asian	Non-Smoker
6	N/A	46	F	Asian	Non-Smoker
COPD patients					
7	N/A	58	M	Caucasian	Past Smoker
8	N/A	54	F	Caucasian	Past Smoker/ tobacco
9	0290072	57	M	Caucasian	Smoker; 30/day; alcohol
Lung Cancer patients					
10	N/A	55	F	Asian	Past Smoker
11	4360497856	57	M	Caucasian	Smoker; 30/day
12	0795624	65	M	Caucasian	30 pack/ year

2.2.12.2 Molecular Biology Methods for RT-qPCR

2.2.12.2.1 Extraction of Total RNA from human lymphocytes

Total RNA was isolated from peripheral blood lymphocytes from healthy individuals and patients (asthma, COPD, and lung cancer) after treatment with GO using the GenElute™ Mammalian Total RNA Miniprep Kit (Sigma, Aldrich, 2017) according to the manufacturer's instructions. Briefly, following treatment of isolated blood lymphocytes with GO (150, and 200 µg/mL) and NC in 6-well petri dishes, the cells were incubated in a cell culture Incubator (37°C, 5% CO₂) for 24 h. Thereafter, they were transferred to Eppendorf Tubes® in a sterile fume hood, centrifuged at a maximum speed (13,000 rpm; 14,243 x g) for 1 min to concentrate the cell. The supernatant RPMI medium was completely removed and cells placed on an ice tray in the sterile fume hood. A volume of 500 µL of RNA Lysis Solution mixture (**Appendix 10**) was added and cells sheared (x 10) using a 20-G insulin needle. Thereafter, they were transferred into a filtration column assembled with a collection tube, followed by centrifugation at a maximum speed (13,000 rpm; 14,243 x g) for 2 min using a Micro Centaur Centrifuge (MSE UK, Ltd). The filtration Column was discarded, and the lysate retained in the collection tube. An equal amount of 70% ethanol (500 µL) was added into the lysate, and the mixture mixed thoroughly with a vortex mixer. From the Lysate/Ethanol mixture, 700 µL was transferred into a DNA binding Column assembled with a Collection tube. The cells were centrifuged to the maximum speed (13,000 rpm; 14,243 x g) for 15 sec and the flow-through liquid discarded while the binding column and the collection tube retained. The process was

repeated if the Lysate/Ethanol mixture was > 700µL. Three column washes were performed to remove contaminants.

2.2.12.2.1.1 First Column Wash

500 µL of Wash Solution 1 was added to the binding column and centrifuged to the maximum speed (13,000 rpm; 14,243 x g) for 15 sec. The flow-through liquid and the collection tube were discarded, and the binding column transferred into a new collection tube.

2.2.12.2.1.2 Second Column Wash

500 µL of diluted Ethanol/Wash Solution 2 Concentrate/ mixture was added into the binding column, and centrifuged to the maximum speed (13,000 rpm; 14,243 x g) for 15 sec. The flow-through liquid was discarded, and the collection tube retained.

2.2.12.2.1.3 Third Column Wash

The step under the second column wash was repeated, by adding 500 µL of diluted Ethanol/Wash Solution 2 Concentrate mixture into the binding column and centrifuged to the maximum speed (13,000 rpm; 14,243 x g) for 2 min.

2.2.12.2.1.4 Optional Spin (to dry the column)

The binding column should be free of ethanol before RNA elution. The column was centrifuged at the maximum speed (13,000 rpm; 14,243 x g) for 1 min.

2.2.12.2.1.5 Elution of Pure RNA

The binding column was transferred into pre-labelled new collection tubes, and 50 μL of Elution Solution pipetted, followed by maximum centrifugation (13,000 rpm; 14243 x g) for 1 min. The purified RNA was eluted (approx. 45 μL) and then stored at - 80°C for future analysis.

2.2.12.2.2 Quantification of RNA concentrations and purity

The frozen RNA samples were thawed on ice, and the concentrations and purity quantified using BioDrop™ Touch Duo Spectrophotometer (BioDrop Ltd, Cambridge, UK) according to the manufacturer's instructions.



Figure 2.9: BioDrop™ Touch Duo Spectrophotometer (BioDrop Ltd 2012)

Briefly, the BioDrop™ equipment was cleaned with 15 μL RNA Elution solution and then calibrated with the same solution. Small volumes of 2 μL of isolated RNAs were dropped onto the optical, pedestal/ measurement surface, and the concentrations (ng/ μL) and purity (ratio of A_{260}/A_{280}) quantified automatically.

2.2.12.2.3 Primer Design

All Primers in Table 2-10 were designed online using basic bioinformatics from Sigma-Aldrich's KiCqStart™ Primers software (Sigma-Aldrich 2013) and Ensemble's website (Ensembl 2019) (see **Figure 2.10**).

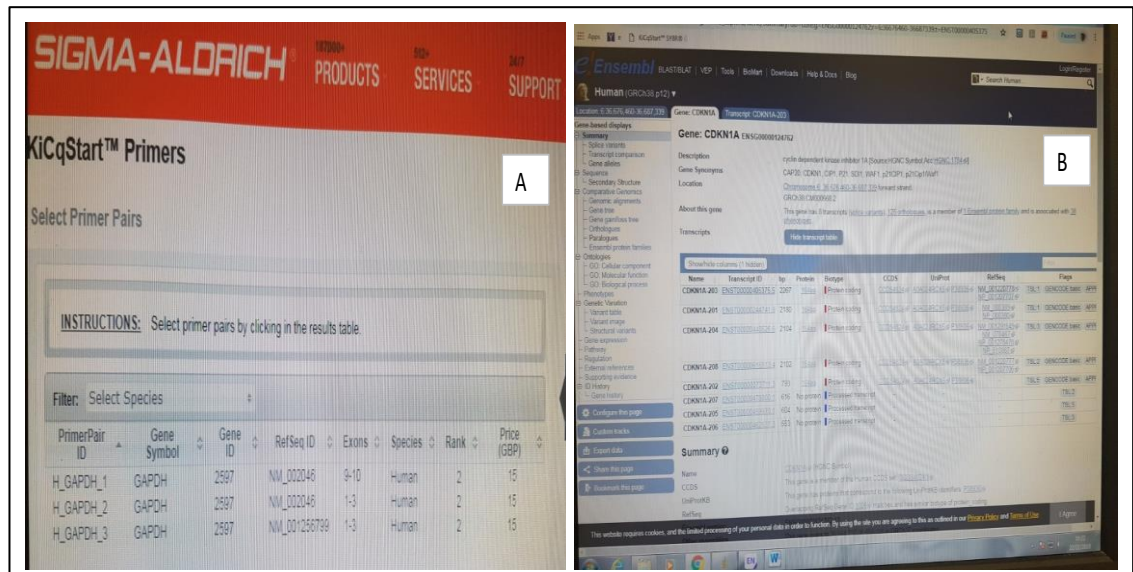


Figure 2.10: Primer design websites: (a) KiCqStart™ (Sigma-Aldrich), and (b) Ensembl website.

Subsequently, the primers were ordered from Sigma-Aldrich (Gillingham, UK). Once they were received, the primers were reconstituted with Nuclease Free Water (NFW) to a final concentration of 100 μ M using the Technical Datasheet that came with the order (Sigma Aldrich, UK, BIN No: 1137).

Table 2-10: Detailed information of the Human Primers used in RT-qPCR, including their sequences (5'-3'), length, conc. (nmol), volume of nuclease free water (μ L) added to reconstitute each primer to 100 μ M and their annealing temperatures

Oligo Name	Cat No (Gene Bank Accession)	Primer design	Human Primers	Primer Sequences (5'-3')	Length	Conc. (nmol)	μ L for 100 μ M	Annealing Temp ($^{\circ}$ C)
FH1_TP53	NM_000546	H_TP53_1	Forward Human 1 TP53	ACCTATGGAACTACTTCCTG	21	70.8	707	56.4
			Reverse Human 1 TP53	ACCATTGTTCAATATCGTCC	20	71	710	58.7
FH1_BCL2	NM_000633	H_BCL2_1	Forward Human 1 BCL2	GATTGTGGCCTTCTTTGAG	19	63.7	637	59.8
			Reverse Human 1 BCL2	GTCCACAAAGGCATCC	17	61.8	617	59
FH1_CDKN1A	NM_000389	H_CDKN1A_1	Forward Human 1 CDKN1A	CAGCATGACAGATTCTACC	20	62.1	621	57.3
			Reverse Human 1 CDKN1A	CAGGGTATGTACATGAGGAG	20	58.8	588	57
FH1_GAPDH	NM_002046	H_GAPDH_1	Forward Human 1 GAPDH	ACAGTTGCCATGTAGACC	18	63.1	631	55.7
			Reverse Human 1 GAPDH	TTGAGCACAGGGTACTTTA	19	57.6	576	55.8

2.2.12.2.4 Reverse Transcription

Isolated RNA was reverse-transcribed into the first-strand complementary DNA (cDNA) using the ImProm-II™ Reverse Transcription System (Promega, USA) according to the manufacturer's instructions. The cDNA reactions were performed with Reverse Transcription mixtures in Table 2-11 and Table 2-12 using the PCR Sprint Thermal Cycler (Thermo Electron Corporation, USA).

2.2.12.2.4.1 Priming with RNA or Oligo (dT)₁₅ Primers

To prepare for the first-strand cDNA synthesis of TP53, CDKN1A, BCL-2, and GAPDH genes, a primer mixture (Mixture No. 1) was prepared using the components in Table 11-12.

Table 2-11: Mixture No. 1: Priming with RNA or Oligo (dT)₁₅ Primer

Priming with isolated RNA			
Description	Volume	Thermal Cycler settings	
Random Hexamer Primer (0.5 µg/µL)	2 µL	Temp.	Time
Isolated Total RNA (1 µg)	8 µL	70 °C	5 min
Total volume	10 µL		

No Template Control priming with Oligo (dT) ₁₅ Primer			
Description	Volume	Thermal Cycler settings	
Oligo (dT) ₁₅ Primer	2 µL	Temp.	Time
Nuclease Free water (NFW)	8 µL	70 °C	5 min
Total volume	10 µL		

Briefly, 2 µL of Random Hexamer Primers (0.5 µg/µl) was mixed with 8 µL of isolated total RNA (1 µg) from healthy individuals and patients (asthma, COPD, and lung cancer) in sterile micro Eppendorf® tubes for each of the genes of interest. For “No Template Control” as the negative control, 2 µL Oligo (dT)₁₅ Primer was mixed with 8 µL of NFW in micro Eppendorf® tubes. Thereafter, they were heated in the PCR Sprint Thermal Cycler (pre-programmed code: A:32 CDNA1) at a temperature of 70°C for 5 min in order to denature and inactivate the RNA. During the 5 min of priming, the Reverse Transcription Mixture (Mixture No. 2) was prepared (See Table 2-12).

2.2.12.2.4.2 Preparation of Reverse Transcription Mixture

Using Table 2-12 below, the Reverse transcription mixture (Mixture No. 2) was prepared in ice cold conditions in a sterile Fume Cupboard.

Table 2-12: Mixture No. 2: Components of Reverse Transcription mixture

Reverse Transcription Mixture		Volume
ImProm-II™ 5 x Reaction buffer		4.0 µL
25mM MgCl ₂		2.4 µL
dNTPs (10 mM)		1.0 µL
NFW		1.1 µL
Recombinant RNasin® (Ribonuclease Inhibitor)		0.5 µL
Improm II RT (Reverse Transcriptase)		1.0 µL
	Total volume	10 µL

Briefly, 4 µL of ImProm-II™ 5 x Reaction buffer was mixed with 2.4 µL of MgCl₂ (25mM), 1 µL of dNTPs (10 mM), 1.1 µL NFW, and 0.5 µL Recombinant RNasin - a Ribonuclease Inhibitor. Finally, a volume of 1 µL of Improm II RT (Reverse Transcriptase) enzyme was added last and the next step, cDNA synthesis, commenced immediately.

2.2.12.2.4.3 Synthesis of Complementary DNA (cDNA)

The Reverse transcription Mixture (Mixture No.2: Table 2-12) was added to Mixture 1, making a total volume of 20 µL reaction mixture. Using the PCR Thermal Cycler (pre-programmed code: A:34 CDNA2), the synthesis of cDNA was performed using the cycling conditions in Table 2-13 below:

Table 2-13: Cycling Conditions for the Synthesis of cDNA

Description	Temperature	Time (min)
Annealing	25°C	5
Extension/cDNA synthesis	42°C	60
Enzyme inactivation	70°C	15


Briefly, the reaction mixtures were incubated at 25°C for 5 min; 42°C for 60 min; and finally, at 70°C for 15 min. Thereafter, the synthesized cDNA (20 µL) was stored at -20°C till when required for qPCR analysis.

2.2.12.2.5 Quantitative Polymerase Chain Reaction (qPCR)

The qPCR assays were performed using qPCR CT000 Touch™ Thermal Cycler (CFX96™ Real-Time System, Bio-Rad). The assays were performed in triplicate, each containing 20 µL reaction mixtures in 96-well Optical reaction plates covered with MicroAmp™ Optical Adhesive films (MicroAmp™ Optical Adhesive Film Kit, Applied Biosystems by Thermo Scientific) following Table 2-14 provided (see page 80).

Table 2-14: qPCR Reaction Mixture (20 μ L) and a photo of a 96-Well plate used for qPCR analysis

20 μ L RT-qPCR Reaction Mixture	
Components	Volume per 20 μ L Reaction
iQ™ SYBR® Green Supermix	10 μ L
Forward primer	0.5 μ L
Reverse Primer	0.5 μ L
DNase/RNase Free water (D/RFW)	4.0 μ L
DNA template (cDNA) (1:10 dilution with DNase/RFW)	5.0 μ L
Final volume of mixture	20 μ L



Each reaction well contained 10 μ L of iQ™ SYBR® Green Supermix (containing SYBR® Green I, enhancers, stabilizers, and fluorescein; iTaq™ DNA Polymerase; MgCl₂; and dNTPs) (Bio-Rad, USA); equal amounts (0.5 μ L) of Forward and Reverse primers of the target genes (BCL-2, CDKN1A, TP53, and GAPDH), 4 μ L of D/RFW, and 5 μ L cDNA template, diluted 1:10 with D/RFW (i.e. 10 μ L of cDNA + 90 μ L of D/RFW). The Human 1 GAPDH was used as an internal control (housekeeping) gene to normalize the test genes of interests. First, the qPCR Thermal Cycler was programmed with annealing temperatures corresponding to the lanes (**E, F, G, H**) of the 96-well plate containing the respective genes, where **Lane E** = BCL-2 (59.7°C); **Lane F** = CDKN1A (57.7°C); **Lane G** = TP53 (56.4°C); and **Lane H** = GAPDH (55.7°C). The reaction mixtures were transferred in triplicate (**NC**: 1, 2, and 3; **150 μ g/mL**: 5, 6, and 7; and **200 μ g/mL**: 9, 10, 11), and sealed with optical films.

Table 2-15: qPCR Thermal Cycling Conditions

Stage	No. of cycles	Steps	Temperature	Time
1	1	Initial template (cDNA) denaturation /polymerase enzyme activation	95°C	30 s
2	40 x	Denaturation/ PCR/Analysis mode	95°C	5 s
		Data Collection	55.7 °C	30 s
3	1	Melt Curve	65°C	2 s
			60°C	60 s
			95°C	15 s

The 96-well optical reaction plates were loaded into the qPCR Thermal cycler preheated to 105°C. qPCR reactions were performed using the thermal cycling conditions above (see Table 2-15). Briefly, the reactions were denatured in one cycle at 95°C for 30 sec and polymerase enzyme activated, and subsequently 40 cycles of denaturation/qPCR analysis at 95 °C for 5 sec and data collection at 55.7°C for 30 sec using qPCR CT000 Touch™ Thermal Cycler (CFX96™ Real-Time System, Bio-Rad). Finally, a Melt Curve was performed at 65°C for 2 sec, 60°C for 60 sec, and 95°C for 15 sec.

2.2.12.2.6 Gene Expression Data Analysis

The RT-qPCR data obtained from each reaction step was analysed using the relevant software (CFX Manager™ Software, version 3.1; Bio-Rad, CA, USA). The quantitative cycles (**Cq**) of samples with the highest cDNA template are expressed first towards the left-hand of the amplification curve, while samples

with lower cDNAs are expressed later towards the right of the curve (see **Figure 2.11**).

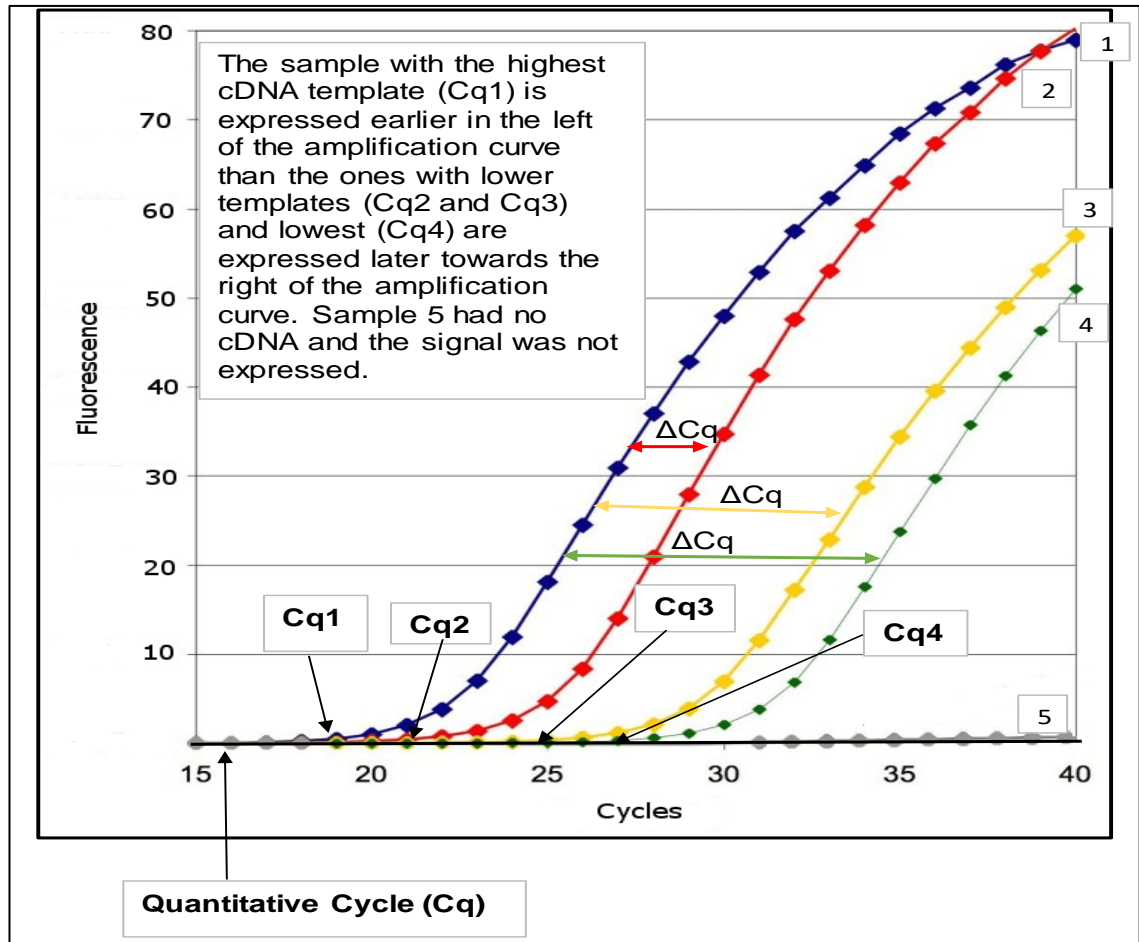


Figure 2.11: Representative example of an amplification plot of 5 samples (1,2,3 and 4). As the cDNA is amplified in the samples, their fluorescence increased. In this plot, sample 1 had the highest amount of cDNA → ↑RNA, and their fluorescence was quickly expressed. On the other hand, sample 4 had the lowest amount of cDNA → ↓RNA, and their fluorescence was expressed last, while sample 5 had no cDNA template and fluorescence was not expressed (BioSistemika 2017).

The relative quantification method, the **Double-Delta Cq ($\Delta\Delta Cq$) (Livak)**

Method: $2^{-\Delta\Delta Cq}$ (Livak and Schmittgen 2001) was used to determine differences in fold-change of genes of interest (GOI) - TP53, CDKN1A, and BCL2 - relative to reference/ housekeeping gene (GAPDH), where Cq = quantitative cycles; ΔCq

= difference in Cq of GOI and GAPDH reference gene; and double-delta Cq ($\Delta\Delta Cq$) = difference in ΔCq of treated samples relative to untreated, NC samples.

2.2.12.2.6.1 Calculation of Relative Gene Expression or Fold-Change using the Double-Delta ($2^{-\Delta\Delta Cq}$) (Livak) Method

The gene expression of TP53, CDKN1A, and BCL-2 genes relative to reference GAPDH gene and untreated samples were calculated as follows:

1. The GOI:

1.1.1 The Cq values of treated samples (TP53, CDKN1A, BCL-2)

1.1.2 The Cq values of controls (untreated, control samples)

2. The Housekeeping, reference genes (GAPDH):

2.1.1 The Cq values of GAPDH (treated samples)

2.1.2 The Cq values of GAPDH (untreated, control samples)

Four further steps were used to calculate Fold Change expression.

2.2.12.2.6.2 Calculation of Average Cq values from triplicate results

The average Cq values of TP53, CDKN1A, BCL2 and GAPDH from the three different concentrations (0, 150 $\mu\text{g/mL}$, and 200 $\mu\text{g/mL}$) for each treatment group (healthy, asthma, COPD, and lung cancer) were calculated and used for normalization (ΔCq).

2.2.12.2.6.3 Normalization (ΔCq) of GOI relative to reference gene

The GOI were normalized (ΔCq) with the reference gene by subtracting the Cq of GAPDH from Cq of target genes (Applied Biosystems 2008). Thus,

$\Delta Cq = Cq$ [Target gene (TP53, CDKN1A, BCL2)] - Cq [Housekeeping gene (GAPDH)].

2.2.12.2.6.4 Normalisation ($\Delta\Delta Cq$) of treated samples (ΔCq) relative to untreated samples (ΔCq)

Treated samples were normalized ($\Delta\Delta Cq$) relative to untreated samples by subtracting the ΔCq of untreated samples (Control) from the ΔCq of treated samples. Thus,

$$\Delta\Delta Cq = \Delta Cq (\text{Treated}) - \Delta Cq (\text{untreated/Control}).$$

1.1 For normalisation of untreated, Control samples:

$$\Delta\Delta Cq (\text{untreated, Control}) = \Delta Cq (\text{untreated, Control}) - \Delta Cq (\text{untreated, Control}) = 0.$$

1.2 For Normalisation of treated samples with the untreated, Control samples:

$$\Delta\Delta Cq (\text{treated samples}) = \Delta Cq (\text{treated}) - \Delta Cq (\text{untreated, Control}).$$

Note:

The $\Delta\Delta Cq$ of the control was set at 0 since the values in 1.1 above cancel out each other.

2.2.12.2.6.5 Calculation of Fold-differences ($2^{-\Delta\Delta Cq}$)

Finally, the fold-change in gene expression was evaluated in Excel package using the Livak formula for gene expression = $2^{-\Delta\Delta Cq}$. The data obtained enabled the

comparison in gene expression of TP53, CDKN1A, and BCL-2 genes in treated samples relative to untreated control samples ($2^{-\Delta\Delta Cq} = 1$).

2.2.12.2.6.6 Statistical Analysis

The significance of the Fold-differences was performed using GraphPad Prism® software, version 8.1.2 (332) (Fay Avenue, La Jolla, CA, USA) with built-in One-Way ANOVA and Dunnett's post-hoc multiple comparison test to determine differences in gene expressions of TP53, CDKN1A, and BCL-2 genes in treated samples (150 and 200 µg/mL of GO NMs) in healthy individuals and patients (asthma, COPD, and lung cancer) relative to the untreated negative control samples in three independent experiments ($2^{-\Delta\Delta Cq}$), n= 3 per sample. Statistical significance was accepted at $p < 0.05$, where * = $p < 0.05$; ** = $p < 0.01$; *** = $p < 0.001$; and ns = not significant.

2.2.13 Protein Expression using Western Blot (WB) Method

2.2.13.1 Materials

Materials and equipment used in WB analysis are list in Sections 2.1.1 and 2.1.2 respectively, while Buffers and mixtures are in **Appendix 11**.

2.2.13.1.1 Demographic Data of participants used in WB analysis

The demographic data, containing Age, Gender, Ethnicity and Smoking history of blood donors used in WB method are listed in Section **2.2.12.1.1**.

2.2.13.2 Molecular Biology Methods in WB

Human PBL were isolated as previously described (Section 2.2.5.1). Cell counts to determine lymphocyte concentrations and cell viability were also performed as

previously described (Sections 2.2.5, 2.2.6, and 2.2.7). The lymphocytes were treated with different concentrations of GO (10, 20, 50 and 100) as previously described in Section 2.2.9.1.2.2. Subsequently, we had enormous difficulties detecting induced proteins of interest at lower non-toxic concentrations. Therefore, the treatment concentrations were increased to 150 µg/mL and 200 µg/mL, respectively to show if they correspond with toxic concentrations.

2.2.13.2.1 Protein Extraction

After 24 hours of incubation, the cells were transferred into Eppendorf® tubes and centrifuged (1,000 rpm; $\approx 418 \times g$) for 5 min to concentrate the cells. The RPMI medium was discarded and cells treated with 100 µL of Halt™ Protease and Phosphatase Inhibitor Cocktail, EDTA-Free (Thermo Scientific). An equal volume 100 µL of Pierce™ Radioimmunoprecipitation assay (RIPA) Buffer (25mM Tris-HCl pH 7.6, 150mM NaCl, 1% NP-40, 1% sodium deoxycholate, and 0.1% SDS, Thermo Fisher) was added. The inhibitor cocktail was added to prevent proteolysis and maintain the phosphorylation status of proteins. The solution was mixed thoroughly with vortex mixer, and then left in ice or refrigerator (4°C) for 60 min. Thereafter; they were sonicated (3-5 pulses with 20% intensity) for about 10-20 seconds. The proteins and DNA were further lysed by shearing with a $28\frac{1}{2}$ Gauge insulin syringe x 10 each, and then centrifuged at maximum speed (13,000 rpm; $14,243 \times g$) for 5 min using a Micro Centaur Centrifuge (MSE UK, Ltd) to concentrate the pellets. The supernatant containing the extracted protein was carefully transferred into new Eppendorf® tubes and stored at -20°C for future use.

2.2.13.2.2 Determination of Protein Concentrations

Protein concentrations were measured using the Quick Start™ Bradford Protein Assay kit 2 (Bio-Rad, USA) – a colorimetric assay kit, consisting of 1 x Dye Reagent (1L) and Quick Start™ Bovine Serum Albumin (BSA) standard sets (2 x 2 mL) of 7 standard BSA concentrations (0.125, 0.250, 0.5, 0.750, 1.00, 1.5 and 2 mg/mL) (Bradford 1976). Briefly, 5 µL of each of the BSA concentrations were pipetted in triplicate in a 96-well plate, followed by the addition of 5 µL of the extracted proteins into the BSA-containing wells. A volume of 250 µL of the 1 x Dye Reagent was added to each well.

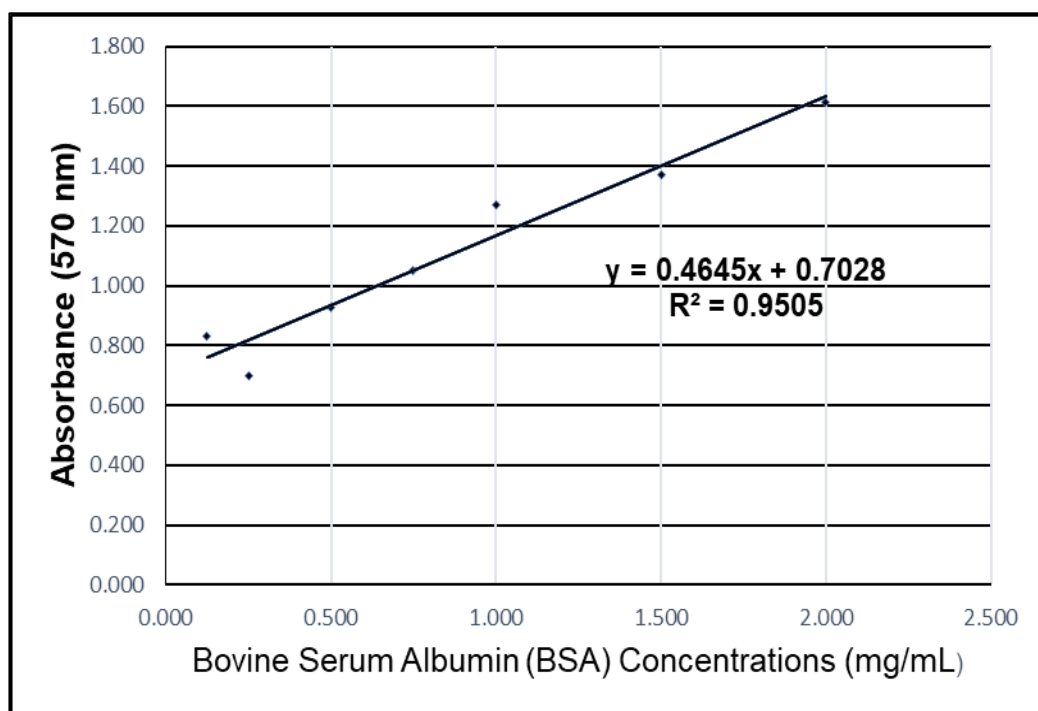


Figure 2.12: Calibration curve obtained using the Bradford assay at 595 nm. Linear regression analysis gives a straight line with $R^2 = 0.9505$

The mixtures were mixed thoroughly with pipette tips and incubated at RT for 60 min. Thereafter, the absorbance was read at 595 nm using a spectrophotometer (Multiscan™ FC Microplate reader, Thermo Fisher Scientific), and BSA protein

concentration standard curves were plotted using Microsoft Excel (**Fig. 2.12**). A straight-line equation, $y = mx + c$, was obtained (where y = absorbance (on y-axis), m = gradient, x = unknown protein concentration, and c = intercept on y-axis).

2.2.13.2.3 Preparation of Sodium Dodecyl Sulfate-Polyacrylamide Gel

Electrophoresis (SDS-PAGE)

2.2.13.2.3.1 Preparation of 12.5% Resolving Gels

Sodium Dodecyl Sulphate-Polyacrylamide Gels were prepared using the table below:

Table 2-16: Reagents for the preparation of Resolving and Stacking Gels

Reagents	Resolving Gel (12.5%; pH 8.8) (2 x 4.5 mL)	Stacking Gel (6%; pH 6.8) (2x 1.25 mL)
Deionised water (dH ₂ O)	3.5 mL	2.1 mL
Acrylamide: Bis-acrylamide (30%)	4.0 mL	630 µL
1.5 M Tris-HCl (pH 8.8)	2.5 mL	---
0.5 M Tris-HCl (pH 6.8)	---	1.3 mL
SDS (10%)	100 µL	1,000 µL
APS (10%)	100 µL	50 µL
TEMED (add last)	15 µL	7.5 µL
Total	10,215 µL	5,087.5 µL

The glass plates were cleaned with 70% ethanol and the WB kits assembled according to the manufacturer's guidance (Bio-Rad). Briefly, the thin, short plates were placed in the front of the thick, spacer plates and both held in place with 2

green plate holding racks, balanced on a flat surface, and the clamps closed as illustrated in **Figure 2.13 (Images A-D)**.

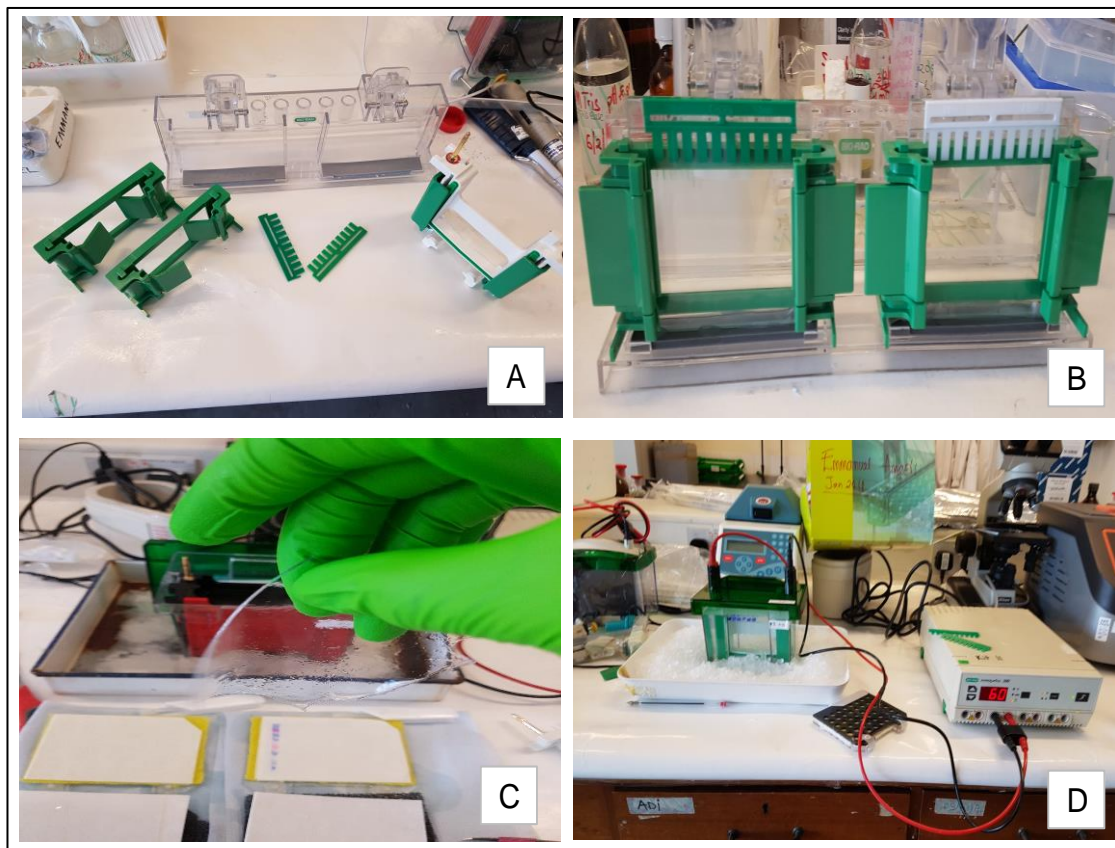


Figure 2.13: Photographic images taken during Western Blot analysis

Subsequently, they were held in position with Perspex Rack holder (image B). To ensure the assembly was air-tight, a piece of cellophane was used to seal the bottom of the plates, followed by addition of 1 mL of water in between the glasses to check for any leakage. The Resolving Gels with higher concentration of polyacrylamide (12.5%) and higher pH of 8.8 were prepared in excess by mixing the reagents optimized in the order shown in Table 2-16 and mixed with a vortex mixer (except TEMED, which was added last). Prior to pouring the gel, 15 μ L of TEMED was added into the solution and mixed thoroughly with a vortex mixer.

Thereafter, using a 5 mL pipette, 4.5 mL of the Resolving Gels were gently introduced between the 2 pairs of glass plates, followed by addition of 1 mL of dH₂O on top of each Resolving Gel to remove excess gel and level up. They were allowed to polymerise at RT for 45 min.

2.2.13.2.3.2 Preparation of 6% Stacking Gels

The purpose of the staging gels is to stack all the proteins to a narrow band so that they all enter the resolving gel almost at the same time. The stacking gels with lower polyacrylamide concentration (6%) and lower pH of 6.8 were prepared by mixing the reagents optimized in the order shown in Table 2-16 and mixed with a vortex mixer (except TEMED which was added last). Prior to pouring the gel, 7.5 µL of TEMED was added into the solution and mixed thoroughly with a vortex mixer. Thereafter, 1.25 mL of the Stacking Gels were gently introduced onto the Resolving Gels and 2 combs inserted immediately, one to each gel and then allowed to polymerise at RT for 45 min.

2.2.13.2.4 Loading Proteins and SDS-PAGE Electrophoresis

Prior to loading proteins onto the SDS-PAGE, equal volume of protein solution was mixed (1:1) with equal amount of x 2 Laemmli buffer (**Appendix 11**). The mixture was heated in a boiling water-bath at 85-100°C for 5-10 min to denature the proteins, and then immediately kept on an ice tray before use. The plates-containing gels and combs were transferred to the electrode and carefully closed and then transferred to the electrophoresis tank (Bio-Rad). Thereafter, 1 Litre of cold running buffer (**Appendix 11**) was poured into the WB tank, first into the inner compartment between 2 two short plates to check for any leakage. A

volume of 7.5-15 μL of a molecular weight marker [a mixture of recombinant proteins from 10-250 kDa with 8 blue stained bands and 2 pink Reference bands at 25 and 75 kDa (Precision Plus Protein™ Dual Colour Standards, Bio-Rad)] was loaded to the first well of each gel. Thereafter, equal amounts of protein (20-40 μg) were loaded into separate wells, and the electrophoresis tank closed with a lid containing two coloured electric cables connected to the power supply (black-to-black and red-to-red). The gel electrophoresis was performed, first at a lower voltage of 50 V for 5 min to stack the proteins, and thereafter the voltage was increased to 200 V to finish the run in 60 min.

2.2.13.2.5 Protein transfer to PVDF membrane

Following protein electrophoresis, the proteins were transferred from the SDS-PAGE gel to PVDF blot membrane (Amersham™ Hybond™, 0.45 μM , GE Healthcare Life Sciences, Germany). Briefly, two PVDF membranes were cut to the size of the gels and a notch made at the top right-hand corner to mark the orientation of the active face of the membrane. They were activated in methanol (10 mL) for 10 min and excess methanol washed off with dH_2O (10 mL) for 10 min. Thereafter, the membranes and four filter papers cut to the size of the gels were transferred to a tray containing transfer buffer (**Appendix 11**) for 10 min. During this period, the membrane sandwich was prepared in a cassette with the PVDF membranes on the **Anode (+)** end and the gel on the **Cathode (-)** end. The negative charged electric current flows from the Cathode to the anode. From the **White Cover** (Anode side): Sponge, 2 filter papers, PVDF membrane, gel, 2 filter papers, sponge, and the **Black Cover** (Cathode). Thereafter, bubbles were removed by pressing a roller on the sandwich, and the cassette transferred

to the WB tank containing transfer buffer and ice block pack, and the tank placed in a tray with ice blocks. Protein transfer was run at 100 V and 10 mA current for 60 min.

2.2.13.2.6 Blocking of unbound Proteins

After blotting, the cassette was removed and the 2 PVDF membranes incubated in a 10 mL of blocking buffer (either 5% BSA in TBST or 5% NFDM in TBST) (**Appendix 11**) for 1 h at RT with gentle agitation in an Orbital shaker set at an appropriate speed.

2.2.13.2.7 Incubation with Primary Antibodies

Following blocking of unbound proteins, the blocking buffer was discarded, and the blots washed (3 x for 5 min each) in cold TBST buffer with gentle agitation in an Orbital Shaker set at an appropriate speed. Thereafter, they were sequentially treated with 5 - 7.5 μ L of different primary anti-bodies [p53 (1:1,000 dilution); p21 (1:2,000 dilution); BCL-2 (1:500 dilution), and GAPDH (1:10,000 dilution)] in 10-15 mL of 5% BSA in TBST according to manufacturer's recommendations (Abcam, UK). They were incubated overnight at 4°C, with gentle agitation in an Orbital shaker set at an appropriate speed.

2.2.13.2.8 Incubation with Secondary Antibody

The following day, the blots were washed (3 x for 5 min) with freshly prepared 5% BSA in TBST buffer. They were incubated with 5 - 7.5 μ L of secondary antibody, conjugated with horseradish peroxidase (HRP) [either a monoclonal Anti-Rabbit IgGVHH Single Domain Anti-body (HRP) (1:1,000 dilution) or Goat Anti-Rabbit

IgG H&L Anti-body (1:2,000 to 1:50,000 dilution)] in 10-15 mL of 5% BSA in TBST. They were incubated for 1 h at RT according to manufacturer's recommendations (Abcam, UK) with gentle agitation in an Orbital shaker set at an appropriate speed. Thereafter, the blots were washed (3 x for 5 mins each) in cold TBST buffer under gentle agitation in an Orbital shaker.

2.2.13.2.9 Detection of proteins with Chemiluminescent Substrate

The chemiluminescent substrates were applied to the blots according to the manufacturer's recommendations (Bio-Rad, UK). Briefly, 5-10 mL of enhanced chemiluminescent substrates (Clarity™ Western ECL, ECL1 + ECL2), containing peroxide and Luminol/ Enhancer Reagents (Bio-Rad, UK) were mixed (1:1) and incubated with the blots for 5 min.

Following the manufacturer's instructions, the blots were transferred to a plastic laminate to avoid drying with the blots facing upwards. The bands were captured automatically using G:Box i Chemi XR Software (GENESys, UK). The blots were mildly stripped and re-probed with multiple primary antibodies, and the steps from incubation to detection repeated for each anti-body of interest.

Chapter 3: Particle Characterization

3.0 Characterization of GO nanomaterials

3.1 Introduction

Particle characterization was performed for DLS and ZP to determine the nanomaterial physical properties in aqueous dispersion including particle distance, shape, surface charge, and polydispersity indices (monodispersity or polydispersity) - a measure of particle size heterogeneity in the medium; and their behaviour in the dry state measured using SEM and TEM.

3.2 Materials

All chemicals and equipment used in particle Characterization are listed in Chapter 2, Sections 2.1.1 and 2.1.2 while GO properties were listed in (Section 2.2.8.1; Table 2-3).

3.3 Methods

The methods used to characterize GO were described in Section 2.2.8.1.2 (DLS); Section 2.2.8.1.3 (Zeta Potential); Section 2.2.8.1.4 (SEM), and Section 2.2.2.8.1.5 (TEM), respectively.

3.4 Results

3.4.1 Agglomeration state / particle size distribution and Zeta Potential (Surface charge) analyses

In this study, we characterized GO NMs for DLS and ZP to determine the agglomeration state / particle size-distribution and surface charge in aqueous solution. The results are shown in

Table 3-1; Figure 3.1 (DLS) and Figure 3.2 (ZP). For the size-distribution, we observed that GO NMs were well dispersed after gentle shaking before the experiment, but gradually agglomerated at the base of the cuvette over time. The average hydrodynamic size (Z-Average (d.nm)) range of each single layer of GO NMs was 35 - 54 nm, while an agglomerate has particle size range from 693.8 to 806.1, a confirmation that the GO NMs used in the study have multiple-layered structure (15-20 sheets); polydispersity indices (Pdl) between 0.768 and 0.92, and surface charges (ZP) between -26.1 mV and -21.7 mV. These data were consistent with work done by others which demonstrated that the ZP of Graphite Carbon nanofibers (GCNF), a member of the GFNM has ZP of -29.7 mV (Mittal et al. 2017). Another researcher elsewhere used GO synthesized in-house, with a 1-2 double-layered structure and found that the average diameter using DLS was 156.4 nm (Liu et al. 2013b), equivalent to 78.2 nm per sheet

Table 3-1: Characterization of GO showing agglomeration states (Z-Average): hydrodynamic diameter (nm), Polydispersity Index and surface charge (Zeta Potential) in aqueous solution assessed using DLS. Particle size range = 693.8 to 806.1 nm; and Zeta Potential = - 21.7 to - 26.1 mV.

No. of Experiments	Dispersant	Agglomeration State: Z-average hydrodynamic diameter (nm)			Polydispersity Index (Pdl)	Surface Charge: Zeta potential (mV)
		15-20 sheets	Size per nano sheet			
Exp. 1	dH ₂ O	806.1	40	54	0.768	-26.1
Exp. 2	"	779.1	38	52	0.899	-21.7
Exp. 3	"	693.8	35	46	0.929	N/A

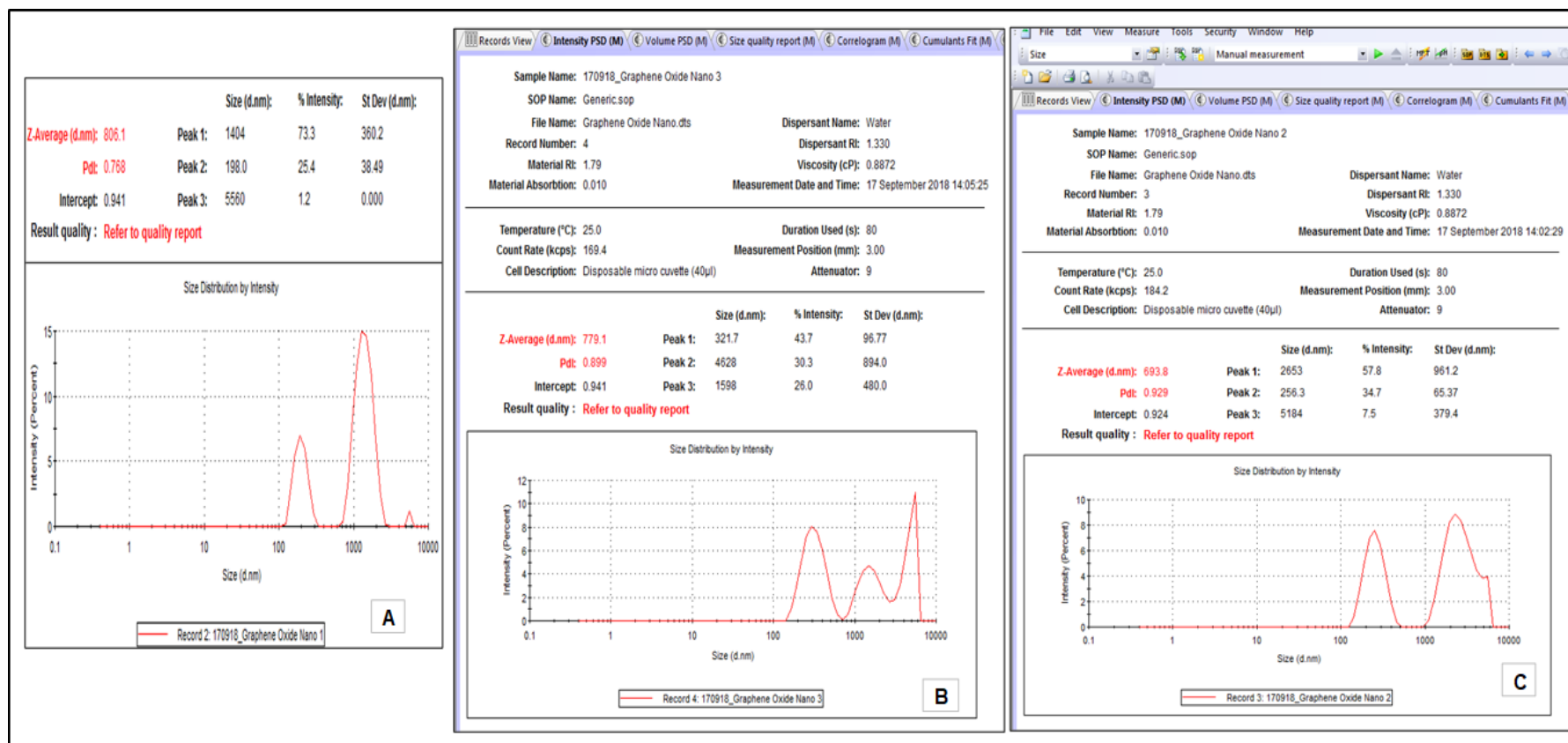


Figure 3.1: Measurement of particle size-distribution (hydrodynamic diameter) by DLS (size vs. intensity) using Zetasizer Nano ZS-90, Model ZEN3600 (Malvern Instruments Ltd, UK). Average particle size of GO (15-20 sheets), Z-Average (d.nm): **A** = 806.1 nm, PDI = 0.768; **B** = 779.1 nm, PDI = 0.899; and **C** = 693.8 nm, PDI = 0.929. Abbreviations: Z-Average = average size; d.nm = diameter; and Pdl = polydispersity index.

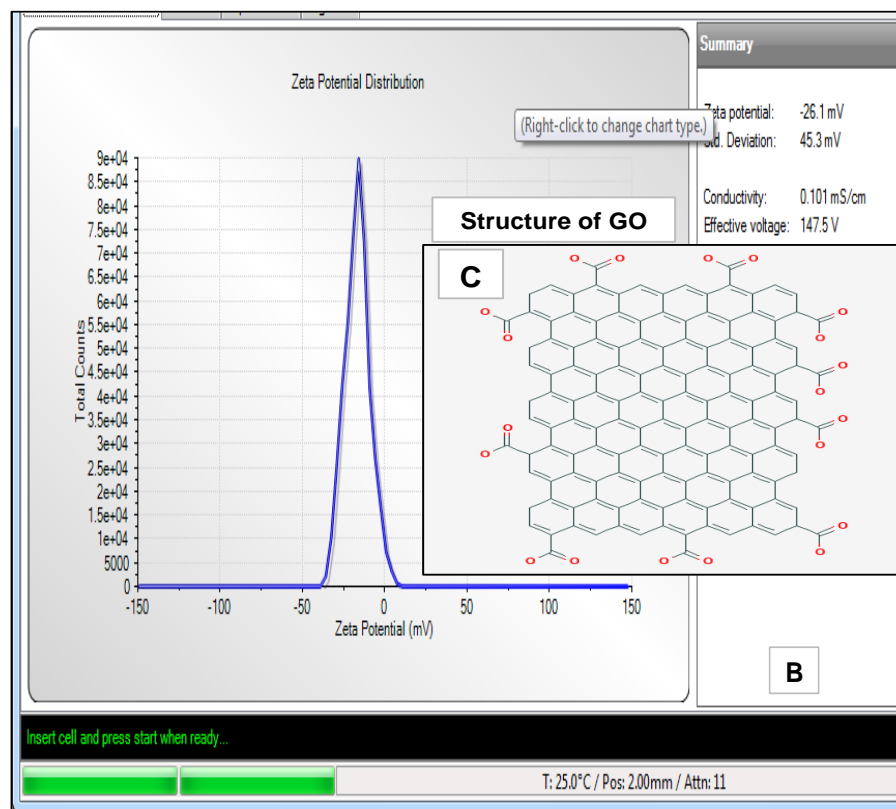
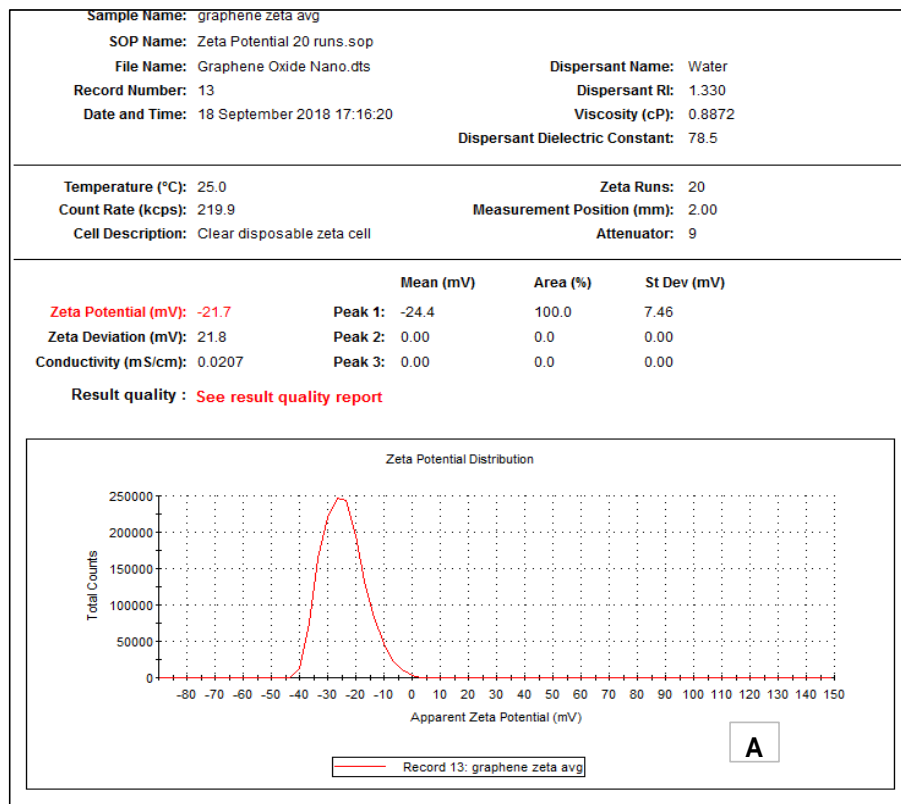


Figure 3.2: Measurement of the Zeta Potential (surface charge) using Zetasizer Nano ZS-90, Model ZEN3600 (Malvern Instruments Ltd, UK). Zeta Potential: (A) = - 21.7 mV; (B) = - 26. 1 mV; and (C) = structure of GO with terminal groups: epoxy /alkoxy (C-O), carboxyl (C=O), aromatic (C=C), etc (Song et al. 2014; PubChem 2018)

3.4.2 SEM and TEM Analyses

The SEM and TEM micrographic images of GO aqueous dispersion at different concentrations (10, 20, 50 and 100 $\mu\text{g/mL}$ respectively) were measured at 20k magnification. In SEM analysis, the range of lateral distance (length) of agglomerates observed in the dry state after evaporation of the dispersion medium ranged from 363.7 to 447.8 nm (see Table 3-2). Two-dimensional (2-D) micrographic images of GO aggregation states were obtained and particle distances or lengths (nm) measured (see **Figure 3.3** and **Figure 3.4**). This is a confirmation that the commercial GO used in this study has multiple-layered structures of up to 15 to 20 sheets as described by the manufacturer (Sigma-Aldrich), compared to the 2-3-layered GO sheets synthesized in-house by other researchers with lower particle distances (109.09, 189.19, 205.07, 224.40, and 257.54) measured using dynamic force microscope (DFM) (see **Table 3-3**). In TEM analysis, differences in the surface morphology, aggregation state, and three-dimensional (3-D) micrographic images (see **Figure 3.5**; **Figure 3.6**; and **Figure 3.7**) were obtained. The TEM micrographs showed massive lumps of GO sheets tightly clogged on top of each other in a highly agglomeration state: aggregated small sheets of GO on top of agglomerated layered, large sheets of GO all competing for space. Due to the higher attractive, intermolecular forces (Van der Waals) between each particle, GO sheets agglomerated in pouches as the molecules of water evaporated during drying, making the sizes very difficult to count.

Table 3-2: Particle distance of GO (10, 20, 50, and 100 µg/mL) measured with SEM and TEM. The average distance was between 360 and 450 nm.

SEM and TEM analysis of the average particle distance (nm) of 15-20 layers of GO dispersed in aqueous solution				
Number of measurements	10 µg/mL	20 µg/mL	50 µg/mL	100 µg/mL
	(nm)	(nm)	(nm)	(nm)
1	286.57	640	208.86	623.98
2	348.75	250	161.72	554.53
3	231.89	220	521.21	605.26
4	434.23	270	604.19	252.43
5	389.08	530	208.16	614.62
6	443.51	450	301.13	290.90
7	454.07	450	420.71	239.68
8	321.38	530	645.60	400.97
Average (15-20)	363.7	417.5	383.9	447.8
Average size per layer	18-24 nm	21-28 nm	19-25 nm	22-29 nm

The table below (Table 3-3) is an example of the mean distances of a non-commercial GO synthesized in-house by other researchers with 2-3 layers (Song et al. 2014).

Table 3-3: Mean distance of 2-3 layers of GO synthesized in-house by other researchers and size distance measured with dynamic force microscope (DFM) (Song et al. 2014)

Mean Distance of 2-3 layers of GO (nm)	Average size per layer
Exp. 1	109.09
Exp. 2	189.19
Exp. 3	205.07
Exp. 4	224.40
Exp. 5	257.54

SEM Micrographs

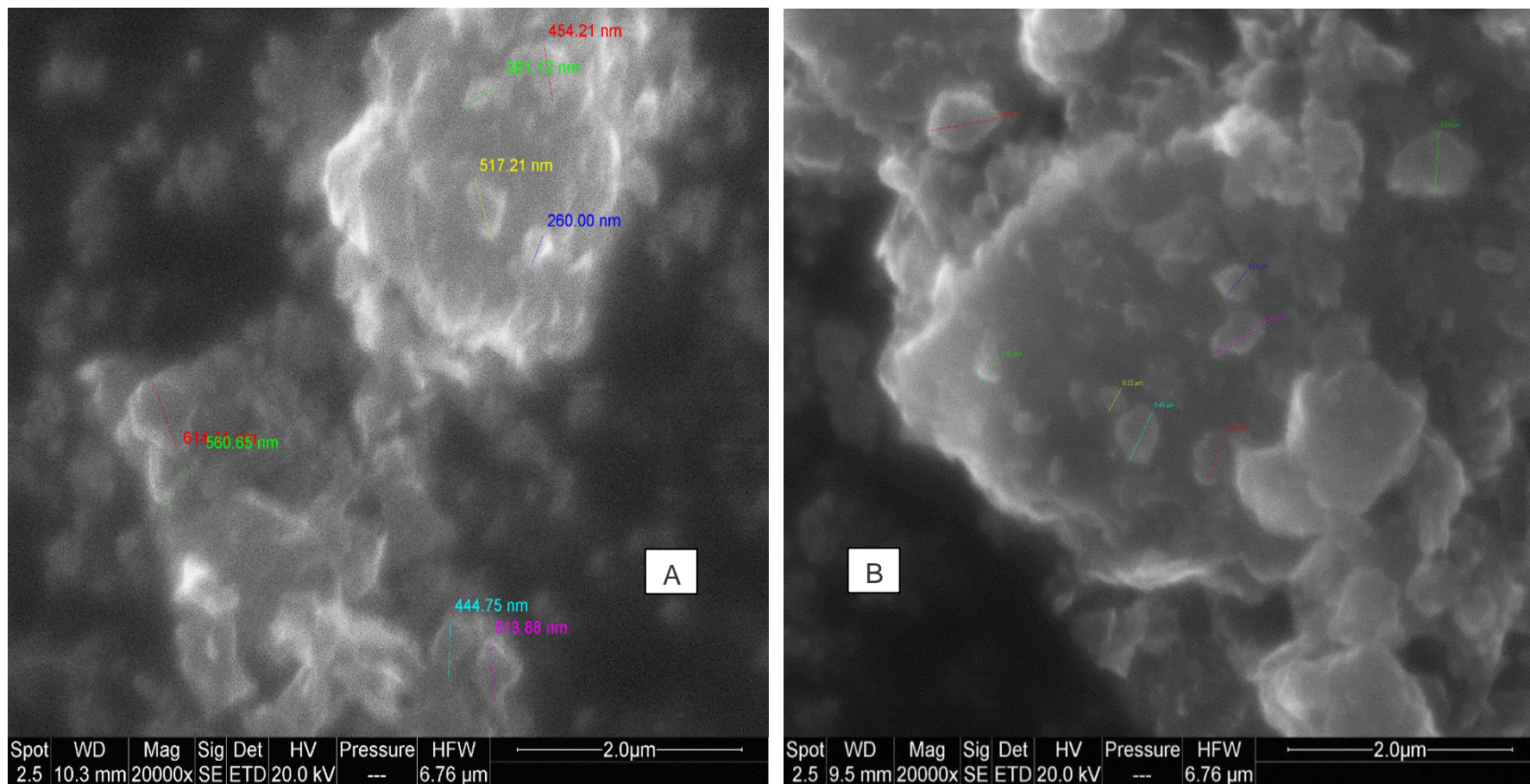


Figure 3.3: 20K SEM micrographs of GO aggregates: (A) in 10 µg/mL; and (B) 20 µg/mL in aqueous solution.

SEM Micrographs

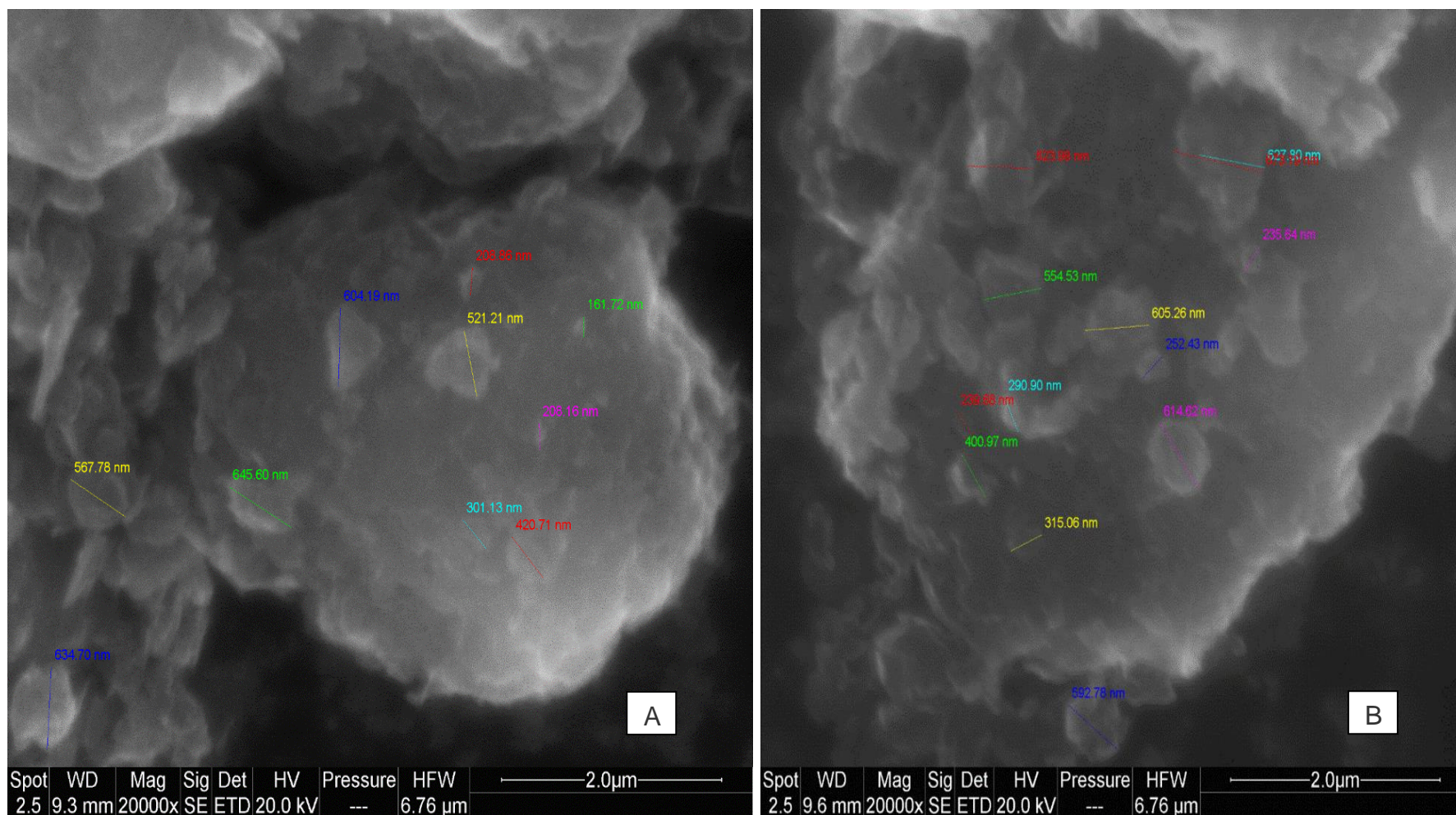


Figure 3.4: 20K SEM micrographs of GO: **(A)** 50 µg/mL suspension in RPMI, and **(B)** in 100 µg/mL suspension in RPM

TEM Micrographs

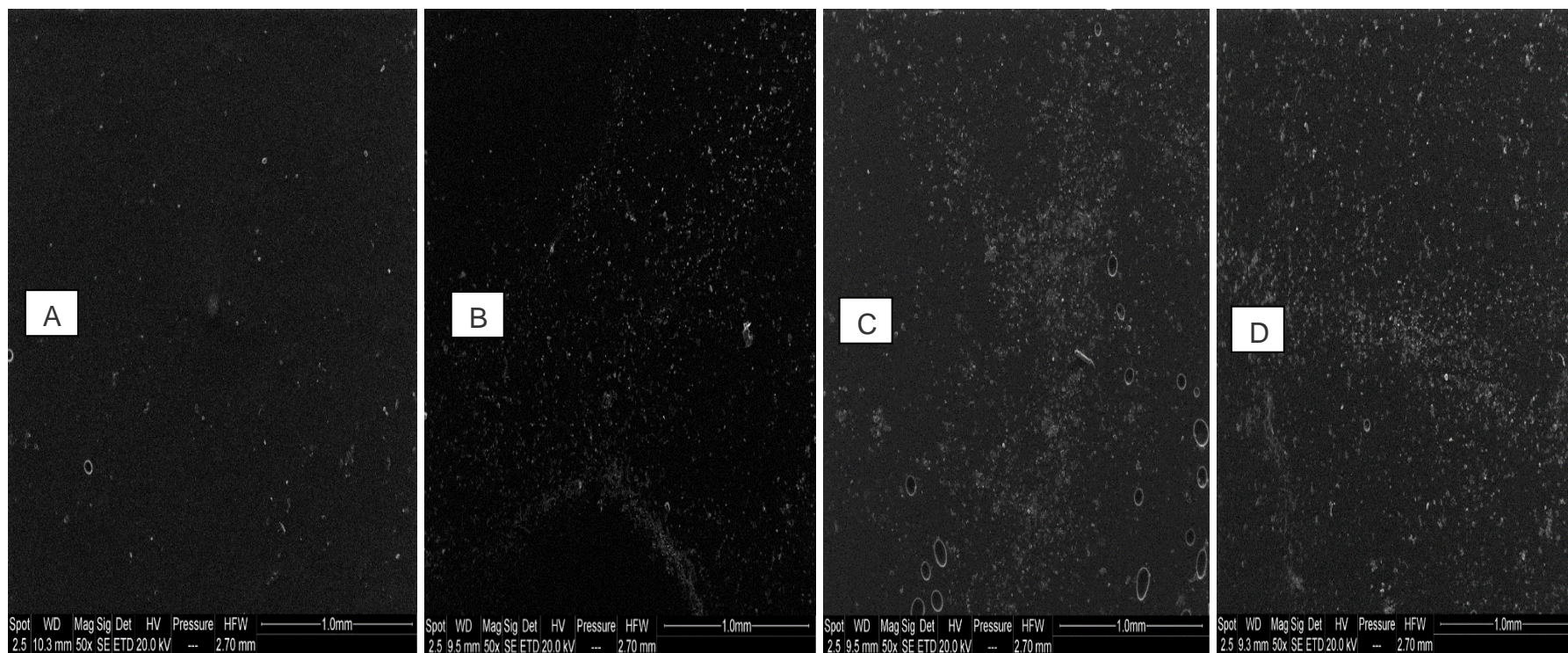


Figure 3.5: TEM micrographs of GO at 50 x magnification: (A) 10 $\mu\text{g/mL}$; (B) 20 $\mu\text{g/mL}$; (C) 50 $\mu\text{g/mL}$, and (D) 100 $\mu\text{g/mL}$

TEM Micrographs

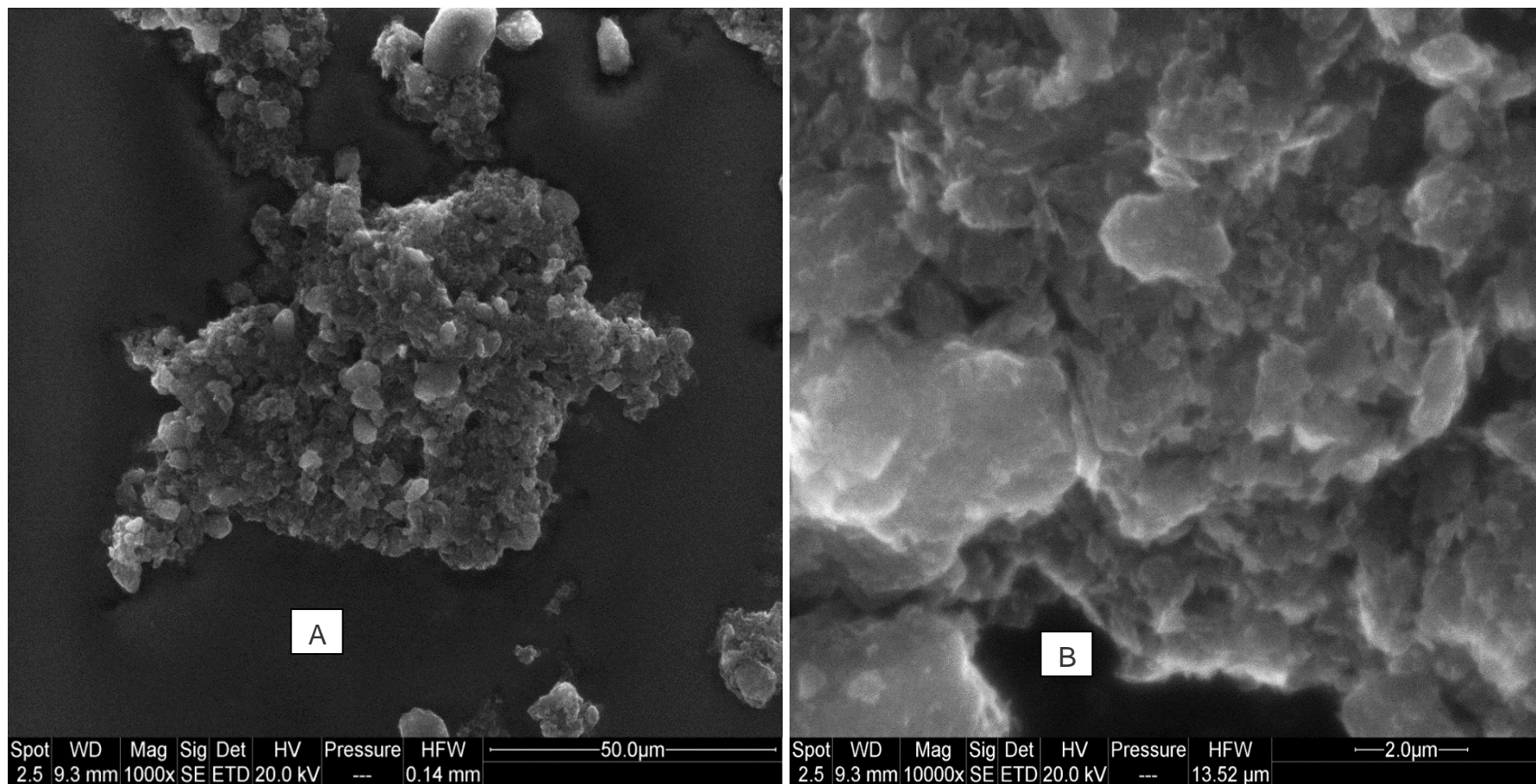


Figure 3.6: TEM micrographs of GO aggregates: (A) x 1K magnification (50 μg/mL) and (B) 10K magnification (20 μg/mL)

TEM Micrographs

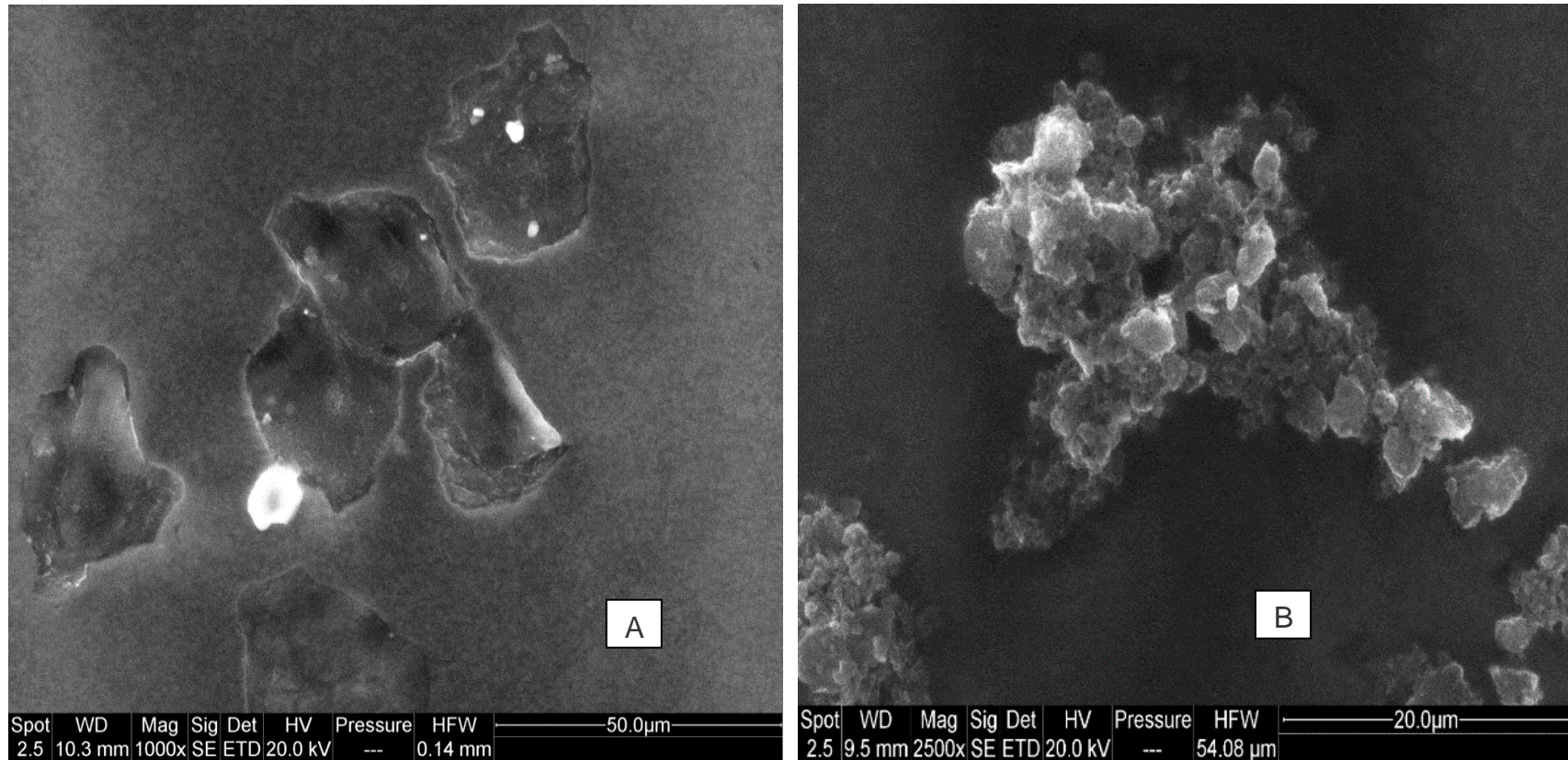


Figure 3.7: TEM micrograph of GO aggregates: (A) x 1K magnification (50 μg/mL) and (B) 2.5K magnification (100 μg/mL)

3.5 Discussion

It is vital to characterise nanoparticles in order to ascertain their physical and chemical properties such as size distribution and surface size since some of their adverse effects have been linked to these properties, and therefore there is a need to assess their safety *in vitro*. DLS size distribution measurements resulted in higher values than those obtained from microscopic analyses (SEM and TEM). One of the reasons could be linked with the state of the materials during measurements. The DLS was measured in the wet state (aqueous dispersion), leading to insertion water molecules (H-H, O⁻) into GO interstitial spaces (Song et al. 2014) as opposed to SEM and TEM analyses in the dry state.

ZP analysis measures the surface charge of particulate matter in solution or colloids using the Zetasizer Nano ZS (Malvern instruments, UK). It offers quantitative data about the stability of nanoparticles in a given dispersion medium. The net-negative zeta potential values (-21.7 and -26.1 mV) obtained showed that GO NMs have net-negative charge on their surface, possibly due to the surface chemistry: unbound hydroxy - OH, carboxyl /ketone C=O, epoxy/alkoxy C-O, and aromatic group C=C groups (Song et al. 2014). This was consistent with research done elsewhere (Ding et al. 2014) where synthesized pristine GO (p-GO) – a highly purified, ideal GO without defects whatsoever - showed negative ZP values. With a ZP value close to ± 30 mV, the GO NMs used in this study were very stable in aqueous dispersion (Mittal et al. 2017).

GO NMs are amphiphilic, and thus possess both hydrophilic (water-loving, polar) and lipophilic (fat-loving) properties in aqueous dispersion (Kim et al. 2012a).

The negative ZP (-21.7 and -26.1 mV) are low, but the inter-particulate forces of attractions (Van der Waals forces) are high which cause GO particles to agglomerate. The higher the ZP (mV), either positive or negative, the more stable the dispersion is. Previous studies on GO showed that the epoxy, carbonyl group (C=O), etc present on the unbound surface of GO (C₁₄H₄₂O₂₀) tend to cause aggregation of the nanomaterials on the graphene plane (Yan and Chou 2010). The range of particle size distribution (length) measurements by DLS (693.8-806.1 nm) were different from those obtained from TEM imaging (363.7-447.8 nm). This discrepancy could be due to its high polydispersity (Pdl = 0.768, 0.899, and 0.929) in aqueous suspension. The limits should be ≤ 0.6 and 0.7 for the DLS measurement to be reliable. When dispersed in water, the hydrophilic properties of GO (C_xH_yO_z) become evident as the sheets of GO NMs absorb molecules of water (H⁺, OH⁻) into their interspace and increase in size, thereby producing false higher particle sizes.

Characterization of the agglomeration state of nanoparticles is commonly performed with DLS using optical techniques to analyse dynamic properties and size distribution. The Zetasizer works by Brownian motion of particles by illuminating monochromatic, laser light through a solution. The intensities of the scattered light waves spread out in all directions and are translated into particulate size (Mountain 1992). Because these particles move in Brownian motion, that means the particle sizes can fluctuate (Wills et al. 2017). Although size measurement with DLS has been widely applied in nanoparticle

characterization especially for monodispersed materials, the DLS technique might be less reliable for highly polydispersed NMs, and thus might not be suitable for size measurements of GO NMs with 15-20 sheets. It has been shown that the intensity of the light scattered by smaller particles in the dispersion medium might be swiftly covered by light intensities from bigger particles, even if the bigger particles are very minute (Powers et al. 2006; Filipe et al. 2010; Bhattacharjee 2016). A second limitation of the DLS is its inability to discriminate particles based on their composition (Hondow et al. 2012). For instance, Nicole Hondow and her colleagues reported that DLS failed to analyse nanoparticle size in the presence of serum proteins forming Protein corona (Barbero et al. 2017) i.e. serum protein-to-particle binding. This effect modifies the particle size and scatter light with higher intensity, which is then translated as a larger particles and false-positive results.

To address some of these limitations in the DLS technique, alternative techniques such as SEM and TEM were used. TEM gives very high resolution because it uses an electron beam with shorter wavelengths. Regardless of any advantages in TEM, a number of limitations were noted elsewhere (Winey et al. 2014). TEM can only analyse one sample at a time, termed drop-cast TEM, where samples dispersed in a medium are dropped and allowed to air-dry in a TEM grid before imaging. Although the particle sizes, shape and sample composition can be analysed in using TEM imaging, this technique may not be a reliable method to measure particle agglomeration since the particles tend to agglomerate as the liquid components evaporate (Hondow et al. 2012; Wills et al. 2017). Another limitation is that the intensity of the ionizing radiation could damage the samples

during TEM analysis and may not be suitable for thermolabile samples. Another key limitation of characterization using TEM is that the micrographs produced are cross-sectional 2-D images of agglomerated particles with several images observed at various points during the analysis which are eventually 3-D images.

To overcome some of the limitations of both the DLS and the electron microscopy, Digital Fourier Microscope (DFM), cryogenic plunge freezing, etc have been suggested (Wills et al. 2017). The cryogenic freezing technique involves snap-freezing a nanoparticle-suspension with enough speed in liquid nitrogen or liquid ethane, freezing the liquid components and preserving them without distorting the integrity of the dispersed NPs. This method is regarded as an excellent technique that can maintain the samples in their most natural form. This alternative method of size measurement gives rise to stable samples adequate for imaging and particle size evaluation and might be suitable for thermolabile NPs. Samples prepared in this way could be warmed under high vacuum, which allows the liquid phase to sublime (change from solid to vapour) without affecting the integrity of the dispersed NPs.

Chapter 4: Cytotoxicity Assays

1.0 Cytotoxicity of GO NMs in human lymphocytes from healthy individuals and patients (asthma, COPD, and lung cancer).

4.1 Introduction

In the previous Chapter (Chapter 3), we characterized GO NMs using Zetasizer Nano instrument for DLS and ZP, and then with electron microscopes using SEM, and TEM analyses. The particle distances obtained in DLS were higher than those obtained in SEM and TEM. Overall, the concentration of GO from 10 to 100 µg/mL resulted in large particle distance due mainly to particle agglomeration.

4.1.1 Hypothesis: GO may be cytotoxic to human lymphocytes

In this chapter, we hypothesised that GO NMs may be cyto-toxic to human lymphocytes and affect their metabolic activities. We came up with this hypothesis because it was reported that the triple particle characteristic (the 3S) - size, shape, and surface chemistry (the surface charge (ZP) and unbound functional groups) (Song et al. 2014) may react with cell membrane, proteins, and DNA and trigger other reactions within the cell (Sanchez et al. 2012; Jaworski et al. 2013). In addition, it has been established that GFNMs with irregular surfaces, small size (= large surface area), and sharp edges are internalized into the cell effortlessly relative to large particles with smooth surfaces (Guo and Mei 2014). The use of human PBL for the assessment of cytotoxicity could be traced back to more than half a century ago due to their remarkable sensitivity (*in vitro* and *in vivo*). Consequently, this had led to the production of WHO guidelines on human biomonitoring of genotoxicity of carcinogenic compounds independent of cancer

and described PBL as surrogate cells and genotoxicity endpoints as either effect biomarkers of exposure or biomarkers of cancer risk (Albertini et al. 2000).

To test this hypothesis, we evaluated the impacts of different concentrations of GO (10, 20, 50, and 100 µg/mL) on human lymphocytes using MTT and NRU Assays. Since human lymphocytes are part of the white blood cells and human immune systems, it was vital to use them in order to understand the role of the immune system in patients with different pathological conditions (asthma, COPD, and lung cancer) and the results compared with those from healthy subjects. The choice of our cytotoxicity assays - MTT and Neutral Red Uptake Assays - were based on their reliability in toxicology and pharmacology screening of drug resistance and cytotoxicity of new anti-cancer drugs (Sargent 2003; Aslantürk 2017).

4.1.2 Materials and Methods

All the chemicals and equipment used in the cytotoxicity assays were listed in Chapter 2, Sections 2.1.1 and 2.1.2; and methods described in Sections 2.2.9.1 (MTT Assay), and 2.2.9.2 (NRU Assay).

4.2 Results

4.2.1 Cytotoxicity of GO NMs in human lymphocytes in the MTT and NRU assays

The application of GO NMs in biomedical sciences has the potential to become toxic threats and health risk when they react with human whole blood. Lymphocytes (T-cells, B-cells, and natural killer cells) are components of the white blood cells which are vital to our immune defence systems. They detect

antigens, and subsequently produce antibodies to destroy cells that could cause damage.

Human lymphocytes from healthy individuals and patients (asthma, COPD, and lung cancer) were treated with different concentrations of GO (10, 20, 50, and 100 µg/mL) for 24 h, followed by treatment with MTT dyes (4 h) and Neutral Red solutions (3 h) to determine the cells' proliferative, metabolic activities or cell survival rates. The results are presented in **Table 4-1** for NRU assay, and **Table 4-2** for MTT assay, respectively, and both the NRU and MTT assay data were presented graphically in **Figure 4.1**, where **Figure 4.1A** = NRU assay; and **Figure 4.1B** = MTT assay. A close observation of the two graphs showed that lower concentrations of GONMs up to 20 µg/mL were cytotoxic as demonstrated by sharp slopes, while higher concentrations from 20 to 100 µg/mL were highly cytotoxic as demonstrated by the continuous decreases of the slopes in each treatment group - healthy individuals (black colour), asthma (blue colour), COPD (green colour), and lung cancer (red colour).

In the NRU assay, the data in **Table 4-1** and **Figure 4.1A** show decreases in the % cell survival after treatment with different concentrations of GO NMs (10, 20, 50, and 100 µg/mL). Specifically, after treatment with 10 µg/mL in healthy individuals, the % cell survival rate decreased in a non-significant manner from 100% to 93.6%; in asthma patients, the %cell survival rate decreased sharply in a statistically significant manner ($p < 0.01$) to 67.29% (33% reduction). In COPD patients, the % of survival rates decreased significantly ($p < 0.05$) to 65.26% (35% reduction), but in lung cancer patients, the % cell survival decreased most

significantly ($p < 0.01$) to the lowest level to just under 60% (41% reduction). As the concentrations increased from 10 $\mu\text{g/mL}$ to 20 $\mu\text{g/mL}$, the % cell survival of lymphocytes from healthy individual controls decreased sharply in a statistically significant manner ($p < 0.01$) to 70.71% (29% reduction), while lymphocytes from patients showed gradual decreases in % cell survival rates in a statistically significant manner ($p < 0.001$) to 61.14% (39% reduction) in asthma patients, to 57.01% (43% reduction) in COPD patients ($p < 0.001$), and to 49.48% (51% reduction) in lung cancer patients ($p < 0.01$). However, when the lymphocytes were treated with much higher GO cytotoxic concentrations, 50 $\mu\text{g/mL}$ and 100 $\mu\text{g/mL}$, the % cell survival rates of lymphocytes decreased continuously in a statistically significant manner ($p < 0.01$) to 69.96% (30% reduction) and 51.21% (49% reduction, $p < 0.01$) in healthy individuals; 57.24% (43% reduction, $p < 0.01$) and 55.57% (44% reduction, $p < 0.01$) in asthma patients; 46.69 (53% reduction, $p < 0.001$) and 38.60% (61% reduction, $p < 0.001$) in COPD patients; and 39.35% (61% reduction, $p < 0.01$) and 27.74% (72% reduction, $p < 0.001$) in lung cancer patients, respectively. Overall, the % cell survival rates of lymphocytes from lung cancer patients were the lowest compared to COPD, asthma, and healthy controls.

In the MTT assay, the data in **Table 4-2** and **Figure 4.1B** show decreases in % cell survival rates after exposure to different concentrations of GO NMs (10, 20, 50, and 100 $\mu\text{g/mL}$). Specifically, after treatment with GO NMs up 10 and 20 $\mu\text{g/mL}$, the % cell survival rates decreased sharply in a concentration-dependent manner and were statistically significant, while samples treated with much higher

cytotoxic concentrations from 50 µg/mL to 100 µg/mL showed interesting responses, especially in asthma patients. For instance, at 10 µg/mL, the % cell survival rates decreased significantly by 17% to 83.08% in healthy individuals ($p<0.01$); a decrease by 20% to 80.01% in asthma patients ($p<0.01$); a decrease by 25% to 74.99% in COPD patients ($p<0.05$); and a decrease by 30% to 70.01% in lung cancer patients ($p<0.01$), demonstrating that patients' DNA, especially in lung cancer patients, was more unstable than in COPD and asthma patients relative to healthy control individuals. When the lymphocytes were treated with higher concentrations of GO NMs, 20, 50, and 100 µg/mL, in healthy individuals, the % cell survival rates decreased significantly to 55.01 % (by 45%, $p<0.001$), 41.99% (by 58%, $p<0.001$), and to 35.02% (by 65%, $p<0.001$), respectively. In asthma patients treated with the aforementioned concentrations (20, 50, and 100 µg/mL), the % cell survival rates decreased significantly with increased by 38% to 61.67% ($p<0.01$), by 55% to 44.97% ($p<0.01$), and by 60% to 40.04% ($p<0.001$). In COPD patients treated with the above three concentrations, the % cell survival rates decreased significantly by 50% to 50.03% ($p<0.01$), by 65% to 34.99% ($p<0.01$), and by 73% to 26.99% ($p<0.001$). However, in lung cancer patients' lymphocytes treated with 20, 50, and 100 µg/mL of GO NMs, the % cell survival rates decreased significantly to their lowest levels by 57% to 43.46% ($p<0.001$), by 70% to 29.99% ($p<0.01$), and by 79% to 20.60% ($p<0.001$). Overall, the % cell survival rates of lymphocytes from lung cancer patients in the MTT assay were the lowest compared to COPD, asthma, and healthy controls.

Table -4-1: NRU Assay measurements of the % cell survival rates and % cell reduction of metabolic activities of human lymphocytes from healthy individuals and patients (asthma, COPD and lung cancer) after treatment with different concentrations of GO (10, 20, 50, and 100 µg/mL) in 3 independent experiments (n = 3). The NC, untreated lymphocytes have 100% metabolic activity.

NRU ASSAY									
GO Concentrations		10 µg/mL		20 µg/mL		50 µg/mL		100 µg/mL	
Treatment Groups	NC	% Cell Survival	% Cell reduction	% Cell Survival	% Cell reduction	% Cell Survival	% Cell reduction	% Cell Survival	% Cell reduction
Healthy	100%	93.96 ^{ns}	6	70.71 ^{**}	29	69.96 ^{**}	30	51.21 ^{**}	49
Asthma	“	67.29 ^{**}	33	61.14 ^{***}	39	57.24 ^{**}	43	55.57 ^{**}	44
COPD	“	65.26 [*]	35	57.01 ^{***}	43	46.69 ^{***}	53	38.60 ^{***}	61
Lung cancer	“	59.14 ^{**}	41	49.48 ^{**}	51	39.35 ^{**}	61	27.74 ^{***}	72

Table 4-2: MTT Assay measurements of the % Cell survival rates and % cell reduction of metabolic activities of human lymphocytes from healthy individuals and patients (asthma, COPD and lung cancer) after treatment with different concentrations of GO (10, 20, 50, and 100 µg/mL) in 3 independent experiments (n = 3). The NC, untreated lymphocytes have 100% metabolic activity.

MTT ASSAY									
GO Concentrations		10 µg/mL		20 µg/mL		50 µg/mL		100 µg/mL	
Treatment Groups	NC	% Cell Survival	% Cell reduction	% Cell Survival	% Cell reduction	% Cell Survival	% Cell reduction	% Cell Survival	% Cell reduction
Healthy	100%	83.08 **	17	55.01 ***	45	41.99 ***	58	35.02 ***	65
Asthma	“	80.01 **	20	61.67 **	38	44.97 **	55	40.04 ***	60
COPD	“	74.99 *	25	50.03 **	50	34.99 **	65	26.99 ***	73
Lung cancer	“	70.01 *	30	43.46 ***	57	29.99 **	70	20.60 ***	79

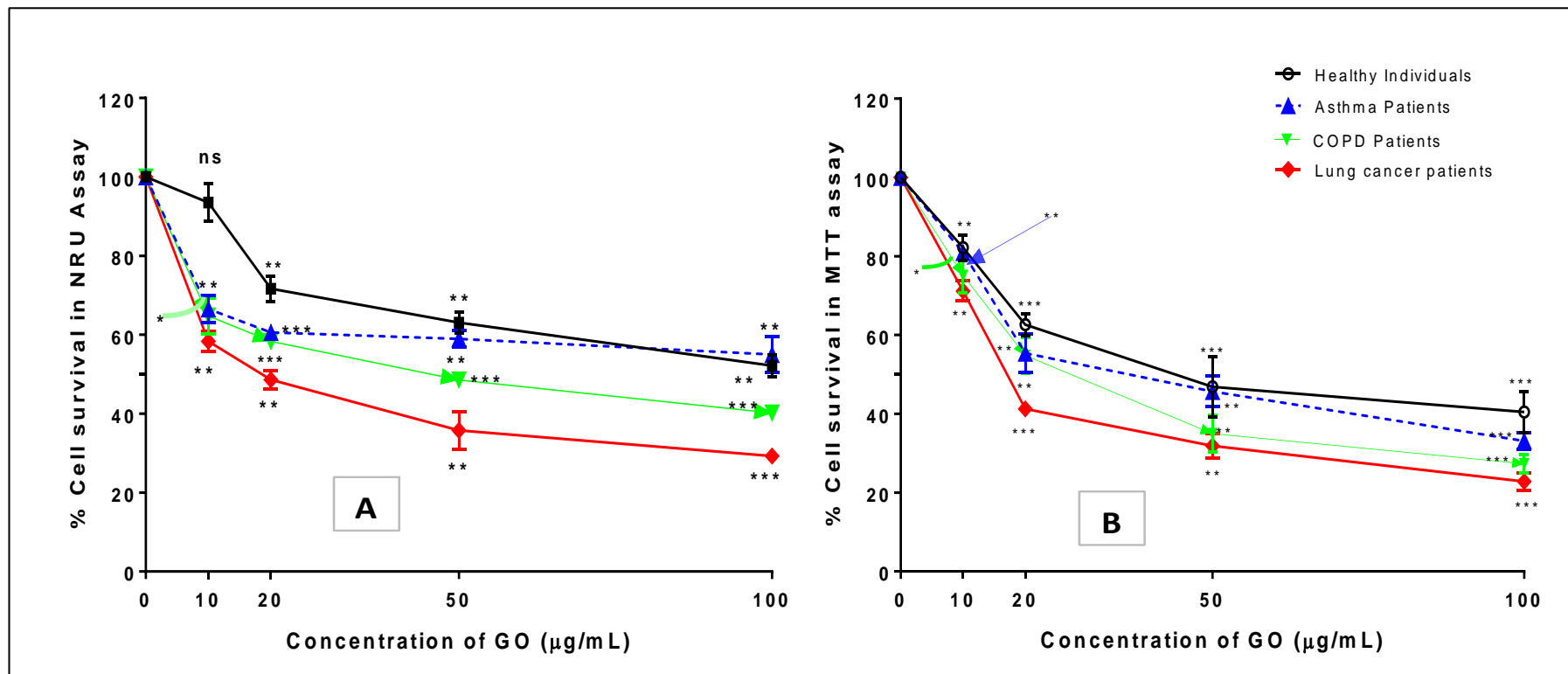


Figure 4.1: Cytotoxicity of Graphene Oxide (15-20 sheets) in peripheral human lymphocytes after 24 h exposure to different concentrations of GO (10, 20, 50 and 100 µg/mL). The mitochondrial activities were assessed with NRU and MTT assays. The percentage (%) of cell survival of treated lymphocytes from healthy individuals (black colour), asthma (blue colour), COPD (Green Colour), and lung cancer (Red Colour) were compared with untreated lymphocytes (0 µg/mL; negative control = 100%). The values represent mean ± SEM of three independent experiments (n=3). *p<0.05; **p<0.01; ***p<0.001; ns = not statistically significant. Bars indicate standard errors.

4.2.2 Confounding Factors

A total of 12 individuals participated in the study, 50 % were males and 50 % were females. There were no confounding effects in healthy individuals and asthma patients due to non-smoking history. The age range of volunteers was between 43-47 in healthy individuals, 26-64 in asthma patients, 54-58 in COPD patients, and 5-65 in lung cancer patients. However, a confounding effect in asthma was observed in gender as all 3 individuals were female. In COPD and lung cancer patients, there was not much confounding differences due to age (54-65), but there were differences in smoking history since 100% of all COPD and lung cancer patients were smokers or past smokers, with some of them smoking up to 30 cigarettes per day.

4.3 Discussion

Performance of cell proliferation rates and /cell viability are some of the excellent ways to determine the cells' metabolic profile or survival in the presence of toxic chemicals. Such chemicals may cause toxicity to cells through various mechanisms including physical destruction of the cell membranes, permanent binding of particles to protein receptors and total inhibition of protein synthesis (Aslantürk 2017).

To evaluate cell death induced by toxic agents, it is vital to select robust and well-established cytotoxicity assays which are cheap, reproducible, and capable of producing reliable results. Before we chose MTT and NRU assays in this study, several factors were considered, including sensitivity and complexity of the protocol. It was the reliability parameters which stood out as these methods are

being used in industries for drug screening (Hansen and Bross 2010). NRU and MTT assays are some of the most frequently used colorimetric assay to assess cytotoxicity or cell viability (Mossman 1983) and have been used to determine cell survival, cell viability or cytotoxicity by evaluating activities of mitochondrial enzymes (Stone et al. 2009).

Human PBL from healthy individuals and patients (asthma, COPD, and lung cancer) were treated with different concentrations of GO (10, 20, 50 and 100 $\mu\text{g}/\text{mL}$) for 24 h. Cytotoxic effects were evaluated by the MTT assay after 4 h incubation with MTT dye solution and NRU assay after 3 h incubation with Neutral Red Solution according to the incubation time recommended by the manufacturers. Our results demonstrated that increases in the concentrations of GO NMs decreased the% cell survival of human lymphocytes according to the pathological state of the individuals. GO NMs caused both genotoxicity and cytotoxicity depending on the concentrations used. Between 10 and 15 $\mu\text{g}/\text{mL}$ and up to 20 $\mu\text{g}/\text{mL}$, GO NMs showed genotoxicity in the absence of cytotoxicity with no artefacts in both NRU and MTT assays, but were more cytotoxic with increased concentrations from 20 to 100 $\mu\text{g}/\text{mL}$. Our results are in agreement with research carried out elsewhere, where lymphocytes from healthy individuals were treated with GO (up to 100 $\mu\text{g}/\text{mL}$) and immunotoxicity assessed using enzyme-linked immunosorbent assay (Guo and Mei 2014). They found concentration-dependent increases in dendric cells with increases in concentration.

In healthy individuals, the MTT assay detected significant levels of cytotoxic events ($p < 0.05$) as shown by the relative number of metabolically active cells present and reduced by the mitochondria reductase enzymes (by 17%, 45%, 58%, and 65%) compared to the much lower levels of reduction ($p < 0.05$) in the NRU assay by 6%, 29%, 30%, and 49% respectively. In patients treated with 10 $\mu\text{g/mL}$ GO, cytotoxic events were detected by NRU as shown by the actual number of cells reduced (33%, 35%, and 41%) compared to the lower number of cells (20%, 25%, and 30) detected in the MTT assay. At higher concentrations (20, 50 and 100 $\mu\text{g/mL}$), the MTT assay detected more cytotoxic events than in the NRU assay, except at 20 $\mu\text{g/mL}$ where the rates of % cell survival in the NRU and the MTT assays were almost the same. This significant level of cytotoxicity was consistent with cytotoxicity assays performed elsewhere using MTT assay which showed that GO decreased cell viability significantly in BEAS-2B human lung cells at concentrations 10-100 $\mu\text{g/mL}$, but the decrease in cell viability in human lung fibroblasts were observed at 100 $\mu\text{g/mL}$ only after extended treatment time (Guo and Mei 2014).

Assessment of the cytotoxicity of GO in vitro is not new, but most of the studies were conducted with HeLa cells, lung cancer cell A549 cells, normal human lung cells, human breast cancer cells, etc (Ding et al. 2014). The same authors argued that human cell lines may not be the ideal tool for biological research as they may contain all sorts of mutation and chromosomal aberration parameters which could have arisen due to several cell duplications. Consequently, the toxicity reports from cell lines may not expansively replicate the actual effects of GO when tested on human lymphocytes and whole blood (Ding et al. 2014). Some previous

research on GO (1-2 layers) on blood cells show conflicting results. For instance, Sasidharan et al showed that GO concentrations up to 75 µg/mL had little or insignificant haemolytic effects on blood cells (Sasidharan et al. 2012), but the work by Liao et al was opposite and demonstrated that GO has concentration-dependent haemolytic effects on red blood cells (Liao et al. 2011). Another research by Singh et al on the haemolytic activity of GO demonstrated that GO as low as 2 µg/mL had effects on the platelets causing thrombo-toxic effects (Singh et al. 2011). A follow-up study by the same group of authors modified the graphene with amine (G-HN2), but the result did not cause thrombo-toxic effects (Singh et al. 2012). Some of these apparent contradictions might be associated with the physicochemical surface properties of GO like surface morphology, composition or even due to artefacts or impurities present in the GO depending on the method through which it was synthesized. To allow for consistency throughout this study, commercial GO was used. Although the MTT and NRU assay results demonstrated a general decrease in cell proliferation or increase in cytotoxicity with increased concentrations, both assays did not follow the same trend. This deviation could be attributed to the cells retaining the GO.

No matter how robust the MTT and NRU assays are, numerous studies have shown that the components of the reagents can interact with carbon NMs resulting in either inflated viability results or false toxic responses. For instance, carbon-based nanomaterials can reduce the MTT reagent, resulting in overestimation of cell viability which could potentially mask cytotoxic responses (Monteiro-Riviere and Inman 2006). Research by Ou L et al. (2016) also showed that the MTT assay could fail to accurately predict GO toxicity due to the

spontaneous reduction results in a false positive GO autofluorescence signal (Wu et al. 2015; Ou et al. 2016). One of the suggested alternative methods is the water-soluble tetrazolium salt reagent (WST-8 assay) to establish that the viability results obtained from the assays were free of any interference /artefacts that might be induced by the GO nanomaterial itself. The viability of the cells at the time of treatments with MTT and NRU dyes should also be considered as a factor that might lead to false toxic results. According to Henderson, et al., the cell viabilities of highest concentration of tested chemicals should be $\geq 75\%$ to evade false positive effects owing to cytotoxicity (Henderson et al. 1998).

It has been largely reported that freshly isolated T Lymphocytes can only keep to viability within 24 h of cell culture (Ding et al. 2014). Since MTT and NRU dye solutions were treated after 24 h isolation, and then incubated for further 4 h and 3 h respectively, it is likely that cell death (apoptosis or necrosis) might have occurred naturally even before the assay completion.

Confounding factors may have also played important roles in the significant cytotoxicity responses observed in both COPD and lung cancer patients since 100% of individuals with COPD and lung cancer were smokers, with some of them smoking up to 30 cigarettes per day.

Next, we tested the hypothesis that GO could induce genotoxicity (DNA damage) on human whole blood using the alkaline Comet Assay, and results and analyses are reported in Chapter 5.

Chapter 5: Genotoxicity Assay

5.0 Genotoxicity (DNA Damage) Effects of GO in vitro in human whole blood from healthy individuals and patients (asthma, COPD, and lung cancer)

5.1 Introduction

In the previous Chapter (Chapter 4), we established that different concentrations of GO (10, 20, 50 and 100 µg/mL) were cytotoxic to human lymphocytes in a concentration-dependent manner after 24 h of treatment, assessed using the MTT and NRU assays. The extent of cytotoxicity was influenced by the disease conditions of the patients (asthma, COPD, and lung cancer) and health status of the healthy control individuals who participated in the study.

The increasing applications of GO NMs in Biomedical Sciences call for urgent analysis of the genetic effects of GO in human whole blood. Most commonly used drug delivery systems like FDA-approved liposomal-Dox preparations (e.g. pegylated Doxil[®] and Lipodox[®], and the non-pegylated Dox (e.g. Myocet[®])) are formulated as intravenous injections (Zhao et al. 2018). It is likely that when formulated with GO, they might interact with human whole blood and induce genetic damage. DNA damage could be in the form of single-strand breaks (SSB), double strand-breaks (DSB), alkali-labile sites (ALS) or changes in chromosomal structure and apparatus.

5.1.1 Hypothesis: GO may be genotoxic in human whole blood

In this chapter, we hypothesize that GO could induce DNA damage in human whole blood. It was vital to assess the genotoxic potential of this particular nanomaterial to support existing genotoxicology research on this GFNM.

Research by others had established a correlation between DNA damage, cellular mutation, and cancer (Ding et al. 2014); COPD being a driving factor in lung cancer (Durham and Adcock 2015); and a significant link between asthma and lung cancer (Rosenberger et al. 2012; Qu et al. 2017).

To test this hypothesis, we evaluated the impacts of different concentrations of GO (10, 20, 50, and 100 µg/mL) on human whole blood using the alkaline Comet assay. We had chosen human whole blood instead of isolated lymphocytes or cancer cell lines because we believe it would be easier and faster to detect changes in blood samples during patients' medical treatment than late detection when much damage had been inflicted, thereby leading to poor prognosis. In this Chapter, we were mindful of the fact that genotoxicity occurs in the absence of cytotoxicity (Henderson et al. 1998).

5.2 Materials and Methods

Reagents, materials, and equipment used in the Alkaline Comet Assay were listed in Sections 2.1.1 and 2.1.2, and methods described in Section 2.2.10.1.2.

5.3 Results

5.3.1 H₂O₂ Concentration-dependent DNA Damage in Healthy individuals

Hydrogen peroxide (H₂O₂) is known to induce DNA damage in biological cells (Driessens et al. 2009). Therefore, the aim of this section was to first establish the highest concentration of H₂O₂ (µM) that induced the greatest DNA damage after treatment with human whole blood from healthy individuals in the alkaline Comet assay compared to untreated whole blood in the absence of cytotoxicity.

That specific, highest concentration was used in the rest of this project in the Comet assay as the positive control (PC). Whole blood samples from healthy individuals were treated with four increasing concentrations of H₂O₂ (10, 30, 60, and 100 µM). Untreated blood samples, without any chemical treatment, served as the negative control (NC). DNA damage was expressed as Olive Tail Moment (OTM) and percentage Tail DNA (% Tail DNA) (Olive and Durand 2005). Results are presented in **Figure 5.1**.

As we can see from Graphs **A** and **B**, different concentrations of H₂O₂ induced DNA damage in a concentration-dependent manner. DNA damage was statistically significant at $p < 0.01$ (**) and <0.001 (***). Although, the DNA damage effects of 60 and 100 µM were almost similar, we selected the higher concentration (100 µM), and this was used as the PC for subsequent Comet assay experiments. Our findings were consistent with other research which showed that H₂O₂ is a typical DNA-damaging chemical and therefore an excellent model system for studying the impacts oxidative stress (Benhusein et al. 2010).

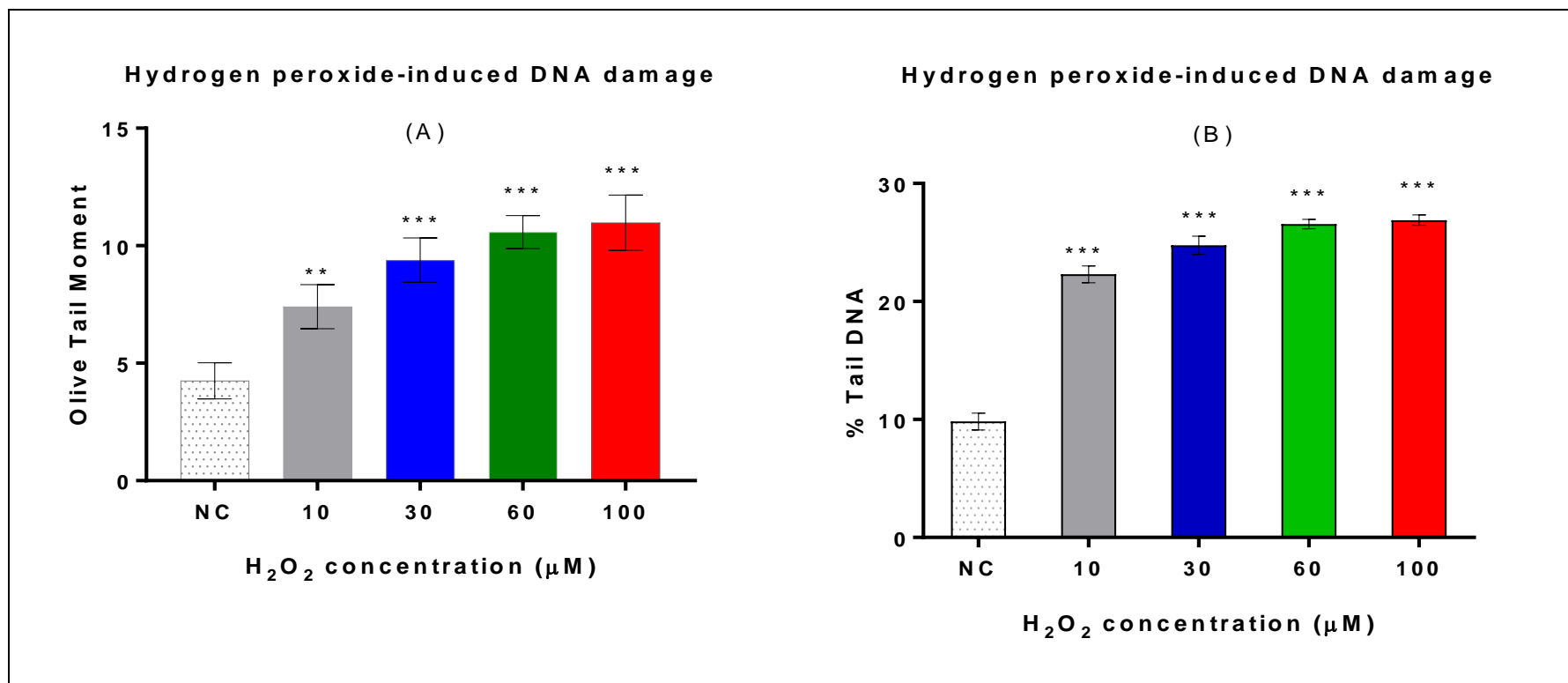


Figure 5.1: H₂O₂ concentration-dependent DNA damage in human whole blood from healthy individuals after exposure to four different concentrations of H₂O₂ (10, 30, 60, and 100 μM) compared with untreated whole blood as the negative control (NC). DNA damage was expressed as: (A) Olive Tail Moment, and (B) % Tail DNA (B). The 60 and 100 μM H₂O₂ showed the highest DNA damage, and were similar, but 100 μM H₂O₂ was selected as the PC. Each graph was plotted with error bars. Statistical significance was rated at p < 0.05; where * = p<0.05; ** = p<0.01; and *** = p <0.001; 5 independent experiments, n=5.

5.3.2 GO-induced DNA damage on human whole blood from Healthy Individuals and patients (asthma, COPD, and lung cancer)

Since 100 μM H_2O_2 induced the highest DNA damage in healthy individuals compared with the control, it was used as the PC. Following the same Comet Assay protocol used in the previous experiments, blood samples from healthy individuals and patients (lung cancer, asthma, and COPD) were treated with four different concentrations of GO (10, 20, 50 and 100 $\mu\text{g}/\text{mL}$) and 100 μM H_2O_2 . (PC). Untreated samples served as the NC. DNA damage parameters - OTM and % Tail DNA - were used to quantify DNA damage in the Comet assay.

Our results are presented in the histograms as shown in **Figure 5.2** (OTM) and **Figure 5.3** (% Tail DNA). GO NMs caused significant DNA damage in a concentration-dependent manner (10, 20, 50 and 100 $\mu\text{g}/\text{mL}$) after 30 min of exposure to human whole blood in all individuals treated samples compared to untreated, NC blood samples. At each GO concentration (10, 20, 50, and 100 $\mu\text{g}/\text{mL}$), blood samples from lung cancer patients showed the highest level of DNA damage as shown by the OTM (Figure 5-2) and % Tail DNA (Figure 5-3) followed by COPD, and asthma patients relative to healthy individuals with the lowest levels of DNA damage.

Specifically, at 10 $\mu\text{g}/\text{mL}$, DNA damage expressed as the % Tail DNA was significantly ($p < 0.001$) highest in lung cancer patients, followed by asthma, and COPD patients relative to the healthy control individuals. A closer observation of the untreated, Negative control samples (Neg. Control) for basal DNA damage in

Figures 5-2 and **5-3** showed significant DNA damage in lung cancer patients ($p < 0.001$) followed by COPD patients ($p < 0.01$). Although basal DNA damage occurred in both healthy individuals and asthma patients, the differences in their DNA damage were not statistically significant. The importance of reporting basal DNA damage is to illustrate the fact that our genome is constantly exposed to genotoxic agents both internally such as ROS produced in our body during normal activities, and externally such as environmental toxicants leading to a continuum of DNA damage and DNA damage-repair cycle. The Comet images (see **Figure 5.4**) from lung cancer patients show various levels of DNA damage induced with different GO concentrations.

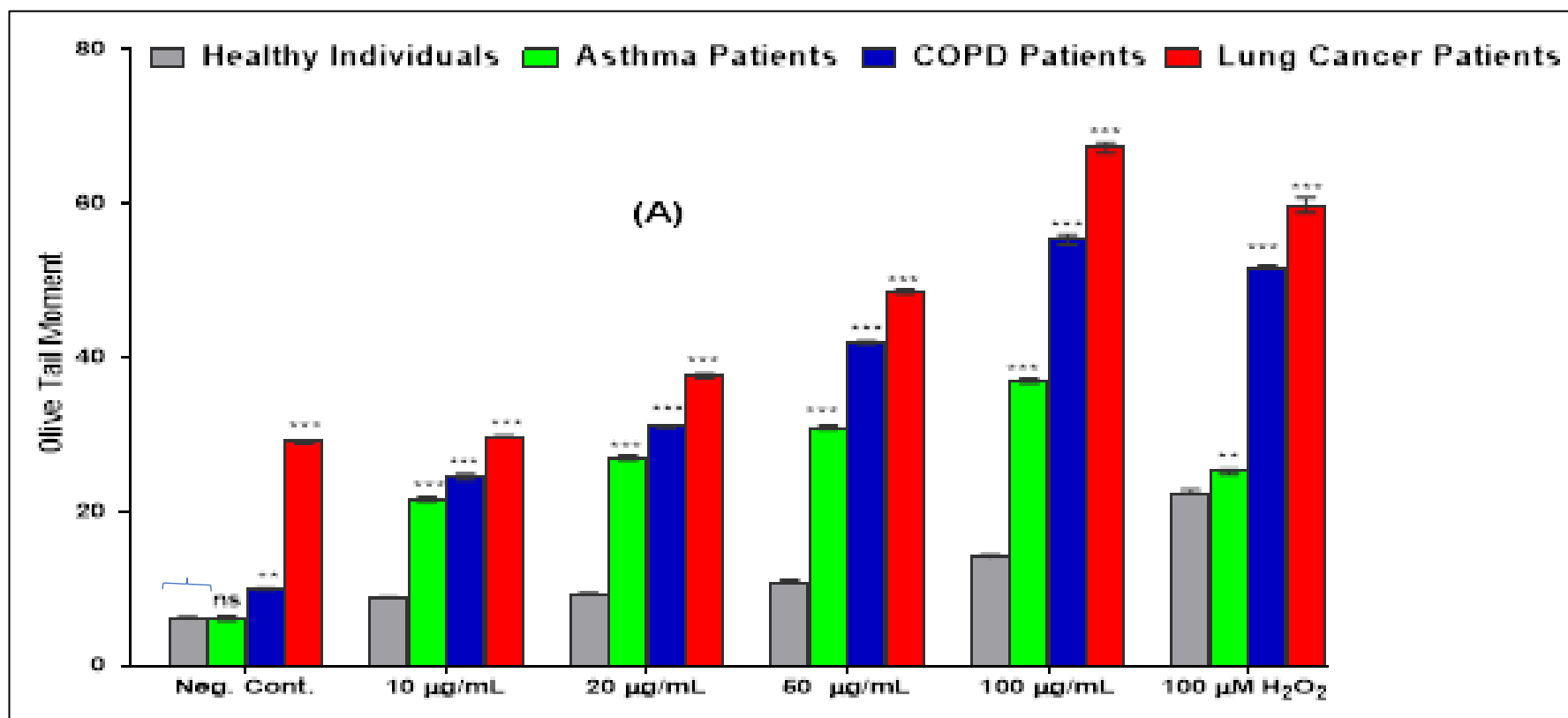


Figure 5.2: GO-induced DNA damage in human whole blood from healthy individuals and patients (Olive tail moment). Blood samples from healthy individuals (Grey colour), asthma (Green colour), COPD (Blue colour), and lung cancer patients (Red colour) were treated with four different concentrations of GO (10, 20, 50, and 100 µg/mL) and 100 µM H₂O₂ (positive control, PC, shown on the right-hand side of the histograms) compared to the untreated whole blood samples (Negative control, shown on the left-hand side of the histograms). DNA damage was expressed as Olive Tail Moment (OTM). Statistical significance was rated at $p < 0.05$; where * = $p < 0.05$; ** = $p < 0.01$; *** = $p < 0.001$; and ns = not significant; 20 x independent Comet assay experiments x 4 per treatment groups; n = 80.

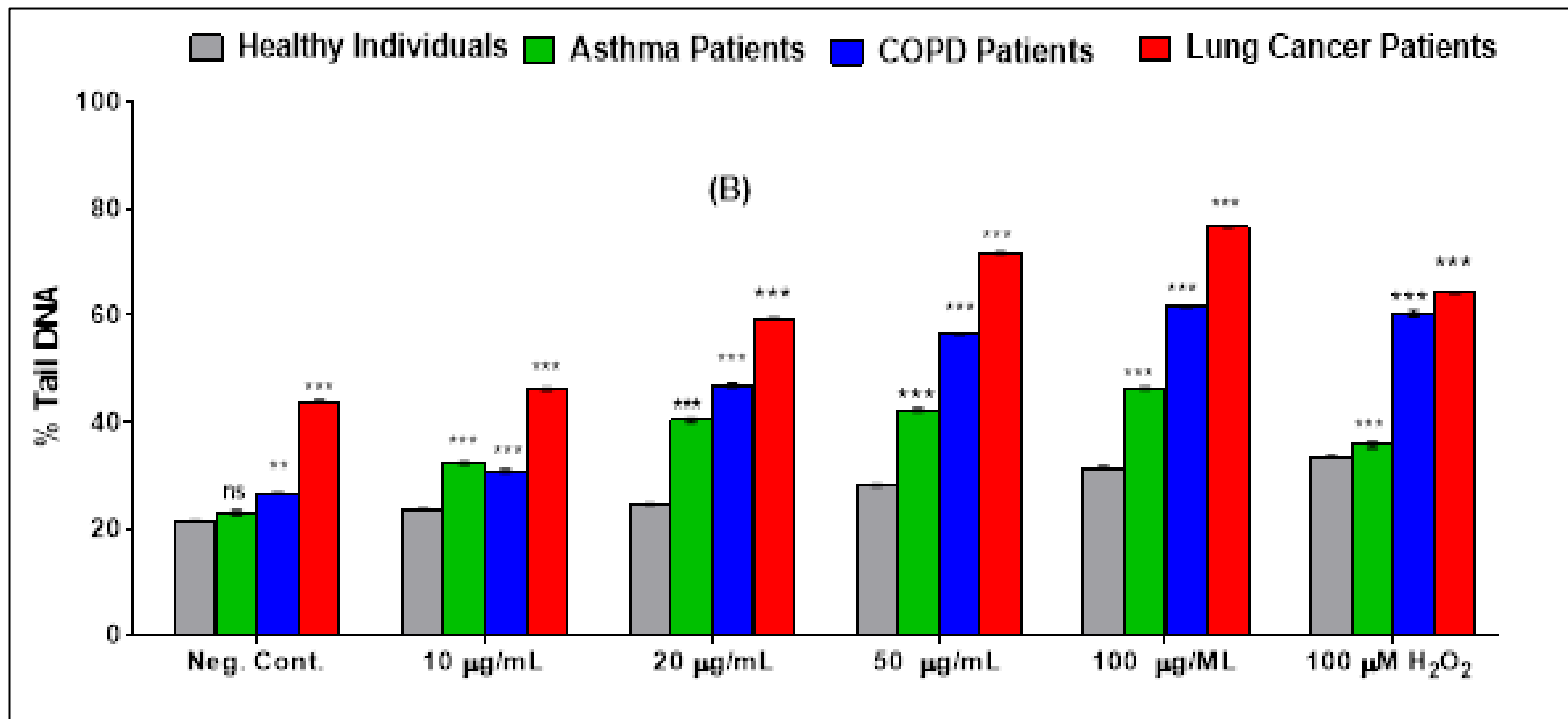


Figure 5.3: GO-induced DNA damage in human whole blood from healthy individuals and patients (% tail DNA). Blood samples from healthy individuals (Grey colour), asthma (Green colour), COPD (Blue colour), and lung cancer patients (Red colour) were treated with four different concentrations of GO (10, 20, 50, and 100 µg/mL) and 100 µM H₂O₂ (positive control, PC, shown on the right-hand side of the histograms) compared to the untreated whole blood samples (Negative control, shown on the left-hand side of the histograms). DNA damage was expressed as the percentage of the DNA in the tail (% Tail DNA). Statistical significance was rated at $p < 0.05$; where * = $p < 0.05$; ** = $p < 0.01$; *** = $p < 0.001$; and ns = not significant; 20 x independent Comet assay experiments x 4 per treatment groups; n = 80.

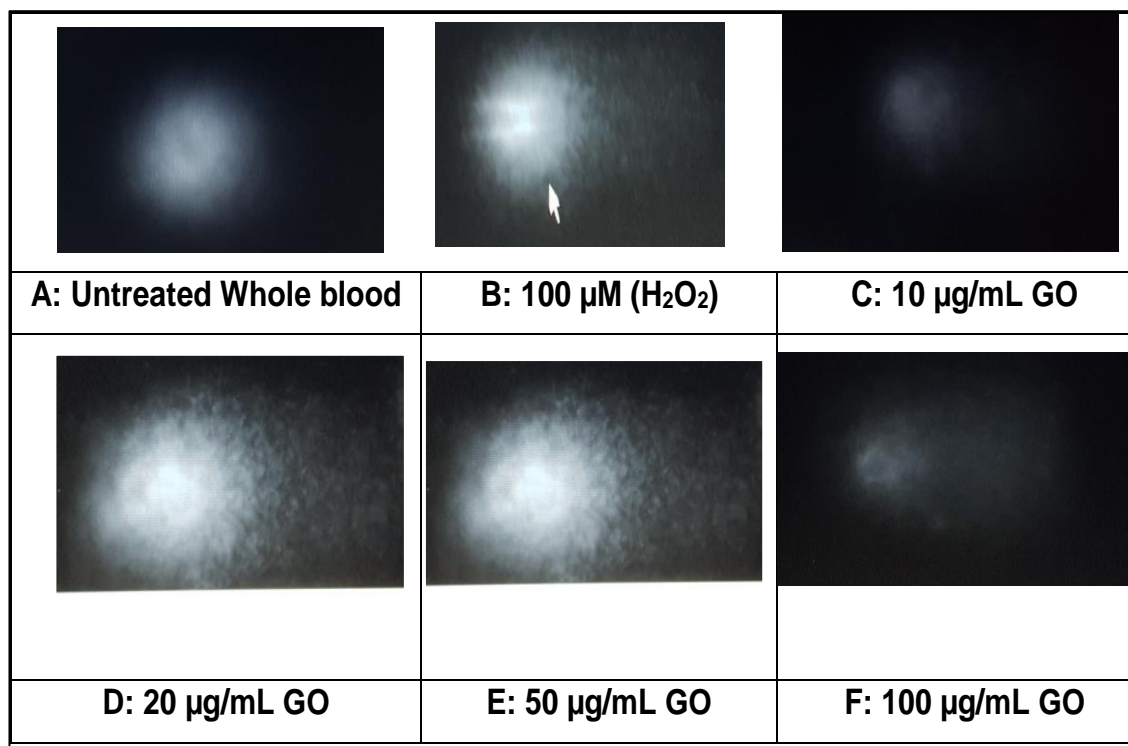


Figure 5.4: Representative Comet images formed after migration of broken DNA fragments from DNA head to the tail (Tail DNA); illustrating the extent of DNA damage on human whole blood from lung cancer patients treated with GO: C = 10 μg/mL; D =20 μg/mL; E = 50; and F = 100 μg/mL); B = 100 μM H₂O₂; while A = NC.

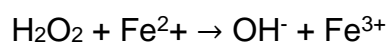
5.3.3 Confounding Factors

A total of 80 individuals participated in the study, 55 % were male [15% healthy, 9% asthma, 16% COPD, and 15% lung cancer] and 45 % were female [10% healthy, 16% asthma, 9% COPD, and 10% lung cancer]. In healthy individuals, there were no confounding effects on smoking history since 100 % of them were non-smokers. However, there appears to be a confounding effect on age as the males had a wide age range (24-69) than those of females (32-56). In asthma patients, there were no confounding effects on age (31-64), but confounding effects were observed due to smoking history (4% males, and 3% females).

In COPD and lung cancer patients, confounding factors were observed in age (49-70) in COPD, and upper age range (50-77) in lung cancer patients. 100% of all COPD patients and 90% of all lung cancer patients had a history smoking.

5.4 Discussion

From our Comet assay results in determining H₂O₂-concentration dependent DNA damage, it was evident that H₂O₂ caused various levels of DNA damage in healthy blood samples after 30 min of treatment. H₂O₂ is a free radical by itself, and it is one of the most commonly produced ROS intermediates (Benhusein et al. 2010) induced through various types of oxidative stress and during normal body physiology such as respiration (Waris and Ahsan 2006). When ROS is produced in excess of the body's normal defence mechanism, the excess ROS overload causes toxic oxidative stress and tissue damage (Benhusein et al. 2010). Excess ROS diffuses through the cellular membranes into the cytoplasm through water channels (also known as aquaporins), and rapidly reaches the nucleus and attacks the DNA. Because of the sensitive nature of the DNA, it is believed that H₂O₂ causes DNA damage by generating hydroxyl-free radicals (OH[•]). The OH[•] attacks the sugar component of the DNA backbone, causing DNA SSB, through the Fenton reaction (Duthie et al. 1997).



In a previous study by Frenzilli et al (2000), DNA damage was analysed after exposure *in-vivo* to rats and *in-vitro* to human leukocytes cell cultures treated with 4 different concentrations of H₂O₂ (25, 50, 100, and 200 µM, respectively) for 4 hours in the Comet assay (Frenzilli et al. 2000). In another study by (Benhusein et al. 2010), the authors treated HepG2 cells (immortalized cell line from human

liver carcinoma cells) with 25 μM and 50 μM of H_2O_2 and DNA damage assessed in a time-dependent manner at 5, 30 and 40 min and then at 1 and 24 h, respectively. Both studies showed that DNA damage increased significantly with increased H_2O_2 concentration in a timely-dependent manner (Benhusein et al. 2010).

Upon treatment of human whole blood with different concentrations of GO (10, 20, 50 and 100 $\mu\text{g}/\text{mL}$) for 30 min, it was evident that DNA damage increased significantly with increased concentrations. Especially in patients with chronic pulmonary diseases (asthma, COPD, and lung cancer), it was generally observed that lung cancer patients had the most significant DNA damage than in COPD patients compared to healthy control individuals as well as to untreated blood samples. Theoretically, this could be attributed to the fact that the DNA of lung cancer patients could be relatively unstable due to various genetic changes (mutations) leading up to lung cancer (U.S. National Library of Medicine 2019) and are therefore weaker and more vulnerable to genotoxic particles. Patients with asthma and healthy individuals almost had the same level of DNA damage. The fact that healthy individuals, assumed to be immunocompetent, suffered various levels of DNA damage within 30 min of exposure to GO could be of concern to public health (industrial exposure) and in nanomedical applications in biomedical science. These results are clear indications of the need for future comprehensive genotoxicity studies of GO (15-20 sheets) both *in-vivo* and *in-vitro* in order to develop better knowledge of DNA damage at the molecular level and resolve the conflicting genotoxicity data available on different types and sizes

of GO as well as detailed information of cell lines used (Liu et al. 2013a; Wu et al. 2015).

We have established using the Comet assay that GO caused DNA damage in human whole blood with increased GO concentration depending on the pathological conditions of the individuals. Previous investigations have shown that GO prepared with chemical exfoliation method (Hummer's method) contains significant amounts of catalytic ions such as Manganese (Mn^{2+}) and ferrous ions (Fe^{2+}) (Liu et al. 2013a). The presence of such impurities may result in unusually high levels of cytotoxicity, genotoxicity, and random scission of DNA, indicating the importance of purification of GO nanomaterials before use. This could lead to false-positive results. In fact, research shows that organic pollutants such as Mn^{2+} impurities on carbon nanotubes induced significant biological effects (Stéfani et al. 2011).

Exposure of human neuroblastoma cells (SH-SY5Y) to Mn^{2+} decreased cell viability in a concentration-dependent manner relative to the negative controls (Stephenson et al. 2013). These authors have shown that Mn^{2+} and Fe^{2+} caused DNA damage in cells when assayed by the alkaline Comet assay. It is, therefore, imperative to assess the presence of impurities in GO, especially commercially purchased GO and if possible, to quantify their levels before comprehensive cytotoxicity and genotoxicity studies could be established.

Next, we tested the hypothesis that GO nanomaterials could induce cytogenetic effects (mutagenicity) in human DNA using the Micronucleus Assay.

Chapter 6: Cytogenetic Assay

6.0 Analysis of the Effects of GO on genetic instability endpoints (Chromosome aberration and Micronuclei (MNi)) in healthy individuals and patients (asthma, COPD, and lung cancer) in the Cytokinesis-Blocked Micronucleus (CBMN) Assay

6.1 Introduction

In the previous chapter (Chapter 5), we established using the Alkaline Comet assay that human whole blood from both patients (asthma, COPD, and lung cancer) and healthy individual treated with different concentrations of GO (10, 20, 50 and 100 µg/mL) for 30 min were genotoxic (DNA damage).

DNA damage, expressed as OTM and % Tail DNA, was concentration-dependent, but according to the pathological state of the individuals. We also observed that DNA damage was significantly ($p > 0.05$) higher in lung cancer patients than in COPD patients, whereas in asthma patients and healthy individuals, DNA damage levels were almost the same. When we compared the DNA damage levels in the 3 untreated samples (the Neg. Controls) in both healthy and patients, we observed that patients with lung cancer and COPD had the highest level of DNA damage, a marker of high instability, vulnerability, and low immune system due to a number of mutational sequences leading up to the development of COPD and lung cancer.

The results obtained were confirmation that there is a close relationship between DNA damage and COPD, with COPD being the greatest risk factor for lung cancer (Adcock et al. 2011). Having established DNA damage in the Comet assay, this chapter dwells on the assessment of chromosome damage parameters with CBMN assay.

6.1.1 Hypothesis: GO may cause mutagenesis in human whole blood

In this chapter, we hypothesised that GO NMs may cause cytogenetic effects/ chromosome breakage through disturbance of the chromosomal formation.

During normal cell cycle, the cells grow, replicate their DNA, and then undergo cell division - mitosis (nuclear division) and cytokinesis (cytoplasmic division) - forming two daughter-cells. These new daughter cells then grow and repeat the same cycle all over again. Once each phase is successfully completed, the cells progress into the next phase, and the phase is activated. However, if cell progression is stopped, or somehow is unable to complete its activities, the cells would enter the resting phase (G_0 -phase), also known as quiescence (Daignan-Fornier and Sagot 2011) (see **Figure 6.1**).

During the interphase, cell growth occurs at the G_1 -phase, and cells are checked at the G_1 -checkpoint to check for any defects. Once completed, the cells progress into S-phase for DNA synthesis, where all chromosomes are duplicated. Thereafter, they progress into the G_2 -phase. It is at the G_2 -checkpoint that duplicated cells are “double-checked” before proceeding into the next phase of nuclear division (mitosis/karyokinesis).

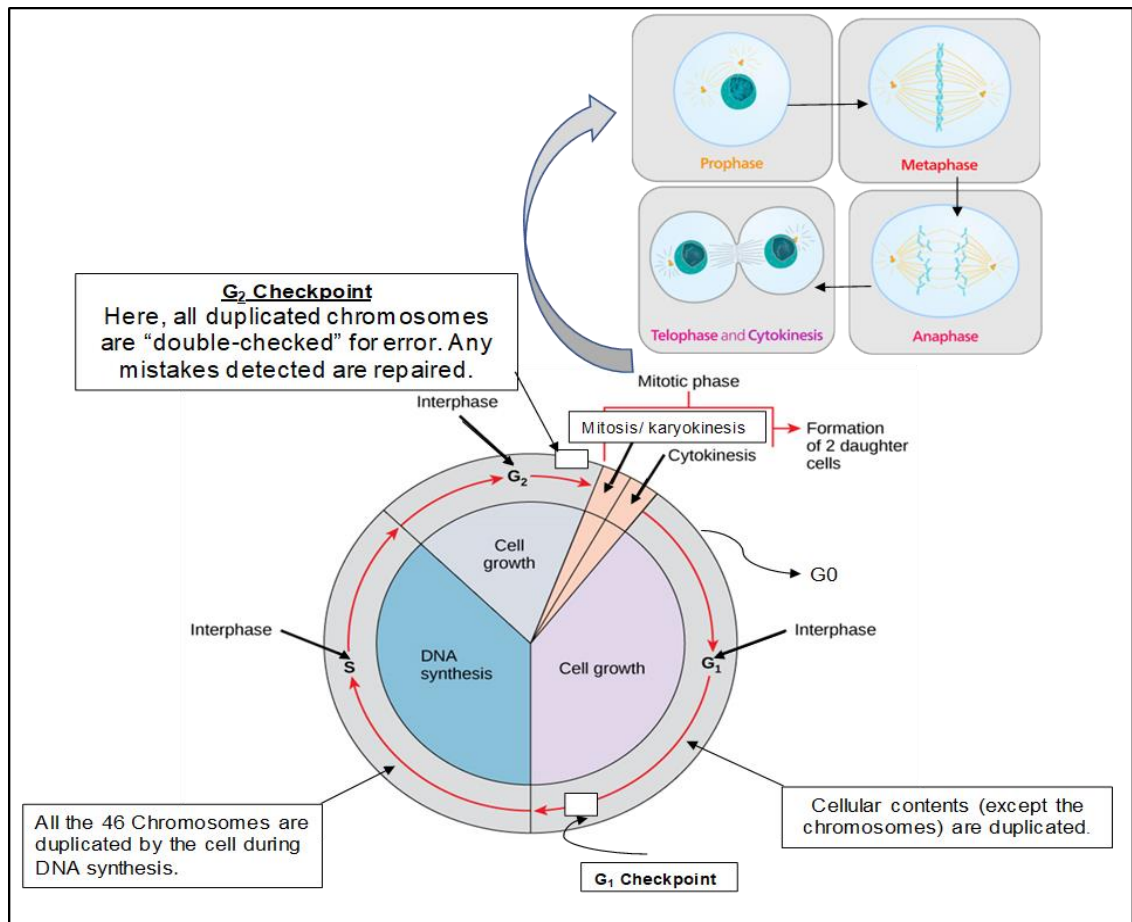


Figure 6.1: Schematic illustration of cell cycle. It comprises two major components: (1) The Interphase (G₀, G₁, S & G₂), and (2) the Mitotic phase (mitosis & cytokinesis) (Lumen Learning 2017; CNX 2019).

The mitotic phase has 4 sequences which cells must undergo in a coordinated manner (**Prophase** → **Metaphase** → **Anaphase** → **Telophase**) and the duplicated chromosomes segregate and are distributed into daughter nuclei. This process is immediately followed by cytokinesis where cell cytoplasmic division takes place, forming two daughter cells. The 2 daughter cells can either start a new cycle or enter the G₀ state (CNX 2019). The cell cycle is an organised order of activities where cells undergoing cell division pass through a sequence of events in a precisely, timely and tightly controlled phases (Kelvinsong 2012; Lumen Learning 2017).

As illustrated in **Figure 6.1**, the cell cycle consists of two major phases: The **Interphase**, and the **M Phase** (Mitotic phase). The **Interphase** comprises 3 phases, namely the **G₁ Phase** (Gap1 phase; Growth Phase), **S-phase** (DNA Synthesis), and **G₂ Phase** (Gap2 phase; Growth Phase), while the **Mitotic Phase** comprises 4 phases, namely the **Prophase, Metaphase, Anaphase, and Telophase** (PMAT). In the **G₁ phase**, the cells actively grow and accumulate building blocks such as chromosomes and proteins essential for DNA synthesis, and the DNA components are checked at the **G₁-Checkpoint** in readiness for the next phase of the cell cycle. In the **S-phase**, all 46 chromosomes of the DNA are duplicated during DNA synthesis to yield two identical DNA molecules (also called sister-chromatids), which then progress into the G₂ phase. Here, the cells continue to grow, producing more proteins and cellular components (e.g. organelles, etc). At the **G₂-Checkpoints**, chromosome arrangements are actively checked for any defects, and any abnormalities identified are repaired ready for the next phase - Mitotic phase (**M Phase**).

At the Mitotic phase, the nuclear DNAs are condensed into chromosomes and cells undergo nuclear divisions to form two nuclei through 4 sub-phases as previously described and illustrated in **Figure 6.1**. In the final phase of the cell-cycle (cytokinesis), the cytoplasm divides into two forming 2 new daughter cells (Cooper 2000; Bryant et al. 2007). The duration of cell cycle varies depending on the cell type. In a rapidly dividing human cell, a cell cycle could be completed in 24 h, comprising 11 h in the G₁ phase; 8 h in the S-Phase; 4 h in G₂ Phase; and 1 h in the Mitotic Phase (Toppr 2018).

The basis of the CBMN assay is its sensitivity in detecting chromosomal aberration parameters (BiNC, MNi, etc) after exposure to mutagenic agents in actively dividing cells. Cytokinesis commences immediately after mitosis (nuclear division) is complete. Cyto-B is a cell-permeable mycotoxin which blocks the cytokinesis stage of the cell cycle and disrupts actin formation – a contractile microfilament ring assembly that is vital for the cell morphology (shape), cytoskeletal framework and structure of cells (Heng and Koh 2010). In addition to cytokinesis inhibition, Cyto-B has an intrinsic DNA damaging property, leading to accumulation of damaged chromosomes (clastogenicity) as well as loss of chromosomes (aneugenicity) (Schwarzbacherova et al. 2016). To test the hypothesis, we used the CBMN assay developed by Schmid (Schmid 1975) to assess chromosome instability parameters in human whole blood after exposure to GO nanomaterials (10, 20, 50, and 100 µg/mL) and MMC as PC.

6.2 Materials and Methods

Reagents, materials, and equipment used in the Micronucleus Assay were listed in Sections 2.1.1 and 2.1.2, and Methods described in Section 2.2.11.1.2.

6.3 Results

6.3.1 Analysis of Genetic Instability Endpoints (Mononucleated cells (MonoNC), Binucleated cells (BiNC), Multinucleated cells (MultiNC), Micronuclei (MNi), Nucleoplasmic bridges (NPBs), and Nuclear Buds (NBUDs)) induced after treatment with GO in healthy individuals and patients (asthma, COPD, and lung cancer) in the CBMN Assay

The results of the cytogenetic (genetic instability) endpoints (frequencies of Mono NC, BiNC, MultiNC, BiNPBs, BiNBUDs, NDI, and BiMNI frequencies) scored in the CBMN assay are summarized in Table 6-1 for healthy individuals; Table 6-2 for asthma patients; Table 6-3 for COPD patients; and Table 6-4 for lung cancer patients, respectively. A total of 20 CBMN assays were performed in this project, comprising 5 CBMN assays each in healthy individuals, asthma, COPD, and lung cancer patients, respectively. Human whole blood samples from the above-mentioned participants were cultured in the appropriate medium for 24 h, followed by treatment with four different concentrations of GO (10, 20, 50 and 100 µg/mL) and 0.4 mM MMC as the PC for 20 h. The untreated blood samples served as the negative control (NC). After 44 h of cell culture or 20 h of chemical treatment, they were treated with Cyto-B to block cytokinesis and prevent cytoplasmic division of the cells. After 72 h, the cells were harvested, fixed in Carnoy's Fixative, and mounted on glass slides before scoring under the microscope. The mitotic and genetic instability parameters were scored, and values reported as the Mean ± SEM.

Generally, we observed that different concentrations of GO (10, 20, 50 and 100 µg/mL) decreased induction of MonoNC significantly ($p < 0.001$) in a concentration-dependent manner across the treatment groups (healthy, asthma, COPD, and lung cancer), while % BiNC, % MultiNC, and NDI increased significantly ($p < 0.001$) in concentration-dependent manner, but not always, especially in the BiMNI, BiNPBs, BiNBUDs and MonoMNI which demonstrated altered levels of chromosome damage parameters.

Mono-nucleated cells (MonoNC)

In healthy individuals (Table 6-1) after treatment with 10, 20, 50 and 100 µg/mL of GO, the MonoNC decreased significantly from 38.12% (NC) to 33.40±0.41% (p<0.001); to 29.76±0.39% (p<0.001); to 27.52±1.02% (p<0.001); and to 24.52±0.63% (p<0.001), respectively. In patients treated with the aforementioned concentrations (10, 20, 50, and 100 µg/mL), induction of MonoNC decreased significantly in asthma patients (Table 6.2) from 35.20% (NC) to 34.28±0.85% (p<0.001); to 30.96±0.32% (p<0.001); to 27.08±0.45% (p<0.001); and to 25.16±0.79% (p<0.001), respectively. In COPD patients exposed to the aforementioned four concentrations of GO NMs (Table 6.3), the % MonoNC decreased significantly from 33.12±0.55% (NC) to 31.84±0.31% (p<0.001); to 29±0.40% (p<0.001); to 24.60±0.45% (p<0.001); and to 21.52±0.55% (p<0.001), respectively. In lung cancer patients treated with the same GO concentrations (10, 20, 50, and 100 µg/mL) (Table 6.4), the % MonoNC decreased significantly from 32.24±1.80% (NC) to 29.56±0.44% (p<0.001); to 25.24±0.99% (p<0.001); to 22.72±0.92% (p<0.001); and to 15.56±1.31% (p<0.001). Therefore, induction of MonoNC was the lowest in cancer patients, followed by COPD and asthma patients, compared with healthy individuals in this order:

% MonoNC Induction: Healthy ≈ asthma > COPD > Lung cancer

Binucleated cells (BiNC)

Induction of BiNC presented some interesting characteristics after treatment with GO concentrations (10, 20, 50, and 100 µg/mL). Generally, induction of BiNC increased significantly (p<0.001) with increased GO concentrations. Specifically,

in healthy individuals, % BiNC increased from $61.16 \pm 1.11\%$ (NC) to $65.72 \pm 0.42\%$ ($p < 0.001$); to $69.08 \pm 0.40\%$ ($p < 0.001$); to $71.12 \pm 0.99\%$ ($p < 0.001$) and to $73.52 \pm 0.26\%$ ($p < 0.001$), respectively. In asthma patients, the same pattern of significant BiNC inductions were also observed after exposure to 10, 20, 50, and 100 $\mu\text{g/mL}$ of GO NMs. Here, the % BiNC increased significantly from $63.84 \pm 0.88\%$ (NC) to $64.76 \pm 0.86\%$ ($p < 0.001$); to $67.80 \pm 0.32\%$ ($p < 0.001$); to $70.72 \pm 0.46\%$ ($p < 0.001$); and to $72.24 \pm 0.72\%$ ($p < 0.001$) with increased GO concentrations. In blood samples of COPD patients treated with GO concentrations (10, 20, 50, and 100 $\mu\text{g/mL}$), BiNC were induced significantly from $65.72 \pm 0.52\%$ (NC) to $66.84 \pm 0.25\%$ ($p < 0.001$); to $69.92 \pm 0.43\%$ ($p < 0.001$); to $72.88 \pm 0.34\%$ ($p < 0.001$); and to $75.84 \pm 0.66\%$ ($p < 0.001$), respectively. Finally, in lung cancer patients exposed to the aforementioned GO concentrations (10, 20, 50, and 100 $\mu\text{g/mL}$), inductions of BiNC were observed to increase significantly from $66.16 \pm 1.64\%$ (NC) to $68.84 \pm 0.46\%$ ($p < 0.001$); to $72.56 \pm 0.95\%$ ($p < 0.001$); to $74.56 \pm 0.84\%$ ($p < 0.001$); and to $80.04 \pm 1.26\%$ ($p < 0.001$) with increased GO concentrations. In summary, BiNC induction followed the following pattern:

% BiNC induction: Lung cancer > COPD > healthy \approx asthma.

Multi-nucleated cells (MultiNC)

The MultiNC are cells formed with 3 or more MonoNC sharing the same cytoplasm. A study conducted elsewhere showed that MultiNC can constantly generate MonoNC in the absence of mitosis (Solari et al. 1995). After exposure to GO NMs at various concentrations (10, 20, 50 and 100 $\mu\text{g/mL}$) for 20 h, the

frequencies of MultiNC observed increased with increased GO concentration in each treatment group.

In healthy individuals treated with the aforementioned concentrations of GO NMs (10, 20, 50 and 100 $\mu\text{g}/\text{mL}$), the % MultiNC increased significantly from $1.44\pm 0.21\%$ to $1.76\pm 0.20\%$ ($p<0.001$); to $2.32\pm 0.15\%$ ($p<0.001$); to $2.72\pm 0.15\%$ ($p<0.001$); and to $4.47\pm 0.41\%$ ($p<0.001$) with increased GO concentrations. In asthma patients, we also observed significant increases in the %MultiNC. At 10 $\mu\text{g}/\text{mL}$, the induction of %MultiNC from $1.92\pm 0.27\%$ (NC) to $1.92\pm 0.08\%$ was not statistically significant. When cells were exposed to higher concentrations (20, 50 and 100 $\mu\text{g}/\text{mL}$), we observed gradual and significant increases in the %MultiNC to $2.48\pm 0.15\%$ ($p<0.001$); to $2.80\pm 0.13\%$ ($p<0.001$); and to $5.20\pm 0.44\%$ ($p<0.001$), respectively. In blood samples of COPD patients, all treated concentrations of GO NMs (10, 20, 50 and 100 $\mu\text{g}/\text{mL}$) showed various levels of inductions of MultiNC. At 10 $\mu\text{g}/\text{mL}$ of GO, the induction of MultiNC increased significantly from $2.32\pm 0.15\%$ (NC) to $2.64\pm 0.16\%$ ($p<0.001$). However, at 20 $\mu\text{g}/\text{mL}$, the %MultiNC was significantly decreased to $2.16\pm 0.10\%$ ($p<0.001$). This decrease could be due to aggregation of particles leading to less contact of the GO NMs with blood cells during the 20 h incubation. At 50, and 100 $\mu\text{g}/\text{mL}$, the proportions of %MultiNC increased significantly to $4.40\pm 0.31\%$ ($p<0.001$) and to $5.28\pm 0.74\%$ ($p<0.001$), respectively. In lung cancer patients, exposure of blood samples to the lowest concentration (10 $\mu\text{g}/\text{mL}$ of GO) did not cause statistically significant changes in the %MultiNC in treated cells ($3.20\pm 0.13\%$, ns) relative to untreated, NC samples ($3.20\pm 0.42\%$). However, when blood samples were

exposed to higher concentrations (20, 50 and 100 $\mu\text{g}/\text{mL}$), we observed significant increases in the %MultiNC to $4.40\pm 1.01\%$ ($p<0.001$); to $5.44\pm 0.30\%$ ($p<0.001$); and to $8.80\pm 0.68\%$ ($p<0.001$), respectively. In summary, MultiNC induction followed the following pattern:

% MultiNC induction: Lung cancer > COPD > healthy \approx asthma

Nuclear division index (NDI)

The NDI values were calculated using the data from the proportions of MonoNC, BiNC, and MultiNC per 1,000 cells scored. A review of the NDI data shows a peculiar pattern. The NDI values increased significantly ($p<0.001$) with increases in GO concentrations (10, 20, 50, and 100 $\mu\text{g}/\text{mL}$) in healthy individuals from 1.63 ± 0.01 (NC) to 1.69 ± 0.02 ($p<0.001$), 1.71 ± 0.00 ($p<0.001$), 1.74 ± 0.01 ($p<0.001$), to 1.79 ± 0.00 ($p<0.001$), respectively. However, in asthma patients, there was a sudden deviation from the above trend. After exposure to 10 and 20 $\mu\text{g}/\text{mL}$ of GO, the NDI values increased significantly from 1.66 ± 0.01 (NC) to 1.67 ± 0.01 and 1.80 ± 0.66 , respectively. When the concentration was increased to 50 $\mu\text{g}/\text{mL}$, the NDI value suddenly dropped significantly to 1.74 ± 0.60 ($p<0.001$), and again increased significantly to 1.77 ± 0.01 ($p<0.001$) at 100 $\mu\text{g}/\text{mL}$. This drop in NDI value – a biomarker of inhibition of cell growth (cytostatic events) - could be attributed to particle aggregation as the sheets of GO particles settled to the bottom of the reaction tubes during 20 h of chemical treatment, and possibly could have had less contact with the cells. In COPD patients, lower concentration (10 $\mu\text{g}/\text{mL}$) did not cause significant induction of the NDI (1.69 ± 0.00 ; ns) relative to the untreated NC samples (1.69 ± 0.01). However, at

higher concentrations (20, 50, and 100 $\mu\text{g}/\text{mL}$), we observed significant concentration-dependent increases in the NDI values to 1.72 ± 0.00 ($p<0.001$); 1.77 ± 0.01 ($p<0.001$), and to 1.81 ± 0.01 ($p<0.001$), respectively. In lung cancer patients, all treated concentrations (10, 20, 50, and 100 $\mu\text{g}/\text{mL}$) caused statistically significant increases in the NDI value from 1.69 ± 0.02 to 1.72 ± 0.00 ($p<0.001$), 1.77 ± 0.01 ($p<0.001$), 1.80 ± 0.01 ($p<0.001$), and 1.89 ± 0.01 ($p<0.001$), respectively.

Frequencies of MNi induction

Regarding the frequencies of MNi, we observed that MNi were induced as BiMNi and MonoMNi, but with some irregularities. In healthy individuals, after treatment with 10 $\mu\text{g}/\text{mL}$ of GO NMs, induction of BiMNi dropped in a statistically significant manner from 1.80 (NC) to 0.80 ($p<0.001$), but peaked to 3.00 ($p<0.001$) at 50 $\mu\text{g}/\text{mL}$ and again dropped to 2.80 ($p<0.001$) at 100 $\mu\text{g}/\text{mL}$ relative to the control. Again, the irregularities observed in the MNi induction at the two extreme concentrations (10 and 100 $\mu\text{g}/\text{mL}$) could be linked to particle behaviour in the culture medium. Either that the 10 $\mu\text{g}/\text{mL}$ concentration did not achieve 100% contacts with cells due to GO particle agglomeration, whereas at 100 $\mu\text{g}/\text{mL}$, GO NPs could have also clogged together leading to less cell contact during incubation. In asthma patients, the proportions of MNi induced in blood samples treated with lower concentrations (10 and 20 $\mu\text{g}/\text{mL}$) were different from those treated with higher concentrations of 50 and 100 $\mu\text{g}/\text{mL}$. GO NMs. After treatment with 10 and 20 $\mu\text{g}/\text{mL}$, induction of MNI decreased significant from 2.40 ± 0.98 (NC) to 1.5 ± 0.26 ($p<0.001$) and to 1.80 ± 0.66 ($p<0.001$), respectively. However, after exposure to 50 and 100 $\mu\text{g}/\text{mL}$, BiMNi induction increased significantly to

5.20±0.80 (p<0.001) and 5.80 ±1.24 (p<0.001), respectively. In COPD patients, blood samples treated with 10 µg/mL of GO NMs caused significant decrease in BiMNI induction from 3.80±80 (NC) to 3.20±0.58 (p<0.001). However, upon treatments with 20, 50, and 100 µg/mL, more BiMNI were significantly induced from 3.80±80 (NC) to 5.60±1.03 (p<0.001), 5.80±1.46 (p<0.001), and to 6.00±0.45 (p<0.001), respectively. In lung cancer patients, GO NMS (10, 20, 50, and 100 µg/mL) caused significant concentration-dependent increases in BiMNI induction from 3.40±0.51 to 4.40±1.14 (p<0.001), 5.80±0.37 (p<0.001), 7.40±0.51 (p<0.001), and to 9.40±0.51 (p<0.001), respectively.

Chromosome Instability Parameters (NPBs, NBUDs, and MonoMNI)

Chromosomal instability parameters such as nucleoplasmic bridges (NPBs) and nuclear buds (NBUDs), as well as MonoMNI frequencies were also scored. **In healthy individuals**, samples treated with 10 and 20 µg/mL equal amounts of BiNPBs induced from 0.00 to 0.20±0.20 (p<0.001), but 50 µg/mL failed to induce BiNPBs. However, when cells were treated with 100 µg/mL, BiNPBs levels were significantly induced to 0.60±0.24 (p<0.001). In the NC and 10 µg/mL samples, BiNBUDs were not induced at all (0.00), and thus were not observed, while samples treated with 20 and 50 µg/mL induced equal amounts of BiNBUDs from 0.00 to 0.20±0.20 (p<0.001). After exposure to 100 µg/mL of GO NMs, BiNBUDs were induced significantly to 0.40±0.24 (p<0.001). The frequencies of the MonoMNI were induced in statistically significant manner with increases in GO NMS concentrations (10, 20,50, and 100 µg/mL). At 10 µg/mL, there was a decrease in MonoMNI induction from 0.40±0.24 to 0.20±0.20 (p<0.001), but the induction

increased significantly after treatment with higher concentrations (20, 50 and 100 $\mu\text{g}/\text{mL}$) to 0.80 ± 0.37 ($p<0.001$), 1.60 ± 0.24 ($p<0.001$), and to 2.60 ± 0.93 ($p<0.001$).

In asthma patients, cells treated with 10 $\mu\text{g}/\text{mL}$ of GO NMs did not induce BiNPBs at all, but cells treated with 20 and 50 $\mu\text{g}/\text{mL}$ induced equal amounts of BiNPBs (0.60 ± 0.40 and 0.60 ± 0.24 ($p<0.001$)). However, when cells were treated with 100 $\mu\text{g}/\text{mL}$ of GO NMs, BiNPBs were induced significantly to 1.20 ± 0.58 ($p<0.001$) relative to the untreated, NC samples (0.00). BiNBUDs and Mono MNi were also induced significantly ($p<0.001$) after treatment with various concentrations of GO NMs. Cells treated with 10, 20, 50, and 100 $\mu\text{g}/\text{mL}$ induced BiNBUDs by 0.50 ± 0.26 ($p<0.001$), 0.40 ± 0.24 (ns), 1.60 ± 0.24 ($p<0.001$), and 1.40 ± 0.60 ($p<0.001$) relative to untreated samples (0.40 ± 0.24). The frequencies of the Mono MNi were also induced significantly after treatment with 10, 20, 50, and 100 $\mu\text{g}/\text{mL}$ of GO NMs by 0.50 ± 0.26 ($p<0.001$), 0.80 ± 0.37 ($p<0.001$), 1.80 ± 0.80 ($p<0.001$), and 5.20 ± 0.97 ($p<0.001$) relative to the untreated cells (1.00 ± 0.32).

In COPD patients, blood samples treated with 10 $\mu\text{g}/\text{mL}$ did not induce BiNPBs, while cells treated with 20 $\mu\text{g}/\text{mL}$ induced significant amounts of BiNPBs by 0.80 ± 0.49 ($p<0.001$). In cells treated with 50 $\mu\text{g}/\text{mL}$, the amounts of BiNPBs induced were decreased by half to 0.40 ± 0.24 ($p<0.001$), but cells treated with 100 $\mu\text{g}/\text{mL}$ of GO NMs increased significantly to 0.60 ± 0.24 ($p<0.001$). The BiNBUDs and Mono MNi were also induced significantly ($p<0.001$) after treatment with various concentrations of GO NMs. Cells treated with 10, 20, 50, and 100 $\mu\text{g}/\text{mL}$ induced BiNBUDs by 0.20 ± 0.20 (ns), 0.80 ± 0.20 ($p<0.001$), 0.80 ± 0.37 ($p<0.001$), and 1.40 ± 0.40 ($p<0.001$) relative to untreated samples

(0.20±0.20). The frequencies of MonoMNI were also induced significantly after treatments with the aforementioned concentrations (10, 20,50, and 100 µg/mL) of GO NMs by 1.40±0.40 (p<0.001), 3.00±0.89 (p<0.001), 3.00±0.84 (p<0.001), and 3.20±1.11 (p<0.001) relative to the untreated cells (2.60±0.40).

In lung cancer patients, blood samples treated with different concentrations of GO NMs 10, 20, 50, and 100 µg/mL, the amounts of BiNPBs induced were significantly low at 0.20±0.20 (p<0.001), 1.00±0.32 (p<0.001), 0.40±0.24 (p<0.001), and 1.00±0.45 (p<0.001) relative to untreated cells (2.00±0.63).

BiNPBs were also induced to various amounts to 0.60±0.24 (p<0.001), 1.20±0.20 (p<0.001), 0.60±0.40 (p<0.001), and to 1.00±0.32 (p<0.001) respectively relative to untreated cells (0.00±0.00). With regard to the MonoMNI inductions, after treatment to the aforementioned concentrations of GO NMS, MonoMNI cells were induced significantly to 3.60±1.37 (p<0.001), 4.80±0.66 (p<0.001), 6.20±0.66 (p<0.001), and to 7.40±0.51 (p<0.001) respectively relative to untreated NC (2.80±0.66).

Photographic Images of the different chromosome instability parameters taken during scoring are shown in **Figures 6.2** and **6.3**.

Table 6-1: Mean values of various genetic instability parameters in human whole blood after treatment with different concentrations of GO (0, 10, 20, 50 and 100 µg/mL) and 0.4 µM MMC in Healthy Individuals in the CBMN Assay. DNA damage events were scored specifically in once divided binucleated cells. Statistical analyses were performed using GraphPad Prism, version 8.1.2 (332) with built-in One-Way ANOVA and Dunnett's multiple comparisons tests to compare cytogenetic parameters in treated samples relative to the negative control (NC). Statistical significance was rated at $p < 0.05$; where * = $p < 0.05$ and ns = not significant; 5 x independent experiments (n = 5).

Healthy Individuals	Chemical Conc.	Mean % MonoNC	Mean % BiNC	Mean % MultiNC	Mean NDI	Mean BiMNi	Mean BiNPBs	Mean BiNBUDs	Mean MonoMNi
NC	0 µg/mL	38.12±1.10	61.16±1.11	1.44±0.20	1.63±0.01	1.80±0.66	0.00±0.00	0.00±0.00	0.40±0.24
MMC (PC)	0.4 µM	18.4±0.70 ***	79.56±0.58 ***	4.08±0.34 ***	1.84±0.01 ***	2.8±0.58 ***	0.80±0.49 ***	0.80±0.37 ***	1.20±0.20 ***
GO (µg/mL)	10	33.40±0.41 ***	65.72±0.42 ***	1.76±0.20 ***	1.69±0.02 ***	0.80±0.37 ***	0.20±0.20 ***	0.00±0.00 ns	0.20±0.20 ***
	20	29.76±0.39 ***	69.08±0.40 ***	2.32±0.15 ***	1.71±0.00 ***	1.00±0.32 ***	0.20±0.20 ***	0.20±0.20 ***	0.80±0.37 ***
	50	27.52±1.02 ***	71.12±0.99 ***	2.72±0.15 ***	1.74±0.01 ***	3.00±0.71 ***	0.00±0.00 ns	0.20±0.20 ***	1.60±0.24 ***
	100	24.52±0.63 ***	73.52±0.26 ***	4.47±0.41 ***	1.79±0.00 ***	2.80±0.66 ***	0.60±0.24 ***	0.40±0.24 ***	2.60±0.93 ***

Where: MMC = Mitomycin C; MonoNC = Mononucleated cells; BiNC = Binucleated cells; MultiNC = Multinucleated cells; NDI = Nuclear Division Index; MNi = Micronuclei; NPBs = Nucleoplasmic bridges; and BUDs = nuclear buds (NBUDs).

Table 6-2: Mean values of various genetic instability parameters in human whole blood after treatment with different concentrations of GO (0, 10, 20, 50 and 100 µg/mL) and 0.4 µM MMC in asthma patients in the CBMN Assay. DNA damage events were scored specifically in once divided binucleated cells. Statistical analyses were performed using GraphPad Prism, version 8.1.2 (332) with built-in One-Way ANOVA and Dunnett's multiple comparisons tests to compare cytogenetic parameters in treated samples relative to the negative control (NC). Statistical significance was rated at $p < 0.05$; where * = $p < 0.05$ and ns = not significant; 5 x independent experiments (n = 5).

Asthma Patients	Chemical Conc.	Mean % MonoNC	Mean % BiNC	Mean % MultiNC	Mean NDI	Mean BiMNI	Mean BiNPBs	Mean BiNBUDs	Mean MonoMNI
NC	0 µg/mL	35.20±0.81	63.84±0.88	1.92±0.27	1.66±0.01	2.40±0.98	0.00±0.00	0.40±0.24	1.00±0.32
MMC (PC)	0.4 µM	23.08±0.34 ***	75.36±0.25 ***	3.12±0.34 ***	1.70±0.08 ***	6.20±0.86 ***	0.80±0.37 ***	0.60±0.40 ***	1.60±0.68 ***
GO (µg/mL)	10	34.28±0.85 ***	64.76±0.86 ***	1.92±0.08 ns	1.67±0.01 ***	1.50±0.26 ***	0.00±0.00 ns	0.50±0.26 ***	0.50±0.26 ***
	20	30.96±0.32 ***	67.80±0.32 ***	2.48±0.15 ***	1.80±0.66 ***	1.80±0.66 ***	0.60±0.40 ***	0.40±0.24 ns	0.80±0.37 ***
	50	27.08±0.45	70.72±0.46 ***	2.80±0.13 ***	1.74±0.60 ***	5.20±0.80 ***	0.60±0.24 ***	1.60±0.24 ***	1.80±0.80 ***
	100	25.16±0.79 ***	72.24±0.72 ***	5.20±0.44 ***	1.77±0.01 ***	5.80±1.24 ***	1.20±0.58 ***	1.40±0.60 ***	5.20±0.97 ***

Where: MMC = Mitomycin C; MonoNC = Mononucleated cells; BiNC = Binucleated cells; MultiNC = Multinucleated cells; NDI = Nuclear Division Index; MNI = Micronuclei; NPBs = Nucleoplasmic bridges; and BUDs = nuclear buds (NBUDs).

Table 6-3: Mean values of various genetic instability parameters in human whole blood after treatment with different concentrations of GO (0, 10, 20, 50 and 100 µg/mL) and 0.4 µM MMC in COPD patients in the CBMN Assay. DNA damage events were scored specifically in once divided binucleated cells. Statistical analyses were performed using GraphPad Prism, version 8.1.2 (332) with built-in One-Way ANOVA and Dunnett's multiple comparisons tests to compare cytogenetic parameters in treated samples relative to the negative control (NC). Statistical significance was rated at $p < 0.05$; where * = $p < 0.05$ and ns = not significant; 5 x independent experiments (n = 5).

COPD Patients	Chemical Conc.	Mean % MonoNC	Mean % BiNC	Mean % MultiNC	Mean NDI	Mean BiMNi	Mean BiNPBs	Mean BiNBUDs	Mean MonoMNi
NC	0 µg/mL	33.12±0.55	65.72±0.52	2.32±0.15	1.69±0.01	3.80±0.80	0.00±0.00	0.20±0.20	2.60±0.40
MMC (PC)	0.4 µM	22.52±1.29 ***	75.52±1.26 ***	3.92±0.32 ***	1.79±0.01 ***	6.80±1.28 ***	0.80±0.37 ***	0.80±0.37 ***	3.40±1.03 ***
GO (µg/mL)	10	31.84±0.31 ***	66.84±0.25 ***	2.64±0.16 ***	1.69±0.00 ns	3.20±0.58 ***	0.00±0.00 ns	0.20±0.20 ns	1.40±0.40 ***
	20	29.00±0.40 ***	69.92±0.43 ***	2.16±0.10 ***	1.72±0.00 ***	5.60±1.03 ***	0.80±0.49 ***	0.80±0.20 ***	3.00±0.89 ***
	50	24.60±0.45 ***	72.88±0.34 ***	4.40±0.31 ***	1.77±0.01 ***	5.80±1.46 ***	0.40±0.24 ***	0.80±0.37 ***	3.00±0.84 ***
	100	21.52±0.55 ***	75.84±0.66 ***	5.28±0.74 ***	1.81±0.01 ***	6.00±0.45 ***	0.60±0.24 ***	1.40±0.40 ***	3.20±1.11 ***

Where: MMC = Mitomycin C; MonoNC = Mononucleated cells; BiNC = Binucleated cells; MultiNC = Multinucleated cells; NDI = Nuclear Division Index; MNi = Micronuclei; NPBs = Nucleoplasmic bridges; and BUDs = nuclear buds (NBUDs).

Table 6-4: Mean values of various genetic instability parameters in human whole blood after treatment with different concentrations of GO (0, 10, 20, 50 and 100 µg/mL) and 0.4 µM MMC in lung cancer patients in the CBMN Assay. DNA damage events were scored specifically in once divided binucleated cells. Statistical analyses were performed using GraphPad Prism, version 8.1.2 (332) with built-in One-Way ANOVA and Dunnett's multiple comparisons tests to compare cytogenetic parameters in treated samples relative to the negative control (NC). Statistical significance was rated at p < 0.05; where * = p<0.05 and ns = not significant; 5 x independent experiments (n = 5).

Lung cancer Patients	Chemical Conc.	Mean % MonoNC	Mean % BiNC	Mean % MultiNC	Mean NDI	Mean BiMNi	Mean BiNPBs	Mean BiNBUDs	Mean MonoMNi
NC	0 µg/mL	32.24±1.80	66.16±1.64	3.20±0.42	1.69±0.02	3.40±0.51	2.00±0.63	0.00±0.00	2.80±0.66
MMC (PC)	0.4 µM	19.44±0.81 ***	77.56±0.66 ***	6.00±0.36 ***	1.84±0.01 ***	8.0±0.45 ***	1.00±0.40 ***	0.40±0.40 ***	5.80±0.37 ***
GO (µg/mL)	10	29.56±0.44 ***	68.84±0.46 ***	3.20±0.13 ns	1.72±0.00 ***	4.40±1.14 ***	0.20±0.20 ***	0.60±0.24 ***	3.60±1.37 ***
	20	25.24±0.99 ***	72.56±0.95 ***	4.40±1.01 ***	1.77±0.01 ***	5.80±0.37 ***	1.00±0.32 ***	1.20±0.20 ***	4.80±0.66 ***
	50	22.72±0.92 ***	74.56±0.84 ***	5.44±0.30 ***	1.80±0.01 ***	7.40±0.51 ***	0.40±0.24 ***	0.60±0.40 ***	6.20±0.66 ***
	100	15.56±1.31 ***	80.04±1.26 ***	8.80±0.68 ***	1.89±0.01 ***	9.40±0.51 ***	1.00±0.45 ***	1.00±0.32 ***	7.40±0.51 ***

Where: MMC = Mitomycin C; MonoNC = Mononucleated cells; BiNC = Binucleated cells; MultiNC = Multinucleated cells; NDI = Nuclear Division Index; MNi = Micronuclei; NPBs = Nucleoplasmic bridges; and BUDs = nuclear buds (NBUDs)

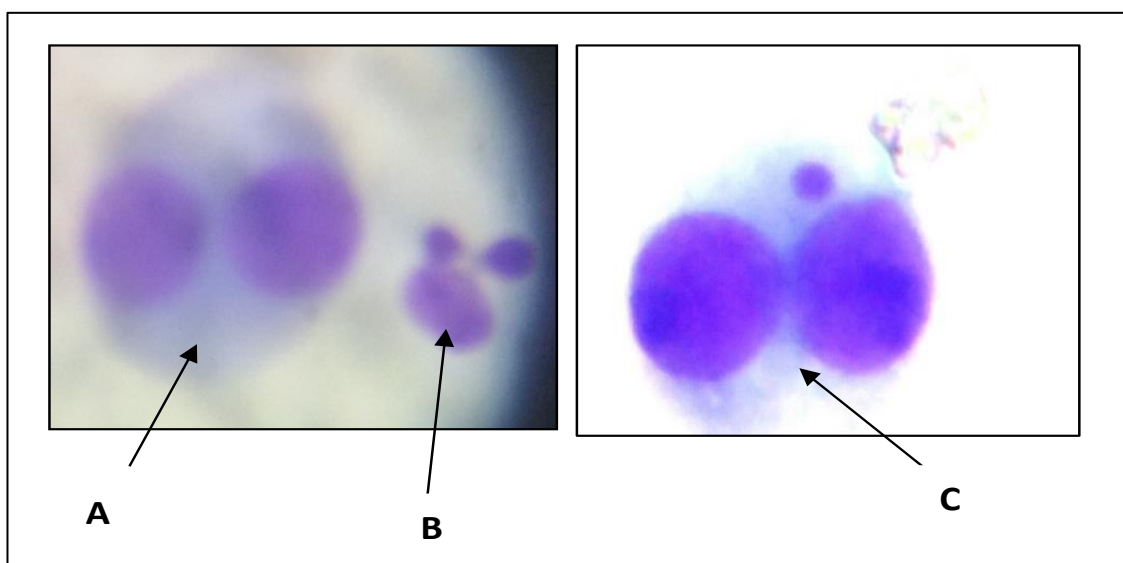


Figure 6.2: Photographs of genetic instability parameters obtained during Micronucleus assay scoring.

Images were acquired with LED Digital binocular Compound microscope equipped with 3.0 Mega Pixel Eyepiece Camera (AmScope, 40X-2500X, USA). Image (A) BiNC with cytoplasm; (B) MonoNC with NBUDs and nucleoplasmic bridge; and (C) Binucleated cells with one MNi.

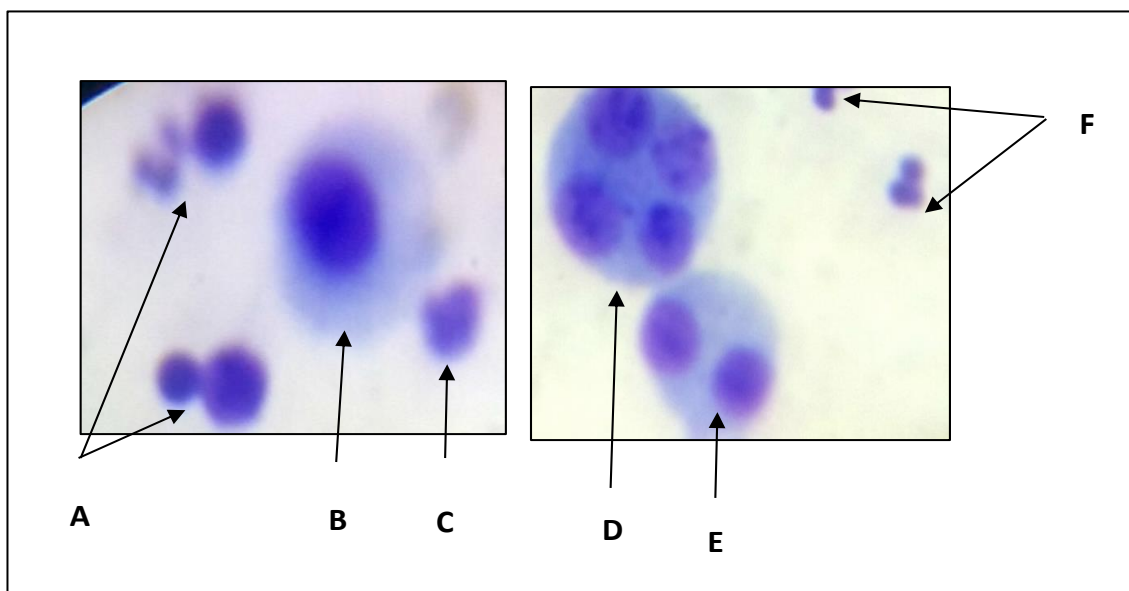


Figure 6.3: Photographs of genetic instability parameters obtained during Micronucleus assay scoring.

Images were acquired with LED Digital binocular Compound microscope equipped with 3.0 Mega Pixel Eyepiece Camera (AmScope, 40X-2500X, USA). Image (A) Mono NC with one MNi and no cytoplasm; (B) Mono NC with cytoplasm; (C) MonoNC without MNi and cytoplasm; (D) MultiNC (4 cells) without MNi, cytoplasm present; (E) BiNC (2 cells) with cytoplasm; and (F) three MNi.

The images in **Figure 6.2** and **Figure 6.3** were live-coloured images captured during scoring with a LED Digital binocular Compound microscope (AmScope, USA) 40X-2500X equipped with 3.0 Mega Pixel Eyepiece Camera. **Figure 6.2** shows Image (A) BiNC with cytoplasm; (B) MonoNC with NBUDs and nucleoplasmic bridge; and (C) BiNC with one MNi. **Figure 6.3** shows (A): MonoNC with one MNi and no cytoplasm; (B) Mono NC with cytoplasm; (C) MonoNC without MNi and cytoplasm; (D) MultiNC (4 cells) without MNi, cytoplasm present; (E) BiNC with cytoplasm; and (F) three MNi. From the results described above, it was evident clear that generation of multinucleated cells was highest in patients with lung cancer followed by COPD and asthma patients, while healthy individuals had the lowest MNi induction.

6.4 Confounding Factors

The discussions on the confounding effects on the blood samples of patients and healthy individuals used in the CMBN assay were discussed in section 5.3.3.

6.5 Discussion

The CBMN assay is a cytogenetic technique based on its ability to evaluate chromosome damage endpoints from cells which have completed, at least, one nuclear division. The inhibition of cytokinesis, the last phase of the cell cycle, by Cyto-B, makes it possible to differentiate cells which had divided in BiNC from those which were caught up in the cytokinesis-blockade and did not divide (MonoNC), thereby avoiding any confusions that might arise from in the cell division processes (Kirsch-Volders and Fenech 2001; Fenech 2002). Chromosome fragment endpoints which failed to engage with the mitotic spindle

or lag prior to cytokinesis include: MNi, BiNC, MonoNC, MultiNC, cytostatic parameters (NDI), genotoxicity endpoints (NPBs and NBUDs) and cytotoxicity parameters (necrotic and apoptotic cells). Accumulation of the above chromosomal endpoints are hall marks of lung cancer (El-Zein et al. 2008) depending on the pathological state of the individuals.

To stimulate T-Lymphocytes into cell division (mitosis), the PHA (a mitogen) was added into the cell culture. The implication of our results could open more curiosity of the genotoxicity of this multi-layered GO used in this study (15-20 sheets) and the necessity for further research. Our data could be interpreted in two ways. In one hand, the significant higher levels of CBMN endpoints observed in both cancer and COPD groups compared to controls were good demonstrations that the GO could be excellent candidates in drug delivery of anti-cancer drugs (Ma et al. 2015) and as nanotherapeutics for the treatment of COPD (Seshadri and Ramamurthi 2018). MNi, a biomarker of genotoxicity and chromosome breakage and/or whole chromosome loss were significantly higher in lung cancer patients (n=5; $p < 0.001$) followed by COPD patients. MNi are chromatin-containing bodies which represent chromosome fragments or even whole chromosomes which lagged behind in the anaphase of mitosis and were not integrated into the daughter cell nucleus at the time of nuclear division (mitosis) (Albertini et al. 2000).

Therefore, GO could be classified as both a **clastogen**, a chemical agent which causes chromosomal breakages by interacting with DNA – and an **aneugen**, an agent which causes chromosome loss by interacting with the spindle apparatus

(Bignold 2009) due to their ability to induce DNA DSBs leading to MNi formation with acentric fragment (i.e. chromosomal fragments lacking centromere). In the CBMN Assay, MNi induction occurred specifically at the anaphase of mitotic phase when the nuclear fragments lagged. Addition of Cyto-B at 44 hours after blood cell culture, or 20 hours after chemical treatments (GO and MMC) stopped the cytokinesis process, leading to the accumulation of MNi.

The implication of significant induction of **cytostatic event** parameters (lower levels of MonoNC, but high levels of MultiNC and BiNC) experienced in lung cancer and COPD patients than in asthma and healthy individuals, could be attributed to the high rate of DNA replication / mutation which occurs in these patients leading up to their chronic pathological conditions (Dai et al. 2017). Our results are consistent with research elsewhere which show that GO have anti-microbial (Li et al. 2013b) and high anticancer properties (Szmidski et al. 2019). Cells from lung cancer and COPD patients may have completed at least one nuclear division yielding more binucleated cells faster than reactions taking place in asthma patients and healthy individuals or they might have escaped the cytokinesis-block after one to two divisions (Albertini et al. 2000). However, MonoNC could also be generated continuously from MultiNC cells in the absence of mitosis (Solari et al. 1995). Increased levels of BiNC is a biomarker of cancer susceptibility, and could be used as predictors of cancer in healthy individuals susceptible to DNA damage (El-Zein et al. 2008). Also, increased levels of NDI values in blood samples of lung cancer and COPD patients compared to normal healthy individuals in the CBMN assays are indicators of high cytotoxicity events in the already proliferating cancer and COPD cells in blood cultures assisted with

PHA (Ionescu et al. 2011). The results in the CBMN assay are clearly in agreement with the concentration-dependent increases in the cytotoxicity of GO we had established earlier on in Chapter 4 using MTT and NRU assays (pp. 106-118), and in the genotoxicity (DNA damage) studies in Chapter 5 using the alkaline Comet assay (pp. 119-131).

Although, the concentrations of GO used in this study may by far exceed the concentrations that might be inhaled from workplace exposure (e.g. 0.1 μg), our results were in sharp contrast to the short-term nose-only inhalation study conducted elsewhere. In that research, 15 male Sprague-Dawley rats were exposed to different concentrations of GO nanoplates (4,60 to 3,760 $\mu\text{g}/\text{m}^3$) (Han et al. 2015) and (760 to 9780 $\mu\text{g}/\text{m}^3$) (Kim et al. 2018) for 6 h daily for 5 days with no significant toxicological effects between 1 to 21 days of recovery period.

Studies by Jaurand et al. (2009) and Yasui et al. (2015) had demonstrated a close relationship between asbestos fibres and multi-walled carbon nanotubes (MWCNTs) (Jaurand et al. 2009; Yasui et al. 2015). MWCNTs have similar chemical structural relationship with GO NMs with 15-20 sheets used in this PhD study, and both nanomaterials possess similar characteristics in cultured experiments such as fibre-like elongated shapes, sizes, surface reactivity, etc. MWCNTs could induce mesothelioma commonly associated with asbestos fibres (NHS Choices 2019). Mesothelioma is a kind of cancer that attacks the mesothelial: the lining that covers certain organs of the body such as the lungs (pleural), intestine (mesentery), and heart (pericardium). Since MWCNTs are made from graphene sheets, theoretically, it is possible to accurately predict GO

toxicity on human organs. Furthermore, studies published elsewhere shows that GO NMs have high protein adsorption efficiency and changes in size and zeta potential due to the formation of protein corona (Wei et al. 2015). Long-term exposure of carbonaceous nanomaterials to the pulmonary system (Skovmand et al. 2018) has been reported to induce oxidative stress and ROS, leading to cellular mutations and carcinogenesis (Waris and Ahsan 2006; Wellen and Thompson 2010; Nita and Grzybowski 2016). On the hand, depending on the concentrations of GO used in injectable nanocarriers, GO NMs may pose cancer risk to human population when in contact with human whole blood (Nichols and Bae 2012).

The journey of a targeted drug delivery carrier starts at the injection site into the bloodstream (Zhou et al. 2014). From there, it circulates throughout the body and passes through a number of stages including extravasation into the extravascular tissues around the site of infusion, biodistribution and accumulation (lung, liver, spleen, intestine, kidney, and brain) (Amrollahi-Sharifabadi et al. 2018), clathrin-mediated endocytosis (Huang et al. 2012; Ding et al. 2014; Linares et al. 2014), endosomal escape (Wong et al. 2015), intracellular localization (Ding et al. 2014), and, lastly action. Effective design of GO drug delivery nanocarriers entails incorporation of the pharmacokinetics and pharmacodynamics parameters in order to maximize drug delivery payload at the tumour sites with little damage to surrounding healthy cells. According to the IPCS guidelines for the monitoring of genotoxicity of carcinogens in humans, increased frequencies of structural and numerical chromosomal aberration parameters after exposure to chemical agents are closely linked with high risk of developing cancer (Albertini et al. 2000).

Chromosome damage parameters observed in healthy individuals assumed to have strong immune systems are clear indicators of the possible damaging potentials of GO up to 20 h of exposure, while patients with chronic pulmonary diseases especially COPD and lung cancer, experienced significant genetic instability compared to healthy control individuals.

Although, the CBMN assay is claimed to be an economic and short-term assay widely used in genetic toxicology studies (İpek et al. 2017), we had encountered various limitations during the course of the experiments. First, it was sensitive in identifying dead cells which had accumulated after cytokinesis was blocked, but the method was time consuming and laborious. We required up to 8 days before the first results could be obtained, including 72 h of cell treatments in sterile conditions, and 1 - 2 h of cell fixation, slide preparation, and Giemsa staining. According to our experience, each duplicate slide took over 30 min to 1 h to score, making the Micronucleus assay unsuitable for field studies where rapid results are required. Furthermore, the CBMN involves the tedious process of manually scoring of 1,000 cells, i.e. 500 cells per concentration using hand-held tally counters. This counting process could lead to human error (Radack et al. 1995) and inter-laboratory discrepancies among various researchers (Fenech et al. 2003a).

To overcome the above limitations, international scoring criteria have been developed as described (Patino-Garcia et al. 2006). An automated method is suggested for this type of assay such as the Metafer - a reliable and fast automation system developed by MetaSystems that could potentially analyse in

vitro and in vivo samples in minutes (MetaSystems 2019). Another factor mitigating against the effectiveness of the CBMN assay is the type and concentration of the mitogen (e.g. Cyto-B) used in the CMN Assay. Cyto-B may induce DNA fragmentation during its use, and thus affect the proliferation rates of the lymphocytes (Albertini et al. 2000). Also, temperature variations within an incubator and across different laboratories could effectively affect the nature of cell culture growth in medium. Also, a long culture time is an important factor which could lead to overestimation of MNi frequencies, probably due to delayed cell division in the already injured cells. Variations in MNi frequencies may occur due to differences in cell proliferation rates.

The significant differences in cytogenetic effects of GO NMs in blood samples from patients with chronic diseases and in healthy individuals could be associated with confounding factors since in this study, 100% of COPD patients and 90% of lung cancer patients had a history of cigarette smoking.

Next, we tested the hypothesis that GO may affect gene expression of cell cycle-signalling genes (TP53, CDKN1A and BCL-2) involved in the cascade of DNA damage. It was reported that pulmonary diseases, especially those of COPD and lung cancer, have long-term alterations in epigenetic regulation of gene expression (Durham and Adcock 2015).

Chapter 7: Gene Expression Analysis

7.0 Effects of GO NMs on the Relative Gene Expression of Cell-Cycle signalling genes (TP53, CDKN1A, and BCL-2) in Human Lymphocytes from healthy individuals and patients (asthma, COPD, and lung cancer) using RT-qPCR Method

7.1 Introduction

Reverse transcription quantitative polymerase chain reaction (RT-qPCR) is a vital technique in modern molecular biology research and clinical medicine for the quantification of micro RNA (mRNA)/DNA, and enables detection of even the smallest amount of gene expression in real time (Ho-Pun-Cheung et al. 2009).

Gene expression of mRNA can be quantified in the RT-qPCR using either absolute or relative quantification methods (Thermo Fisher Scientific 2019?).

While absolute quantification results give an accurate number of copies of the target gene of interest (mRNA/DNA), it requires the use of known standard concentrations to create a calibration curve, from where an unknown sample can be determined. On the other hand, relative quantification expresses the quantity of the target gene of interest (mRNA/DNA) as an n-fold difference relative to a calibrator, which is usually an untreated, NC control sample (Livak and Schmittgen 2001; Cikos et al. 2007). Although this method requires data normalization in order to give biologically relevant results, it is the most commonly used method to compare fold-changes in mRNA expression between different samples (Cikos et al. 2007).

Previous research on DNA amplification of GO NMs were conducted using 2-3 layers of GO nanosheets, and higher GO concentrations such as 200, 300, 400, 500, and 600 $\mu\text{g}/\text{mL}$ in different experimental models (e.g. MDA-MB-231 (human breast cancer cells, skin fibroblasts, animal models, etc.) have been reported

(Liao et al. 2011; Liu et al. 2013b; Ding et al. 2014; Wang et al. 2017). There is, therefore, the need to evaluate the commercially sourced, multi-layered GO NMs (15-20 sheets) in order to understand what really goes on at the molecular level of gene expression of the cell-cycle signalling genes.

7.1.1 Hypothesis: GO may affect gene expression of cell-cycle signalling genes involved in the cascade of DNA damage

In this chapter, we hypothesised that GO NMs could affect the gene expression of cell-cycle signalling genes (TP53, CDKN1A, and BCL-2) involved in the cascade of DNA damage in human lymphocytes.

7.2 Materials and Methods

The Reagents and equipment used in the RT-qPCR were listed in Chapter 2 (sections 2.1.1 and 2.1.2) and the method described in section 2.2.12.2. To test the hypothesis that GO NMs may affect gene expression of cell-cycle signalling genes listed above, we evaluated the impacts of higher concentrations of GO - 150 and 200 µg/mL, respectively than lower concentrations 10 to 100 µg/mL we had used in the previous three assays (cytotoxicity, Comet, and CBMN assays).

At the lower concentrations, there were no significant changes in response. Although it is anticipated that such exposures will be encountered at workplace in the range where non-toxicity occurs, we increased the concentrations to determine if there would be any changes on the genes.

7.3 Results

7.3.1 Effects of GO NMs on the Relative Gene Expression of cell-cycle signalling genes (TP53, CDKN1A, BCL-2) relative to GAPDH in Human Lymphocytes from healthy individuals and patients (asthma, COPD, and lung cancer) using the RT-qPCR Method

The lymphocytes were treated with different concentrations of GO (0, 150 and 200 µg/mL) for 24 h and mRNA expression levels of TP53, CDKN1A, BCL-2 were evaluated relative to GAPDH. The RT-qPCR results showing differential levels of mRNA expression in healthy individuals and patients are listed in Table 7-1 (healthy individuals), Table 7-2 (asthma patients), Table 7-3 (COPD patients), and Table 7-4 (lung cancer patients). Generally, the mRNA levels of **TP53 genes** were mostly upregulated in patients at both concentrations (150 and 200 µg/mL) ($p < 0.001$) relative to untreated samples, an indication of DNA damage, but was downregulated at 150 µg/mL in healthy individuals.

In healthy individuals, **TP53 genes** were downregulated by 0.8-fold ($p < 0.001$) and upregulated by 2.3-fold ($p < 0.001$) after treatment with 150 and 200 µg/mL of GO NMs, respectively. In asthma patients, TP53 genes were significantly upregulated by 2.6- and 2.5-folds ($p < 0.001$) compared with COPD patients with less expression levels by 1.9- and 1.4-fold ($p < 0.001$) after exposure to 150 and 200 µg/mL of GO NMs, relative to untreated, NC samples. Interestingly, TP53 tumour suppressor genes were upregulated significantly in lung cancer patients by 3.3-fold ($p < 0.001$) and maximally by 10-fold ($p < 0.001$) after treatment with 150 and 200 µg/mL of GO NMs, respectively.

However, **CDKN1A genes** were upregulated by 2.0- and 5.8-folds ($p < 0.001$) in healthy individuals; and by 3.4- and 9.9-fold ($p < 0.001$) in asthma patients after treatment with 150 and 200 $\mu\text{g}/\text{mL}$ of GO, respectively relative to untreated cells. In COPD patients, CDKN1A genes were significantly downregulated by 0.3- and 0.4-fold ($p < 0.001$) after treatment with 150 $\mu\text{g}/\text{mL}$ and 200 $\mu\text{g}/\text{mL}$ GO relative to untreated cells. In lung cancer patients, there were no fold-differences in gene expression of CDKN1A genes (ns) after treatment of cells with 150 $\mu\text{g}/\text{mL}$ GO NMs relative to untreated NC samples. However, as the treatment concentration in lung cancer patients was increased to 200 $\mu\text{g}/\text{mL}$, the CDKN1A genes were downregulated in a statistically significant manner by 0.90-fold ($p < 0.001$) relative to the untreated cells.

The **BCL-2 genes** have dual functions depending on the signal type received, the severity of the DNA damage, and the health status of the individuals with regard to their immune systems. On one hand, the BCL-2 genes are pro-apoptotic genes, i.e. they respond to pro-apoptotic signals promoting programmed cell deaths if DNA damage is severe beyond repair, and in doing so can avoid accumulation of death and cancerous cells. On the other hand, the BCL-2 genes can function as anti-apoptotic genes, promoting cell growth and contribute to tumour development. After treatments with GO (150 and 200 $\mu\text{g}/\text{mL}$), BCL-2 genes were significantly downregulated in healthy individuals by 0.5- and 0.7-folds ($p < 0.001$) and in asthma patients by 0.8- and 0.7-folds ($p < 0.001$), respectively relative to untreated, NC samples. However, they were significantly upregulated by 1.6- and 1.3-folds ($p < 0.001$) in COPD patients compared with 1.3-

and 1.2-folds ($p < 0.001$) in lung cancer patients relative to untreated, NC samples after exposure to the GO NMs.

Table 7-1: Relative Gene Expression of cell-cycle signalling genes (TP53, CDKN1A, and BCL2) normalized with reference gene (GAPDH) in human lymphocytes from healthy individuals after 24 h treatment with different concentrations of GO (150 and 200 µg/mL) in RT-qPCR. Relative gene expression was expressed as fold-change/fold difference of treated samples relative to untreated samples using the double delta method ($2^{-\Delta\Delta Cq}$). Statistical analyses were performed using GraphPad Prism, version 8.1.2 (332) with built-in One-Way ANOVA and Dunnett's multiple comparisons tests to compare expressed genes of interest in treated samples relative to the untreated. Statistical significance was rated at $p < 0.05$; where * = $p < 0.05$ and ns = not significant.); three independent experiments (n=3) were performed in triplicate.

			HEALTHY							$2^{-\Delta\Delta Cq}$	
HEALTHY	TP53			TP53	GAPDH			GAPDH	ΔCq	$\Delta\Delta Cq$	(Fold difference in TP53 expression relative to untreated)
Treatments	Exp. 1 (Av.)	Exp. 2 (Av.)	Exp. 3 (Av.)	Av. Cq	Exp. 1 (Av.)	Exp. 2 (Av.)	Exp. 3 (Av.)	Av. Cq	(TP53-GAPDH)	ΔCq (treated-untreated)	
Untreated	27.72	27.99	27.91	27.87	26.57	26.44	26.55	26.52	1.35	0.00	1.0
150 µg/mL	25.34	25.59	25.22	25.38	23.72	23.74	23.76	23.74	1.64	0.29	0.8 ***
200 µg/mL	25.75	25.59	26.29	25.88	25.72	25.73	25.66	25.70	0.17	-1.18	2.3 ***
			HEALTHY							$2^{-\Delta\Delta Cq}$	
	CDKN1A			CDKN1A	GAPDH			GAPDH	ΔCq	$\Delta\Delta Cq$	(Fold difference in CDKN1A expression relative to untreated)
Treatments	Exp. 1	Exp. 2	Exp. 3	Av.Cq	Exp. 1	Exp. 2	Exp. 3	Av. Cq	(CDKN1A-GAPDH)	ΔCq (treated-untreated)	
Untreated	28.48	28.75	28.45	28.56	26.57	26.44	26.55	26.52	2.04	0.00	1.0
150 µg/mL	24.85	24.97	24.58	24.80	23.72	23.74	23.76	23.74	1.06	-0.98	2.0 ***
200 µg/mL	25.20	25.20	25.20	25.20	25.72	25.73	25.66	25.70	-0.50	-2.54	5.8 ***
			HEALTHY							$2^{-\Delta\Delta Cq}$	
	BCL-2			BCL-2	GAPDH			GAPDH	ΔCq	$\Delta\Delta Cq$	(Fold difference in BCL-2 expression relative to untreated)
Treatments	Exp. 1 (Av.)	Exp. 2 (Av.)	Exp. 3 (Av.)	Av. Cq	Exp. 1 (Av.)	Exp. 2 (Av.)	Exp. 3 (Av.)	Av.Cq	(BCL-2-GAPDH)	ΔCq (treated-untreated)	
Untreated	29.14	29.25	29.71	29.37	26.57	26.44	26.55	26.52	2.85	0.00	1.00
150 µg/mL	27.70	27.69	27.74	27.71	23.72	23.74	23.76	23.74	3.97	1.12	0.5***
200 µg/mL	29.14	29.24	29.11	29.16	25.72	25.73	25.66	25.70	3.46	0.61	0.7***

Table 7-2: Relative Gene Expression of cell-cycle signalling genes (TP53, CDKN1A, and BCL2) normalized with reference gene (GAPDH) in human lymphocytes from asthma patients after 24 h treatment with different concentrations of GO (150 and 200 µg/mL) in RT-qPCR. Relative gene expression was expressed as fold-change/fold difference of treated samples relative to untreated samples using the double delta method ($2^{-\Delta\Delta Cq}$). Statistical analyses were performed using GraphPad Prism, version 8.1.2 (332) with built-in One-Way ANOVA and Dunnett's multiple comparisons tests to compare expressed genes of interest in treated samples relative to the untreated. Statistical significance was rated at $p < 0.05$; where * = $p < 0.05$ and ns = not significant.); three independent experiments (n=3) were performed in triplicate.

				ASTHMA								$2^{-\Delta\Delta Cq}$
ASTHMA	TP53			TP53	GAPDH			GAPDH	ΔCq	$\Delta\Delta Cq$	(Fold difference in TP53 expression relative to untreated)	
Treatments	Exp. 1 (Av.)	Exp. 2 (Av.)	Exp. 3 (Av.)	Av. Cq	Exp. 1 (Av.)	Exp. 2 (Av.)	Exp. 3 (Av.)	Av. Cq	(TP53-GAPDH)	ΔCq (treated-untreated)		
Untreated	31.12	30.40	30.45	30.66	28.35	28.51	28.34	28.40	2.26	0.00	1.0	
150 µg/mL	25.13	25.43	25.40	25.32	24.47	24.55	24.38	24.47	0.85	-1.40	2.6***	
200 µg/mL	26.27	26.21	26.48	26.32	25.48	25.35	25.34	25.39	0.93	-1.33	2.5***	
				CDKN1A								$2^{-\Delta\Delta Cq}$
ASTHMA	CDKN1A			CDKN1A	GAPDH			GAPDH	ΔCq	$\Delta\Delta Cq$	(Fold difference in CDKN1A expression relative to untreated)	
Treatments	Exp. 1 (Av.)	Exp. 2 (Av.)	Exp. 3 (Av.)	Av. Cq	Exp. 1 (Av.)	Exp. 2 (Av.)	Exp. 3 (Av.)	Av. Cq	(CDKN1A-GAPDH)	ΔCq (treated-untreated)		
Untreated	32.96	32.40	30.41	31.92	28.35	28.51	28.34	28.40	3.52	0.00	1.0	
150 µg/mL	27.44	25.77	25.43	26.21	24.47	24.55	24.38	24.47	1.75	-1.78	3.4***	
200 µg/mL	27.52	24.84	24.45	25.60	25.48	25.35	25.34	25.39	0.21	-3.31	9.9***	
				BCL-2								$2^{-\Delta\Delta Cq}$
ASTHMA	BCL-2			BCL-2	GAPDH			GAPDH	ΔCq	$\Delta\Delta Cq$	(Fold difference in BCL-2 expression relative to untreated)	
Treatments	Exp. 1 (Av.)	Exp. 2 (Av.)	Exp. 3 (Av.)	Av. Cq	Exp. 1 (Av.)	Exp. 2 (Av.)	Exp. 3 (Av.)	Av. Cq	(BCL-2-GAPDH)	ΔCq (treated-untreated)		
Untreated	31.85	31.10	30.21	31.05	28.35	28.51	28.34	28.40	2.65	0.00	1.0	
150 µg/mL	27.00	27.75	27.42	27.39	24.47	24.55	24.38	24.47	2.92	0.27	0.8***	
200 µg/mL	28.43	28.51	28.58	28.51	25.48	25.35	25.34	25.39	3.12	0.46	0.7***	

Table 7-3: Relative Gene Expression of cell-cycle signalling genes (TP53, CDKN1A, and BCL2) normalized with reference gene (GAPDH) in human lymphocytes from COPD patients after 24 h treatment with different concentrations of GO (150 and 200 µg/mL) in RT-qPCR. Relative gene expression was expressed as fold-change/fold difference of treated samples relative to untreated samples using the double delta method ($2^{-\Delta\Delta Cq}$). Statistical analyses were performed using GraphPad Prism, version 8.1.2 (332) with built-in One-Way ANOVA and Dunnett's multiple comparisons tests to compare expressed genes of interest in treated samples relative to the untreated. Statistical significance was rated at $p < 0.05$; where * = $p < 0.05$ and ns = not significant.); three independent experiments (n=3) were performed in triplicate.

				COPD				$2^{-\Delta\Delta Cq}$			
COPD	TP53			TP53	GAPDH			GAPDH	ΔCq	$\Delta\Delta Cq$	(Fold difference in TP53 expression relative to untreated)
Treatments	Exp. 1 (Av.)	Exp. 2 (Av.)	Exp. 3 (Av.)	Av. Cq	Exp. 1 (Av.)	Exp. 2 (Av.)	Exp. 3 (Av.)	Av. Cq	(TP53-GAPDH)	ΔCq (treated-untreated)	
Untreated	28.30	28.60	28.39	28.43	25.02	24.99	24.98	25.00	3.43	0.00	1.0
150 µg/mL	27.24	27.40	27.56	27.40	25.30	24.72	24.58	24.87	2.53	-0.90	1.9***
200 µg/mL	28.05	28.67	28.35	28.36	25.45	25.40	25.39	25.41	2.94	-0.49	1.4***
				CDKN1A				$2^{-\Delta\Delta Cq}$			
	CDKN1A			CDKN1A	GAPDH			GAPDH	ΔCq	$\Delta\Delta Cq$	(Fold difference in CDKN1A expression relative to untreated)
Treatments	Exp. 1 (Av.)	Exp. 2 (Av.)	Exp. 3 (Av.)	Av. Cq	Exp. 1 (Av.)	Exp. 2 (Av.)	Exp. 3 (Av.)	Av. Cq	(CDKN1A-GAPDH)	ΔCq (treated-untreated)	
Untreated	27.17	26.74	26.63	26.85	25.02	24.99	24.98	25.00	1.85	0.00	1.0
150 µg/mL	28.40	28.56	28.65	28.54	25.30	24.72	24.58	24.87	3.67	1.82	0.3***
200 µg/mL	28.74	28.41	28.38	28.51	25.45	25.40	25.39	25.41	3.10	1.25	0.4***
				BCL-2				$2^{-\Delta\Delta Cq}$			
	BCL-2			BCL-2	GAPDH			GAPDH	ΔCq	$\Delta\Delta Cq$	(Fold difference in BCL-2 expression relative to untreated)
Treatments	Exp. 1 (Av.)	Exp. 2 (Av.)	Exp. 3 (Av.)	Av. Cq	Exp. 1 (Av.)	Exp. 2 (Av.)	Exp. 3 (Av.)	Average Cq	(BCL2-GAPDH)	ΔCq (treated-untreated)	
Untreated	29.20	29.40	29.21	29.27	25.02	24.99	24.98	25.00	4.27	0.00	1.0
150 µg/mL	28.60	28.45	28.30	28.45	25.30	24.72	24.58	24.87	3.58	-0.69	1.6***
200 µg/mL	30.28	29.18	28.51	29.32	25.45	25.40	25.39	25.41	3.91	-0.36	1.3***

Table 7-4: Relative Gene Expression of cell-cycle signalling genes (TP53, CDKN1A, and BCL2) normalized with reference gene (GAPDH) in human lymphocytes from lung cancer patients after 24 h treatment with different concentrations of GO (150 and 200 µg/mL) in RT-qPCR. Relative gene expression was expressed as fold-change/fold difference of treated samples relative to untreated samples using the double delta method ($2^{-\Delta\Delta Cq}$). Statistical analyses were performed using GraphPad Prism, version 8.1.2 (332) with built-in One-Way ANOVA and Dunnett's multiple comparisons tests to compare expressed genes of interest in treated samples relative to the untreated. Statistical significance was rated at $p < 0.05$; where * = $p < 0.05$ and ns = not significant.); three independent experiments (n=3) were performed in triplicate.

				LUNG CANCER								$2^{-\Delta\Delta Cq}$		
LUNG CANCER	TP53			TP53	GAPDH			GAPDH	ΔCq	$\Delta\Delta Cq$	(Fold difference in TP53 expression relative to untreated)			
Treatments	Exp. 1 (Av.)	Exp. 2 (Av.)	Exp. 3 (Av.)	Av. Cq	Exp. 1 (Av.)	Exp. 2 (Av.)	Exp. 3 (Av.)	Av. Cq	(TP53-GAPDH)	ΔCq (treated-untreated)				
Untreated	30.33	29.36	29.61	29.77	24.98	24.95	25.03	24.99	4.78	0.00	1.0			
150 µg/mL	29.33	27.58	27.79	28.23	25.23	25.16	25.11	25.17	3.07	-1.71	3.3***			
200 µg/mL	27.22	26.74	26.66	26.87	25.55	25.33	25.36	25.41	1.46	-3.32	10.0***			
				CDKN1A								$2^{-\Delta\Delta Cq}$		
LUNG CANCER	CDKN1A			CDKN1A	GAPDH			GAPDH	ΔCq	$\Delta\Delta Cq$	(Fold difference in CDKN1A expression relative to untreated)			
Treatments	Exp. 1 (Av.)	Exp. 2 (Av.)	Exp. 3 (Av.)	Av. Cq	Exp. 1 (Av.)	Exp. 2 (Av.)	Exp. 3 (Av.)	Av. Cq	(CDKN1A-GAPDH)	ΔCq (treated-untreated)				
Untreated	30.95	30.27	29.92	30.38	24.98	24.95	25.03	24.99	5.39	0.00	1.0			
150 µg/mL	30.82	30.84	30.06	30.57	25.23	25.16	25.11	25.17	5.41	0.01	1.0 ns			
200 µg/mL	31.52	30.90	30.45	30.96	25.55	25.33	25.36	25.41	5.54	0.15	0.9***			
				BCL-2								$2^{-\Delta\Delta Cq}$		
LUNG CANCER	BCL-2			BCL-2	GAPDH			GAPDH	ΔCq	$\Delta\Delta Cq$	(Fold difference in BCL-2 expression relative to untreated)			
Treatments	Exp. 1 (Av.)	Exp. 2 (Av.)	Exp. 3 (Av.)	Av. Cq	Exp. 1 (Av.)	Exp. 2 (Av.)	Exp. 3 (Av.)	Av. Cq	(BCL2-GAPDH)	ΔCq (treated-untreated)				
Untreated	30.19	30.39	30.79	30.46	24.98	24.95	25.03	24.99	5.47	0.00	1.0			
150 µg/mL	30.44	30.28	30.22	30.31	25.23	25.16	25.11	25.17	5.15	-0.32	1.3***			
200 µg/mL	31.17	30.26	30.55	30.66	25.55	25.33	25.36	25.41	5.25	-0.22	1.2***			

7.3.2 Confounding Factors

The blood samples of donors used in the MTT and NRU assays were also used for the RT-qPCR assay. The discussions on the confounding effects were discussed in section 4.2.2.

7.4 Discussion

The RT-qPCR assay used in this study was based on the SYBR™ Green (iQ™ SYBR® Green Supermix, Bio-Rad, USA). It quantitatively measures the amount of DNA amplification using the fluorescence dye. The intensity of fluorescence generated increases in proportion with each cycle of the amplification. The cycle at which fluorescence was detected is termed the quantitative cycle (Cq) and it is the most vital data required in the RT-qPCR analysis. The Cq is the cycle at which fluorescent signal can be detected, at the detection-threshold level automatically set up by the qPCR machine. The Cq result is the main reason behind qPCR analysis and is inversely proportional to the amount of cDNA in the sample being detected. The lower the Cq values, the higher the amount of cDNA template in the sample → the higher the amount of RNA and → and the earlier it is expressed to the left in the amplification curve, and vice-versa; the higher the Cq values, the smaller the amount of cDNA templates in the sample vis-à-vis the smaller the RNA concentration, and the amplification curve is expressed later to the right of the curve (BioSistemika 2017).

We used the Livak method (relative quantification) to quantify different levels of genes expressed between various samples. This method was selected because it assumes that all primers used in the reaction mixtures have equal efficiency

when samples were treated under the same conditions. The amplification efficiency of each reaction is taken to be 100%, or that each of the qPCR cycle doubles the amplicon. Since all the genes were analysed in single RT-qPCR reaction steps, the GAPDH reference gene and the target genes, TP53, CDKN1A, and BCL-2 are assumed to be paired data points. p53/TP53 genes/proteins are tumour suppressors (Suzuki and Matsubara 2011) responsible for maintaining genomic stability when cells are exposed to genotoxic agents. They are like the guardian angels (Chakarov et al. 2012) activated to protect the DNA in two ways. On the one hand, when DNA damage is not severe and below a certain threshold, TP53 activation stimulates CDKN1A/p21 genes to help with cell-cycle arrest and activate DNA repair mechanisms. The cell-cycle arrest allows damaged DNA to recover and be repaired before proceeding into the next phase of replication/mitosis (Williams and Schumacher 2016).

Treatment of human PBL with GO (150 and 200 µg/mL) led to altered gene expression in both healthy individuals and patients, a clear demonstration of DNA damage. High level of DNA damage and very fragile genome in lung cancer patients could be why a maximum level of gene expression by 10-fold ($p < 0.001$) was recorded for TP53 after exposure to 200 µg/mL of GO, compared with much lower levels of TP53 expressed in asthma patients (2.5-fold, $p < 0.001$), healthy individuals (2.3-fold, $p < 0.001$) and in COPD patients (by 1.4-fold, $p < 0.001$) at the same concentration. On the other hand, when DNA damage is severe beyond repair, and above a certain threshold, the TP53 protective mechanism against tumour growth (cancer) is disabled leading to accumulation of dead cells (De Zio et al. 2013). It is the loss of functional p53 that forms one of the key stages in the

cascade of neoplasm (Sionov et al. 2000-2013). Depending on the cell type, such as leukaemia or transformed fibroblast, TP53 activation leads directly to apoptosis (pro-apoptosis) (Chen 2016). TP53 genes switches into pro-apoptotic mode and sends irreversible, apoptotic signals to the BCL-2 genes leading to programmed cell death (cell-suicide) in order to remove, excess dead cells. The BCL-2 family of genes/proteins are known as anti-apoptotic or pro-apoptotic genes/proteins depending of the severity of the DNA damage. In our present study, we found that BCL-2 genes were upregulated in COPD patients (1.6- and 1.3-fold, $p < 0.001$) than in lung cancer patients (1.3- and 1.2-fold, $p < 0.001$). In healthy individuals (0.5- and 0.7-fold, $p < 0.001$) and asthma patients (0.8- and 0.7-fold, $p < 0.001$), BCL-2 expressions were downregulated to almost the same level relative to untreated, NC samples.

Our results agree with other research performed elsewhere where high level of p53 expression corresponded to a decrease in BCL-2 in the absence of mutagenesis (Wu et al. 2013). However, our results were in sharp contrast to the research by Liu et al (2013) where DNA damage induced by the carbonaceous GO in human breast cancer cells and animal models did not demonstrate clear induction of mutagenesis (Liu et al. 2013b). It is general knowledge that the TP53 gene is one the most frequently mutated genes in human cancer (Muller and Vousden 2014), and approximately half of all cancers (50%) have inactive TP53 (Deepthi Ch et al. 2011). The only explanation on why we had more BCL-2 genes expressed in COPD patients than in lung cancer patients is that both COPD and lung cancer may have a common cause such as cigarette smoking, etc and pro-apoptotic BCL-2 genes are activated to fight against COPD complications .

people with COPD are at increased risks of developing lung cancer, heart disease, etc. (Le et al. 2005). On the other hand, slight upregulation of BCL-2 genes in lung cancer patients could be associated with the anti-apoptotic mechanism that even the presence of the BCL-2 genes was not enough to stop lung cancer progression in these patients who were already immunocompromised at the time of blood sample collection. Next, we attempted to test the hypothesis that GO NMs may affect protein expression of cell-cycle signalling proteins (p53, p21, and BCL-2) involved in the cascade of DNA damage.

Chapter 8: Protein Expression Analysis

8.0 Analysis of the Effects of GO on Protein Expression of Cell-Cycle signalling proteins (p53, p21, BCL-2) relative to GAPDH in Human Lymphocytes from healthy individuals and patients (asthma, COPD, and lung cancer) using Western Blot Method

8.1 Introduction

In the previous Chapter (Chapter 7), we established that GO (150 and 200 µg/mL) affected gene expression of TP53, CDK1A and BCL-2 genes relative to untreated samples. Genotoxic chemicals can also disrupt proteins involved in DNA replication, cell division (Nohmi 2018), cell-cycle control and apoptosis (Narayanan et al. 2015). Cell-cycle proteins such as p53, p21, and BCL-2 are a class of highly preserved proteins involved in the cascade of DNA damage (Pucci et al. 2000). WB is an analytical technique used in molecular/cancer biology for the detection of specific proteins of interest in a given sample (Mahmood and Yang 2012; Bio-Rad 2018). It uses the principles of gel electrophoresis to separate native or denatured proteins according to their molecular weight. Proteins with small molecular weights migrate faster and are separated towards the bottom of the gel, while proteins with large molecular weights migrate slowly and are separated towards the top of the gel.

After protein electrophoresis, proteins are blotted to a PVDF membrane under electric current and subsequently probed with primary antibodies (e.g. anti-p53, anti-p21, anti-BCL-2, and anti-GAPDH antibodies) specific to the target proteins of interest. The expressed proteins are then visualized using a secondary antibody (Horseradish Peroxidase (HRP) enzyme) and detected with Enhanced Chemiluminescent substrates (ECL, Bio-Rad), containing peroxide and Luminol/Enhancer Reagents (1:1). The bands are captured using relevant Software (e.g.

GENESys, UK) and band intensity quantified using relevant software (e.g. ImageJ, Invitrogen iBright Imaging Systems, etc).

8.1.1 Hypothesis: GO may affect protein expression in the cell-cycle signalling pathways (p53, p21, and BCL-2 relative to GAPDH) involved in the cascade of DNA Damage

8.2 Materials and Methods

The Reagents and equipment used in WB were listed in Chapter 2, sections 2.1.1 and 2.1.2, and Molecular Biology Methods are described in section 2.2.13.2.

8.3 Results

8.3.1 Effects of GO on Protein Expression on the Cell-Cycle signalling proteins (p53, p21, BCL-2) in Human Lymphocytes from healthy individuals and patients (asthma, COPD, and lung cancer) using WB Method

In the WB method, we first treated human lymphocytes with four different concentrations of GO (10, 20, 50, and 100 µg/mL). Due to technical issues, we were unable to detect proteins induced at two lower concentrations (10 and 20 µg/mL). Therefore, two more concentrations (150, and 200 µg/mL) were added and final concentrations used were 50, 100, 150, and 200 µg/mL.

A total of 36 WB assays were performed between Jan 2018 and Jan 2019), and the expressed proteins (p53, p21, and BCL-2) were detected in healthy individuals using GAPDH as an internal control (see

Figure 8.1). However, we were unsuccessful at detecting these proteins in all lymphocytes from patients (asthma, COPD, and lung cancer). A number of studies have shown upregulation of p53 and downregulation of BCL-2 proteins in COPD patients (Sigasaki et al. 2010), while cells treated with pristine GO (p-GO) (an ideal, pure GO without defects) caused 50% downregulation of BCL-2 relative to control, an indication of passive apoptosis (Ding et al. 2014).

Our results confirm previous qPCR experiments in Chapter 7 which support the hypothesis that GO NMs may affect protein expression of p53, p21, and BCL-2 proteins. We, therefore, recommend future work on this area, using WB assay and other methods such as immunohistochemistry in formalin-fixed, paraffin-embedded lymphocytes from both healthy individuals and patients.

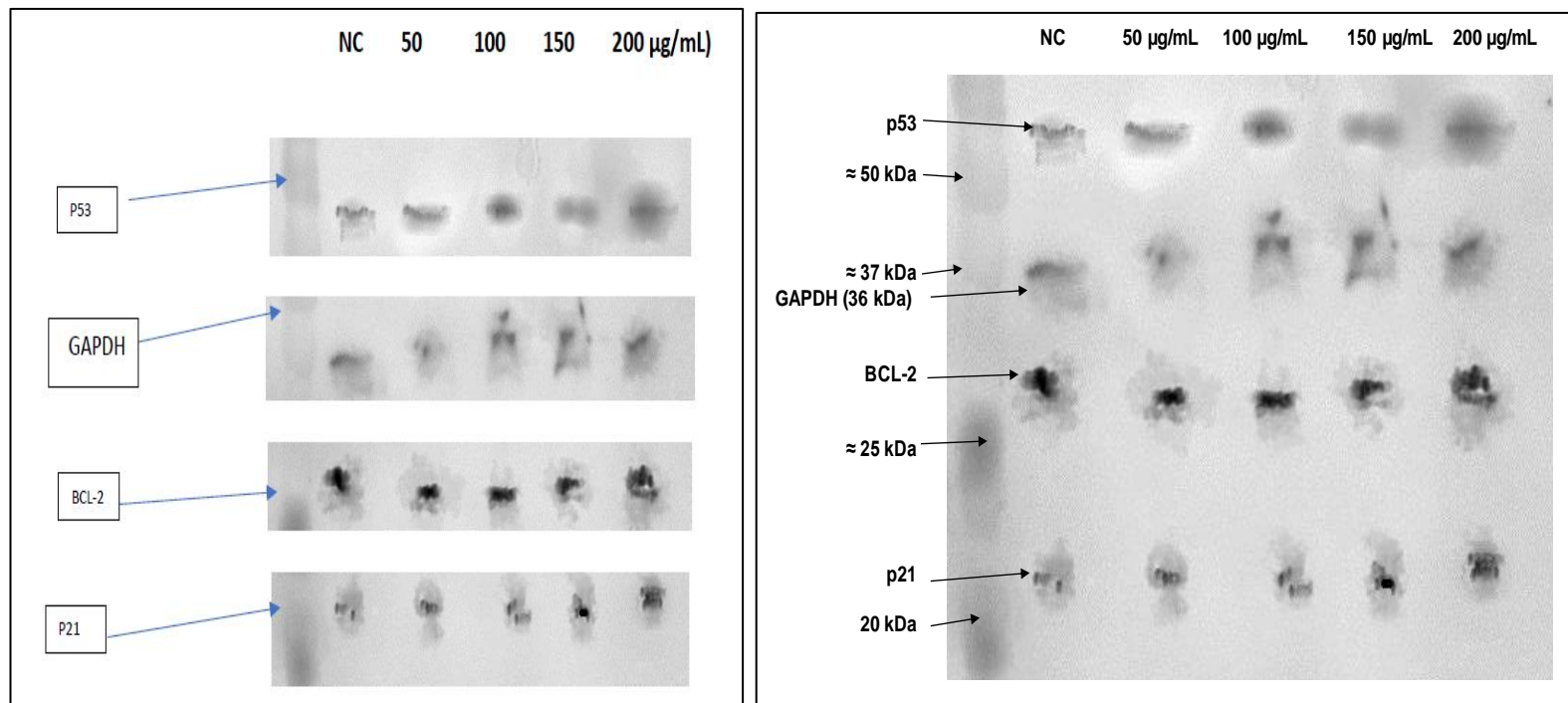


Figure 8.1: Effects of GO (50, 100, 150, and 200 µg/mL) on the induction of p53, BCL-2, and p21 proteins relative to GAPDH human lymphocytes from healthy individuals. The protein bands were differentially induced.

8.3.2 Confounding Factors

The blood samples of donors used in the MTT, NRU, and RT-qPCR assays were also used for the WB assay. The discussions on the confounding effects on the blood samples were discussed in section 4.2.2.

8.4 Discussion

In this Chapter, we investigated the effects of different concentrations of GO (50, 100, 150, and 200 µg/mL) on induction of p53, p21, and BCL-2 proteins after 24 h exposure to human lymphocytes from healthy individuals relative to GAPDH as an internal control. GO oxide could have reacted with the cell membrane in various ways before proteins are induced and at the entry into the cytoplasm. Such mechanisms include cellular diffusion, interaction with receptors, adhesion to surface, and membrane puncturing due to sharp edges.

At normal, oxidative physiological conditions, entry of GO NMs into the cytoplasm causes oxidative stress, and primarily generates ROS. ROS triggers most of the biological responses and triggers various signalling pathways and induces oxidative damage to DNA and cellular proteins. The location of p53 (either in the cytoplasm or the nucleus) is vital in its response to DNA damage. In the cytoplasm, p53 activates **cellular stress** (e.g. DNA damage, hypoxia, oncogene activation, depletion of ribonucleotide, telomere erosion, and prevents autophagy), whereas in the nucleus, p53 activates **cellular responses** (e.g. cell-cycle arrest, DNA damage repair, differentiation, senescence/aging or apoptosis) (Hientz et al. 2017). BCL-2 proteins are located in the mitochondria, and when activated can either be anti-apoptotic or pro-apoptotic depending on the nature

of DNA damage. BCL-2 contributes to cell death by causing the release of cytochrome-c which then activates caspase-family enzymes. Oxidative damage of cellular proteins activates unfolded protein responses (UPR), which trigger chaperones to rebuild the proteins leading to cell survival.

However, in patients diagnosed with cancer and COPD, the p53 guardian angels are no longer protective in nature; they are downregulated, but any upregulation does not necessarily lead to cell-cycle arrest. With no changes in Bax activity, BCL-2 activation leads to inactivation of Caspases, no apoptotic response, and uncontrolled cell growth which ultimately leads to tumorigenesis.

Chapter 9: General Discussion

9.0 General Discussion

Evaluation of the cytotoxicity and genotoxicity profiles of GO are crucial in order to understand their behaviour at the molecular level which in turn provide more information for future design of GO materials free of toxicity for nanomedical applications. The objective of this PhD thesis has been to evaluate the genotoxic potential of commercially available aqueous suspension of GO (1mg/mL; 15-20 sheets, and 4-10% edge-oxidized), *in vitro* on DNA damage on human whole blood and PBL from healthy individuals and patients with chronic pulmonary conditions (asthma, COPD, and lung cancer). We were particularly interested on the use of human whole blood and isolated PBL as blood samples were quicker to collect from patients at the hospital than collection of cell lines. Furthermore, it is better and faster to detect COPD and cancer's DNA in the blood sample at the early stages of chronic disease development than late detection using cell lines (cancer cell-lines, etc) when the disease had already spread and malignant.

The physicochemical properties of GO such as particle diameter, shape, surface charge, etc are important factors which influence the toxicity of nanomaterials. In order to accurately compare results with other researchers and appreciate the genotoxicity potential of this particular GO used in this thesis, it is essential to maintain consistency in every parameter of the GO studies: consistencies on the GO concentrations, incubation time, use of the same cell types (e.g. lymphocytes, cancer cell lines, etc), *in vivo* or *in vitro*, continuous validation of effectiveness of the assays used, and most importantly, consistency on the same source of GO. The last point is so important to ensure consistency and systematic particle size control (Gies and Zou 2018). Previous studies have used non-commercial GO

(with 2-3 layers of GO sheets) synthesized locally in their laboratories across the world, and genotoxicity studies performed using different assay methods and test models [e.g. animal (Liu et al. 2013b); human erythrocytes and skin fibroblasts (Liao et al. 2011); human lymphocytes and serum albumin (Ding et al. 2014); normal human lung cells (BEAS-2B) (Vallabani et al. 2011); human hepatoma HepG2 (Yuan et al. 2011); macrophages (Sasidharan et al. 2012); and different administration routes in mice such as i.v. administration (Zhang et al. 2011)]. Other previous studies have also shown that some of these discrepancies observed in cell responses were due to differences in cell lines (Gies and Zou 2018). Furthermore, the variability of human error from the individuals performing these studies could contribute to conflicting data among researchers

To accomplish our objective, we first characterized GO NMs in the aqueous state using Zetasizer Nano for DLS and zeta potential to evaluate their dynamic particle diameter and surface charge and explore their aggregation state after dispersion. We also studied particle size and aggregation using electron microscope (SEM and TEM). Thereafter, we assessed the cytotoxicity of GO (50, 100, 150, and 200 µg/mL) after 24 h exposure to human lymphocytes from healthy individuals and patients (asthma, COPD, and lung cancer) using two colorimetric assays - NRU and MTT assays, respectively - to evaluate the % cell survival after 3 and 4 hrs of exposure to the dyes. Further, we determined the genotoxicity (DNA damage) of GO and 100 µM H₂O₂ as the PC for 30 min on human whole blood from healthy individuals and patients (asthma, COPD, and lung cancer) using the Alkaline Comet assay. Damaged DNA particles (negatively charged) under electric field migrate towards the positively charged electrode according to their molecular

weights and appear as comets: the smaller the molecular weights, the faster the migration, and vice-versa, the bigger the molecular weight, the slower the migration. DNA damage was quantified using two parameters – OTM and % tail DNA. We followed our curiosity and further ascertained the cytogenetic potential of GO (0, 10, 20, 50 and 100 µg/mL) and 50 µL of Mitomycin C (MMC) as the PC on freshly collected human whole blood from healthy individuals and patients (asthma, COPD, and lung cancer) using the CBMN assay. The cytogenetic endpoints (MNI, MonoNC, BiNC, MultiNC, NBUDs, and NPBs) were scored and the NDI calculated per 1,000 cells counted. Thereafter, we assessed the impacts of higher concentrations of GO (150 and 200 µg/mL) on human lymphocytes from healthy and patients on the relative gene expression of cell-cycle signalling genes (TP53, CDKN1A, and BCL-2) in RT-qPCR using GAPDH as an internal control, followed by WB analysis of protein expression of p53, p21 and BCL-2 proteins relative to GAPDH in human lymphocytes (healthy and patients) after exposure to GO NMs.

9.1 Discussion on GO particle characterization (Chapter 3)

Systematic evaluation of the entire toxicity profile of GO at the molecular level of DNA damage is vital for the safe and future development of GO-based biomedical applications such as nanocarriers in drug delivery of anti-cancer therapy (Liu et al. 2013a); anti-microbial agents for teeth and bone grafting (Priyadarsini et al. 2018); imaging (Zhou and Liang 2014) and many more. Despite these overwhelming biomedical applications, existing literature on the overall characterization methods (particle size measurements using different

techniques), cytotoxicity and genotoxicity of GO are conflicting and inconsistent. Here, we characterized commercially purchased GO (Sigma-Aldrich) using DLS, ZP, SEM and TEM. We did not prepare the GO NMs in our laboratory since such preparation could possibly differ in composition and purity when compared to the commercially sourced GO NMs. Sigma-Aldrich and other commercial graphene oxide manufacturers have established quality control systems which guarantee controlled particle size and consistency in purity of GO NMs.

The range of particle size distribution obtained in our study has shown the type of discrepancies already pointed out in the earlier paragraph. In DLS (under aqueous solution), the particle size range for GO NMs (15-20 sheets) was between 690 and 806 nm, while the particle size range per sheet of GO was between 35 and 54 nm, and high polydispersity indices (PDI) of 0.768, 0.899, and 0.929. On the hand, particle size analyses of GO NMs (15-20 sheets) using electron microscope (SEM and TEM) revealed much smaller particle size distances between 363.7 and 447.8 nm, while the particle size range per sheet of GO was between 18 and 29 nm. Therefore, more precise, and consistent methods for the characterization of GO materials are required. GO has both hydrophilic and hydrophobic properties depending on the interacting surface. The hydrophilic properties were evident in DLS analysis as GO sheets dispersed in H₂O absorbed molecules of water into their interstitial space and expand in size. DLS cannot discriminate the actual particle size from H-bond reactions such as GO-protein reactions (protein corona), leading to misleading results. Finally, the implication of the negative surface charge of GO NMs (-21.7 and -26.1 mV) in our results is that although these negatively charges may be low to repel

intermolecular forces of attraction (Van der Waal forces) between particles, hence causing agglomeration, they are in fact sufficient enough to stabilise GO NMs in aqueous dispersion medium. Even after agglomeration had occurred, the particles can be re-dispersed homogenously with gentle agitation. Although, it has been reported that differences in cellular cytotoxicity was due to differences in physicochemical properties (Ng et al. 2011), and that GO sheets absorbed culture medium, nutrients, amino acids, etc causing cellular oxidative stress (Guo et al. 2008; Liu et al. 2009), it is likely theoretically that the GO NMs used in this study could have induced cytotoxicity and genotoxicity through oxidative DNA damage mechanisms.

9.2 Discussion on the cytotoxicity of GO NMs in human lymphocytes from healthy individuals and patients (asthma, COPD, and lung cancer) using MTT and NRU assays (Chapter 4)

GO NMs are potential candidates for biomedical applications such as bio-sensors, nanomedical devices, gene therapy as well as nano-carriers in drug delivery of anti-cancer agents (e.g. Dox) (Wu et al. 2015). These biomedical applications have stimulated much debate on the safety of GO and more research interest on their cytotoxicity in human systems. This has led to several biocompatibility analyses (Wang et al. 2011a; Zhang et al. 2011; Ding et al. 2014).

In view of that, the present study has provided conclusive evidence that GO can be cytotoxic in human lymphocytes [healthy and patients (asthma, COPD, and lung cancer)] over a range of concentrations and using well-known assays such

as MTT and NRU assays to evaluate cell proliferation / mitochondrial metabolic activities (Jedrzejczak-Silicka and Mijowska 2018). Interaction of Graphene nanomaterials with cell membranes has been reported (Liao et al. 2018) leading to membrane damage and cytotoxicity. Our results demonstrated increased cytotoxicity/ decreased metabolic activities with increased GO concentrations (10, 20, 50 and 100 µg/mL) relative to the untreated NC samples. Our results are also in agreement with work conducted elsewhere which showed that GO caused significant decrease in cell viability on normal human fibroblast cells using the MTT assay (Wang et al. 2013). In another study, different concentrations of GO between 10-100 µg/mL, significantly decreased cell viabilities in human lung cancer cells (BEAS-2B) after 24 h treatment and assessed using the MTT assay (Vallabani et al. 2011).

The viability assays and methods used to calibrate cytotoxicity may further influence cytotoxicity results. In a study by Jiao, Guozheng et al, the results following the analysis of cytotoxicity of graphene on HepG2 and Chang liver cell lines using both MTT and CCK-8 assays were inconsistent (Jiao et al. 2015). It is known that carbon nanotubes and other nanomaterials interfere with the MTT assay. Pulmonary toxicity of different sizes of graphene family nanomaterials such as SWCNTs has also been conducted on NR8383 rat alveolar macrophages using the instillation test and *in vitro* cell-based assays (Fujita et al. 2015), leading to acute lung inflammation soon after inhalation, thereby linking respiratory toxicity to particle size.

9.3 Discussion on the genotoxicity (DNA damage) of GO NMs in human whole blood from patients and patients (asthma, COPD, and lung cancer) using the Alkaline Comet Assay (Chapter 5)

The alkaline Comet assay, also known as single-cell gel electrophoresis, is a sensitive and simple method for the assessment of DNA damage at the molecular level (Pu et al. 2015). Under electrical conditions, damaged DNA particles migrate from the negatively charged Cathode to the positively charged anode, and the rate of migration is dependent on the size: the smaller the DNA particles, the faster the migration and appear as a Comet. Performance of the Comet assay under alkaline conditions (pH >13) is regarded as the best version of the Comet assay for assessment of DNA damage events. The assay is able to detect various types of DNA damage events, including DNA SSB, DNA DSB, alkali-labile sites (ALS), and DNA-DNA/DNA-protein cross-linking (Tice et al. 2000).

In this study, human whole blood samples from healthy individuals and patients (asthma, COPD, and lung cancer) were treated with different concentrations of GO (0, 10, 20, 50 and 100 µg/mL) in a final RPMI culture volume of 1,000 µL for 30 min and DNA damage scored and quantified using OTM and % Tail DNA. DNA damage was significantly higher in patients than in healthy individuals. Specifically, DNA damage was higher in lung cancer patients than in COPD patients, whereas DNA damage in asthma and healthy individuals was almost the same. The differences in DNA damage may be due to the nature of the cell and patients' pathological conditions. Several studies on the cytotoxicity and genotoxicity of GO have been reported. The work of Hu et al. (2010) showed that GO caused inhibition of bacterial growth, while on human alveolar epithelia A549

cells, minimal toxicity was observed (Hu et al. 2010). Using the same A549 cells, Chang et al (2011) proposed that GO cannot enter A549 cells irrespective of their size or concentration (Chang et al. 2011).

Studies by Wang et al. (2010) have demonstrated that GO nanomaterials can cause concentration-dependent toxicity in human fibroblast cells (CRL-2522) at concentrations > 50 µg/mL (Wang et al. 2011a). This research agrees with our studies which showed that GO exerted considerable DNA damage in a concentration-dependent manner in patients according to their medical conditions as well as in healthy individuals. GO nanomaterials may therefore pose a health risk to humans through their biomedical applications when they inadvertently get into human blood. On the other hand, this genotoxicity potential is a confirmation of the kind of toxicity GO nanomaterials could produce when used medically in drug delivery as a nanocarrier system in the treatment of lung cancer and COPD.

9.4 Discussion on the cytogenetic (mutagenesis) effects of GO on human whole blood from patients and patients (asthma, COPD, and lung cancer) using CBMN Assay (Chapter 6)

Nanotechnology has become integrated into our human society with the growing biomedical applications of GO and other GFNMs. This increase in popularity has been associated with their unique physical and chemical properties such as size, large surface area, 2D surface planar, surface chemistry, etc. These properties project GO as promising agents as nanocarriers in the design and delivery of advanced drug delivery systems and a wide range of therapeutics. It has been reported that the same properties which make nanomaterials unique could be responsible for their genotoxicity potentials (Landsiedel et al. 2009).

The inconsistencies in the cytotoxicity and genotoxicity profiles of GO and other GFNMs have led to increased research on the safety of these materials. Previous studies on CBMN assay had been performed on a number of test models, including erythrocytes, peripheral blood lymphocytes, epithelial cells, etc (Speit et al. 2011). In one of such studies, El-Yamany NA, et al. (2017) investigated effects of different concentrations of GO nanosheets (10, 50, 100, 250, and 500 µg/kg b.w.) on mice by injecting them intraperitoneally on weekly basis, and chromosome aberrations tested after 7, 28 and 56 days after treatment (El-Yamany et al. 2017). Their results demonstrated variable structural chromosomal aberrations (SCA) in the mice bone marrow, which are reflections of chromosomal DNA damage. In another study by Liu, Y. et al (2013), 1-2 layers of GO NMs were synthesised in house and particle size determined using TEM. Kunming mice (25-30 g) were intravenously administered with different

concentrations of the GO (5, 10, and 20 mg/kg) daily for 5 days as well as *ex vivo*, and mutagenicity performed using the CBMN assay. Their results showed that GO NMs induced mutagenesis in both *in vivo* and *in vitro* studies (Liu et al. 2013b).

In this study, cytogenetic potential of different concentrations of GO (0, 10, 20, 50 and 100 µg/mL) was assessed in human whole blood, and chromosome instability parameters (BiNC, MNi, MonoNC, MultiNC, NDI, etc) scored in the CBMN Assay. Like the Comet assay, our results as described in Chapter 6, show significant increases in chromosome aberration endpoints which are clear indications of the cytogenetic effects of GO nanomaterials in human whole blood. Unlike in the Comet assay where whole blood samples were treated for 30 min, in the CBMN Assay, whole blood samples were treated for 20 h – a much longer period of exposure. The long incubation time meant that more cells reacted with the GO leading to significant DNA fragmentation and high number of cytotoxic endpoints as observed (Nabi et al. 2014), but less than longer treatment times of 7, 28 and 56 days conducted elsewhere (El-Yamany et al. 2017).

One of the main advantages of the CBMN assay is the ability to measure both structural and numerical changes in the chromosomes (Doepker et al. 1998). Chromosome endpoints are induced due to GO insult to actively dividing cells. Cytokinesis process commences immediately after telophase, the last stage of mitosis, is completed. On the 44th hour of cell culture or 20 h of chemical treatment when Cytochalasin B (a cell-permeable mycotoxin) was added to the cell culture (Chang et al. 2016), it immediately blocks cytokinesis and disrupts actin formation

– a contractile microfilament ring assembly vital for the cell morphology (shape), cytoskeletal framework and structure of cells (Heng and Koh 2010).

Although the CBMN assay is very sensitive for scoring chromosomal abnormalities after exposure to chemical agents, a number of factors could impact on the results (Golbamaki et al. 2015), such as the presence of impurities in the compound during synthesis; differences in physical characteristics among different laboratories such as particle size, size distribution, size of aggregates in the dispersion medium; crystal structure; surface areas of materials with similar average size; differences in coatings; and differences in assay types and models. The CBMN assay has several limitations among them is the Cyto-B itself. Naturally, Cyto-B is a well-known mycotoxin produced by fungi and causes death and diseases in both humans and animals. This toxic effects on cells could work synergistically with GO nanomaterials resulting in significant GO-induced chromosome aberrations leading to overestimation of cytogenetic events (Fenech and Morley 1985; Schwarzbacherova et al. 2016).

9.5 Discussion on the Effects of GO on Gene and Protein Expression of p53/TP53, CDKN1A/p21, and BCL-2 on human lymphocytes from healthy individuals and patients (asthma, COPD, and lung cancer) using the RT-qPCR Method (Chapter 7)

Tumour suppressor genes (TP53/p53 and CDKN1A/p21) and apoptotic/ anti-apoptotic BCL2 genes/ proteins are important transcription factors involved in cell-cycle regulation in response to DNA damage. They play key roles in the suppression of cell invasion, control cell growth arrest and apoptosis (Kim et al. 2017). When DNA damage is irreparable, p53 interacts with BCL2 proteins in the mitochondria and initiate apoptosis (Roufayel 2016). Expression of tumour suppressor genes /proteins (TP53/p53 and CDKN1A/p21) have been known to be upregulated in response to DNA damage, while BCL-2 is stimulated towards either pro-apoptotic or anti-apoptotic, upregulation or downregulation depending on the extent of DNA damage. However, it was reported that p21 can be upregulated independently of p53 activation (Abbas and Dutta 2009; Li et al. 2014).

However, the effects of GO on gene and protein expression in humans after exposure to human lymphocytes are not yet fully explored. To the best of our knowledge, there are no reports so far, specifically on the effects of GO (15-20 sheets) on p53/TP53, CDKN1A/p21, BCL-2 and GAPDH on human lymphocytes from 4 different individuals – 3 patient groups diagnosed in the hospital setting to have asthma, COPD and lung cancer and healthy individual groups simultaneously. To address this question, gene, and protein expression of

p53/TP53, CDKN1A/21, and BCL-2 genes/ proteins were analysed using RT-qPCR and Western Blotting (WB), respectively using GAPDH as an internal control. For RT-qPCR, different human lymphocytes from patients (asthma, COPD, and lung cancer) and healthy individuals were exposed to two GO (150, and 200 µg/mL) for 24 h and gene expression of TP53, CDKN1 and BCL-2 genes, normalized with GAPDH as an internal control, was evaluated relative to untreated, NC using RT-qPCR. In the WB analyses, human lymphocytes from patients (asthma, COPD, and lung cancer) and healthy individuals were treated with four concentrations of GO (50, 100, 150 and 200 µg/mL). We were unable to detect bands at lower concentrations (10 and 20 µg/mL) and the proteins of interest appeared to be unaffected with no alterations at these non-toxic concentrations.

Remarkably, induced TP53 genes were observed in all samples treated with 150 and 200 µg/mL of GO as a confirmation of DNA damage relative to the untreated cells. The TP53 genes were significantly expressed by 3.3- and 10-fold in lung cancer patients after exposure to 150 and 200 µg/mL, respectively; by 2.6- and 25-fold in asthma; by 2.6- and 2.5-fold in COPD patients; and minimally expressed by 0.8- and 2.3-fold in healthy individuals after exposure to the respective aforementioned treatment concentrations relative to the untreated cells. The CDKN1A genes were upregulated variably after treatment with 150 and 200 µg/mL. In asthma lymphocytes, CDKN1A genes were significantly upregulated by 3.4- and 9.9-fold; in healthy individuals, the genes were upregulated by 2- and 5.8-fold after exposure to the aforementioned

concentrations respectively relative to untreated samples. In lymphocytes from COPD patients, the CDKN1A genes were downregulated by 0.3- and 0.4 after treatment with 150 and 200 µg/mL of GO NMs, respectively. However, in lymphocytes of lung cancer patients, there were no changes in fold-differences after exposure to 150 µg/mL ($2^{-\Delta\Delta Cq} = 1$), but the CDKN1A genes were downregulated by 0.9-fold after exposure to 200 µg/mL of GONMs. These changes were clear indications that activation of TP53 genes due to genetic injury leads to activation of cyclin- dependent kinase inhibitor (CDKN1A) genes as part of the tumour suppressor pathway, but the CDKN1A genes are less active in patients with serious chronic diseases (e.g. COPD and lung cancer). Also, upregulation of BCL-2 genes in the worst cases of chronic lung diseases in COPD patients (1.6- and 1.3-fold) and lung cancer patients (1.3- and 1.2-fold) compared with the downregulation of BCL-2 genes observed in asthma patients (0.8- and 0.7-fold) and healthy individuals (0.5- and 0.7-fold) were indications of the non-apoptotic activities of the BCL-2 genes in patients with serious pulmonary diseases (COPD and lung cancer).

In the WB analysis, p53, p21, BCL-2, and GAPDH were expressed and detected in healthy individuals. These findings are confirmations of the DNA damaging potential of GO. It may also be possible that expression of these proteins in patient's lymphocytes (asthma, COPD, and lung cancer) are possible. Unfortunately, we encountered enormous difficulties in WB analysis of lymphocytes from patients. Due to technical issues with Abcam monoclonal Secondary antibody (Anti-Rabbit IgGVHH Single Domain Antibody (HRP) (ab191866), we were unable to detect p53, p21, and BCL-2 proteins in asthma,

COPD, and lung cancer patients throughout the 12 months (Jan 2018-Jan 2019) spent in the laboratory conducting Western blot and RT-qPCR experiments.

However, in September 2018, a complaint was made to Abcam UK regarding the authenticity of the quality of the secondary antibody we had purchased from them. A free replacement Secondary antibody (Goat Anti-Rabbit IgG H&L (HRP) was sent to us and acknowledged on Monday, 24th September 2018. Thereafter, we successfully obtained bands only in healthy individuals, suggesting that the proteins of interest were more abundant in healthy individuals.

9.6 Conclusion

GO NMs are increasingly becoming popular because of their versatile applications, especially in nanomedicine as a drug delivery carrier of anticancer drugs. Knowledge about its genotoxicity in humans still remains very scarce. The increasing need to find a cure for chronic pulmonary diseases such as lung cancer, asthma and COPD justifies the urgent need to assess the genotoxicity of GO before being used in humans.

In the present study, we had rigorously analysed the commercially available GO (15-20 sheets; 4-10% edge-oxidized; Concentration: 1 mg/mL; Dispersion in H₂O) synthesized through the modified Hummers' method (Hummers and Offeman 1958) and purchased from Sigma-Aldrich, USA (PCode: 1002087404; 794341) (PubChem 2018; Sigma-Aldrich 2018). A study of GO Safety Data Sheet (SDS) in **Appendix 14** shows that none of the components used in the synthesis of GO was at levels $\geq 0.1\%$, a concentration threshold identified by the International Agency for Research on Cancer (IARC) above which chemical agents become carcinogenic in humans (IARC 2017).

Every effort was made to ascertain from Sigma-Aldrich if there were any impurities contained in the commercially produced GO during manufacture. The company's representative was contacted by email on 15th and 18th January 2019 to request for any information or data they might have regarding the purity, quantity of impurities, and any previous toxicology studies. However, we were informed that there was no toxicology data available, and that all the information

they had on their GO was available in the SDS sheet online (See **Appendix 15: E-mail Correspondences with Sigma-Aldrich**).

In the absence of any genotoxicity information on GO (15-20) sheets, we anticipate that our research has fulfilled the knowledge gap and make an original contribution to support existing research on multi-walled GO NMs. To the best of our knowledge, this study was the first of its kind in the genetic toxicology assessments of this class of GO on human whole blood and human peripheral lymphocytes from 3 real-life patients clinically diagnosed in the hospital with chronic pulmonary diseases (asthma, COPD, and lung cancer) and healthy control individuals.

First, GO NMs were characterised using DLS, ZP, SEM and TEM. Although the range of particle size distance measured between DLS (693.8 nm to 806.1 nm) and TEM (363.7 nm to 447.8 nm) differed remarkably, the implication is that DLS, which measures particle size distribution in the liquid dispersion phase, might not after all be the suitable tool to accurately measure GO NMs. The reason being that since water molecules are absorbed in-between particles and swell up, this change may not be taken into consideration by the scattered light, and the size is reported as large. The thickness of GO was also influenced by the amount of oxygen-containing functional groups present (Song et al. 2014). The morphology observed in SEM and TEM micrographs show that GO particles agglomerated as piles of multiple flakes of GO sheets, tightly packed together on top of each other in various thicknesses and rough edges, and thus precisely matched the 15-20 layers of GO as described by the manufacturer. The results of the *in vitro* studies

may differ remarkably from the *in vivo* reactions inside the body. When administered i.v. as a nano-carrier in drug delivery, GO reacts with the blood components such as proteins, forming a **Protein corona** around nanomaterials, and consequently affect the surface properties as well as the final drug dose which reaches the tumour site (Dawson et al. 2009; Wills et al. 2017). The negative value of the ZP demonstrated that GO particles exist as negatively charged materials in aqueous dispersion, which impart good stability and dispersity in the aqueous solution. However, the negatively charged surface vis-a-viz aqueous stability might be altered *in vivo* depending on the pH and temperature of the surrounding environment (Farazi et al. 2018). Reports show that the efficiency of drug released into the tumour site is dependent on the body temperature (from 25-37°C) and pH (from 7.4 to 5.4) of the tumour environment (Farazi et al. 2018).

The cytotoxicity data from MTT and NRU assays showed that GO caused a concentration-dependent decrease in cellular metabolic profile in human lymphocytes according to the pathological conditions of the individuals. Since GO-induced cytotoxicity levels in lung cancer and COPD patients were significantly higher compared to asthma and healthy individuals, GO may play a synergistic role as a nanocarrier of anticancer (Dox) and COPD drugs (Pan et al. 2012; Zhou et al. 2014; Wu et al. 2015). In the Comet assay, DNA damage was quantified as OTM and % Tail DNA. H₂O₂, a well-known genotoxic agent, demonstrated concentration-dependent increases in DNA damage on human whole blood from healthy individuals. The concentration with the highest DNA damage (100 µM H₂O₂,) was used as the positive control (PC). Like results

obtained in the cytotoxicity assessments (MTT and NRU assays), DNA damage was significantly higher in lung cancer patients followed by COPD patients. DNA damage in asthma was almost like those of healthy individuals.

In the CBMN assay, our results showed various degrees of chromosome damage after 20 h of exposure to different concentrations of GO (10, 20, 50 and 100 $\mu\text{g}/\text{mL}$). Chromosomal aberration parameters (BiNC, MultiNC, MNi, NDI, etc) increased with increase in GO concentration, especially in healthy individuals and lung cancer patients compared to untreated NC samples. In asthma and COPD patients, cytogenetic affects were also observed at various levels. These are indicators of DNA damaging potential of GO concentrations used in this study. Gene expressions of TP53, CDKN1A and BCL-2 relative to GAPDH after exposure of human lymphocytes (healthy, asthma, COPD, and lung cancer) to GO (150 and 200 $\mu\text{g}/\text{mL}$) were analysed using RT-qPCR, followed by WB analyses after exposure to GO (50, 100, 150 and 200 $\mu\text{g}/\text{mL}$). Both results showed altered gene expression levels and protein induction in healthy individuals which are clear demonstrations of DNA damage. In RT-qPCR, tumour suppressor TP53 genes were maximally expressed in lung cancer patients by 10-fold ($p < 0.001$) after exposure to 200 $\mu\text{g}/\text{mL}$ of GO relative to untreated samples, followed by 2.5-fold in asthma ($p < 0.001$), 2.3-fold in healthy individuals ($p < 0.001$) and 1.4-fold in lung cancer patients ($p < 0.001$) at the same concentration. Our data agree with work by Wang, et al (2010) which showed GO as a double-edge sword that might pose a potential health risk at workplace. Wang et al. found that GO concentrations between 100 and 250 μg did not show clear toxicity in mice within 1-7 days of exposure. However, after 30 days, GO at a very high

concentration of 400 µg caused severe lethal side effects to the mice, and killing over 44% of them, while the rest of the mice suffered granuloma in the lungs and injury to other vital parts of their body (Wang et al. 2011a). Confounding factors such as age, cigarette smoking, etc were taken into consideration and could have contributed to DNA fragmentation.

In conclusion, the concentrations of GONMs (10, 20, 50, 100, 150 and 200 µg/mL) used in this study caused lethal damage to human whole blood and PBL from patients with lung cancer, COPD, and asthma than in healthy individuals. If GO NMs are pharmaceutically formulated as nanocarriers in drug delivery to target lung cancer cells and COPD, our results suggest that they could potentially cause damage to COPD and lung cancer's DNA. However, the cytotoxicity, genotoxicity (DNA damage), chromosome aberrations, and alteration in gene expression - biomarkers of cancer pathogenesis - observed *in vitro* in human whole blood and PBL from healthy control individuals are of concern to public health especially on the workforce who might be exposed at micro levels overtime at the workplace. The responses obtained in this PhD study further contribute to existing literature on the cytotoxicity and genotoxicity of the various types of GO nanomaterials.

9.7 Future work

Previous research has shown that GO NMs react with MTT dye, and cytotoxicity assessment using the MTT assay could lead to overestimated of toxicity results (Liao et al. 2011). Therefore, alternative methods such as the water-soluble tetrazolium salt (WST-8), ROS, etc are suggested to further support the MTT assay results obtained in this project.

Furthermore, we recommend future work on the Western Blot analysis of the effects of GO (10, 20, 50, 100, 150 and 200 µg/mL) on different protein regulatory pathways which control protein expressions of p53, p21, and BCL-2 in response to DNA damage in human whole blood or lymphocytes from patients (asthma, COPD, and lung cancer). In the absence of WB analysis, Immunohistochemistry (IHC) could be used as an alternative to WB to selectively identify induced antigens (proteins) in GO-treated human lymphocytes or whole blood by exploiting the same anti-body-antigen binding specificity used in WB method.

References

References

- Abbas, T. and Dutta, A. (2009) p21 in cancer: intricate networks and multiple activities. *Nature Reviews Cancer* 9 (7), 460-461.
- ACS Material (2019) *High Surface Area Graphene Oxide*.
<https://www.acsmaterial.com/high-surface-area-graphene-oxide-1069.html>
Accessed 09 Mar 2019.
- Adcock, I. M., Caramori, G. and Barnes, P. J. (2011) Chronic Obstructive Pulmonary Disease and Lung Cancer: New Molecular Insights. *Respiration* 81 (4), 265-284.
- Albertini, R. J., Anderson, D., Douglas, G. R., Hagmar, L., Hemminki, K., Merlo, F., Natarajan, A. T., Norppa, H., Shuker, D. E. G., Tice, R., Waters, M. D. and Aitio, A. (2000) IPCS guidelines for the monitoring of genotoxic effects of carcinogens in humans. International Programme on Chemical Safety. *Mutation Research-Reviews in Mutation Research* 463 (2), 111-172.
- American Cancer Society (2018) *High-Dose Chemotherapy/Radiation Therapy and Stem Cell Transplant for Neuroblastoma*. Online.
<https://www.cancer.org/cancer/neuroblastoma/treating/high-dose-chemo-radiation.html> Accessed 08 Mar 2019.
- Amrollahi-Sharifabadi, M., Koochi, M. K., Zayerzadeh, E., Hablolvarid, M. H., Hassan, J. and Seifalian, A. M. (2018) In vivo toxicological evaluation of graphene oxide nanoplatelets for clinical application. *International journal of nanomedicine* 13, 4757-4769.
- AMS Biotechnology (2016) *Amsbio*. <http://www.amsbio.com/Comet-Assays.aspx>
Accessed 25 Mar 2019.
- Andem, A. B., Agbor, B. and Ekpo, I. A. (2013) Review of Comett Assay: A reliable tool for assessing DNA damage in Animal Models. *Journal of Current Research in Science* 1 (6), 405-427.
- Anderson, D., Najafzadeh, M., Gopalan, R., Ghaderi, N., Scally, A. J., Britland, S. T., Jacobs, B. K., Reynolds, P. D., Davies, J., Wright, A. L., Al-Ghazal, S., Sharp, D. and Denyer, M. C. (2014) Sensitivity and specificity of the empirical lymphocyte genome sensitivity (LGS) assay: implications for improving cancer diagnostics. *The FASEB Journal* 28, 1-9.
- Applied Biosystems (2008) *Guide to Perform Relative Quantitation of Gene Expression Using Real-Time Quantitative PCR*. https://assets.thermofisher.com/TFS-Assets/LSG/manuals/cms_042380.pdf Accessed 13th January 2019.
- Aslantürk, Ö. S. (2017) In Vitro Cytotoxicity and Cell Viability Assays: Principles, Advantages, and Disadvantages. *IntechOpen*.
- Asthma UK (2016) *Asthma and Other Conditions*. Online: Asthma UK.
https://www.asthma.org.uk/advice/manage-your-asthma/other-conditions/?qclid=EAlaIqObChMlqs6Ww-mw1QIV7bztCh3P1qpHEAAYASAAEqJ-YfD_BwE#copd Accessed 30 July.
- Avelar-Freitas, B. A., Almeida, V. G., Pinto, M. C. X., Mourão, F. A. G., Massensini, A. R., Martins-Filho, O. A., Rocha-Vieira, E. and Brito-Melo, G. E. A. (2014) Trypan blue exclusion assay by flow cytometry. *Brazilian Journal of Medical and Biological Research* 47 (4), 307-315.

- Bahadar, H., Maqbool, F., Niaz, K. and Abdollahi, M. (2016) Toxicity of nanoparticles and an overview of current experimental models. *Iranian Biomedical Journal* 20 (1), 1-11.
- Barbero, F., Russo, L., Vitali, M., Piella, J., Salvo, I., Borrajo, M. L., Busquets-Fité, M., Grandori, R., Bastús, N. G., Casals, E. and Puntès, V. (2017) Formation of the Protein Corona: The Interface between Nanoparticles and the Immune System. *Seminars in Immunology* 34, 52-60.
- Bengtson, S., Kling, K., Madsen, A. M., Noergaard, A. W., Jacobsen, N. R., Clausen, P. A., Alonso, B., Pesquera, A., Zurutuza, A., Ramos, R., Okuno, H., Dijon, J., Wallin, H. and Vogel, U. (2016) No cytotoxicity or genotoxicity of graphene and graphene oxide in murine lung epithelial FE1 cells in vitro: Graphene and Graphene Oxide in Vitro. *Environmental and Molecular Mutagenesis* 57 (6), 469-482.
- Benhusein, G. M., Mutch, E., Aburawi, S. and Williams, F. M. (2010) Genotoxic effect induced by hydrogen peroxide in human hepatoma cells using comet assay. *The Libyan journal of medicine* 5 (1), 4637.
- Bernard, P. S. and Wittwer, C. T. (2002) Real-Time PCR Technology for Cancer Diagnostics. *Clinical Chemistry* 48 (8), 1178-1185.
- Bharadwaj, M., Mifsud, N. A. and McCluskey, J. (2012) Detection and Characterisation of Alloreactive T Cells In: Christiansen F., Tait B. (eds) Immunogenetics. Methods in Molecular Biology (Methods and Protocols), vol 882. Humana Press, Totowa, NJ. *Immunogenetics* 882, 309-337.
- Bhattacharjee, S. (2016) DLS and zeta potential – What they are and what they are not? *Journal of Controlled Release* 235, 337-351.
- Bignold, L. P. (2009) Mechanisms of clastogen-induced chromosomal aberrations: A critical review and description of a model based on failures of tethering of DNA strand ends to strand-breaking enzymes. *Mutation Research-Reviews in Mutation Research* 681 (2), 271-298.
- Bio-Rad (2018) *Western Blotting*. <https://www.bio-rad-antibodies.com/western-blotting.html>
- BioDrop Ltd (2012) *BioDrop micro-volume measurement platforms*. Online: <https://www.biodrop.co.uk/index.php?where=snaptait> Accessed 19 Mar 2019.
- BioSistemika (2017) *Real-Time PCR (qPCR) Technology Basics*. 4 Jul 2017. Online: BioSystemika. <https://biosistemika.com/blog/qpcr-technology-basics/> Accessed 19 Mar 2019.
- Bishop, G. B. and Einhorn, T. A. (2007) Current and future clinical applications of bone morphogenetic proteins in orthopaedic trauma surgery. *International Orthopaedics* 31 (6), 721-727.
- Bousquet, J., Clark, T. J. H., Hurd, S., Khaltaev, N., Lenfant, C., O'Byrne, P. and Sheffer, A. (2007) GINA guidelines on asthma and beyond. *Allergy* 62 (2), 102-112.
- Bradford, M. M. (1976) A rapid and sensitive method for the quantitation of microgram quantities of protein utilizing the principle of protein-dye binding. *Analytical biochemistry* 72 (1-2), 248-254.
- British Lung Foundation (2017) *Lung disease in the UK - big picture statistics*. British Lung Foundation. <https://statistics.blf.org.uk/lung-disease-uk-big-picture> Accessed 11th May 2017.
- Bryant, J. A., Francis, D. and Society for Experimental, B. (2007) *The eukaryotic cell cycle*. Vol. 59. London: Taylor & Francis.

- Burnette, W. N. (1981) "Western Blotting": Electrophoretic transfer of proteins from sodium dodecyl sulfate-polyacrylamide gels to unmodified nitrocellulose and radiographic detection with antibody and radioiodinated protein A. *Analytical Biochemistry* 112 (2), 195-203.
- Bustin, S. A. and Mueller, R. (2005) Real-time reverse transcription PCR (qRT-PCR) and its potential use in clinical diagnosis. *Clinical Science* 109 (4), 365-379.
- Böyum, A. (1968) Separation of leukocytes from blood and bone marrow. Introduction. *Scand J Clin Lab Invest Suppl.* 97 (7).
- Cancer Research UK (2015) *Lung Cancer Statistics*. Online: <https://www.cancerresearchuk.org/health-professional/cancer-statistics/statistics-by-cancer-type/lung-cancer#heading-One> Accessed 16 Mar 2019.
- Cancer Research UK (2016) *Fluorouracil (5FU)*. Online: <https://www.cancerresearchuk.org/about-cancer/cancer-in-general/treatment/cancer-drugs/drugs/fluorouracil> Accessed 09 Mar 2019.
- Cancer Research UK (2017) *Treatment for Cancer*. Online: <https://www.cancerresearchuk.org/about-cancer/cancer-in-general/treatment> Accessed 08 Mar 2019.
- Chakarov, S., Petkova, R. and Russev, G. C. (2012) p53-Guardian Angel and Archangel. *Biotechnology & Biotechnological Equipment* 26 (1), 2695.
- Chang, H.-T., Chou, C.-T., Chen, I. S., Yu, C.-C., Lu, T., Hsu, S.-S., Shieh, P., Jan, C.-R. and Liang, W.-Z. (2016) Mechanisms underlying effect of the mycotoxin cytochalasin B on induction of cytotoxicity, modulation of cell cycle, Ca²⁺ homeostasis and ROS production in human breast cells. *Toxicology* 370, 1-19.
- Chang, Y., Yang, S.-T., Liu, J.-H., Liu, Y., Dong, E., Wang, H., Wang, Y. and Cao, A. (2011) In vitro toxicity evaluation of graphene oxide on A549 cells. *Toxicology Letters* 200 (3), 201-210.
- Chen, B., Liu, M., Zhang, L., Huang, J., Yao, J. and Zhang, Z. (2011) Polyethylenimine-functionalized graphene oxide as an efficient gene delivery vector. *Journal of Materials Chemistry* 21 (21), 7736-7741.
- Chen, J. (2016) The Cell-Cycle Arrest and Apoptotic Functions of p53 in Tumor Initiation and Progression. *Cold Spring Harbor perspectives in medicine* 6 (3), a026104.
- Chovancova, P., Merk, V., Marx, A., Leist, M. and Kranaster, R. (2017) Reverse-transcription quantitative PCR directly from cells without RNA extraction and without isothermal reverse-transcription: a 'zero-step' RT-qPCR protocol. *Biology Methods and Protocols* 2 (1), 1-6.
- Cikos, S., Bukovská, A. and Koppel, J. (2007) Relative quantification of mRNA: comparison of methods currently used for real-time PCR data analysis. *BMC molecular biology* 8 (1), 113-113.
- CNX, O. (2019) *The Cell Cycle*. https://cnx.org/contents/GFy_h8cu@9.87:1tJ55Ot6@7/The-Cell-Cycle Accessed 20 Mar 2019.
- Collins, A. (2004) The Come Assay for DNA damage and repair: principles, applications, and limitations. *Molecular Biotechnology* 6, 249-61.
- Cooper, G. M. (2000) The Eukaryotic Cell Cycle. *The Cell: A Molecular Approach. 2nd edition*. Sunderland (MA): Sinauer Associates, Inc.
- Çelik, T. I. A. k. (2018) *Introductory Chapter: Cytotoxicity*. IntechOpen Limited.

- Dahl, R. (2006) Systemic side effects of inhaled corticosteroids in patients with asthma. *Respiratory Medicine* 100 (8), 1307-1317.
- Dai, J., Yang, P., Cox, A. and Jiang, G. (2017) Lung cancer and chronic obstructive pulmonary disease: From a clinical perspective. *Oncotarget* 8 (11), 18513.
- Daignan-Fornier, B. and Sagot, I. (2011) Proliferation/Quiescence: When to start? Where to stop? What to stock? *Cell division* 6 (1), 20-20.
- Dana-Farber Cancer Institute (2018) *How is Gene Therapy Being Used to Treat Cancer?* Online: <https://blog.dana-farber.org/insight/2018/04/gene-therapy-used-treat-cancer/> Accessed 08 Mar 2019.
- Daniels, T. R., Delgado, T., Helguera, G. and Penichet, M. L. (2006) The transferrin receptor part II: Targeted delivery of therapeutic agents into cancer cells. *Clinical Immunology* 121 (2), 159-176.
- Dasari, S. and Bernard Tchounwou, P. (2014) Cisplatin in cancer therapy: Molecular mechanisms of action. *European Journal of Pharmacology* 740, 364-378.
- Dasari Shareena, T. P., McShan, D., Dasmahapatra, A. K. and Tchounwo, P. B. (2018) A Review on Graphene-Based Nanomaterials in Biomedical Applications and Risks in Environment and Health. *Nano-Micro Lett.* 10:53, 1-34.
- Dawson, K. A., Salvati, A. and Lynch, I. (2009) Protein-nanoparticle interactions What does the cell see? *Nature Nanotechnology* 4 (9), 546-547.
- De La Fuente, J. (2013) *Graphene & Graphite - How do they compare?* Online: <https://www.graphenea.com/pages/graphene-graphite#> Accessed 30 Jul 2017.
- De Zio, D., Cianfanelli, V. and Cecconi, F. (2013) New Insights into the Link Between DNA Damage and Apoptosis. *Antioxidants & Redox Signaling* 19 (6), 559-571.
- Deepthi Ch, N., Kumar, V. V. L. P., babu, R. and darshini, U. I. (2011) Role of Tumor Suppressor Protein p53 in Apoptosis and Cancer Therapy. *Journal of Cancer Science & Therapy* 3 (6).
- Denholm, R., Crellin, E., Arvind, A. and Quint, J. (2017) Asthma and lung cancer, after accounting for co-occurring respiratory diseases and allergic conditions: a systemic review protocol. *BMJ* (7).
- Dimai, H. P., Linkhart, S. G., Linkhart, T. A., Donahue, L. R., Beamer, W. G., Rosen, C. J., Farley, J. R. and Baylink, D. J. (1998) Alkaline phosphatase levels and osteoprogenitor cell numbers suggest bone formation may contribute to peak bone density differences between two inbred strains of mice. *Bone* 22 (3), 211-216.
- Dinauer, N., Balthasar, S., Weber, C., Kreuter, J., Langer, K. and von Briesen, H. (2005) Selective targeting of antibody-conjugated nanoparticles to leukemic cells and primary T-lymphocytes. *Biomaterials* 26 (29), 5898-5906.
- Ding, Z., Zhang, Z., Ma, H. and Chen, Y. (2014) In vitro hemocompatibility and toxic mechanism of graphene oxide on human peripheral blood T lymphocytes and serum albumin. *ACS applied materials & interfaces* 6 (22), 19797-19807.
- Doepker, C. L., Livingston, G. K., Schumann, B. L. and Srivastava, A. K. (1998) Structural and numerical chromosomal aberrations in a metabolically competent human lymphoblast cell line (MCL-5). *Mutagenesis* 13 (3), 275-280.
- Driessens, N., Versteyhe, S., Ghaddhab, C., Burniat, A., Deken, X. D., Sande, J. V., Dumont, J.-E., Miot, F. and Corvilain, B. (2009) Hydrogen peroxide induces DNA single- and double-strand breaks in thyroid cells and is therefore a potential mutagen for this organ. *Endocrine-Related Cancer* 16 (3), 845-856.

- Durham, A. L. and Adcock, I. M. (2015) The Relationship between COPD and lung cancer. *Lung Cancer* 90 (2), 121-7.
- Duthie, S. J., Collins, A. R., Duthie, G. G. and Dobson, V. L. (1997) Quercetin and myricetin protect against hydrogen peroxide-induced DNA damage (strand breaks and oxidised pyrimidines) in human lymphocytes. *Mutation Research/Genetic Toxicology and Environmental Mutagenesis* 393 (3), 223-231.
- El-Yamany, N. A., Mohamed, F. F., Salaheldin, T. A., Tohamy, A. A., Abd El-Mohsen, W. N. and Amin, A. S. (2017) Graphene oxide nanosheets induced genotoxicity and pulmonary injury in mice. *Experimental and Toxicologic Pathology* 69 (6), 383-392.
- El-Zein, R. A., Fenech, M., Lopez, M. S., Spitz, M. R. and Etzel, C. J. (2008) Cytokinesis-Blocked Micronucleus Cytome Assay Biomarkers Identify Lung Cancer Cases Amongst Smokers. *Cancer Epidemiol Biomarkers Prev.* 17 (5), 1111-1119.
- Ensembl (2019) Gene: *CDKN1A ENSG00000124762*. Jan 2019.
https://www.ensembl.org/Homo_sapiens/Gene/Summary?db=core
- Fahmy, H. (2014) Effect of Low Radiation Dose on Cisplatin Induced Hepato- Testicular Damage in Male Rats. *British Journal of Pharmaceutical Research* 4 (9), 1053-1066.
- Farazi, R., Vaezi, M. R., Molaei, M. J., Saeidifar, M. and Behnam-Ghader, A. A. (2018) Effect of pH and temperature on doxorubicin hydrochloride release from magnetite/graphene oxide nanocomposites. *Materials Today: Proceedings* 5 (7), 15726-15732.
- Fenech and Michael (2007) Cytokinesis-block Micronucleus Assay. *Nature Protocols* 2 (5), 1084-1104.
- Fenech, M. (2002) Chromosomal biomarkers of genomic instability relevant to cancer. *Drug Discovery Today* 7 (Generic), 1128-1137.
- Fenech, M. (2007) Cytokinesis-block micronucleus cytome assay. *Natural Protoc* (2), 1084-1104.
- Fenech, M., Bonassi, S., Turner, J., Lando, C., Ceppi, M., Chang, W. P., Holland, N., Kirsch-Volders, M., Zeiger, E., Bigatti, M. P., Bolognesi, C., Cao, J., De Luca, G., Di Giorgio, M., Ferguson, L. R., Fucic, A., Lima, O. G., Hadjidekova, V. V., Hrelia, P., Jaworska, A., Joksic, G., Krishnaja, A. P., Lee, T.-K., Martelli, A., McKay, M. J., Migliore, L., Mirkova, E., Müller, W.-U., Odagiri, Y., Orsiere, T., Scarfi, M. R., Silva, M. J., Sofuni, T., Suralles, J., Trenta, G., Vorobtsova, I., Vral, A. and Zijno, A. (2003a) Intra- and inter-laboratory variation in the scoring of micronuclei and nucleoplasmic bridges in binucleated human lymphocytes: Results of an international slide-scoring exercise by the HUMN project. *Mut.Res.-Genetic Toxicology and Environmental Mutagenesis* 534 (1), 45-64.
- Fenech, M., Chang, W. P., Kirsch-Volders, M., Holland, N., Bonassi, S. and Zeiger, E. (2003b) HUMN project: detailed description of the scoring criteria for the cytokinesis-block micronucleus assay using isolated human lymphocyte cultures. *Mut.Res.-Genetic Toxicology and Environmental Mutagenesis* 534 (1), 65-75.
- Fenech, M. and Morley, A. A. (1985) Measurement of micronuclei in lymphocytes. *Mutation research* 147 (1-2), 29.
- Feng, L., Zhang, S. and Liu, Z. (2011) Graphene based gene transfection. *Nanoscale* 3 (3), 1252-1257.

- Filipe, V., Hawe, A. and Jiskoot, W. (2010) Critical Evaluation of Nanoparticle Tracking Analysis (NTA) by NanoSight for the Measurement of Nanoparticles and Protein Aggregates. *Pharmaceutical Research* 27 (5), 796-810.
- Fisher, S., Al-Fayea, T. M., Winget, M., Gao, H. and Butts, C. (2012) Uptake and tolerance of chemotherapy in elderly patients with small cell lung cancer and impact on survival. *Journal of cancer epidemiology* 2012, 708936-9.
- Foldvari, M., Chen, D. W., Nafissi, N., Calderon, D., Narsineni, L. and Rafiee, A. (2016) Non-viral gene therapy: Gains and challenges of non-invasive administration methods. *Journal of Controlled Release* 240, 165-190.
- Frenzilli, G., Bosco, E. and Barale, R. (2000) Validation of single cell gel assay in human leukocytes with 18 reference compounds. *Mutation Research / Genetic Toxicology and Environmental Mutagenesis* 468 (2), 93-108.
- Fu, P. P., Xia, Q., Hwang, H.-M., Ray, P. C. and Yu, H. (2014) Mechanisms of nanotoxicity: generation of reactive oxygen species. *Journal of food and drug analysis* 22 (1), 64-75.
- Fujita, K., Fukuda, M., Endoh, S., Maru, J., Kato, H., Nakamura, A., Shinohara, N., Uchino, K. and Honda, K. (2015) Size effects of single-walled carbon nanotubes on in vivo and in vitro pulmonary toxicity. *Inhalation Toxicology* 27 (4), 207-223.
- Gautschi, O., Frey, S. and Zellweger, R. (2007) Bone Morphogenetic Proteins in Clinical Applications. *ANZ Journal of Surgery* 77 (8), 626-631.
- Ge, C., Du, J., Zhao, L., Wang, L., Liu, Y., Li, D., Yang, Y., Zhou, R., Zhao, Y., Chai, Z. and Chen, C. (2011) Binding of blood proteins to carbon nanotubes reduces cytotoxicity. *Proceedings of the National Academy of Sciences of the United States of America* 108 (41), 16968-16973.
- Gies, V. and Zou, S. (2018) Systematic toxicity investigation of graphene oxide: evaluation of assay selection, cell type, exposure period and flake size. *Toxicology research* 7 (1), 93.
- Global Initiative For Asthma (2014) *Diagnosis of Diseases of Chronic Airflow Limitation: Asthma, COPD and Asthma-COPD Overlap Syndrome (ACOS)*. Online: <http://www.everyday-breathing.com/media/15569/asthmacopdoverlap.pdf> Accessed 30 July.
- Golbamaki, N., Rasulev, B., Cassano, A., Marchese Robinson, R. L., Benfenati, E., Leszczynski, J. and Cronin, M. T. D. (2015) Genotoxicity of metal oxide nanomaterials: review of recent data and discussion of possible mechanisms. *Nanoscale* 7 (6), 2154-2198.
- Grant, R. (2014) *File:MTT reaction.png* 15 Sep 2014. Online: Wikimedia Commons. https://commons.wikimedia.org/wiki/File:MTT_reaction.png Accessed 18 Mar 2019.
- Gunasekarana, V., Raj, G. V. and Chand, P. (2015) A Comprehensive Review on Clinical Applications of Comet Assay. *Journal of Clinical and Diagnostic Research* 9 (3), GE01-GE05.
- Guo, L., Von Dem Bussche, A., Buechner, M., Yan, A., Kane, A. B. and Hurt, R. H. (2008) Adsorption of essential micronutrients by carbon nanotubes and the implications for nanotoxicity testing. *Small (Weinheim an der Bergstrasse, Germany)* 4 (6), 721-727.
- Guo, X. and Mei, N. (2014) Assessment of the toxic potential of graphene family nanomaterials. *Journal of food and drug analysis* 22 (1), 105-115.

- Han, S. G., Kim, J. K., Shin, J. H., Hwang, J. H., Lee, J. S., Kim, T.-G., Lee, J. H., Lee, G. H., Kim, K. S., Lee, H. S., Song, N. W., Ahn, K. and Yu, I. J. (2015) Pulmonary Responses of Sprague-Dawley Rats in Single Inhalation Exposure to Graphene Oxide Nanomaterials. *BioMed research international* 2015, 376756-9.
- Handy, R. D. and Shaw, B. J. (2007) Toxic effects of nanoparticles and nanomaterials: Implications for public health, risk assessment and the public perception of nanotechnology. *Health, Risk & Society* 9 (2), 125-144.
- Hansen, J. and Bross, P. (2010) A cellular viability assay to monitor drug toxicity. *Methods Mol Biol.* 648, 303-11.
- Hatto, P. (2011) ISO consensus definitions relevant to nanomaterials and nanotechnologies. http://ec.europa.eu/health/sites/health/files/nanotechnology/docs/ev_20110329_co04_en.pdf Accessed 25 Mar 2019
- Haubruck, P., Kammerer, A., Korff, S., Apitz, P., Xiao, K., Büchler, A., Biglari, B., Zimmermann, G., Daniel, V., Schmidmaier, G. and Moghaddam, A. (2016) The treatment of nonunions with application of BMP-7 increases the expression pattern for angiogenic and inflammable cytokines: A matched pair analysis. *Journal of Inflammation Research* 9, 155-165.
- He, Y.-C., Chen, J.-W., Cao, J., Pan, D.-Y. and Qiao, J.-G. (2003) Toxicities and therapeutic effect of 5-fluorouracil controlled release implant on tumor-bearing rats. *World J Gastroenterol.* 9 (8), 1795-1798.
- Henderson, L., Wolfreys, A., Fedyk, J., Bourner, C. and Windebank, S. (1998) The ability of the Comet assay to discriminate between genotoxins and cytotoxins. *Mutagenesis* 13 (1), 89-94.
- Heng, Y.-W. and Koh, C.-G. (2010) Actin cytoskeleton dynamics and the cell division cycle. *International Journal of Biochemistry and Cell Biology* 42 (10), 1622-1633.
- Hientz, K., Mohr, A., Bhakta-Guha, D. and Efferth, T. (2017) The role of p53 in cancer drug resistance and targeted chemotherapy. *Oncotarget* 8 (5), 8921.
- Ho-Pun-Cheung, A., Bascoul-Molleivi, C., Assenat, E., Boissière-Michot, F., Bibeau, F., Cellier, D., Ychou, M. and Lopez-Crapez, E. (2009) Reverse transcription-quantitative polymerase chain reaction: description of a RIN-based algorithm for accurate data normalization. *BMC molecular biology* 10 (1), 31-31.
- Hondow, N., Brydson, R., Wang, P., Holton, M. D., Brown, M. R., Rees, P., Summers, H. D. and Brown, A. (2012) Quantitative characterization of nanoparticle agglomeration within biological media. *Journal of Nanoparticle Research* 14 (7), 1-15.
- Hu, W., Peng, C., Luo, W., Lv, M., Li, X., Li, D., Huang, Q. and Fan, C. (2010) Graphene-Based Antibacterial Paper. *ACS Nano* 4 (7), 4317-4323.
- Huang, J., Zong, C., Shen, H., Liu, M., Chen, B., Ren, B. and Zhang, Z. (2012) Mechanism of cellular uptake of graphene oxide studied by surface-enhanced Raman spectroscopy. *Small (Weinheim an der Bergstrasse, Germany)* 8 (16), 2577-2584.
- Hummers, W. S. and Offeman, R. E. (1958) Preparation of Graphitic Oxide. *Journal of the American Chemical Society* 80 (6), 1339-1339.
- IARC (2017) *Some Nanomaterials and some Fibres/IARC Monographs on the evaluation of carcinogenic risks to humans*. Vol. III. Lyon, France: IARC.
- İpek, E., Ermiş, E., Uysal, H., Kızılet, H., Demirelli, S., Yıldırım, E., Ünver, S., Demir, B. and Kızılet, N. (2017) The relationship of micronucleus frequency and nuclear division

index with coronary artery disease SYNTAX and Gensini scores. *Anatol J Cardiol* 17 (6), 483-489.

- Ionescu, M. E., Ciocirlan, M., Becheanu, G., Nicolaie, T., Ditescu, C., Teiusanu, A. G., Gologan, S. I., Arbanas, T. and Diculescu, M. M. (2011) Nuclear Division Index may Predict Neoplastic Colorectal Lesions. *Maedica (Buchar)* 6 (3), 173-178.
- Jaurand, M.-C. F., Renier, A. and Daubriac, J. (2009) Mesothelioma: Do asbestos and carbon nanotubes pose the same health risk? *Part Fibre Toxicol* 6 (1), 16-16.
- Jaworski, S., Sawosz, E., Grodzik, M., Winnicka, A., Prasek, M., Wierzbicki, M. and Chwalibog, A. (2013) In vitro evaluation of the effects of graphene platelets on glioblastoma multiforme cells. *International journal of nanomedicine* 8, 413.
- Jedrzejczak-Silicka, M. and Mijowska, E. (2018) *General Cytotoxicity and Its Application in Nanomaterial Analysis*.
- Jeevanandam, J., Barhoum, A., Chan, Y. S., Dufresne, A. and Danquah, M. K. (2018) Review on nanoparticles and nanostructured materials: history, source, toxicity and regulations. *Beilstein J Nanotechnol* 9, 1050-1074.
- Ježek, J., Cooper, K. F. and Strich, R. (2018) Reactive Oxygen Species and Mitochondrial Dynamics: The Yin and Yang of Mitochondrial Dysfunction and Cancer Progression. *Antioxidants (Basel, Switzerland)* 7 (1), 13.
- Jiao, G., He, X., Li, X., Qiu, J., Xu, H., Zhang, N. and Liu, S. (2015) Limitations of MTT and CCK-8 assay for evaluation of graphene cytotoxicity. *RSC Advances* 5 (66), 53240-53244.
- Kamm, Y. J. L., Peters, G. J., Hull, W. E., Punt, C. J. A. and Heerschap, A. (2003) Correlation between 5-fluorouracil metabolism and treatment response in two variants of C26 murine colon carcinoma. *British journal of cancer* 89 (4), 754-762.
- Karbaschi, M. and Cooke, M. S. (2014) Novel method for the high-throughput processing of slides for the comet assay. *Scientific reports* 4, 7200.
- Kelvinsong (2012) *Animal cell cycle*.
https://commons.wikimedia.org/wiki/File:Animal_cell_cycle-en.svg Accessed 20 Mar 2019.
- Kenyon, N. J., Bratt, J. M., Lee, J., Luo, J., Franzi, L. M., Zeki, A. A. and Lam, K. S. (2013) Self-assembling nanoparticles containing dexamethasone as a novel therapy in allergic airways inflammation. *PLoS One* 8 (10), e77730.
- Kiew, S. F., Kiew, L. V., Lee, H. B., Imae, T. and Chung, L. Y. (2016) Assessing biocompatibility of graphene oxide-based nanocarriers: A review. *Journal of Controlled Release* 226, 217-228.
- Kim, E. M., Jung, C.-H., Kim, J., Hwang, S.-G., Park, J. K. and Um, H.-D. (2017) The p53/p21 Complex Regulates Cancer Cell Invasion and Apoptosis by Targeting Bcl-2 Family Proteins. *Cancer research* 77 (11), 3092-3100.
- Kim, J., Cote, L. J. and Huang, J. (2012a) Two Dimensional Soft material: new faces of Graphene Oxide. *Accounts of chemical research* 45 (8), 1356-1364.
- Kim, J. S., Sung, J. H., Song, K. S., Lee, J. H., Kim, S. M., Lee, G. H., Ahn, K. H., Lee, J. S., Shin, J. H., Park, J. D. and Yu, I. J. (2012b) Persistent DNA damage measured by comet assay of sprague dawley rat lung cells after five days of inhalation exposure and 1 month post-exposure to dispersed multi-wall carbon nanotubes (MWCNTS) generated by new MWCNT aerosol generation system. *Toxicological Sciences* 128 (2), 439-448.

- Kim, Y. H., Jo, M. S., Kim, J. K., Shin, J. H., Baek, J. E., Park, H. S., An, H. J., Lee, J. S., Kim, B. W., Kim, H. P., Ahn, K. H., Jeon, K., Oh, S. M., Lee, J. H., Workman, T., Faustman, E. M. and show, I. J. Y. (2018) Short-term inhalation study of graphene oxide nanoplates. *Nanotoxicology* 12 (3), 224-238.
- Kirsch-Volders, M. and Fenech, M. (2001) Inclusion of micronuclei in non-divided mononuclear lymphocytes and necrosis/apoptosis may provide a more comprehensive cytokinesis block micronucleus assay for biomonitoring purposes. *Mutagenesis* 16 (1), 51-58.
- Konios, D., Stylianakis, M. M., Stratakis, E. and Kymakis, E. (2014) Dispersion behaviour of graphene oxide and reduced graphene oxide. *Journal of Colloid and Interface Science* 430, 108-112.
- La, W.-G., Jin, M., Park, S., Yoon, H.-H., Jeong, G.-J., Bhang, S. H., Park, H., Char, K. and Kim, B.-S. (2014) Delivery of bone morphogenetic protein-2 and substance P using graphene oxide for bone regeneration. *International Journal of Nanomedicine* 9 (1), 107-116.
- Landsiedel, R., Kapp, M. D., Schulz, M., Wiench, K. and Oesch, F. (2009) Genotoxicity investigations on nanomaterials: Methods, preparation and characterization of test material, potential artifacts and limitations—Many questions, some answers. *Mutation Research-Reviews in Mutation Research* 681 (2), 241-258.
- Le, H.-V., Minn, A. J. and Massagué, J. (2005) Cyclin-dependent Kinase Inhibitors Uncouple Cell Cycle Progression from Mitochondrial Apoptotic Functions in DNA-damaged Cancer Cells. *Journal of Biological Chemistry* 280 (36), 32018-32025.
- Lefebvre, P., Duh, M. S., Lafeuille, M.-H., Gozalo, L., Desai, U., Robitaille, M.-N., Albers, F., Yancey, S., Ortega, H., Forshag, M., Lin, X. and Dalal, A. A. (2015) Acute and chronic systemic corticosteroid-related complications in patients with severe asthma. *The Journal of allergy and clinical immunology* 136 (6), 1488-1495.
- Lei, M., Zhang, L., Lei, J., Zong, L., Li, J., Wu, Z. and Wang, Z. (2015) Overview of emerging contaminants and associated human health effects. *BioMed Research International* 2015, 1-12.
- Li, B., Yang, J., Huang, Q., Zhang, Y., Peng, C., Zhang, Y., He, Y., Shi, J., Li, W., Hu, J. and Fan, C. (2013a) Biodistribution and pulmonary toxicity of intratracheally instilled graphene oxide in mice. *NPG Asia Materials* 5 (4), e44.
- Li, C., Wang, X., Chen, F., Zhang, C., Zhi, X., Wang, K. and Cui, D. (2013b) The antifungal activity of graphene oxide–silver nanocomposites. *Biomaterials* 34 (15), 3882-3890.
- Li, L., Deng, R., Su, Y. and Yang, C. (2017) Dual-targeting nanoparticles with excellent gene transfection efficiency for gene therapy of peritoneal metastasis of colorectal cancer. *Oncotarget* 8 (52), 89837-89847.
- Li, X., Fang, P., Mai, J., Choi, E. T., Wang, H. and Yang, X.-f. (2013c) Targeting mitochondrial reactive oxygen species as novel therapy for inflammatory diseases and cancers. *Journa of Hematology & Oncology* 6 (19).
- Li, Y., Wu, Q., Zhao, Y., Bai, Y., Chen, P., Xia, T. and Wang, D. (2014) Response of MicroRNAs to In Vitro Treatment with Graphene Oxide. *ACS Nano* 8 (3), 2100-2110.
- Li, Y.-F. and Chen, C. (2011) Fate and toxicity of metallic and metal-containing nanoparticles for biomedical applications. *Small* 7 (21), 2965-2980.

- Liao, C., Li, Y. and Tjong, S. C. (2018) Graphene Nanomaterials: Synthesis, Biocompatibility, and Cytotoxicity. *International journal of molecular sciences* 19 (11), 3564.
- Liao, K.-H., Lin, Y.-S., Macosko, C. W. and Haynes, C. L. (2011) Cytotoxicity of graphene oxide and graphene in human erythrocytes and skin fibroblasts. *ACS applied materials & interfaces* 3 (7), 2607-2615.
- Linares, J., Matesanz, M. C., Vila, M., Feito, M. J., Gonçalves, G., Vallet-Regí, M., Marques, P. A. A. P. and Portolés, M. T. (2014) Endocytic mechanisms of graphene oxide nanosheets in osteoblasts, hepatocytes and macrophages. *ACS applied materials & interfaces* 6 (16), 13697-13706.
- Liu, B., Salgado, S., Maheshwari, V. and Liu, J. (2016) DNA adsorbed on graphene and graphene oxide: Fundamental interactions, desorption and applications. *Current Opinion in Colloid and Interface Science* 26, 41-49.
- Liu, J., Cui, L. and Losic, D. (2013a)
Graphene and graphene oxide as new nanocarriers for drug delivery applications. *Acta biomaterialia* 9 (12), 9243-9257.
- Liu, J., Yang, L. and Hopfinger, A. J. (2009) Affinity of drugs and small biologically active molecules to carbon nanotubes: a pharmacodynamics and nanotoxicity factor? *Molecular pharmaceutics* 6 (3), 873-882.
- Liu, Y., Luo, Y., Wu, J., Wang, Y., Yang, X., Yang, R., Wang, B., Yang, J. and Zhang, N. (2013b) Graphene oxide can induce in vitro and in vivo mutagenesis. *Scientific reports* 3, 3469.
- Liu, Y., Luo, Y., Wu, J., Wang, Y., Yang, X., Yang, R., Wang, B., Yang, J. and Zhang, N. (2013c) Graphene oxide can induce in vitro and in vivo mutagenesis. *Scientific reports* 3, 3469.
- Liu, Y., Peterson, D. A., Kimura, H. and Schubert, D. (1997) Mechanism of cellular 3-(4,5-dimethylthiazol-2-yl)-2,5-diphenyltetrazolium bromide (MTT) reduction. *Journal of Neurochemistry* 69 (2), 581-593.
- Liu, Z., Robinson, J. T., Sun, X. and Dai, H. (2008) PEGylated nanographene oxide for delivery of water-insoluble cancer drugs. *Journal of the American Chemical Society* 130 (33), 10876-10877.
- Livak, K. J. and Schmittgen, T. G. (2001) Analysis of Relative Gene Expression Data Using Real-Time Quantitative PCR and the 2DeltaDeltaCT Method. *Methods* 25 (4), 402-408.
- Lodish, H., Berk, A., Zipursky, S., Lawrence, Matsudaira, P., Baltimore, D. and Darnell, J. (2000) Section 16.2: Electron Transport and Oxidative Phosphorylation. *Molecular Cell Biology. 4th edition.* New York: W. H. Freeman.
- Lu, X., Zhu, T., Chen, C. and Liu, Y. (2014) Right or left: the role of nanoparticles in pulmonary diseases. *Int J Mol Sci* 15 (10), 17577-17600.
- Lumen Learning (2017) *The Cell Cycle*. Online: Lumen Learning. <https://courses.lumenlearning.com/vccs-bio101-17fa/chapter/the-cell-cycle/> Accessed 20 Mar 2019.
- Ma, N., Liu, J., He, W., Li, Z., Luan, Y., Song, Y. and Garg, S. (2017) Folic acid-grafted bovine serum albumin decorated graphene oxide: An efficient drug carrier for targeted cancer therapy. *Journal of Colloid and Interface Science* 490, 598-607.

- Ma, N., Zhang, P., Zhang, B., Liu, J., Li, Z. and Luan, Y. (2015) Green fabricated reduced graphene oxide: evaluation of its application as nano-carrier for pH-sensitive drug delivery. *International Journal of Pharmaceutics* 496 (2), 984-992.
- MacMillan Cancer Support (2012) *Chemotherapy for non-small cell lung cancer*. <https://www.macmillan.org.uk/cancerinformation/cancertypes/lung/treating-non-small-cell-lung-cancer/chemotherapy.aspx> Accessed 09 Mar 2019.
- MacMillan Cancer Support (2018) *Cisplatin*. Online: <https://www.macmillan.org.uk/information-and-support/treating/chemotherapy/drugs-and-combination-regimens/individual-drugs/cisplatin.html> Accessed 09 Mar 2019.
- MacNee, W. (2005) Pathogenesis of chronic obstructive pulmonary disease. *Proceedings of the American Thoracic Society* 2 (4), 258-266.
- Mahmood, T. and Yang, P.-C. (2012) Western blot: technique, theory, and trouble shooting. *North American journal of medical sciences* 4 (9), 429-34.
- Malvern Panalytical Ltd (2018) *Zetasizer μ V*. Online: Malvern Panalytical Ltd. <https://www.malvernpanalytical.com/en/products/product-range/zetasizer-range/zetasizer-microv> Accessed 19/09/2018.
- Medscape (2019) *Cisplatin (Rx): Dosage Forms & Strengths*. Online. <https://reference.medscape.com/drug/platinol-aq-cisplatin-342108> Accessed 09 Mar 2019.
- MetaSystems (2019) *Toxicology and Radiation Biology*. <https://metasystems-international.com/en/applications/tox/> Accessed 21 Mar 2019.
- Mintzer, M. A. and Simanek, E. E. (2009) Nonviral vectors for gene delivery. *Chemical Reviews* 109 (2), 259-302.
- Mittal, S., Sharma, P. K., Tiwari, R., Rayavarapu, R. G., Shankar, J., Chauhan, L. K. S. and Pandey, A. K. (2017) Impaired lysosomal activity mediated autophagic flux disruption by graphite carbon nanofibers induce apoptosis in human lung epithelial cells through oxidative stress and energetic impairment. *Particle and fibre toxicology* 14 (1), 15-25.
- Mody, V. V., Siwale, R., Singh, A. and Mody, H. R. (2010) Introduction to metallic nanoparticles. *Journal of pharmacy & bioallied sciences* 2 (4), 282-289.
- Mohamadi, S. and Hamidi, M. (2017) The new nanocarriers based on graphene and graphene oxide for drug delivery applications. *Nanostructures for Drug Delivery: Micro and Nano Technologies*. Online: 107-147.
- Monteiro-Riviere, N. A. and Inman, A. O. (2006) Challenges for assessing carbon nanomaterial toxicity to the skin. *Carbon* 44 (6), 1070-1078.
- Mossman, T. (1983) Rapid colorimetric assay for cellular growth and survival: Application to proliferation and cytotoxicity assays. *Journal of Immunological Methods* 65 (1-2), 55-63.
- Mountain, R. D. (1992) Laser light scattering: Basic principles and practice. *Journal of Colloid and Interface Science* 152 (2), 593.
- Muller, Patricia A. J. and Vousden, Karen H. (2014) Mutant p53 in Cancer: New Functions and Therapeutic Opportunities. *Cancer Cell* 25 (3), 304-317.
- Muralidharan, P., Malapit, M., Mallory, E., Hayes, D. and Mansour, H. M. (2015) Inhalable nanoparticulate powders for respiratory delivery. *Nanomedicine: Nanotechnology, Biology, and Medicine* 11 (5), 1189-1199.

- Nabi, A., Khalili, M. A., Halvaei, I. and Roodbari, F. (2014) Prolonged incubation of processed human spermatozoa will increase DNA fragmentation. *Andrologia* 46 (4), 374-379.
- Naldini, L., Blömer, U., Gallay, P., Ory, D., Mulligan, R., Gage, F. H., Verma, I. M. and Trono, D. (1996) In Vivo Gene Delivery and Stable Transduction of Nondividing Cells by a Lentiviral Vector. *Science* 272 (5259), 263-267.
- Nandhakumar, S., Parasuraman, S., Shanmugam, M. M., Rao, K. R., Chand, P. and Bhat, B. V. (2011) Evaluation of DNA damage using single-cell gel electrophoresis (Comet Assay). *Journal of Pharmacology & pharmacotherapeutics* 2 (2), 107-111.
- Narayanan, K. B., Ali, M., Barclay, B. J., Cheng, Q. S., D'Abbronzo, L., Dornetshuber-Fleiss, R., Ghosh, P. M., Gonzalez Guzman, M. J., Lee, T.-J., Leung, P. S., Li, L., Luanpitpong, S., Ratovitski, E., Rojanasakul, Y., Romano, M. F., Romano, S., Sinha, R. K., Yedjou, C., Al-Mulla, F., Al-Temaimi, R., Amedei, A., Brown, D. G., Ryan, E. P., Colacci, A., Hamid, R. A., Mondello, C., Raju, J., Salem, H. K., Woodrick, J., Scovassi, A. I., Singh, N., Vaccari, M., Roy, R., Forte, S., Memeo, L., Kim, S. Y., Bisson, W. H., Lowe, L. and Park, H. H. (2015) Disruptive environmental chemicals and cellular mechanisms that confer resistance to cell death. *Carcinogenesis* 36 Suppl 1 (Suppl 1), S89-S110.
- Nasongkla, N., Shuai, X., Ai, H., Weinberg, B. D., Pink, J., Boothman, D. A. and Gao, J. (2004) cRGD-functionalized polymer micelles for targeted doxorubicin delivery. *Angewandte Chemie - International Edition* 43 (46), 6323-6327.
- Netdoctor (2012) *Cisplatin: What is it used for?*
<https://www.netdoctor.co.uk/medicines/cancer-drugs/a6411/cisplatin/>
 Accessed 09 Mar 2019.
- Ng, K. W., Khoo, S. P. K., Heng, B. C., Setyawati, M. I., Tan, E. C., Zhao, X., Xiong, S., Fang, W., Leong, D. T. and Loo, J. S. C. (2011) The role of the tumor suppressor p53 pathway in the cellular DNA damage response to zinc oxide nanoparticles. *Biomaterials* 32 (32), 8218-8225.
- NHS Choices (2019) *Mesothelioma*. 8 Jan 2019. Website: NHS England.
<http://www.nhs.uk/conditions/mesothelioma/Pages/Definition.aspx> Accessed 26 Mar 2019.
- Nichols, J. W. and Bae, Y. H. (2012) Odyssey of a cancer nanoparticle: From injection site to site of action. *Nano Today* 7 (6), 606-618.
- Niles, A. L., Moravec, R. A. and Riss, T. L. (2009) In vitro viability and cytotoxicity testing and same-well multi-parametric combinations for high throughput screening. *Current Chemical Genomics* 3 (1), 33-41.
- Nita, M. and Grzybowski, A. (2016) The Role of the Reactive Oxygen Species and Oxidative Stress in the Pathomechanism of the Age-Related Ocular Diseases and Other Pathologies of the Anterior and Posterior Eye Segments in Adults. *Oxidative medicine and cellular longevity* 2016, 3164734-23.
- Nohmi, T. (2018) Thresholds of Genotoxic and Non-Genotoxic Carcinogens. *Toxicological research* 34 (4), 281-290.
- Oberdörster, G., Ferin, J. and Lehnert, B. E. (1994) Correlation between Particle Size, In Vivo Particle Persistence, and Lung Injury. *Environmental Health Perspectives* 102 (5), 173-179.

- Olive, P. L., Banath, J. P. and Durand, R. E. (1990) Detection of etoposide resistance by measuring DNA damage in individual Chinese hamster cells. *J Natl Cancer Inst* 82 (9), 779-83.
- Olive, P. L. and Durand, R. E. (2005) Heterogeneity in DNA damage using the comet assay. *Cytometry Part A* 66A (1), 1-8.
- Omlor, A. J., Nguyen, J., Bals, R. and Dinh, Q. T. (2015) Nanotechnology in respiratory medicine. *Respiratory Research* 16 (1), 64.
- Osman, I., Baumgartner, A., Anderson, D., Cemeli-Carratala, E. and Fletcher, J. N. (2010) Genotoxicity and cytotoxicity of zinc oxide and titanium dioxide in HEp-2 cells.
- Ou, L., Song, B., Liang, H., Liu, J., Feng, X., Deng, B., Sun, T. and Shao, L. (2016) Toxicity of graphene-family nanoparticles: a general review of the origins and mechanisms. *Particle and fibre toxicology* 13 (1), 57.
- Pan, Y., Sahoo, N. G. and Li, L. (2012) The application of graphene oxide in drug delivery. *Expert Opinion on Drug Delivery* 9 (11), 1365-1376.
- Pantel, K. (2016) Blood-Based Analysis of Circulating Cell-Free DNA and Tumor Cells for Early Cancer Detection. *PLoS Medicine* 13 (12).
- Parveen, S., Misra, R. and Sahoo, S. (2012) Nanoparticles: a boon to drug delivery, therapeutics, diagnostics and imaging. *Nanomedicine* 8 (2), 147-166.
- Patino-Garcia, B., Hoegel, J., Varga, D., Hoehne, M., Michel, I., Jainta, S., Kreienberg, R., Maier, C. and Vogel, W. (2006) Scoring variability of micronuclei in binucleated human lymphocytes in a case-control study. *Mutagenesis* 21 (3), 191-197.
- Powers, K. W., Brown, S. C., Krishna, V. B., Wasdo, S. C., Moudgil, B. M. and Roberts, S. M. (2006) Research strategies for safety evaluation of nanomaterials. Part VI. Characterization of nanoscale particles for toxicological evaluation. *Toxicological sciences : an official journal of the Society of Toxicology* 90 (2), 296-303.
- Priyadarsini, S., Mohanty, S., Mukherjee, S., Basu, S. and Mishra, M. (2018) Graphene and graphene oxide as nanomaterials for medicine and biology application. *Journal of Nanostructure in Chemistry* 8 (2), 123-137.
- Pu, X., Wang, Z. and Klaunig, J. E. (2015) Alkaline Comet Assay for Assessing DNA Damage in Individual Cells. *Curr Protoc Toxicol* 65, 3.12.1.
- PubChem (2018) *Graphene oxide, 15-20 sheets, 4-10% edge-oxidized, 1 mg/mL, dispersion in H2O*. 14 Mar 2019. Online: National Centre for Biotech Information. <https://pubchem.ncbi.nlm.nih.gov/substance/329768441> Accessed 18 Mar 2019.
- Pucci, B., Kasten, M. and Giordano, A. (2000) Cell Cycle and Apoptosis. *Neoplasia* 2 (4), 291-299.
- Qu, Y.-L., Liu, J., Zhang, L.-X., Wu, C.-M., Chu, A.-J., Wen, B.-L., Ma, C., Yan, X.-Y., Zhang, X., Wang, D.-M., Lv, X. and Hou, S.-J. (2017) Asthma and the risk of lung cancer: a meta-analysis. *Oncotarget* 8 (7), 11614.
- Radack, K. L., Pinney, S. M. and Livingston, G. K. (1995) Sources of variability in the human lymphocyte micronucleus assay: a population-based study. *Environ Mol Mutagen* 26 (1), 26-36.
- Radiant Insights (2014) *Healthcare Nanotechnology (Nanomedicine) Market Analysis By Application (Drug Delivery System, Molecular Diagnostics, Clinical Oncology, Clinical Neurology, Clinical cardiology, Anti-inflammatory, Anti-infective) And Segment Forecasts To 2020*. Online: Grand View Research. <http://www.radiantinsights.com/research/healthcare-nanotechnology->

[nanomedicine-market-analysis-by-application-drug-delivery-system-molecular-diagnostics-clinical-oncology-clinical-neurology-clinical-cardiology-anti-inflammatory-anti-infective-and-segment-forecasts-to-2020/](#) Accessed 14 Apr 2017.

- Rameshwar, P. and Gascon, P. (1995) Substance P (SP) mediates production of stem cell factor and interleukin- 1 in bone marrow stroma: Potential autoregulatory role for these cytokines in SP receptor expression and induction. *Blood* 86 (2), 482-490.
- Rebuttni, V., Fazio, E., Santangelo, S., Neri, F., Caputo, G., Martin, C., Brousse, T., Favier, F. and Pinna, N. (2015) Chemical Modification of Graphene Oxide through Diazonium Chemistry and Its Influence on the Structure–Property Relationships of Graphene Oxide–Iron Oxide Nanocomposites. *Chemistry – A European Journal* 21 (35), 12465-12474.
- Rim, K.-T., Song, S.-W. and Kim, H.-Y. (2013) Oxidative DNA Damage from Nanoparticle Exposure and Its Application to Workers' Health: A Literature Review. *Safety and Health at Work* 4 (4), 177-186.
- Roa, W. H., Azarmi, S., Al-Hallak, M. H. D. K., Finlay, W. H., Magliocco, A. M. and Löbenberg, R. (2011) Inhalable nanoparticles, a non-invasive approach to treat lung cancer in a mouse model. *Journal of Controlled Release* 150 (1), 49-55.
- Roggen, E. L. (2011) In vitro Toxicity Testing in the Twenty-First Century. *Frontiers in pharmacology* 2, 3.
- Rosenberger, A., Bickeböller, H., McCormack, V., Brenner, D. R., Duell, E. J., Tjønneland, A., Friis, S., Muscat, J. E., Yang, P., Wichmann, H. E., Heinrich, J., Szeszenia-Dabrowska, N., Lissowska, J., Zaridze, D., Rudnai, P., Fabianova, E., Janout, V., Bencko, V., Brennan, P., Mates, D., Schwartz, A. G., Cote, M. L., Zhang, Z.-F., Morgenstern, H., Oh, S. S., Field, J. K., Raji, O., McLaughlin, J. R., Wiencke, J., LeMarchand, L., Neri, M., Bonassi, S., Andrew, A. S., Lan, Q., Hu, W., Orlov, I., Park, B. J., Boffetta, P. and Hung, R. J. (2012) Asthma and lung cancer risk: A systematic investigation by the international lung cancer consortium. *Carcinogenesis* 33 (3), 587-597.
- Roufayel, R. (2016) Regulation of stressed-induced cell death by the Bcl-2 family of apoptotic proteins. *Molecular membrane biology* 33 (6-8), 89-99.
- Sager, T. M., Kommineni, C. and Castranova, V. (2008) Pulmonary response to intratracheal instillation of ultrafine versus fine titanium dioxide: Role of particle surface area. *Particle and Fibre Toxicology* 5 (1), 17-17.
- Sanchez, V. C., Jachak, A., Hurt, R. H. and Kane, A. B. (2012) Biological Interactions of Graphene-Family Nanomaterials: An Interdisciplinary Review. *Chemical Research in Toxicology* 25 (1), 15-34.
- Sanchez, V. C., Pietruska, J. R., Miselis, N. R., Hurt, R. H. and Kane, A. B. (2009) Biopersistence and potential adverse health impacts of fibrous nanomaterials: what have we learned from asbestos? *Wiley Interdisciplinary Reviews: Nanomedicine and Nanobiotechnology* 1 (5), 511-529.
- Sargent, J. M. (2003) The use of the MTT assay to study drug resistance in fresh tumour samples. *Recent results in cancer research. Fortschritte der Krebsforschung. Progres dans les recherches sur le cancer* 161, 13.
- Sasidharan, A., Panchakarla, L. S., Sadanandan, A. R., Ashokan, A., Chandran, P., Girish, C. M., Menon, D., Nair, S. V., Rao, C. N. R. and Koyakutty, M. (2012)

- Hemocompatibility and macrophage response of pristine and functionalized graphene. *Small (Weinheim an der Bergstrasse, Germany)* 8 (8), 1251-1263.
- Schmid, W. (1975) The micronucleus test. *Mutation Research/Environmental Mutagenesis and Related Subjects* 31 (1), 9-15.
- Schwarzbacherova, V., Šiviková, K., Holečková, B. and Dianovský, J. (2016) Micronucleus assay in genotoxicity assessment. *Acta fytotechnica et zootechnica* 19 (Special issue), 93-95.
- Seshadri, D. R. and Ramamurthi, A. (2018) Nanotherapeutics to Modulate the Compromised Micro-Environment for Lung Cancers and Chronic Obstructive Pulmonary Disease. *Frontiers in pharmacology* 9, 759.
- Shimizu, K., Nakaya, N., Saito-Nakaya, K., Akechi, T. O. A., Fujisawa, D., Sone, T., Yoshiuchi, K., Goto, K., Tsugane, M. I. S. and Uchitomi, Y. (2015) Personality traits and coping styles explain anxiety in lung cancer patients to a greater extent than other factors. *Japanese Journal of Clinical Oncology* 45 (5), 456-463.
- Shinryuu (2010) *MTT Plate*. Online: Wikipedia Commons.
https://commons.wikimedia.org/wiki/File:MTT_Plate.jpg Accessed 18 Mar 2019.
- Siganaki, M., Koutsopoulos, A. V., Neofytou, E., Vlachaki, E., Psarrou, M., Soultziz, N., Pentilas, N., Schiza, S., Siafakas, N. M. and Tzortzaki, E. G. (2010) Deregulation of apoptosis mediators' p53 and bcl2 in lung tissue of COPD patients. *Respiratory research* 11 (1), 46-46.
- Sigma-Aldrich (2013) *KiCqStart™ Primers*. 2013. Online: Sigma-Aldrich.
<https://www.kicqstart-primers-sigmaaldrich.com/KiCqStartPrimers.php>
 Accessed 19 Mar 2019.
- Sigma-Aldrich (2017) *Product Information Sheet: Mytomycin C*. [Product Information Sheet] http://www.sigmaaldrich.com/content/dam/sigmaaldrich/docs/Sigma/Product_Information_Sheet/2/m0503pis.pdf Accessed 26 Mar 2019.
- Sigma-Aldrich (2018) Safety Data Sheet; Graphene Oxide, 15-20 sheets, 4-10% edge-oxidized, 1mg/mL dispersion in H₂O; Version5; Revision Date: 08/08/14; Section 11: Toxicology Information, p.4. 1-6.
<https://www.sigmaaldrich.com/MSDS/MSDS/DisplayMSDSPage.do?country=G&language=en&productNumber=794341&brand=ALDRICH&PageToGoToURL=https%3A%2F%2Fwww.sigmaaldrich.com%2Fcatalog%2Fproduct%2Faldrich%2F794341%3Flang%3Den> Accessed 28 Nov 2018
- Sigma-Aldrich USA (2018) *In Vitro Toxicology Assay Kit Neutral Red Based*. Online:
<https://www.sigmaaldrich.com/content/dam/sigmaaldrich/docs/Sigma/Bulletin/tox4bul.pdf>
- Singh, S. K., Singh, M. K., Kulkarni, P. P., Sonkar, V. K., Grácio, J. J. A. and Dash, D. (2012) Amine-Modified Graphene: Thrombo-Protective Safer Alternative to Graphene Oxide for Biomedical Applications. *ACS Nano* 6 (3), 2731-2740.
- Singh, S. K., Singh, M. K., Nayak, M. K., Kumari, S., Shrivastava, S., Grácio, J. J. A. and Dash, D. (2011) Thrombus Inducing Property of Atomically Thin Graphene Oxide Sheets. *ACS Nano* 5 (6), 4987-4996.
- Sionov, R. V., Hayon, I. L. and Haupt, Y. (2000-2013) The Regulation of p53 Growth Suppression. In: Madame Curie Bioscience Database [Internet].

- Skovmand, A., Jacobsen Lauvås, A., Christensen, P., Vogel, U., Sørig Hougaard, K. and Goericke-Pesch, S. (2018) Pulmonary exposure to carbonaceous nanomaterials and sperm quality. *Particle and fibre toxicology* 15 (1), 10.
- Smart, E., Lopes, F., Rice, S., Nagy, B., Anderson, R. A., Mitchell, R. T. and Spears, N. (2018) Chemotherapy drugs cyclophosphamide, cisplatin and doxorubicin induce germ cell loss in an in vitro model of the prepubertal testis. *Scientific reports* 8 (1), 1773-15.
- Solari, F., Domenget, C., Gire, V., Woods, C., Lazarides, E., Rousset, B. and Jurdic, P. (1995) Multinucleated cells can continuously generate mononucleated cells in the absence of mitosis: a study of cells of the avian osteoclast lineage. *Journal of Cell Science* 108, 3233-3241.
- Song, J., Wang, X. and Chang, C.-T. (2014) Preparation and Characterization of Graphene Oxide. *Journal of Nanomaterials* 2014, 1-6.
- Speit, G., Zeller, J. and Neuss, S. (2011) The in vivo or ex vivo origin of micronuclei measured in human biomonitoring studies. *Mutagenesis* 26 (1), 107-110.
- STEMCELL Technologies (2017) *Lymphoprep Density Gradient Medium for the Isolation of mononuclear cells*. 2017. Online: STEMCELL Technologies Canada Inc. https://cdn.stemcell.com/media/files/pis/29283-PIS_1_3_0.pdf?qa=2.11894386.777538854.1552913845-1383156917.1552913845
- Stephenson, A. P., Schneider, J. A., Nelson, B. C., Atha, D. H., Jain, A., Soliman, K. F. A., Aschner, M., Mazzi, E. and Renee Reams, R. (2013) Manganese-induced oxidative DNA damage in neuronal SH-SY5Y cells: Attenuation of thymine base lesions by glutathione and N-acetylcysteine. *Toxicology Letters* 218 (3), 299-307.
- Stone, V., Johnston, H. and Schins, R. (2009) Development of in vitro systems for nanotoxicology: methodological considerations. *Crit Rev Toxicol.* 39 (7), 613-26.
- Stéfani, D., Paula, A. J., Vaz, B. G., Silva, R. A., Andrade, N. F., Justo, G. Z., Ferreira, C. V., Filho, A. G. S., Eberlin, M. N. and Alves, O. L. (2011) Structural and proactive safety aspects of oxidation debris from multiwalled carbon nanotubes. *Journal of Hazardous Materials* 189 (1), 391-396.
- Sun, X., Liu, Z., Welsher, K., Robinson, J. T., Goodwin, A., Zaric, S. and Dai, H. (2008) Nano-graphene oxide for cellular imaging and drug delivery. *Nano Res.* 1 (3), 203-212.
- Sur, U. K. (2012) Graphene: A Rising Star on the Horizon of Materials Science. *International Journal of Electrochemistry* 2012, 1-12.
- Suzuki, K. and Matsubara, H. (2011) Recent advances in p53 research and cancer treatment. *Journal of biomedicine & biotechnology* 2011, 978312-7.
- Szmidt, M., Stankiewicz, A., UrbaAska, K., Jaworski, S., Kutwin, M., Wierzbicki, M., Grodzik, M., BurzyAska, B., Gora, M., Chwalibog, A. and Sawosz, E. (2019) Graphene oxide down-regulates genes of the oxidative phosphorylation complexes in a glioblastoma. *BMC Molecular Biology* 20 (1), 1-9.
- Tang, H., Zhao, Y., Yang, X., Liu, D., Shao, P., Zhu, Z., Shan, S., Cui, F. and Xing, B. (2017) New Insight into the Aggregation of Graphene Oxide Using Molecular Dynamics Simulations and Extended Derjaguin–Landau–Verwey–Overbeek Theory. *Environmental Science & Technology* 51 (17), 9674-9682.
- Tang, S., Wang, M., Germ, K. E., Du, H.-M., Sun, W.-J., Gao, W.-M. and Mayer, G. D. (2015) Health implications of engineered nanoparticles in infants and children. *World J Pediatr* (11), 197-206.

- The Project on Emerging Nanotechnologies (2019) *Nanotech-enabled Consumer Products Continue to Rise*. Online: The Project on Emerging Nanotechnologies. <http://www.nanotechproject.org/news/archive/9231/> Accessed 16 Mar 2019.
- Thermo Fisher Scientific (2018) *Trypan Blue Exclusion*. Online: <https://www.thermofisher.com/uk/en/home/references/gibco-cell-culture-basics/cell-culture-protocols/trypan-blue-exclusion.html> Accessed 18 Mar 2019.
- Thermo Fisher Scientific (2019?) *Absolute vs. Relative quantification for qPCR*. Online: <https://www.thermofisher.com/uk/en/home/life-science/pcr/real-time-pcr/real-time-pcr-learning-center/real-time-pcr-basics/absolute-vs-relative-quantification-real-time-pcr.html#1> Accessed 21 Mar 2019.
- ThermoFisher-Scientific (2015) *Overview of Western Blotting*. <https://www.thermofisher.com/uk/en/home/life-science/protein-biology/protein-biology-learning-center/protein-biology-resource-library/pierce-protein-methods/overview-western-blotting.html#> Accessed 07/05/2016.
- Tice, R. R., Agurell, E., Anderson, D., Burlinson, B., Hartmann, A., Kobayashi, H., Miyamae, Y., Rojas, E., Ryu, J. C. and Sasaki, Y. F. (2000) Single cell gel/comet assay: Guidelines for in vitro and in vivo genetic toxicology testing. *Environmental and Molecular Mutagenesis* 35 (3), 206-221.
- Toppr (2018) *Cell cycle and Cell Division: Cell Cycle*. <https://www.toppr.com/quides/biology/cell-cycle-and-cell-division/cell-cycle/> Accessed 20 Mar 2019.
- Towbin, H., Staehelin, T. and Gordon, J. (1979) Electrophoretic Transfer of Proteins from Polyacrylamide Gels to Nitrocellulose Sheets: Procedure and Some Applications. *Proceedings of the National Academy of Sciences of the United States of America* 76 (9), 4350-4354.
- Tuder, R. M. and Petrache, I. (2012) Pathogenesis of chronic obstructive pulmonary disease. *Journal of Clinical Investigation* 122 (8), 2749-2755.
- U.S. National Library of Medicine (2019) *Lung Cancer*. Online: <https://ghr.nlm.nih.gov/condition/lung-cancer> Accessed 20 Mar 2019.
- Vallabani, N. V. S., Mittal, S., Shukla, R. K., Pandey, A. K., Dhakate, S. R., Pasricha, R. and Dhawan, A. (2011) Toxicity of Graphene in Normal Human Lung Cells (BEAS-2B). *Journal of biomedical nanotechnology* 7 (1), 106-107.
- Vance, M. E., Kuiken, T., Vejerano, E. P., McGinnis, S. P., Hochella, J. M. F., Rejeski, D. and Hull, M. S. (2015) Nanotechnology in the real world: Redeveloping the nanomaterial consumer products inventory. *Beilstein journal of nanotechnology* 6 (1), 1769-1780.
- Vijayan, V. K. (2013) Chronic obstructive pulmonary disease. *Indian Journal of Medical Research* 137 (2), 251-269.
- Vinardell, M. P. and Mitjans, M. (2015) *Antitumor activities of metal oxide nanoparticles*. *Nanomaterials* 5 (2), 1004-1021.
- Wacker, M. J. and Godard, M. P. (2005) Analysis of one-step and two-step real-time RT-PCR using superscript III. *Journal of Biomolecular Techniques* 16 (3), 266-271.
- Wang, A., Pu, K., Dong, B., Liu, Y., Zhang, L., Zhang, Z., Duan, W. and Zhu, Y. (2013) Role of surface charge and oxidative stress in cytotoxicity and genotoxicity of graphene oxide towards human lung fibroblast cells. *Journal of Applied Toxicology* 33 (10), 1156-1164.

- Wang, K., Ruan, J., Song, H., Zhang, J., Wo, Y., Guo, S. and Cui, D. (2011a) Biocompatibility of Graphene Oxide. *Nanoscale Research Letters* 6 (1), 1-8.
- Wang, Y., Wang, F., Wang, H. and Song, M. (2017) Graphene oxide enhances the specificity of the polymerase chain reaction by modifying primer-template matching. *Scientific reports* 7 (1), 16510-10.
- Wang, Y., Wang, J., Li, J., Li, Z. and Lin, Y. (2011b) Graphene and graphene oxide: biofunctionalization and applications in biotechnology. *Trends in Biotechnology* 29 (5), 205-212.
- Waris, G. and Ahsan, H. (2006) Reactive oxygen species: role in the development of cancer and various chronic conditions. *J Carcinog* 5 (14).
- Wei, X.-Q., Hao, L.-Y., Shao, X.-R., Zhang, Q., Jia, X.-Q., Zhang, Z.-R., Lin, Y.-F. and Peng, Q. (2015) Insight into the Interaction of Graphene Oxide with Serum Proteins and the Impact of the Degree of Reduction and Concentration. *Applied Materials Interfaces* 7 (24), 13367-13374.
- Wellen, K. E. and Thompson, C. B. (2010) Cellular Metabolic Stress: Considering How Cells Respond to Nutrient Excess. *Molecular Cell* 40 (2), 323-332.
- WHO (2017) *WHO Guidelines on Protecting Workers from potential risks of manufactured nanomaterials*. Online: World Health Organization (WHO).
- Williams, A. B. and Schumacher, B. (2016) p53 in the DNA-Damage-Repair Process. *Cold Spring Harbor perspectives in medicine* 6 (5), a026070.
- Williams, D. A. (2014) Curing genetic disease with gene therapy. *Transactions of the American Clinical and Climatological Association* 125, 122.
- Wills, J. W., Summers, H. D., Hondow, N., Sooresh, A., Meissner, K. E., White, P. A., Rees, P., Brown, A. and Doak, S. H. (2017) Characterizing Nanoparticles in Biological Matrices: Tipping Points in Agglomeration State and Cellular Delivery In Vitro. *ACS Nano* 11 (12), 11986-12000.
- Winey, M., Meehl, J. B., O'Toole, E. T. and Giddings, J. T. H. (2014) Conventional transmission electron microscopy. *Molecular biology of the cell* 25 (3), 319-323.
- Wong, A. S. M., Mann, S. K., Czuba, E., Sahut, A., Liu, H., Suekama, T. C., Bickerton, T., Johnston, A. P. R. and Such, G. K. (2015) Self-assembling dual component nanoparticles with endosomal escape capability. *Nano* 11 (15), 2993.
- Wu, S., Liu, B., Zhang, Q., Liu, J., Zhou, W., Wang, C., Li, M., Bao, S. and Zhu, R. (2013) Dihydromyricetin reduced Bcl-2 expression via p53 in human hepatoma HepG2 cells. *PloS one* 8 (11), e76886.
- Wu, S.-Y., An, S. S. A. and Hulme, J. (2015) Current applications of graphene oxide in nanomedicine. *International journal of nanomedicine* 10 Spec Iss, 9-24.
- Xia, T., Kovichich, M., Liong, M., Zink, J. I. and Nel, A. E. (2008) Cationic polystyrene nanosphere toxicity depends on cell-specific endocytic and mitochondrial injury pathways. *ACS Nano* 2 (1), 85-96.
- Yan, J. A. and Chou, M. Y. (2010) Oxidation functional groups on graphene: Structural and electronic properties. *Phys. Rev. B* 82 (125403).
- Yang, K., Zhang, S., Zhang, G., Sun, X., Lee, S.-T. and Liu, Z. (2010) Graphene in mice: Ultrahigh in vivo tumor uptake and efficient photothermal therapy. *Nano Letters* 10 (9), 3318-3323.
- Yang, Z. R., Wang, H. F., Zhao, J., Peng, Y. Y., Wang, J., Guinn, B. A. and Huang, L. Q. (2007) Recent developments in the use of adenoviruses and immunotoxins in cancer gene therapy. *Cancer Gene Therapy* 14 (7), 599-615.

- Yasui, M., Kamoshita, N., Nishimura, T. and Honma, M. (2015) Mechanism of induction of binucleated cells by multiwalled carbon nanotubes as revealed by live-cell imaging analysis. *Genes and Environ.* 37 (1), 6.
- Yuan, J., Gao, H. and Ching, C. B. (2011) Comparative protein profile of human hepatoma HepG2 cells treated with graphene and single-walled carbon nanotubes: An iTRAQ-coupled 2D LC-MS/MS proteome analysis. *Toxicology Letters* 207 (3), 213-221.
- Zhang, M., Zhou, N., Yuan, P., Su, Y., Shao, M. and Chi, C. (2017) Graphene oxide and adenosine triphosphate as a source for functionalized carbon dots with applications in pH-triggered drug delivery and cell imaging. *RSC Advances* 7 (15), 9284-9293.
- Zhang, X., Yin, J., Peng, C., Hu, W., Zhu, Z., Li, W., Fan, C. and Huang, Q. (2011) Distribution and biocompatibility studies of graphene oxide in mice after intravenous administration. *Carbon* 49 (3), 986-995.
- Zhao, N., Woodle, M. C. and Mixson, A. J. (2018) Advances in delivery systems for doxorubicin. *Journal of nanomedicine & nanotechnology* 9 (5), 519.
- Zhao, X., Yang, L., Li, X., Jia, X., Liu, L., Zeng, J., Guo, J. and Liu, P. (2015) Functionalized graphene oxide nanoparticles for cancer cell-specific delivery of antitumor drug. *Bioconjugate chemistry* 26 (1), 128-136.
- Zhi, L. and Müllen, K. (2008) A bottom-up approach from molecular nanographenes to unconventional carbon materials. *Journal of Materials Chemistry* 18 (13), 1472-1484.
- Zhou, T., Zhou, X. and Xing, D. (2014) Controlled release of doxorubicin from graphene oxide based charge-reversal nanocarrier. *Biomaterials* 35 (13), 4185-4194.
- Zhou, X. and Liang, F. (2014) Application of graphene/graphene oxide in biomedicine and biotechnology. *Current Medicinal Chemistry* 21 (7), 855-69.
- Zhu, Y., Murali, S., Cai, W., Li, X., Suk, J. W., Potts, J. R. and Ruoff, R. S. (2010) Graphene and graphene oxide: Synthesis, properties, and applications. *Advanced Materials* 22 (35), 3906-3924.
- Ziello, J. E., Huang, Y. and Jovin, I. S. (2010) Cellular endocytosis and gene delivery. *Molecular Medicine* 16 (5-6), 222-229.

Appendix

Appendix 1: Consent Forms



UNIVERSITY OF
BRADFORD
MAKING KNOWLEDGE WORK

School of Life Sciences

PARTICIPATION INFORMATION SHEET FOR PATIENTS

Study title: Genetic and environmental effects in lymphocytes from different cancerous, precancerous and inflammatory conditions using various genetic endpoints

**Reviewed by Leeds East Research Ethics Committee (REC)
(REC reference number: 12/YH/0464)**

Invitation to the research study

We would like to invite you to take part in a research study. Before you decide you need to understand why the research is being done and what it would involve for you. Please take time to read the following information carefully. Talk to others about the study if you wish to and you will be allowed around 24hours to consider this.

(Part 1 tells you the purpose of this study and what will happen to you if you take part. Part 2 gives you more detailed information about the conduct of the study).

Ask us if there is anything that is not clear or if you would like more information. Take time to decide whether or not you wish to take part.

Part 1

In this study white blood cells will be treated in a test tube with chemical solutions or particles or UV radiation to determine if patients with cancerous and inflammatory diseases are more at risk after exposure. A blood sample of around 2 teaspoons (5-7 ml) will be taken. Samples will be stored only for the duration of the study and used for studies of a similar nature or to check original responses. This is for various research programmes involving post doctoral fellows and PhDs.

Why have I been invited?

You have been invited because you have a disease state and we should like to determine if these chemicals or UV irradiation could be more harmful to people with a disease state than those without such a disease.

Do I have to take part?

It is up to you to decide. We shall outline the study and go through this information sheet, which we shall then give to you. We shall ask you to sign a consent form to show you have agreed to take part. You are free to withdraw at any time, without giving a reason.

Part 2

What will happen to me if I take part?

Only a single blood sample will be taken for this research study. A brief questionnaire will need to be completed by the researchers.

Each individual will be given a coded study number so that your clinical data can be linked in an anonymous way with the research results.

The data obtained will only be available to the research team and will **not** be returned to you. Responses will be compared only on a group basis i.e. collective responses from patients with diseases compared to collective responses from people without diseases. Results could be published in the form of scientific papers. The work will benefit the medical and scientific community at large, but will not be of direct benefit to you as an individual. If, however, you would like more information, the Consultant and research team will be prepared to talk to you individually about study results.

People who cannot take part in the study

People who are not well enough to take part will be excluded (e.g those with anaemia).

If you have any further questions, you could contact the research team:

Prof Badie Jacob, NHS Trust, **Bradford Royal Infirmary** and **St Lukes Hospital**
Bradford Teaching Hospitals NHS Foundation Trust, BD5 0NA .
Telephone: 01274-542200

Professor Diana Anderson, Established Chair in Biomedical Sciences, BSc, MSc, PhD, DipEd, FSB, FATS, FRCPath, FIFST, FBTS, FHEA, University of Bradford, Richmond Road, Bradford, BD7 1DP and Honorary Research Consultant to Bradford NHS Trust.

e-mail: d.anderson1@bradford.ac.uk

Dr Mojgan Najafzadeh MD, PhD Post Doctoral Fellow. Division of Medical Sciences, University of Bradford, Richmond Road, Bradford, BD7 1DP
and Honorary Research Consultant to Bradford NHS Trust.

DATA COLLECTION FORM

(To be completed by the Doctor)

STUDY TITLE: Genetic and environmental effects in lymphocytes from different cancerous, precancerous and inflammatory conditions using various genetic endpoints

REVIEWED BY LEEDS East RESEARCH ETHICS COMMITTEE (REC)

(REC REFERENCE NUMBER: 12/YH/0464)

PATIENT NUMBER DATE OF SAMPLE

AGE

SEX (PLEASE TICK) M F CONSENT Y/N
ETHNIC GROUP INFORMATION SHEET Y/N

OCCUPATION

CURRENT SMOKER Y/N PAST SMOKER Y/N HOW MANY/MUCH PER DAY?
CIGARETTES CIGARS PIPE
ALCOHOL Y/N UNITS PER WEEK

DIET WESTERN ASIAN OMNIVORE VEGETARIAN VEGAN

VITAMINS / ANTI-OXIDANTS (PLEASE LIST)

PRESCRIBED DRUG USE (PLEASE LIST)

RECREATIONAL DRUG USE Y/N

IF YES PLEASE LIST
MEDICAL

CANCER Inflammatory disease
EXTENT SITE HISTOLOGY SURGERY

CANCER Inflammatory disease
Pre cancerous state
OTHER MEDICAL CONDITIONS (PLEASE LIST)
Family history of cancer and Inflammatory disease
Chemotherapy or radiotherapy

MOST RECENT MEASURE

	RESULT	DATE	OTHERS	RESULT	DATE
WEIGHT	<input type="text"/>	<input type="text"/>	<input type="text"/>	<input type="text"/>	<input type="text"/>
HEIGHT	<input type="text"/>	<input type="text"/>	<input type="text"/>	<input type="text"/>	<input type="text"/>
BMI	<input type="text"/>	<input type="text"/>	<input type="text"/>	<input type="text"/>	<input type="text"/>

Centre Number:

CONSENT FORM FOR PATIENTS

Title of Project: **Genetic and environmental effects in lymphocytes from different cancerous, precancerous and inflammatory conditions using various genetic endpoints**

**Reviewed by Leeds East Research Ethics Committee (REC)
(REC reference number: 12/YH/0464)**

Names of Researchers: Prof. D Anderson, Dr. Mojgan Najafzadeh, Prof Badie Jacob

Please tick
box

1. I confirm that I have read and understand the information sheet for the above study. I have had the opportunity to consider the information, ask questions and have had these answered satisfactorily.
2. I understand that my participation is voluntary and that I am free to withdraw at any time without giving any reason, without my medical care or legal rights being affected.
3. I understand that relevant sections of my medical notes and data collected during the study may be looked at by individuals from the NHS Trust or the University of Bradford, where it is relevant to my taking part in this research. I give permission for these individuals to have access to my records.
4. I agree that the sample I have given and the information gathered about me can be stored at the University of Bradford, as described in the attached information sheet.
5. I agree to take part in the above study.

Patient number

Date

Name of Person
taking consent

Date

Signature

When completed, 1 for patient; 1 for researcher site file; 1 (original) to be kept in medical notes

Participant Information Sheet for healthy volunteers (Version 4, 28/01/2013)

Study title: Genetic and environmental effects in lymphocytes from different cancerous, precancerous and inflammatory conditions using various genetic endpoints.

**Reviewed by Leeds East Research Ethics Committee (REC)
(REC reference number: 12/YH/0464)**

Invitation to the research study

We should like to invite you to take part in a research study. Before you decide you need to understand why the research is being done and what it would involve for you. Please take the time to read the following information carefully. Talk to others about the study if you wish and you will be allowed around 24 hours to consider this.

(Part 1 tells you the purpose of this study and what will happen to you if you take part.

Part 2 gives you more detailed information about the conduct of the study).

Ask us if there is anything that is not clear or if you would like more information. Take time to decide whether or not you want to take part.

Part 1**What is the purpose of the study?**

In this study white blood cells will be treated in a test tube with very small chemical particles or UVA (Ultra Violet A light) to determine if patients with different diseases are more at risk after exposure compared to healthy individuals. For example, chemicals and UV (Ultra Violet) can break and damage the DNA of white blood cells. Further examination of this resulting damage may improve our knowledge of the cancers and other inflammatory diseases. The tests are not predictive for any kind of diseases and the test results will not impact on you or the patients with whom you are compared.

A blood sample of around 2-4 teaspoons (20 ml) will be taken. Samples will be stored only until the end of the study (after 8 years) and used for studies of a similar nature or to check original responses. The research is also used for some PhD programmes.

Why have I been invited

You have been invited because you are healthy and do not have the disease of the patients we are comparing you with. We should like to determine if these small chemical particles or UVA could be more harmful to people with diseases than those without diseases.

Do I have to take part?

No, it is up to you to decide. We shall outline the study and go through this information sheet, which we shall then give to you. We shall ask you to sign a consent form to show you have agreed to take part. You are free to withdraw at any time, without giving a reason.

Part 2

What will happen to me if I take part?

Only a single blood sample will be taken for this research study. A brief questionnaire will need to be completed by the researchers.

Each individual will be given a coded study number so that your clinical data will be linked in an anonymous way with the research results.

The study tests are not predictive for you

The data obtained will only be available to the research team and will **not** be returned to you. Responses will be compared only on group basis i.e. collective responses from patients with that individual disease compared to collective responses from people without that disease. Results could be published in the form of scientific papers. The work may benefit the medical and scientific community at large, but will not be of direct benefit to you as an individual. If, however, you would like more information, the appropriate consultant will be prepared to talk to you individually about study results.

The data will be stored until the study is completed at the end of 8 years.

People who cannot take part in the study.

People who are not well enough to take part will be excluded (e.g those with anaemia).

If you have any further questions, you could contact the research team:

Prof Badie Jacob, NHS Trust, **Bradford Royal Infirmary and St Lukes Hospital**
Bradford Teaching Hospitals NHS Foundation Trust, BD5 0NA .

Telephone: 01274-542200

Professor Diana Anderson, Established Chair in Biomedical Sciences, BSc, MSc, PhD, DipEd, FIBiol, FATS, FRCPath, FIFST, FBTS, FHEA, University of Bradford, Richmond Road, Bradford, BD7 1DP and Honorary Research Consultant to Bradford NHS Trust.
e-mail: d.anderson1@bradford.ac.uk

Dr Mojgan Najafzadeh MD, PhD, Honorary Research Consultant to Bradford NHS Trust, University Medical Research Fellow, Division of Medical Sciences, University of Bradford, Richmond Road, Bradford, BD7 1DP.

Centre Number:

CONSENT FORM FOR HEALTHY VOLUNTEERS

Title of Project: **Genetic and environmental effects in lymphocytes from different cancerous, precancerous and inflammatory conditions using various genetic endpoints**

**Reviewed by Leeds East Research Ethics Committee (REC)
(REC reference number: 12/YH/0464)**

Names of Researchers: Prof. D Anderson, Dr. Mojgan Najafzadeh, Prof Badie Jacob

Please tick
box

1. I confirm that I have read and understand the information sheet (version.01) for the above study. I have had the opportunity to consider the information, ask questions and have had these answered satisfactorily.
2. I understand that my participation is voluntary and that I am free to withdraw at any time without giving any reason, without my medical care or legal rights being affected.
3. I understand data collected during the study may be looked at by individuals from the NHS Trust or the University of Bradford, where it is relevant to my taking part in this research. I give permission for these individuals to have access to my records.
4. I agree that the sample I have given and the information gathered about me can be stored at the University of Bradford, as described in the attached information sheet.
5. I agree to take part in the above study.

Healthy volunteer number

Date

Name of Person
taking consent

Date

Signature

When completed, 1 for healthy volunteer; 1 for researcher site file; 1 (original) to be kept in medical note

Appendix 2: Abstracts & Oral Presentations attended

Appendix 2.1: NANO Boston Conference under the “Emerging Researcher Forum;” Crown Plaza, Boston-Newton, Boston, MA, USA, 22-24 April 2019

Title: In-vitro investigation into the Genotoxic effects of Graphene Oxide on human DNA before and after exposure to blood samples from healthy individuals and pulmonary disease patients: asthma, COPD, and lung cancer patients.

Emmanuel Eni Amadi,¹ * Mojgan Najafzadeh¹, Adi Baumgartner², Badie K Jacob³, Diana Anderson¹

¹School of Chemistry and Bioscience, Faculty of Life Sciences, University of Bradford, Richmond Road, Bradford, West Yorkshire, BD7 1DP UK.

²School of Health Sciences, York St John University, Lord Mayor's Walk, York, YO31 7EX, UK.

³Bradford Royal Infirmary, Bradford, BD9 6RJ and St. Luke's Hospital, Bradford, BD5 ONA, UK.

*Presenter Contact Details: **Emmanuel Eni Amadi:** E.E.Amadi@bradford.ac.uk

Abstract

Graphene nanomaterials are increasingly becoming popular in the past few decades due to their unique properties such as mechanical, chemical, and electronic properties. The proposed application of the water-soluble derivative, Graphene Oxide, in biomedical sciences as a nano carrier in cancer therapeutics had led scientists to increase research in this nanomaterial. Despite their intended nanomedical applications, there are concerns about their potential toxicity in human DNA. To our knowledge, this is the first research on in-vitro studies of genotoxic potential of the 2D nanomaterials in human whole blood from real-life patients clinically diagnosed with asthma, COPD, and lung cancer by a

Consultant Physician. In this study, blood samples from healthy individuals, asthma, COPD, and lung cancer patients were treated with four different concentrations of Graphene oxide (10, 20, 50 and 100 µg/mL). Genotoxicity was performed using the Comet and cytokinesis-blocked micronucleus (CBMN) assays. Quantification of DNA damage parameters showed concentration-dependent increase in DNA damage in each of the treated samples. However, pulmonary diseases patients showed more DNA damage than the healthy individuals' group. Specifically, lung cancer patients showed highest DNA damage than in COPD patients, while DNA damage levels in asthma patients and healthy individuals were similar compared to untreated samples. These findings are indications that low concentrations of GO used in this study were genotoxic to human DNA. Therefore, more caution is required when formulating Graphene Oxide as a nano carrier or in nanomedical sciences.

Author Biography:

Emmanuel Eni Amadi is a PhD Candidate in Biomedical Sciences, under Professor Diana Anderson, Faculty of Life Sciences, University of Bradford, UK. He holds an Executive MBA from Lancaster University Management School, UK (2009-2011); PG. Diploma in Pharmacy, University of Brighton, UK (2005-2006); MSc in Analytical & Pharmaceutical Sciences, Loughborough University, UK (2002-2003) and a Bachelor of Pharmacy degree from the University of Nigeria, Nsukka. He was the Founder, CEO and Superintendent Pharmacist for **EE AMADI LTD** t/a **Drugs4U Pharmacy** Manchester, UK (2009-2018). Currently, he sits on the Board as a Non-Executive Director / Member of Trustee to a Multi-Academy Trust in Bury, Greater Manchester, UK. **His Scientific Fields,**

expertise and interests are on Pulmonary Nanotoxicity and Genotoxicity of Graphene Oxide nanoparticles in drug delivery; nanomedicines / nanomedical devices in the treatment of **asthma, COPD, and lung cancer patients**; mainly on the DNA damage mechanisms of 2D Graphene Oxide nanoparticles in human whole blood before and after exposure to the genotoxic agent.

14:25-14:45	Mengjiste L. Debasu, University of Aveiro, Portugal Highly Sensitive Near-Infrared (GdNd) ₃ O ₉ Nanothermometers Operating in the Biological Windows
14:45-15:00	Tianyuan Zhang, Zhejiang University, China Mesenchymal Stem Cell Engineering using Ferrimagnetic Nanocube for an Improved Ischemic Stroke Treatment
15:00-15:15	Cheva Harish, University of North Carolina at Greensboro, NC Study of Growth Science of Bottom-Up and Solid-State Silver Nanowires (Ag NWs) and their Potential Application in Surface Enhance Raman Scattering (SERS) and Antibacterial Activities
15:15-15:30	Khalaf Jasim, University of Central Florida, FL Targeted Chemotherapy Approach Based on Iron-Releasing Nanoparticle Conjugates for Triggered Metastatic Melanoma Therapy <i>in vitro</i>
15:30-15:45	Tea Break
15:45-16:00	Marta Dziejwiecka, University of Silesia in Katowice, Poland Evaluation of Selected Biological Parameters in <i>Acheta domestica</i> after Long-Lasting Exposure to Graphene Oxide Nanoparticles in Food
16:00-16:15	Emmanuel Eni Amadi, University of Bradford, United Kingdom <i>In vitro</i> Investigation into the Genotoxic Effects of Graphene Oxide on Human DNA before and after Exposure to Human Whole Blood from Healthy Individuals and Pulmonary Disease Patients: Asthma, COPD and Lung Cancer Patients
16:15-16:30	Thamonwan Angkuratipakorn, Thammasat University, Thailand Tailoring Cellulose Nanocrystals by Food Grade Cationic Surfactant (Lauric Arginate) for Stabilizing Edible Pickering Oil-in-Water Emulsion
16:30-16:45	Ching Chang, National Tsing Hua University, Taiwan Growth of Nitrogen-Incorporated Ultra-Nano Crystalline Diamond with Acicular-Shaped Grains Using Si ₃ N ₄ as Interface Layer and Study Its Application in Biosensor
16:45-17:00	Ajmeeta Sangtani, University of Maryland-College Park, MD Intracellularly-Actuated Nanoparticle-Drug Bioconjugates for Overcoming Multidrug Resistance in Cancer Cells
17:20-18:15	Posters Session

@ University C Room



Appendix 2.2: Postgraduate Research Symposium, Faculty of Life Sciences, University of Bradford; Mon. 4th June 2018; Abstract Book, p6.

Abstract title: The Medium Throughput Alkaline Comet Assay as A Sensitive and Reliable Tool for Rapid Assessment of DNA Damaging Potential of Graphene Oxide Nanoparticles in Human Whole Blood from Healthy Individuals.

E.E. Amadi^{1,2}, S. Fraga^{3,4}, J. P. Teixeira^{3,4} and D. Anderson^{1, *}

¹School of Chemistry and Bioscience, Faculty of Life Sciences, University of Bradford, Bradford, UK; ²The Leverhulme Trade Charities Trust, London, UK; ³EPIUnit - Instituto de Saúde Pública, Universidade do Porto, 4050-600 Porto, Portugal; ⁴Departamento de Saúde Ambiental, Instituto Nacional de Saúde Doutor Ricardo Jorge, 4000-055 Porto, Portugal.

Introduction: Graphene Oxide Nanoparticles have become increasingly popular in the past 2 decades due to their applications in biomedical sciences, especially their proposed application as drug delivery-carrier conjugates for the treatment of pulmonary diseases (asthma, COPD, or lung cancer). Therefore, there is urgent need to assess their genetic /DNA damage using multiple blood samples at a relatively short period of time, before being used in nanomedicine. The standard Alkaline Comet assay is the most commonly used method to assess nanotoxicity/genotoxicity of nanoparticles. However, this assay has various limitations such as low throughput, which invariably had limited its wider application in clinical medicine. To remove these limitations, the standard Comet assay has undergone extensive modifications, leading to the evolution of another technique known as the Medium Throughput Alkaline Comet Assay (MTACA): a 12-Gel Comet Assay Unit [™] consisting of 12 wells (i.e. 6 duplicates) and an aluminium base plate holder.

Method: Human whole blood (WB) samples were collected after informed consent from 5 different healthy individuals from the Environmental Health Institute, Portuguese National Health Institute, Porto, Portugal. WB samples were treated with different concentrations of Graphene Oxide Nanoparticles (0, 10, 20, 50 and 100 µg/mL) and 100 µM H₂O₂ (30% w/w) (PC) for 30 min at 37°C in an atmosphere of 5 % CO₂, where 0µg/mL = untreated blood sample (NC). Using the MTACA format, 5 µL of agarose-cell mixture (NC, PC, 10, 20, 50, and 100 µg/mL) were loaded in duplicate onto a dry microscope slide, pre-coated with 1% normal-melting point (NMP) agarose, forming 12-Mini Gels on a single microscope slide. The cells were lysed, DNA unwound, electrophoresed, and stained. DNA damaged cells were scored with Comet Assay IV (Perceptive Instruments, Suffolk, UK). Fifty cells (i.e. 25 from each of the 2 replicate gels) per treatment were counted. 5 slides were used.

Results: Parametric data analyses were performed by means of one-way ANOVA, with Dunnett post-hoc test for multiple comparisons, to determine significant differences relative to the NC. Significance was accepted at a *P*-value < 0.05. DNA damage was concentration dependent.

Conclusion: Like the standard Comet assay, the results were rapid and sensitive. However, the MTACA used less materials (slides, chemicals, buffers/solutions) in each stage of the experiment. Moreover, it was less labour intensive with better throughput for simultaneous analysis of multiple samples at the same time, and in the same experimental conditions. Finally, the MTACA was energy efficient, cost effective (££) and saved time by 60%.

Appendix 2.3: Postgraduate Research Symposium, Faculty of Life Sciences, University of Bradford; Abstract & Oral Presentation: Wed. 7th June 2017; Abstract Book, pp10-11.

Title: Comparison of DNA Damaging Effects of Graphene Oxide Nanoparticles on Human Whole Blood from Healthy Individuals and Pulmonary Disease patients: Asthma, COPD, and lung cancer.

Emmanuel Eni Amadi, Mojgan Najafzadeh, and Diana Anderson, School of Medical Sciences, University of Bradford, UK.

In the past 4 decades, metal nanoparticles (M-NPs) or particles of metals in the nano-particulate form, has cut through our everyday life: from being used in healthcare products as sunscreens to toothpastes. From tissue engineering, imaging techniques, photodynamic therapies and gene delivery, graphene oxide (GO) nanoparticles (GO-NPs) are now among the most highly researched NPs in recent years due to its biomedical applications. This is due to their current application in medicine as drug delivery carrier-conjugates for the treatment of pulmonary diseases such as asthma, COPD, and lung cancer. In the nano-form, GO in human lungs and alveoli behave similarly to asbestos fibres (causing asbestosis), ultra-fine dusts/particles, and combustion exhaust smokes from diesel car engines and locomotives/trains. Despite these overwhelming applications and their close resemblance to other genotoxic agents, there is little research in the database about their potential DNA damaging effects on patients with respiratory diseases.

The aim of this PhD project is to address some of the deficiencies found in previous studies:

1. GO comes in various forms, sizes, shapes, and surface area. Studies by previous authors have failed to indicate the type of GO used in their studies. In the world of nanotechnology and graphene for human medicines, the type of GO and the number of layers/sheets used in an experiment are paramount. This is because the DNA damaging effects of a single-layered GO could be significantly less compared to GO with 10-15 layers. Result from such investigations had shown that GO induces low cell toxicity why others showed increase in airway hypersensitivity. Therefore, entire results are inconsistent and conflicting. There are safety and toxicity concerns.

2. Moreover, previous studies were conducted using animal models such as mice/ rats, pigs, macrophages, lymphocytes, and cancer cell lines. No genotoxicity studies were conducted using real life patients, nor their whole blood samples, prior to GO nano being used as a drug delivery carrier.

Materials & Methods: The Graphene Oxide (GO) used in this PhD study is the edge-oxidized Graphene Oxide (EOGO); 4-10% edge oxidized; Number of Layers: 15-20 sheets; Conc.1mg/mL. It is commercially available from Sigma-Aldrich (UK), Product Code: 1002087404; **794341**-50mL; Lot #: MKBW0818V). This few-layered graphene has a high spec ratio (1-5 nm in thickness and 400 nm in diameter).

Blood Sample collection: Healthy blood samples were collected from healthy individual donors; while pulmonary disease blood samples (asthma, COPD, and lung Cancer) were collected from clinically diagnosed patients from the

Respiratory Clinic of Professor Badie Jacob, Bradford Royal Infirmary & St Luke's Hospital.

Genotoxicity Studies:

□ **The Comet assay** (to determine DNA damage): A total of **85** comet assays were conducted: **5** Healthy individuals for **H₂O₂** Concentration-dependent responses as PC; **20** Healthy individuals as a negative control (NC); **20** asthma; **20** COPD and **20** lung cancer patients.

□ **The Micronucleus assay**: A total of **19** experiments were conducted: **5** on healthy individuals as NC; **5** on asthma, **5** on COPD, and **4** on lung cancer patients.

Results/Discussions: The results are being analysed and would be presented in the final PhD Transfer Report, due before 1st August 2017.

Appendix 3: Poster Presentation: Life Sciences Research and Development Open Day, Tuesday 5th June 2018; Faculty of Life Sciences, University of Bradford, UK.



The Medium Throughput Alkaline Comet Assay as a Sensitive and reliable tool for rapid assessment of DNA Damaging Potential of Graphene Oxide Nanoparticles in Human Whole Blood from Healthy Individuals

LEVERHULME TRUST

Emmanuel Eni Amadi¹; Sónia Fraga^{2,3}, João Paulo Teixeira^{2,3}; Diana Anderson¹

¹School of Chemistry and Bioscience, Faculty of Life Sciences, University of Bradford, Bradford, UK; ²EPIUnit - Instituto de Saúde Pública, Universidade do Porto, 4050-600 Porto, Portugal; ³Departamento de Saúde Ambiental, Instituto Nacional de Saúde Doutor Ricardo Jorge, 4000-055 Porto, Portugal

ABSTRACT

The Standard Comet Assay is the most commonly used assay to assess DNA damage caused by nanoparticles. Functionalised graphene oxide nanoparticles are increasingly being applied in Nanomedicine, with proposed use as drug delivery-carrier conjugate for the treatment of Pulmonary diseases. In the present study, a modified form of the Comet assay known as the Medium throughput Alkaline Comet assay (MTACA). The objective was to ascertain if any differences exist in each stage of the assay compared with the standard Comet assay. Our findings demonstrated that DNA damage was concentration-dependent and MTACA was still sensitive similar to the standard Comet assay. However, the MTACA technique had many advantages: better throughput; required less materials; highly reproducible and the amount of time spent in the lab was reduced by 60% compared to the standard Comet assay.

INTRODUCTION

Graphene Oxide Nanoparticles (GONPs) have become increasingly popular in the past 2 decades due to their applications in biomedical sciences, especially their proposed application as drug delivery-carrier conjugates for the treatment of pulmonary diseases (asthma, COPD or lung cancer). Therefore, there is urgent need to multiple assessment of their genetic /DNA damage at a relatively short period of time, before being applied in nanomedicine.

The standard Alkaline Comet assay is the most sensitive and most commonly used assay to assess nanotoxicity/ genotoxicity of nanoparticles^{1,2}. However, this assay has a number of limitations such as low sample throughput and the lengthy sample workup procedures, which invariably limit its wider application in clinical medicine³. To eliminate some of these limitations, the standard Comet assay has undergone extensive modifications to accommodate even the smallest amount of samples⁴ leading to a newer assay known as the Medium Throughput Alkaline Comet Assay (MTACA)⁵.

AIM

To assess the DNA damaging potential of Graphene Oxide Nanoparticles in Human Whole Blood from Healthy individuals using the MTACA.

The objective was determine if there are any advantages of MTACA method over the standard Comet assay currently being used at the University of Bradford.

MATERIALS & METHODS

All reagents, including aqueous suspension of graphene oxide nanoparticles were purchased from Sigma Aldrich unless otherwise specified. Blood samples were taken after informed consent from 5 different healthy individuals at the Environmental Health Department, Portuguese National Health Institute, Porto, Portugal. Whole blood samples were treated with GONPs (10, 20, 50 and 100 µg/mL). Samples treated with 100 µM H₂O₂ (30% w/w) were the positive control (PC) while untreated blood samples were the negative control (NC). They were incubated for 30 min at 37°C in an atmosphere of 5 % CO₂. The cells were centrifuged and the pellets resuspended in 100 µL of 0.5% low melting point (LMP) agarose (Biolin, UK). Using the template (Fig.1), and the 12-Gel Comet Assay Unit™ (Severn Biotech Ltd®, Worcestershire, UK) (Fig. 2), 5 µL from each of the agarose-cell mixtures were loaded in duplicate (a & b) onto a dry microscope slide, pre-coated with 1% normal melting point (NMP) agarose (Biolin, UK), forming 12-Mini Gels (Fig. 3) per slide. The cells were lysed, DNA unwound, electrophoresed (29V, I=296-310 mA) for 20 min, and stained (0.07% SYBR® Gold solution). DNA damage was scored manually using Comet Assay IV (Perceptive Instruments, Suffolk, UK). Fifty cells (i.e. 25 from each of the 2 replicate gels) per treatment concentration were counted. To quantify DNA damage, the Tail moment and the Tail Intensity were used.



Fig. 1. A diagrammatic representation of MTACA template, with a & b being duplicates of treatment concentrations.



Fig. 2. 12-Gel Comet Assay Unit™ Fig. 3. A slide with 12-mini gels with aluminium base plate holder

STATISTICAL ANALYSIS

Parametric data analyses were performed by means of one-way ANOVA, with Dunnett post-hoc test for multiple comparisons, to determine significant relative to NC using GraphPad Prism® software, version 7.03 (Fay Avenue, La Jolla, CA, USA). Significance was accepted at a P-value < 0.05 (*).

RESULTS

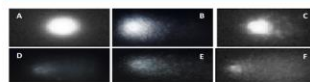


Fig. 4. Representative Comet images after exposure to different concentrations of GONPs, where A = negative control (NC); B = 100 µM H₂O₂ (PC); C = 10 µg/mL; D = 20 µg/mL; E = 50 µg/mL; and F = 100 µg/mL. The images were captured using the Comet IV software (Perceptive Instruments, UK).

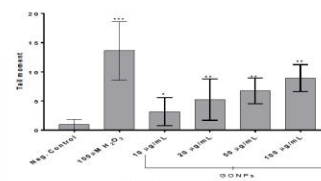


Figure 4 GONPs-induced DNA damage in human whole blood from healthy individuals expressed as Tail Moment. ANOVA, *p<0.05; **p<0.01; ***p<0.001, relative to untreated blood samples

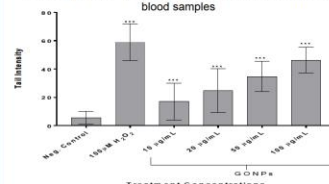


Figure 5 GONPs-induced DNA damage in human whole blood from healthy individuals, expressed as Tail Intensity. ANOVA, *p<0.05; **p<0.01; ***p<0.001, relative to untreated control.

Key Measurable parameters for 5 diff. blood samples	Standard Comet Assay	Medium Throughput Comet Assay
No. of slides	60 (12 x 5 samples)	5 (1 per sample)
0.5% LMP Agarose-Cell mixture	100 µL	5 µL
Cover slips	120 • 12 - to flatten Cell-agarose Mixture • 12 - during DNA scoring	5 (req'd. during DNA scoring)
Vol. of Lysis Buffer	1 L (5 x 200 mL)	200 mL
Vol. of Electrophoresis buffer	≈ 10 L (1,900 mL x 5)	≈ 1 L (1,900 mL x 1)
Labour Intensity	High (laborious)	Low, Time by 60%
Energy consumption	High 0.3 Kwh	Low 0.04 Kwh
Reproducibility	Low	High
Throughput	Low	Medium
Cost impact (€€€)	High: ~ €4,125 based on May 2018 Tariff @ 13.75p for Large businesses	Low: ~ €0.55p

DISCUSSION

From the results above in this study, we can conclude that despite the various modifications of the standard Comet assay to newer versions such as the MTACA, both methods are still very sensitive and reliable techniques for nanotoxicity and genotoxicity analysis of nanoparticles⁶. However, the MTACA technique has many advantages in almost each stage in the Comet assay. Therefore, it makes economic sense where rapid assessment of multiple samples are required for quick turnaround⁷. Finally, the MTACA decreased assay time by 60%³.

REFERENCES

- Anderson, D. and Laubenthal, J. (2013) Analysis of DNA damage via single-cell electrophoresis. *Methods Mol Biol* 1054, 209-18.
- Langie, S. A. S., Azqueta, A. and Collins, A. R. (2015) The comet assay: past, present, and future. *Frontiers in genetics* 6, 266.
- Karbaschi, M. and Cooke, M. S. (2014) Novel method for the high-throughput processing of slides for the comet assay. *Scientific reports* 4, 7200.
- Tebbs, R. S., Cleaver, J. E., Pedersen, R. A. and Hartmann, A. (1999) Modification of the Comet assay for the detection of DNA strand breaks in extremely small tissue samples. *Mutagenesis* 14 (4), 437-438.
- Lavies, A., Dijke, E. V., Wenzel, J. F. and Pretorius, P. J. (2014) Using a medium-throughput comet assay to evaluate the global DNA methylation status of single cells. *Frontiers in Genetics* 5, 21-6.
- The Najafzadeh, M. and Anderson, D. (2016) The use of isolated peripheral lymphocytes and human whole blood in the comet assay. *Protocol Exchange*.
- Moller, P., Knudsen, L., Loft, S. and Wallin, H. (2000) The comet assay as a rapid test in biomonitoring occupational exposure to DNA-damaging agents and effect of confounding factors. *Cancer Epidemiol Biomarkers Prev* 9 (10), 1005-15.

ACKNOWLEDGEMENT

The authors are grateful to the Short-Term Scientific Mission (STSM) for funding (COST Action CA1532; Reference No: 38499). EE Amadi wishes to acknowledge the PhD Bursary award by the Leverhulme Trade Charities Trust, London.

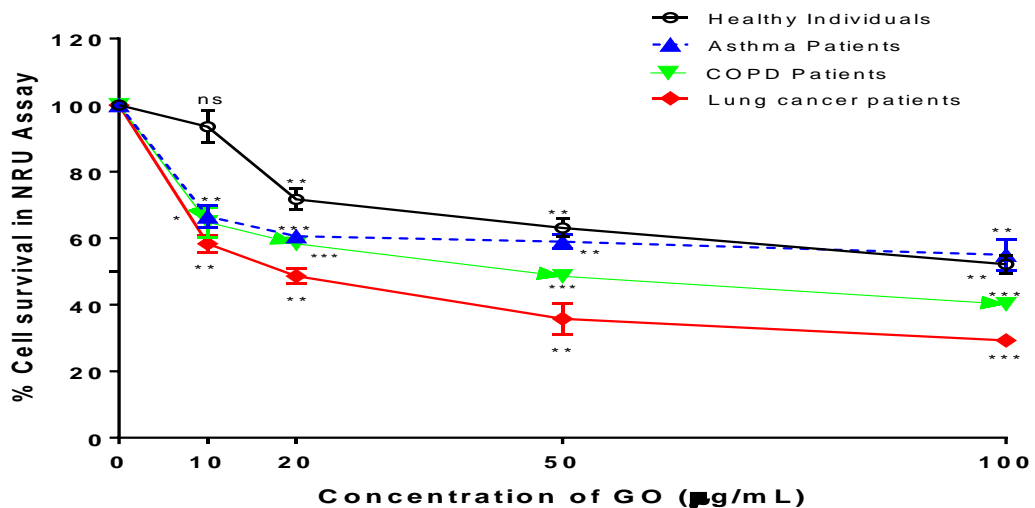
Appendix 4: Raw Date for Neutral Red Uptake Assay

Neutral Red Uptake Assay		30/10/2018				
NRU in COPD patients (n=3)						
	0 µg/mL	10 µg/mL	20 µg/mL	50 µg/mL	100 µg/mL	
Blank (RPMI) (540 nm)	2.010	2.967	3.743	3.256	2.979	
Minus empty well (540nm)	0.064	0.054	0.051	0.054	0.064	
Adjusted Ab of Control	1.946	2.913	3.692	3.202	2.915	
*Corrected Ab of Control (540nm-595nm)	1.716	2.569	3.054	2.780	2.593	
Absorbance of Sample (540nm)	3.766	3.474	3.640	2.738	2.342	
Minus empty well	0.052	0.112	0.056	0.048	0.052	
Corrected absorbance (540nm)-well	3.714	3.362	3.584	2.690	2.290	
Actual sample absorbance (@ 540-595nm)	3.000	2.931	3.044	2.269	1.750	
Background absorbance at 595nm						
Blank wells (RPMI)	0.287	0.398	0.687	0.474	0.378	
Minus Empty Wells	0.057	0.054	0.049	0.052	0.056	
	0.23	0.344	0.638	0.422	0.322	
Samples @ 595nm	0.764	0.53	0.594	0.468	0.594	
minus Empty wells	0.05	0.099	0.054	0.047	0.054	
	0.714	0.431	0.54	0.421	0.54	
	174.83	114.09	99.67	81.62	67.49	
$\frac{OD\ of\ Test}{OD\ of\ Control} \times 100$	100.00	65.26	57.01	46.69	38.60	
% Cell proliferation (where 0 µg/mL = 100%)						
HEALTHY						
	0	10 µg/mL	20 µg/mL	50 µg/mL	100 µg/mL	
Absorbance of Treated samples (540 nm) (1)	3.694	2.881	2.033	1.554	1.497	
2	3.505	3.017	2.564	1.498	1.594	
3	3.679	3.494	2.419	2.003	1.992	
Average (A)	3.626	3.131	2.339	1.685	1.694	
Empty wells	0.047	0.045	0.052	0.049	0.048	
Adjusted Absorbance (A2)	3.579	3.086	2.287	1.636	1.646	
Absorbance of Treated sample at 595 nm						
1	0.584	0.472	0.492	0.325	0.295	
2	0.764	0.528	0.501	0.319	0.309	
3	0.689	0.491	0.468	0.311	0.326	

Average	0.679	0.497	0.487	0.3183	0.31
Empty wells	0.048	0.047	0.051	0.047	0.047
Adjusted	0.63	0.45	0.436	0.27	0.26
OD of Sample (540-595 nm)	2.948	2.636	1.851	1.365	1.383
Absorbance of Control/RPMI (540)	3.682	3.528	3.792	2.821	3.489
Absorbance of Background of Control/RPMI (595)	0.196	0.211	0.697	0.258	0.295
OD of Control (Ab at 540-595)	3.486	3.317	3.095	2.563	3.194
%	84.57	79.46	59.80	53.24	43.31
% Cell proliferation (where 0 µg/mL = 100%)	100%	93.96	70.71	62.96	51.21
ASTHMA PATIENTS					
Absorbance of Treated samples (540 nm)					
	0	10 µg/mL	20 µg/mL	50 µg/mL	100 µg/mL
1	2.889	2.451	1.584	1.028	1.258
2	2.756	2.012	2.564	1.947	1.539
3	2.876	3.901	2.615	2.101	2.938
Average (A)	2.840	2.788	2.254	1.692	1.912
Empty wells	0.047	0.045	0.052	0.049	0.048
Adjusted Absorbance (A2)	2.793	2.743	2.202	1.643	1.864
Absorbance of Treated sample at 595 nm					
	0.854	0.401	0.492	0.496	0.537
2	0.647	0.817	0.501	0.583	0.484
3	0.764	0.531	0.499	0.584	0.499
Average	0.755	0.583	0.497	0.5543	0.507
Empty wells	0.049	0.048	0.052	0.048	0.049
Adjusted	0.706	0.535	0.445	0.51	0.46
OD of Sample (540-595 nm)	2.087	2.208	1.757	1.137	1.406
Absorbance of Control/RPMI (540)	3.574	4.351	3.792	2.821	3.489
Absorbance of Background of Control/RPMI (595)	0.286	0.471	0.394	0.473	0.497
OD of Control (Ab at 540-595)	3.288	3.88	3.398	2.348	2.992
Relative %	63.48	56.91	51.71	48.41	46.99
% Cell proliferation (where 0 µg/mL = 100%)	100%	67.29	61.14	57.24	55.57
LUNG CANCER					
Absorbance of Treated samples (540 nm)					
	0	10 µg/mL	20 µg/mL	50 µg/mL	100 µg/mL
1	3.784	2.649	2.803	1.147	0.858
2	3.891	2.558	1.926	1.295	0.791
3	3.677	3.001	1.790	1.991	2.101

Average (A)	3.784	2.736	2.173	1.478	1.250
Empty wells	0.048	0.047	0.046	0.045	0.045
Adjusted Absorbance (A2)	3.736	2.689	2.127	1.433	1.205
Absorbance of Treated sample at 595 nm					
1	0.999	0.834	0.801	0.531	0.734
2	0.811	0.826	0.761	0.671	0.841
3	0.941	0.729	0.691	0.899	0.773
Average	0.917	0.796	0.751	0.700	0.783
Empty wells	0.045	0.048	0.046	0.049	0.045
Adjusted	0.87	0.748	0.705	0.65	0.74
OD of Sample (540-595 nm)	2.864	1.941	1.422	0.781	0.467
Absorbance of Control/RPMI (540)	3.574	4.351	3.792	2.821	2.489
Absorbance of Background of Control/RPMI (595)	0.286	0.471	0.394	0.473	0.497
OD of Control (Ab at 540-595)	3.288	3.88	3.398	2.348	1.992
Relative %	87.10	50.02	41.85	33.28	23.46
% Cell proliferation (where 0 $\mu\text{g/mL}$ = 100%)	100%	59.14	49.48	39.35	27.74

Graph for NRU



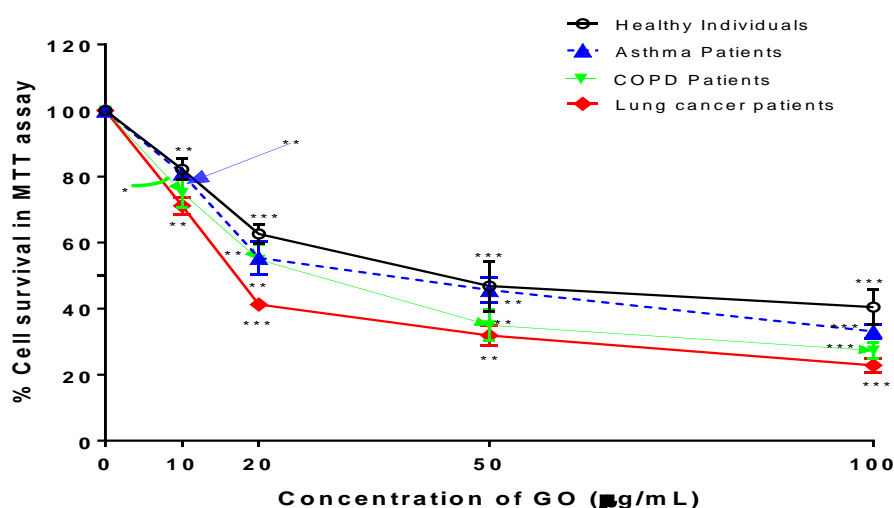
% Cell Survival in NRU of human lymphocytes from patients (asthma, COPD, and lung cancer) compared with healthy individuals after 24 h treatment with different concentrations of GO (10, 20, 50 and 100 $\mu\text{g/mL}$), followed by 3 h incubation with Neutral Red dye. Untreated lymphocytes = 100% % cell survival (n = 3).

Appendix 5: Raw Date for MTT Assay

MTT Assay					
	Neg. Conc.	10 µg/mL	20 µg/mL	50 µg/mL	100 µg/mL
Medium +MTT (Blank = No cell)	0.054	0.054	0.047	0.058	0.050
Background	0.049	0.047	0.047	0.048	0.047
	0.005	0.007	0	0.01	0.003
Treated Cells					
1	0.966	0.114	1.836	0.450	0.253
2	1.692	0.956	0.155	0.592	1.727
3	1.213	0.527	0.783	1.843	1.608
Adjusted					
1	0.961	0.107	1.836	0.44	0.25
2	1.687	0.949	0.155	0.582	1.724
3	1.208	0.52	0.783	1.833	1.605
Average	1.285	0.525	0.925	0.952	1.193
% Cell Survival in MTT	100%	40.87	71.94	74.04	92.82
Healthy Individual 30/10/2018					
Medium +MTT (Blank = No cell)	0.056	0.067	0.070	0.087	0.075
minus background	0.047	0.048	0.046	0.046	0.048
	0.009	0.019	0.024	0.041	0.027
1	1.692	1.354	1.095	0.761	0.677
2	1.513	1.210	0.908	0.681	0.605
3	1.539	1.231	0.923	0.692	0.616
Av.	1.581	1.265	0.975	0.711	0.633
% Cell survival	100.00	80.01	61.67	44.97	40.04
Asthma patients					
Medium +MTT (Blank = No cell)	0.054	0.058	0.056	0.049	0.054
minus background	0.052	0.048	0.050	0.048	0.052
	0.002	0.01	0.006	0.001	0.002
1	1.536	1.198	0.845	0.645	0.538
2	1.510	1.178	0.831	0.634	0.529
3	1.457	1.365	0.801	0.612	0.510
Av	1.501	1.247	0.826	0.630	0.526
% Cell survival	100	83.08	55.01	41.99	35.02
COPD					

Medium +MTT (Blank = No cell)	0.054	0.054	0.049	0.058	0.050
minus background	0.047	0.048	0.047	0.056	0.048
	0.007	0.006	0.002	0.002	0.002
Sample Absorbance	0 µg/mL	10 µg/mL	20 µg/mL	50 µg/mL	100 µg/mL
1	1.407	1.055	0.704	0.492	0.380
2	1.329	0.997	0.665	0.465	0.359
3	1.253	0.940	0.627	0.439	0.338
Av	1.330	0.997	0.665	0.465	0.359
% cell survival	100.00	74.99	50.03	34.99	26.99
Lung cancer					
Medium +MTT (Blank = No cell)	0.054	0.058	0.056	0.049	0.054
minus background	0.047	0.048	0.05	0.047	0.048
	0.007	0.01	0.006	0.002	0.006
Sample Absorbance	0 µg/mL	10 µg/mL	20 µg/mL	50 µg/mL	100 µg/mL
1	1.427	0.999	0.642	0.428	0.285
2	1.324	0.927	0.596	0.397	0.289
3	1.317	0.922	0.530	0.395	0.264
Av	1.356	0.949	0.589	0.407	0.279
% Cell survival	100	70.01	43.46	29.99	20.60

Graph for MTT assay



% Cell Survival in MTT assay of human lymphocytes from patients (asthma, COPD, and lung cancer) compared with healthy individuals after 24 h treatment with different concentrations of GO (10, 20, 50 and 100 µg/mL), followed by 4 h incubation with MTT dye solution. Untreated lymphocytes = 100% % cell survival (n = 3).

Appendix 6: Reagents for Comet assay

Cold Lysis Stock Solution (445 mL)

Components	Quantity	Conc.
NaCl	73.05 g	2.5 M
NaOH	4.0 g	
Disodium EDTA (Na ₂ EDTA.2H ₂ O)	18.61 g	100 mM
Trizma Base (Tris)	0.61 g	10 mM
Dissolve in dH ₂ O	350 mL	

Mix the components and dissolve in 350 mL of dH₂O, and adjust to pH 10 with NaOH, then make up to 445 mL.

Lysis buffer (Working Stock)

Components	Quantity	Conc.
Lysis Stock Solution	178 mL	
DMSO	20 mL	10%
Triton X-100	2 mL	1%

10 M NaOH (Alkaline Electrophoresis Buffer Stock Solution 1) x 200 mL

Components	Quantity
NaOH	80 g
dH ₂ O	150 mL

Dissolve 80 g of NaOH in 150 mL of dH₂O (Exothermic reaction). Keep flask in ice blocks until cool and store at RT.

200 mM EDTA (Alkaline Electrophoresis Buffer Stock solution 2) x 100 mL

Components	Quantity
Na ₂ EDTA.2H ₂ O	7.44 g
dH ₂ O	100 mL

Dissolve Na₂EDTA.2H₂O in 80 mL of dH₂O. Adjust to pH 10 with NaOH, and then make up to 100 mL (Exothermic reaction). Keep flask in ice blocks until cool and store at RT.

Electrophoresis Buffer (Work Solution, pH = >13)

Components	Quantity
10 M NaOH	30 mL
EDTA	5 mL
Make up with dH ₂ O to	1,000 mL

To prepare a fresh electrophoresis buffer (better prepared fresh on the day) per 1 Litre, add 30 mL of 10 M NaOH and 5.0 mL EDTA and make up with distilled water to 1,000 mL and mix well. Before use, check the pH of the buffer is >13 and adjust accordingly.

Neutralisation Buffer

Components	Quantity
Trizma Base	12.11 g
dH ₂ O	250 mL

Dissolve Trizma base in 200 mL of dH₂O and adjust to pH 7.5 with HCl. Make up to 250 mL final volume. Filter and sterilize.

Appendix 7: Raw data of DNA damage in the Comet assay.

Appendix 7.1: H₂O₂-concentration dependent DNA damage in healthy individuals (n=5)

Treatments	OTM (Mean ± S.E.)	% Tail DNA (Mean ± S.E.)
Neg. Control (NC)	12.15±1.46	28.41±1.63
10 µM H ₂ O ₂	15.63±2.65 **	35.6±1.90 ***
30 µM H ₂ O ₂	18.59±1.87 ***	38.73±1.78 ***
60 µM H ₂ O ₂	24.17±1.57 ***	52.74±0.98 ***
100 µM H ₂ O ₂	35.75±0.48 ***	66.14±1.66 ***

Appendix 7.2: Effects of GO and 100 μM H_2O_2 on human DNA in vitro on human whole blood from Healthy individuals and patients (asthma, COPD, and lung Cancer) in the Comet assay.

TREATMENT GROUPS		OTM (Mean \pm SEM)	% Tail DNA (Mean \pm SEM)
HEALTHY (n = 20)			
	Untreated WB	6.35 \pm 0.05	21.54 \pm 0.07
	100 μM H_2O_2	22.51 \pm 0.36 ***	33.53 \pm 0.11 ***
GO	10 $\mu\text{g}/\text{mL}$	8.87 \pm 0.04 ***	23.65 \pm 0.07 ***
	20 $\mu\text{g}/\text{mL}$	9.45 \pm 0.04 ***	24.53 \pm 0.11 ***
	50 $\mu\text{g}/\text{mL}$	10.92 \pm 0.21 ***	28.17 \pm 0.19 ***
	100 $\mu\text{g}/\text{mL}$	14.12 \pm 0.27 ***	31.49 \pm 0.14 ***
ASTHMA (n = 20)			
	Untreated WB	6.27 \pm 0.28 ns	22.95 \pm 0.34 ns
	100 μM H_2O_2	25.25 \pm 0.16 ***	35.73 \pm 0.22 ***
GO	10 $\mu\text{g}/\text{mL}$	21.63 \pm 0.11 ***	32.03 \pm 0.36 ***
	20 $\mu\text{g}/\text{mL}$	27.05 \pm 0.21 ***	40.37 \pm 0.26 ***
	50 $\mu\text{g}/\text{mL}$	30.96 \pm 0.34 ***	42.27 \pm 0.16 ***
	100 $\mu\text{g}/\text{mL}$	37.07 \pm 0.27 ***	46.04 \pm 0.53 ***
COPD (n = 20)			
	Untreated WB	10.03 \pm 0.12 **	26.81 \pm 0.15 **
	100 μM H_2O_2	51.81 \pm 0.22 ***	60.44 \pm 0.17 ***
GO	10 $\mu\text{g}/\text{mL}$	24.56 \pm 0.37 ***	30.90 \pm 0.13 ***
	20 $\mu\text{g}/\text{mL}$	31.03 \pm 0.12 ***	46.89 \pm 0.10 ***
	50 $\mu\text{g}/\text{mL}$	42.00 \pm 0.16 ***	56.53 \pm 0.10 ***
	100 $\mu\text{g}/\text{mL}$	55.35 \pm 0.66 ***	61.70 \pm 0.15 ***
LUNG CANCER (n = 20)			
	Untreated WB	29.08 \pm 0.17 ***	43.90 \pm 0.16 ***
	100 μM H_2O_2	59.82 \pm 1.00 ***	64.20 \pm 0.16 ***
GO	10 $\mu\text{g}/\text{mL}$	29.77 \pm 0.12 ***	46.02 \pm 0.11 ***
	20 $\mu\text{g}/\text{mL}$	37.67 \pm 0.28 ***	59.44 \pm 0.15 ***
	50 $\mu\text{g}/\text{mL}$	48.67 \pm 0.27 ***	71.75 \pm 0.12 ***
	100 $\mu\text{g}/\text{mL}$	67.30 \pm 0.67 ***	76.75 \pm 0.07 ***

Appendix 8: Reagents used in the CBMN Assay

Buffers for CBMN Assays	
Carnoy's Solution	Quantity
glacial acetic acid	30 mL
Methanol	90 mL
110mM Cold Potassium chloride (KCl) (4°C)	
KCl	8.20 g
ddH ₂ O	1,000 mL
Preparation of Sorenson Buffer, pH 6.8	
Monobasic (0.2M NaH ₂ PO ₄)	51 mL
Dibasic (0.2M Na ₂ HPO ₄)	49 mL
Distilled water (dH ₂ O)	100 mL
Total volume	200 mL
5% Giemsa Stain solution	
Giemsa stain, R66 Gurr®	10 mL
Sorensen's Buffer	190 mL

Appendix 9: Summary of Chemical Treatments, volumes, and treatment sequences in the CBMN assay

Flask labels	Chemical Treatments	Volume
Flask No. 1	Untreated flask (Negative Control)	0 µL
Flask No. 2	0.4 µM Mitomycin – C (Positive Control)	50 µL
Flask No. 3	10 µg/mL Graphene oxide in aq. suspension	50 µL
Flask No. 4	20 µg/mL Graphene oxide aq. suspension	50 µL
Flask No. 5	50 µg/mL Graphene oxide aq. suspension	50 µL
Flask No. 6	100 µg/mL Graphene oxide aq. suspension	50 µL

Day	Time Point	Activities	Volume need
Preparations under sterile conditions (Sterile Hood with lamina flow)			
Day 1	0-hour	Blood cell culturing 1. Basic culture Medium (previously prepared, stored frozen and defrosted an hour before procedure): 2. Phytohaemagglutinin M-form (PHA)	4.5 mL 130 µL 400 µL

		3. Human whole blood (Freshly collected)	
Day 2	24-hour	Chemical Treatments NC, PC (with Mitomycin-C), and four different concentrations of Graphene Oxide in aqueous suspension (10, 20, 50 and 100µg/mL)	50 µL
Day 3	44-hours	Addition of Cyto-B	30 µL
Non-sterile Conditions (on the work bench) at 48 hours after chemical exposure			
Day 4	72-hours	Cell Preparations 1. Hypotonic shock: with cold KCl 2. Fixations: 2.1 Fixation with Formaldehyde (once) 2.2 Fixation without formaldehyde (x2)	
Day 5	Any time	Slide Preparation: leave cells to dry overnight	2 x 20µL
Day 6	“	Staining with %5 Giemsa in Sorenson’s buffer: leave to dry overnight	
Day 7 (end us lab work)	“	Mounting Glass Cover slips: Mounting glass covers with DPX Mountant on a hot plate. The slides are then left to dry overnight.	
Day 8	“	Slides are ready for scoring – can be done at home or at the office.	

Appendix 10: Chemicals and mixtures used in RNA Isolation

Chemicals/components	Quantity
Lysis Solution	70 mL
2-Mercapto Ethanol (2-ME)	0.9 mL
Wash Solution 1	40 mL
Wash Solution 2 Concentrate	15 mL
Elution Solution	10 mL
Filtration Columns	70 pcs
Binding Columns	70 pcs
Collection Tubes (2 mL)	280 pcs

RNA Lysis Solution Mixture		
Description	X 1	X 3 For 3 treatments (NC, 150, and 200 µg/mL)
2-ME	10 µL	30 µL
RNA Lysis Solution	1 mL	3 mL

Dilution of Wash Solution 2 Concentrate	
Wash Solution 2 Concentrate	15 mL
Ethanol	60 mL

Appendix 11: Western Blot materials

Description of Abcam antibodies used	Predicted molecular weight (kDa)	Dilution in TBST
Anti-p21 (CDK)	21	1:1,000-1:10,000
Anti-BCL-2	26	1:500-1:2,000
Anti-GAPDH	36	1:10,000
Ant-p53	53	1:500-1:1,000

Target protein size against percentage T of separation gel (% T)

The size of the Separation Gel used in the WB depends on the size of proteins of interest. Here, 12.5% of separating Gel was chosen since the protein sizes of p53, p21, BCL-2 and GAPDH lie between 14 and 66 KDa as shown in the table (Antibodies, Molecular weight, and Dilution range). Predicted protein sizes of p53, p21, BCL-2, and GAPDH as well as their recommended dilutions by Abcam.

Target Protein size range (kDa)	% T in Separation Gel
26-2015	5.0%
24-205	7.5%
14-205	10.0%
14-66	12.5%
14-45	15.0%

Preparation of Stock solutions for Western Blot

TBST x 10 stock solution (use cold at 4°C)

TBST (Tris Base Saline – Tween 20) x10 – 1 Litre	
Description	Quantity
Sodium Chloride (NaCl)	8.80 g
Tris Base	24.20 g
0.1% Tween [®] -20	1,000 µL

The TBST was used as a Wash Buffer and antibody dilution/incubation buffer.

To make, add NaCl, Tris Base and Tween[®]-20 to 800 mL of dH₂O. Adjust to pH 7.4 with 1 M HCl, stored at 4-25°C.

Stock preparation of Sample Loading Buffer (= 2x Laemmli Buffer x 10 mL)

Preparation of 0.5 M Tris-HCl, pH6.8

Chemical	Quantity
Tris Base	6.05 g
dH ₂ O	100 mL

6.05g of Tris base was dissolved in 100 mL of dH₂O and pH adjusted to 6.8 with 1M HCl.

Preparation of 1 M Tris-HCl, pH6.8

Chemical	Quantity
Tris Base	12.10 g
dH ₂ O	100 mL

12.10 g of Tris base was dissolved in 100 mL of dH₂O and pH adjusted to 6.8 with 1M HCl.

Preparation of 10% SDS

Chemical	Quantity
SDS	1 g
dH ₂ O	10 mL

1 g of SDS was dissolved in 10 mL of dH₂O and heated to 68°C to solubilize it and pH adjusted to pH6.6

Preparation of 20% Glycerol

Chemical	Quantity
Glycerol	1 mL
dH ₂ O	5 mL

1 mL of Glycerol was made up with dH₂O to 5 mL.

Preparation of 10% 2-mercaptoethanol

Chemical	Quantity
2-mercaptoethanol (10%)	1 mL
dH ₂ O	10 mL

2-mercaptoethanol is a reducing agent in a sample buffer in WB to reduce protein disulphide bonds before polyacrylamide gel electrophoresis (SDS-PAGE). 10% 2-mercaptoethanol was prepared by pipetting 1 mL of 2-mercaptoethanol and made up to 10 mL with dH₂O.

Preparation of 1% Bromophenol Blue (BPB)

Chemical	Quantity
BPB (1%)	10 mg
dH ₂ O	1,000 μ L

1% of BPB was prepared by weighing 10 mg of BPB and dissolving in 1,000 μ L dH₂O.

Recipe used for Loading buffer (= 2x Laemmli Buffer)

Description	Quantity
1 M Tris-HCL, pH 6.8	1 mL
10% SDS	4 mL
20% Glycerol	2 mL
2-mercaptoethanol	2.5 mL
1% Bromophenol Blue	500 μ L
dH ₂ O to	10 mL

Each of the components was added and adjusted to pH 6.8 and kept for future use.

Preparation of 10% APS

Chemical	Quantity
APS	100 mg
dH ₂ O	1 mL

0.1 g (100 mg) of APS was weighed and added to 1 mL of dH₂O. The solution was frozen at -20°C and thawed before use.

Preparation of Blocking Buffer (5% BSA or 5% Non-Fat Dry Milk (NFDM) in TBST)

Chemical	Quantity
BSA or NFDM	2.5 g
TBST	50 mL

2.5g of BSA or NFDM was weighed and dissolved in 50 mL of TBST. They were prepared fresh each day, filtered, and stored in the refrigerator at 4°C or used cold before use.

Stock Running Buffer 10x (1L), stored at 4°C

Description	Quantity
Tris base (250 mM)	30.30 g
Glycine (192 M)	144 g
SDS (35 mM)	10.08g

Dissolve Tris, Glycine and SDS in 700 mL of dH₂O, and make up to 1 Litre with dH₂O. No pH adjustment is required. Store at 4°C. Dilute 1x as shown below before use.

Dilution of Stock Running Buffer x 10 (1L) prior to use

Chemical	Quantity
Stock Running Buffer x 10	100 mL
dH ₂ O	900 mL

Take 100 mL of stock (Running Buffer x 10) and make up to 1 Litre with dH₂O.

Stock Transfer Buffer (10 x 1 Litre)

Description	Quantity
Tris base (250 mM)	30.30 g
Glycine (192 mM)	144.00 g

Dissolve Tris Base and Glycine together in 600 mL of dH₂O. Check pH and adjust pH to 8.30. Then make up to 1 Litre with dH₂O. Prepare in advance and cool down in the refrigerator at 4°C before use.

Dilution of Stock Transfer Buffer (10 x 1L) before Use

Description	Quantity
Transfer buffer (10 x 1 L)	100 mL
(20%) Methanol	200 mL
dH ₂ O	700 mL
Total	1 L

Before use, take 100 mL of stock and add 200 mL of methanol. And finally make up to 1 Litre.

Preparation of Mild Stripping Buffer x 1 L (Abcam)

Reagents	Quantity
Glycine	15 g
SDS	1 g
Tween-20	10 mL

Dissolve the reagents in 800 mL of dH₂O. Adjust the pH to 2.2 with conc. HCl, 12M and bring the volume up to 1 L with distilled water.

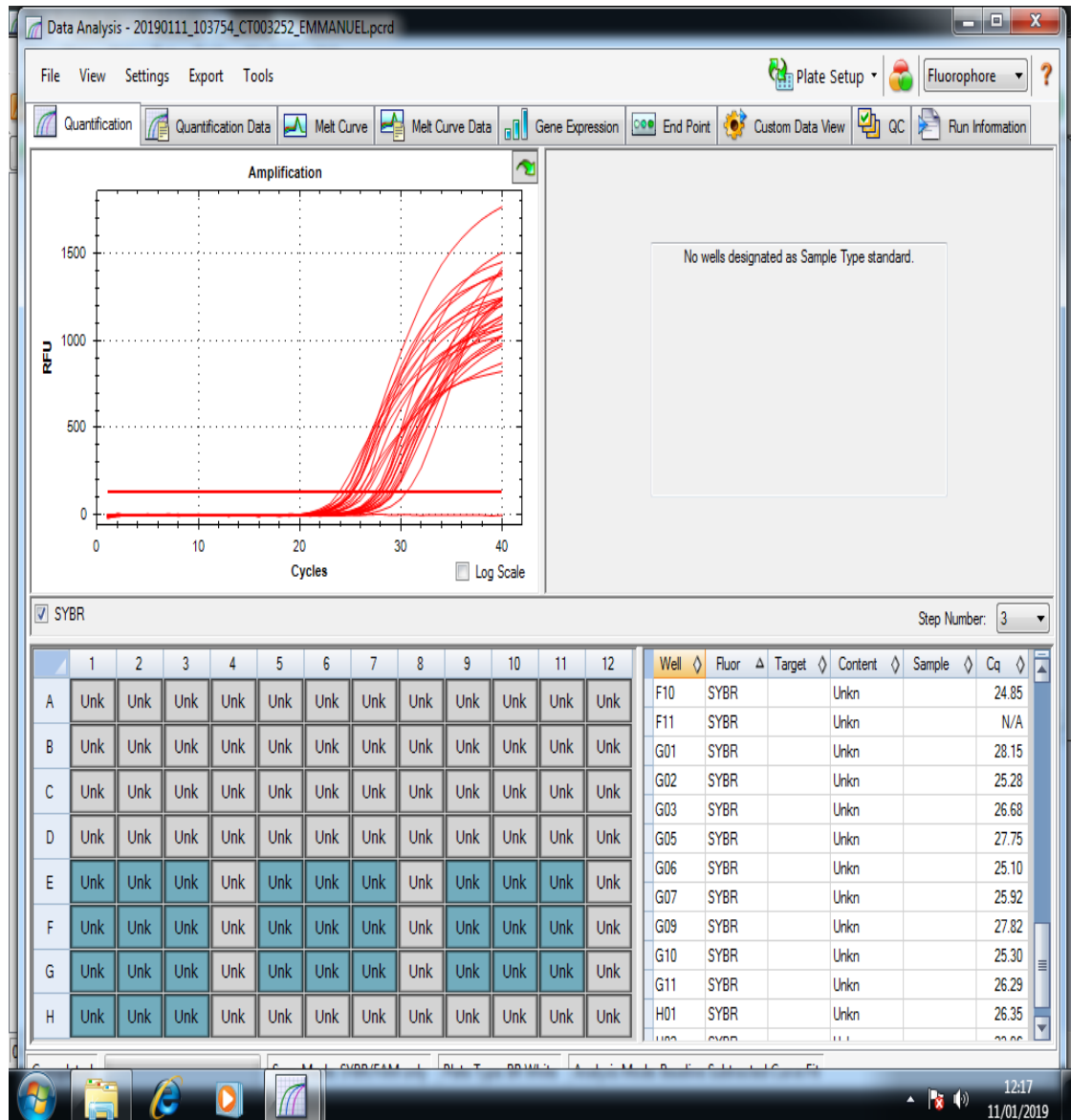
Stripping Procedures

Using a volume that would cover the whole membrane, incubate the stripping buffer with PVDF membrane at RT for 5-10 min.

1. Discard the buffer thereafter;
2. Repeat step 1 (with fresh stripping buffer) and Step 2
3. Wash for 10 min in PBS (x 2)
4. Wash for 5 mins in TBST (x 2)
5. The membrane is ready for blocking.

Appendix 12: Amplification curves obtained during qPCR data analysis

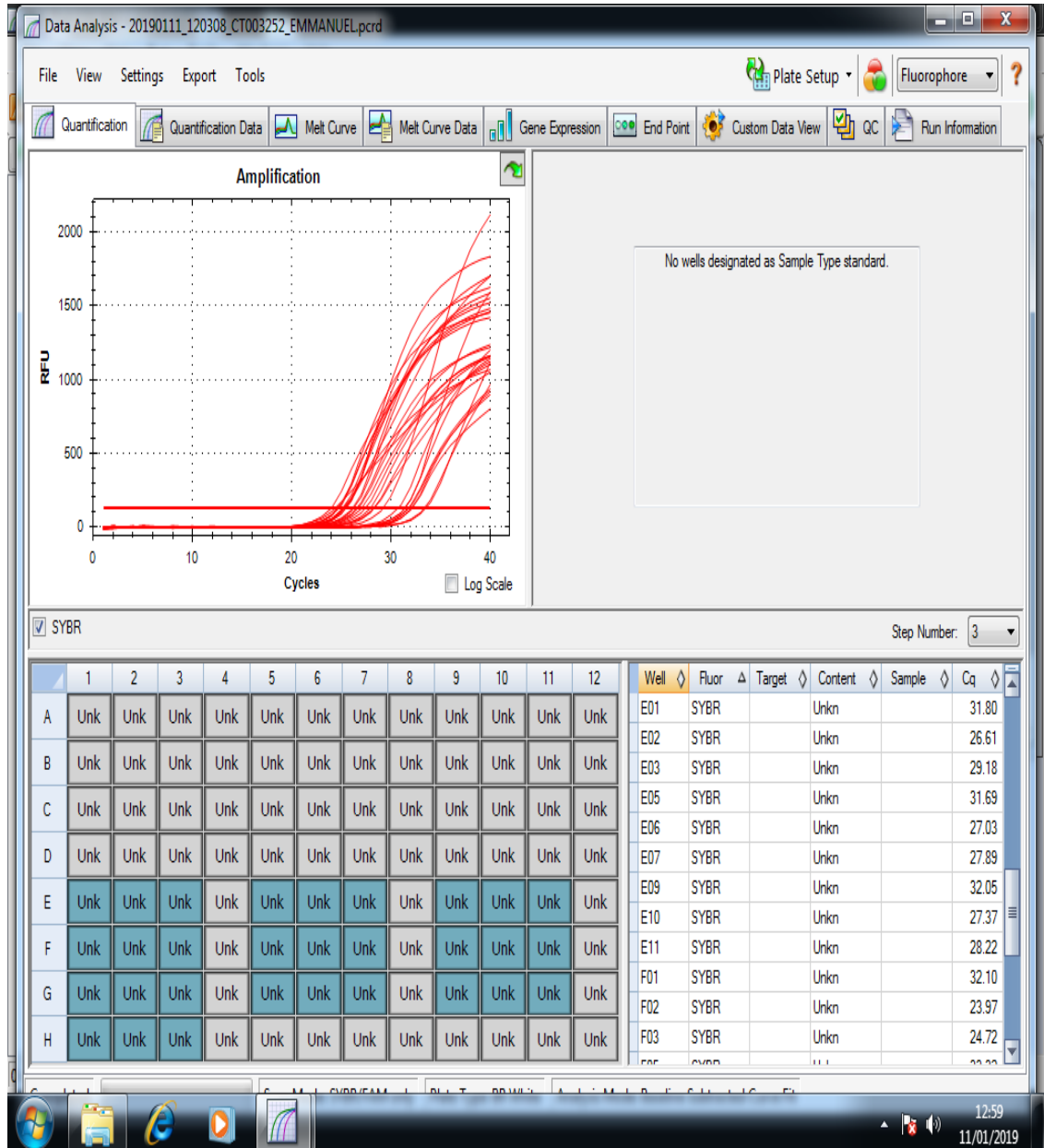
Appendix 12.1: Amplification curves for Healthy Individuals



RT-qPCR amplification signals obtained for Healthy Individuals,

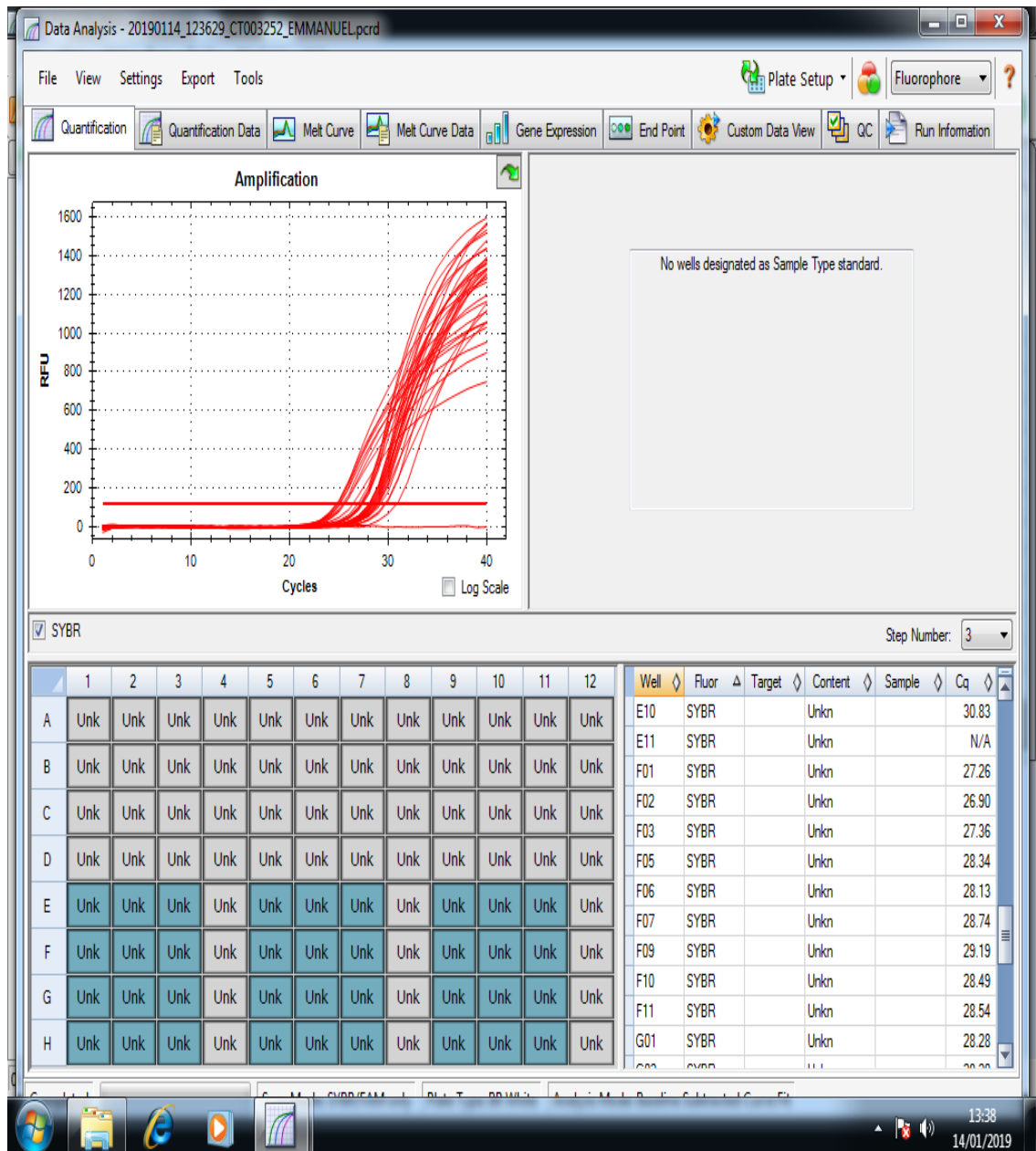
Where: **E** = BCL2; **F** = CDKN1A; **G** = TP53; **H** = GAPDH

Appendix 12.2: Amplification curves for asthma Patients



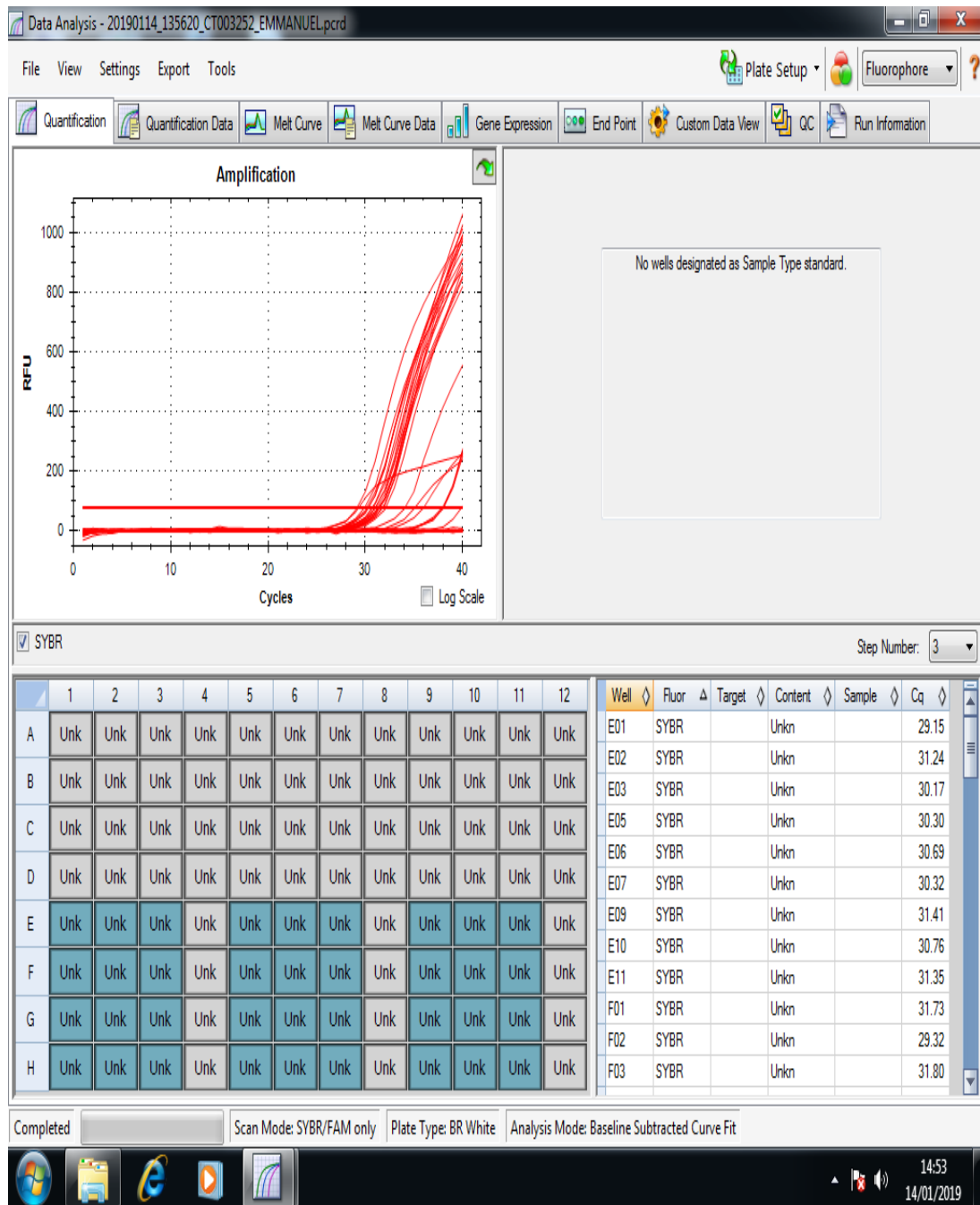
Where: **E** = BCL-2; **F** = CDKN1A; **G** = TP53; **H** = GAPDH

Appendix 12.3: Amplification curves for COPD patients



Where: **E** = BCL-2; **F** = CDKN1A; **G** = TP53; **H** = GAPDH

Appendix 12.4: Amplification curves for lung cancer patients



Where: **E** = BCL-2; **F** = CDKN1A; **G** = TP53; **H** = GAPDH

Appendix 13: RT-qPCR RAW DATA

Appendix 13.1 RT-qPCR raw data for Healthy

		EXPERIMENT 1												
		Cq Values in Healthy Individuals												
		Annealing	NC				150 µ/mL				200 µ/mL			
Genes	Temp (degree Cel.)		1	2	3	Av	1	2	3	Av.	1	2	3	Av.
E	BCL2	59.7	28.29	29.58	29.56	29.14	27.72	27.55	27.85	27.70	28.50	29.75	29.18	29.14
F	CDKN1A	57.7	28.54	28.37	28.54	28.48	25.37	24.42	24.76	24.85	25.55	25.74	25.85	25.20
G	TP53	56.4	28.26	27.66	27.25	27.72	25.35	25.29	25.39	25.34	25.73	25.63	25.91	25.75
H	GAPDH	55.7	26.57	26.39	26.75	26.57	23.57	23.68	23.91	23.72	25.58	25.94	25.64	25.72

		EXPERIMENT 2												
		Cq Values in Healthy Individuals												
		Annealing	NC			Av	150 µ/mL			Av.	200 µ/mL			Av.
Genes	Temp (degree Cel.)		1	2	3		1	2	3		1	2	3	
E	BCL2	59.7	29.57	28.49	29.69	29.25	27.83	27.80	27.46	27.69	28.98	28.74	29.99	29.24
F	CDKN1A	57.7	28.68	28.79	28.78	28.75	25.44	24.57	24.90	24.97	25.68	25.89	25.58	25.20
G	TP53	56.4	28.60	27.79	27.58	27.99	25.67	25.43	25.67	25.59	25.43	25.89	25.47	25.59
H	GAPDH	55.7	26.78	26.28	26.26	26.44	23.78	23.72	23.72	23.74	25.68	25.65	25.87	25.73

		EXPERIMENT 3												
		Cq Values in Healthy Individuals												
		Annealing Temp.	NC			Av	150 µ/mL			Av.	200 µ/mL			Av.
Genes	Temp. (degree Cel.)		1	2	3		1	2	3		1	2	3	
E	BCL2	59.7	29.29	30.58	29.26	29.71	27.72	27.45	28.05	27.74	29.40	28.85	29.07	29.11
F	CDKN1A	57.7	28.43	28.45	28.47	28.45	24.46	24.42	24.85	24.58	25.15	25.24	25.34	25.20
G	TP53	56.4	28.15	27.75	27.82	27.91	25.28	25.10	25.30	25.22	26.68	25.92	26.29	26.29
H	GAPDH	55.7	26.35	26.40	26.90	26.55	23.96	23.47	23.86	23.76	25.74	25.30	25.95	25.66

Appendix 13.2 RT-qPCR raw data for asthma patients

EXPERIMENT 1														
Cq Values in Asthma Patients														
		Annealing	NC			Av	150 µ/mL			Av.	200 µ/mL			Av.
	Genes	Temp (degree Cel.)	1	2	3		1	2	3		1	2	3	
E	BCL2	59.7	31.80	31.69	32.05	31.85	26.61	27.03	27.37	27.00	29.18	27.89	28.22	28.43
F	CDKN1A	57.7	32.10	33.32	33.46	32.96	27.97	27.26	27.09	27.44	27.72	27.60	27.23	27.52
G	TP53	56.4	30.67	31.36	31.34	31.12	24.56	25.43	25.40	25.13	26.20	26.11	26.50	26.27
H	GAPDH	55.7	28.26	28.74	28.04	28.35	24.34	24.79	24.28	24.47	25.18	25.79	25.48	25.48

Experiment 2														
Cq Values in Asthma Patients														
		Annealing	NC			Av	150 µ/mL			Av.	200 µ/mL			Av.
	Genes	Temp (degree Cel.)	1	2	3		1	2	3		1	2	3	
E	BCL2	59.7	30.50	31.94	30.86	31.10	27.85	27.57	27.82	27.75	28.57	28.68	28.27	28.51
F	CDKN1A	57.7	32.83	32.11	32.27	32.40	26.57	25.48	25.27	25.77	24.89	24.55	25.07	24.84
G	TP53	56.4	30.67	30.26	30.26	30.40	25.48	25.52	25.30	25.43	26.27	26.21	26.15	26.21
H	GAPDH	55.7	28.16	28.61	28.76	28.51	24.28	24.56	24.81	24.55	25.48	25.45	25.11	25.35

Experiment 3														
Cq Values in Asthma Patients														
		Annealing	NC			Av	150 µ/mL			Av.	200 µ/mL			Av.
	Genes	Temp (degree Cel.)	1	2	3		1	2	3		1	2	3	
E	BCL2	59.7	30.28	30.23	30.12	30.21	27.22	27.43	27.62	27.42	28.50	28.53	28.71	28.58
F	CDKN1A	57.7	30.25	30.55	30.43	30.41	25.75	25.22	25.33	25.43	24.24	24.64	24.47	24.45
G	TP53	56.4	30.55	30.37	30.42	30.45	25.24	25.83	25.14	25.40	26.50	26.51	26.42	26.48
H	GAPDH	55.7	28.27	28.49	28.27	28.34	24.61	24.32	24.22	24.38	25.25	25.23	25.55	25.34

Appendix 13.3 RT-qPCR raw data for COPD Patients

		EXPERIMENT 1												
		Cq Values in COPD patients												
Genes	Annealing Temp (degree Cel.)	NC			Av.	150 µg/mL			Av.	200 µg/mL			Av.	
		1	2	3		1	2	3		1	2	3		
E	BCL2	59.7	29.04	28.94	29.61	29.20	28.32	28.83	28.66	28.60	29.73	30.83	30.28	
F	CDKN1A	57.7	27.26	26.90	27.36	27.17	28.34	28.13	28.74	28.40	29.19	28.49	28.54	28.74
G	TP53	56.4	28.28	28.20	28.43	28.30	27.35	27.13	27.22	27.24	28.05	28.04	28.07	28.05
H	GAPDH	55.7	25.07	24.90	25.09	25.02	26.37	24.70	24.81	25.30	25.34	25.48	25.55	25.45

		EXPERIMENT 2												
		Cq values in COPD patients												
Genes	Annealing Temp (degree Cel.)	NC			Av.	150 µg/mL			Av.	200 µg/mL			Av.	
		1	2	2		1	2	3		1	2	3		
E	BCL2	59.7	29.23	29.25	29.73	29.40	28.44	28.66	28.24	28.45	29.45	28.22	29.88	29.18
F	CDKN1A	57.7	27.36	26.58	26.28	26.74	28.48	28.57	28.63	28.56	28.27	28.48	28.49	28.41
G	TP53	56.4	28.63	28.28	28.88	28.60	27.12	27.44	27.62	27.40	28.83	28.72	28.48	28.67
H	GAPDH	55.7	25.18	24.48	25.32	24.99	25.44	24.29	24.43	24.72	25.30	25.58	25.32	25.40

Genes	Annealing Temp (degree Cel.)	EXPERIMENT 3												
		Cq values in COPD patients												
		NC				150 µg/mL				200 µg/mL				
		1	2	3	Av.	1	2	3	Av.	1	2	3	Av.	
E	BCL-2	59.7	29.29	29.27	29.06	29.21	28.47	28.22	28.2	28.30	28.43	28.64	28.47	28.51
F	CDKN1A	57.7	27.44	26.27	26.17	26.63	28.35	28.89	28.71	28.65	28.72	28.22	28.21	28.38
G	TP53	56.4	28.22	28.32	28.64	28.39	27.81	27.61	27.24	27.56	28.27	28.49	28.29	28.35
H	GAPDH	55.7	25.38	24.28	25.29	24.98	25.28	24.18	24.27	24.58	25.48	25.42	25.29	25.39

Appendix 13.4 RT-qPCR raw data for lung cancer patients

EXPERIMENT 1														
Cq Values in Lung cancer Patients														
		Annealing	NC				150 µ/mL				200 µ/mL			
	Genes	Temp (degree Cel.)	1	2	3	Av.	1	2	3	Av.	1	2	3	Av.
E	BCL2	59.7	29.15	31.24	30.17	30.19	30.30	30.69	30.32	30.44	31.41	30.76	31.35	31.17
F	CDKN1A	57.7	31.73	29.32	31.80	30.95	29.93	31.05	31.49	30.82	32.10	31.43	31.04	31.52
G	TP53	56.4	30.05	30.92	30.02	30.33	30.00	28.09	29.91	29.33	27.24	27.32	27.11	27.22
H	GAPDH	55.7	25.06	24.80	25.08	24.98	26.27	24.60	24.81	25.23	25.44	25.58	25.65	25.55

EXPERIMENT 2														
Cq Values in Lung cancer Patients														
		Annealing	NC				150 µ/mL				200 µ/mL			
	Genes	Temp (degree Cel.)	1	2	3	Av.	1	2	3	Av.	1	2	3	Av.
E	BCL2	59.7	30.24	30.54	30.39	30.39	30.12	30.48	30.25	30.28	30.22	30.44	30.13	30.26
F	CDKN1A	57.7	30.45	29.87	30.49	30.27	29.88	31.37	31.28	30.84	30.13	31.28	31.29	30.90
G	TP53	56.4	29.44	29.37	29.28	29.36	27.22	27.52	28.01	27.58	26.48	26.21	27.53	26.74
H	GAPDH	55.7	25.21	24.32	25.32	24.95	26.42	24.26	24.78	25.16	25.24	25.49	25.26	25.33

EXPERIMENT 3														
Cq Values in Lung cancer Patients														
		Annealing	NC				150 µ/mL				200 µ/mL			
	Genes	Temp (degree Cel.)	1	2	3	Av.	1	2	3	Av.	1	2	3	Av.
E	BCL2	59.7	31.65	30.27	30.45	30.79	30.29	30.23	30.13	30.22	30.92	30.25	30.47	30.55
F	CDKN1A	57.7	30.29	29.26	30.22	29.92	29.41	30.38	30.38	30.06	30.45	30.69	30.22	30.45
G	TP53	56.4	29.56	29.48	29.79	29.61	27.18	27.29	28.92	27.79	26.22	26.37	27.37	26.66
H	GAPDH	55.7	25.73	24.26	25.11	25.03	26.34	24.72	24.26	25.11	25.14	25.28	25.67	25.36

Appendix 14: Graphene Oxide Safety Data Sheet

SIGMA-ALDRICH		<i>sigma-aldrich.com</i>
		SAFETY DATA SHEET
		according to Regulation (EC) No. 1907/2006 Version 5.0 Revision Date 08.08.2014 Print Date 22.03.2019
SECTION 1: Identification of the substance/mixture and of the company/undertaking		
1.1 Product identifiers		
Product name	:	Graphene oxide, 15-20 sheets, 4-10% edge-oxidized, 1mg/mL dispersion in H ₂ O
Product Number	:	794341
Brand	:	Aldrich
REACH No.	:	A registration number is not available for this substance as the substance or its uses are exempted from registration, the annual tonnage does not require a registration or the registration is envisaged for a later registration deadline.
1.2 Relevant identified uses of the substance or mixture and uses advised against		
Identified uses	:	Laboratory chemicals, Manufacture of substances
1.3 Details of the supplier of the safety data sheet		
Company	:	Sigma-Aldrich Company Ltd. The Old Brickyard NEW ROAD, GILLINGHAM Dorset SP8 4XT UNITED KINGDOM
Telephone	:	+44 (0)1747 833000
Fax	:	+44 (0)1747 833313
E-mail address	:	eurtechserv@sial.com
1.4 Emergency telephone number		
Emergency Phone #	:	+44 (0)870 8200418 (CHEMTREC)
SECTION 2: Hazards identification		
2.1 Classification of the substance or mixture		
	Not a hazardous substance or mixture according to Regulation (EC) No. 1272/2008. Not a hazardous substance or mixture according to EC-directives 67/548/EEC or 1999/45/EC.	
2.2 Label elements		
	The product does not need to be labelled in accordance with EC directives or respective national laws.	
2.3 Other hazards - none		
SECTION 3: Composition/information on ingredients		
3.1 Substances		
	No components need to be disclosed according to the applicable regulations.	
SECTION 4: First aid measures		
4.1 Description of first aid measures		
If inhaled		
	If breathed in, move person into fresh air. If not breathing, give artificial respiration.	
Aldrich - 794341		Page 1 of 6

In case of skin contact

Wash off with soap and plenty of water.

In case of eye contact

Flush eyes with water as a precaution.

If swallowed

Never give anything by mouth to an unconscious person. Rinse mouth with water.

4.2 Most important symptoms and effects, both acute and delayed

The most important known symptoms and effects are described in the labelling (see section 2.2) and/or in section 11

4.3 Indication of any immediate medical attention and special treatment needed

no data available

SECTION 5: Firefighting measures

5.1 Extinguishing media

Suitable extinguishing media

Use water spray, alcohol-resistant foam, dry chemical or carbon dioxide.

5.2 Special hazards arising from the substance or mixture

no data available

5.3 Advice for firefighters

Wear self contained breathing apparatus for fire fighting if necessary.

5.4 Further information

no data available

SECTION 6: Accidental release measures

6.1 Personal precautions, protective equipment and emergency procedures

Avoid breathing vapours, mist or gas.
For personal protection see section 8.

6.2 Environmental precautions

Do not let product enter drains.

6.3 Methods and materials for containment and cleaning up

Keep in suitable, closed containers for disposal.

6.4 Reference to other sections

For disposal see section 13.

SECTION 7: Handling and storage

7.1 Precautions for safe handling

For precautions see section 2.2.

7.2 Conditions for safe storage, including any incompatibilities

Store in cool place. Keep container tightly closed in a dry and well-ventilated place. Containers which are opened must be carefully resealed and kept upright to prevent leakage.

7.3 Specific end use(s)

Apart from the uses mentioned in section 1.2 no other specific uses are stipulated

SECTION 8: Exposure controls/personal protection

8.1 Control parameters

Components with workplace control parameters

Contains no substances with occupational exposure limit values.

8.2 Exposure controls

Appropriate engineering controls

General industrial hygiene practice.

Personal protective equipment

Eye/face protection

Use equipment for eye protection tested and approved under appropriate government standards such as NIOSH (US) or EN 166(EU).

Skin protection

Handle with gloves. Gloves must be inspected prior to use. Use proper glove removal technique (without touching glove's outer surface) to avoid skin contact with this product. Dispose of contaminated gloves after use in accordance with applicable laws and good laboratory practices. Wash and dry hands.

The selected protective gloves have to satisfy the specifications of EU Directive 89/686/EEC and the standard EN 374 derived from it.

Body Protection

Impervious clothing. The type of protective equipment must be selected according to the concentration and amount of the dangerous substance at the specific workplace.

Respiratory protection

Respiratory protection not required. For nuisance exposures use type OV/AG (US) or type ABEK (EU EN 14387) respirator cartridges. Use respirators and components tested and approved under appropriate government standards such as NIOSH (US) or CEN (EU).

Control of environmental exposure

Do not let product enter drains.

SECTION 9: Physical and chemical properties

9.1 Information on basic physical and chemical properties

a) Appearance	Form: liquid
b) Odour	no data available
c) Odour Threshold	no data available
d) pH	no data available
e) Melting point/freezing point	no data available
f) Initial boiling point and boiling range	no data available
g) Flash point	no data available
h) Evaporation rate	no data available
i) Flammability (solid, gas)	no data available
j) Upper/lower flammability or explosive limits	no data available
k) Vapour pressure	no data available
l) Vapour density	no data available
m) Relative density	no data available
n) Water solubility	no data available
o) Partition coefficient: n-octanol/water	no data available
p) Auto-ignition	no data available

- temperature
- q) Decomposition temperature no data available
- r) Viscosity no data available
- s) Explosive properties no data available
- t) Oxidizing properties no data available

9.2 Other safety information
no data available

SECTION 10: Stability and reactivity

10.1 Reactivity

no data available

10.2 Chemical stability

Stable under recommended storage conditions.

10.3 Possibility of hazardous reactions

no data available

10.4 Conditions to avoid

no data available

10.5 Incompatible materials

Strong oxidizing agents

10.6 Hazardous decomposition products

Hazardous decomposition products formed under fire conditions. - Nature of decomposition products not known.
In the event of fire: see section 5

SECTION 11: Toxicological information

11.1 Information on toxicological effects

Acute toxicity

no data available

Skin corrosion/irritation

no data available

Serious eye damage/eye irritation

no data available

Respiratory or skin sensitisation

no data available

Germ cell mutagenicity

no data available

Carcinogenicity

IARC: No component of this product present at levels greater than or equal to 0.1% is identified as probable, possible or confirmed human carcinogen by IARC.

Reproductive toxicity

no data available

Specific target organ toxicity - single exposure

no data available

Specific target organ toxicity - repeated exposure

no data available

Aspiration hazard

no data available

Additional Information

RTECS: Not available

To the best of our knowledge, the chemical, physical, and toxicological properties have not been thoroughly investigated.

SECTION 12: Ecological information**12.1 Toxicity**

no data available

12.2 Persistence and degradability

no data available

12.3 Bioaccumulative potential

no data available

12.4 Mobility in soil

no data available

12.5 Results of PBT and vPvB assessment

PBT/vPvB assessment not available as chemical safety assessment not required/not conducted

12.6 Other adverse effects

no data available

SECTION 13: Disposal considerations**13.1 Waste treatment methods****Product**

Offer surplus and non-recyclable solutions to a licensed disposal company.

Contaminated packaging

Dispose of as unused product.

SECTION 14: Transport information**14.1 UN number**

ADR/RID: -

IMDG: -

IATA: -

14.2 UN proper shipping name

ADR/RID: Not dangerous goods

IMDG: Not dangerous goods

IATA: Not dangerous goods

14.3 Transport hazard class(es)

ADR/RID: -

IMDG: -

IATA: -

14.4 Packaging group

ADR/RID: -

IMDG: -

IATA: -

14.5 Environmental hazards

ADR/RID: no

IMDG Marine pollutant: no

IATA: no

14.6 Special precautions for user

no data available

SECTION 15: Regulatory information

This safety datasheet complies with the requirements of Regulation (EC) No. 1907/2006.

15.1 Safety, health and environmental regulations/legislation specific for the substance or mixture

no data available

15.2 Chemical Safety Assessment

For this product a chemical safety assessment was not carried out

SECTION 16: Other information

Further information

Copyright 2014 Sigma-Aldrich Co. LLC. License granted to make unlimited paper copies for internal use only.

The above information is believed to be correct but does not purport to be all inclusive and shall be used only as a guide. The information in this document is based on the present state of our knowledge and is applicable to the product with regard to appropriate safety precautions. It does not represent any guarantee of the properties of the product. Sigma-Aldrich Corporation and its Affiliates shall not be held liable for any damage resulting from handling or from contact with the above product. See www.sigma-aldrich.com and/or the reverse side of invoice or packing slip for additional terms and conditions of sale.

Appendix 15: E-mail Correspondences with Sigma-Aldrich

On Fri, Feb 15, 2019 at 10:49 PM <E.E.Amadi@bradford.ac.uk> wrote:

ProdSafety_Request - United Kingdom

Form ID : ProdSafety_Request

first_name_haht : Emmanuel

last_name_haht : Amadi

country_haht : GB

state_haht :

e_mail_address_haht : E.E.Amadi@bradford.ac.uk

email_permission_haht : 0

register : no

ProdSafety_ProdNumber : 794341-200ML

ProdSafety_ProdName : Graphene oxide 15-20 sheets, 4-10 edge-oxidized, 1 mg/mL,

ProdSafety_Brand : SIGMA

ProdSafety_Question : Dear Sir/Madam, I am a 4th Year PhD student in Biomedical Sciences, Faculty of Life Sciences, University of Bradford, UK. I had been working on above product since 2016, purchased from from Sigma-Aldrich, UK. I was just informed by some academics that Commercial GO (15-20 sheets) may contain significant amount of Mn₂, Fe₂ and catalytic ions which may give false-positive results in Comet assay (DNA damage), which may not be due to GO itself. Could you please provide me with the following information: (1) The method used to prepare the GO (2) Chemical artefacts /impurities present (3) size of each particle, (4) size of the 15-20 GO. TEM SEM analysis shows that its size is over 600 to 800 nm in diameter. I have been calling this GO nanoparticles or Nanomaterials, but my supervisor and other academics dispute this because they say the size of this GO is outside (100 nm) the classification. I am confused. (5) Nanomaterial particle Characterisation data you might have. Many thanks. Emmanuel Amadi (PhD Candidate)

haht_form_name : ProdSafety_Request

page_link : <https://webpwpublish.sial.com:80/safety-center/email-product-safety.html>

referr_page : <https://www.sigmaaldrich.com/safety-center.html>

thank_you_text :

elqFormName : ProdSafety_Request

elqSiteID : 832461399

----- Forwarded message -----

From: E.E.Amadi@bradford.ac.uk

Date: Mon, Feb 18, 2019 at 06:08 PM

Subject: Chemical Properties

To: ukorders@sial.com;

Dear Sir/Madam,

I am a final year PhD Student (4th Year) in Biomedical Sciences, Faculty of Life Sciences, University of Bradford. Since Feb 2016, I have been working on the toxicity of Graphene Oxide, 15-20 sheets, 14-10% edge-oxidized; 1 mg/mL; dispersion in H₂O (Product No: 794341) due to its popularity in Biomedical applications and to support existing research. I was wondering if you could provide me with data about this product which are not in the Safety Data Sheet available online.

(1) I have read from your website that it was prepared by Chemical Exfoliation method. Is this method the modified Hummer's method commonly found in the literature regarding synthesis of GO?

(2) What are the levels of the Chemical impurities present? I understand that it contains high amount of Mn²⁺, Fe²⁺, and catalytic ions making them give false-positive results.

(3) Nanoparticle characterization + size distribution: Using DLS and TEM, I obtained size ranges from 600 to 800 nm (DLS) and 300 to 450 nm (TEM). Please could you provide me with the data you have for comparison. I was told by other academics that since the size obtained is > 100 nm, that I should not call this GO a nanoparticle.

(4) What is the correct name for GO with 15-20 sheets? Nanoparticles, Nanomaterials or simply Graphene Oxide?

(5) Do you have any genotoxicology data available? We believe that effects of 1-2 sheets of GO on cells might be different from GO with multi-layers (15 to 20).

I look forward to reading from you soon.

Yours Sincerely,

Emmanuel

.....One Reply

noreply@salesforce.com on behalf of

LabWE North TS 4 <technicalservice@merckgroup.com>

Mon 18/02, 21:42

Emmanuel Amadi

Hi Emmanuel,

thank you very much for contacting us at Merck.

The information available on the website, through the specification sheet and the SDS, is everything we have in terms of impurities and safety profile of the product. We don't carry out additional characterizations other than what is stated on the specs/CoA.

Particle size is not measured so you can simply call it graphene oxide.

I hope this is of help, if you have any further questions, please feel free to contact us at technicalservice@merckgroup.com.

Best regards

Sebastiano Rupiani, PhD

Technical Service Scientist - North Area

Customer Excellence | Research & Applied Solutions Commercial - Western Europe
Life Science, Merck

E-mail: technicalservice@merckgroup.com

Phone UK: 01923 813 365 | EI: 016058401 | DK: 82 33 28 21 | FI 0981 710 366 | NO:
81 06 26 46 | SE: 0851 992 488

Sigma-Aldrich is now part of Merck

Mandatory information can be found at <http://www.merckgroup.com/mandatories>